DISSERTATION

THE INFLUENCE OF SOIL HYDRAULIC PROPERTY ESTIMATION ON THE PREDICTIVE ACCURACY OF SOLUTE TRANSPORT MODELING

Submitted by

Mark Alan Prieksat

Department of Soil and Crop Sciences

In partial fulfillment of the requirements

for the Degree of Doctor of Philosophy

Colorado State University

Fort Collins, Colorado

Spring 1999

COLORADO STATE UNIVERSITY

April 2, 1999

WE HEREBY RECOMMEND THAT THE THESIS PREPARED UNDER OUR SUPERVISION BY MARK ALAN PRIEKSAT ENTITLED THE INFLUENCE OF SOIL HYDRAULIC PROPERTY ESTIMATION ON THE PREDICTIVE ACCURACY OF SOLUTE TRANSPORT MODELING BE ACCEPTED AS FULFILLING IN PART REQUIREMENTS FOR THE DEGREE OF DOCTOR OF PHILOSOPHY.

Committee on Graduate Work

Adviser

Department Head

ABSTRACT

THE INFLUENCE OF SOIL HYDRAULIC PROPERTY ESTIMATION ON THE PREDICTIVE ACCURACY OF SOLUTE TRANSPORT MODELING

Because of the complexity of processes governing water and chemical movement in the unsaturated zone, numerical models will necessarily play a key role in predicting the fate and transport of chemicals. If models are to fulfill their role as a tool in managing agrichemicals, then clearly models need to be tested for sensitivity to the method used to measure the soil hydraulic properties used in the model. The objectives of this study were to compare hydraulic parameter estimates obtained using alternative methods and to evaluate the affect of the parameter estimation method on the predictive accuracy of the HYDRUS-2D model. Soil hydraulic parameters were determined at multiple depths within a 2 meter deep soil profile using a variety of methods; field methods included the instantaneous profile method (IPM) and tension infiltrometry at two scales (5.08 cm-diameter (4TI) and 20.32 cm-diameter (8TI)); lab methods included determination of saturated hydraulic conductivity using the falling head method and analysis of moisture retention using pressure plate analysis at two scales (5.08 cm-diameter x 5.08 cm-long soil cores (2C) and 10.16 cm-diameter x 5.08 cm-long soil cores (4C)); indirect methods (IND) included determining hydraulic parameters

from three literature sources based on soil textural data. In addition, identical parameter estimates were made under two tillage treatments (non-tilled (NT) and tilled (T)). It was found that estimation of soil hydraulic properties was sensitive to the measurement method selected. Estimation of the α and K_s parameters was more sensitive to method and scale than was estimation of the n and θ_s parameters. The IPM method showed the least variability in parameter estimates. Tillage introduced significant changes in the hydraulic properties and increased spatial variability in the parameter estimates.

Data obtained using the alternative estimation methods was used as input to the HYDRUS-2D model to predict water and solute movement. Water content and solute concentration profiles estimated using the model were compared with observed water content and solute concentration profiles obtained during a field-scale solute transport study using bromide tracer. Most of the parameter estimation methods resulted in simulated water content that were within about 2 to 5 percent of the measured data. The IND method had the largest deviations (about 10 percent) from the measured data. Under T soil conditions, all the methods (except the IND) predicted bromide movement well and simulated bromide concentration data were well correlated to measured data at all times throughout the simulation. Under NT conditions, all methods, except the 8TI, under-predicted the center of mass movement of bromide. Analysis of the simulation data revealed that the hydraulic properties of the surface soil are extremely important in controlling water and solute movement. Results indicate that the IPM is probably

the most reliable method, but other estimation methods may result in similar predictions of water and solute movement when made in repetition.

Mark Alan Prieksat
Department of Soil and Crop Sciences
Colorado State University
Fort Collins, CO 80523
Spring 1999

ACKNOWLEDGMENTS

This investigation was supported by the Agricultural Research Service, ARS-USDA, in cooperation with the Colorado State University Department of Soil and Crop Sciences. Support was initiated under the National Needs Fellowship Program in Water Science.

I wish to thank my advisor Dr. Greg L. Butters for his participation and inspiration during the course of this investigation and for his continued persistence to see that my program of study came to a completion. I also would like to thank my committee members Dr. Laj Ahuja, Dr. Grant Cardon, and Dr. David McWhorter for their participation and advice. Much is owed to my wife Patience who has supported me both mentally and financially over the past year. Her name rings true in her persistence and attitude towards me over the past three years. All the abilities that I have are attributed to God and through him all things are possible. I have been given the grace to finish this work and for that I am thankful.

TABLE OF CONTENTS

LIST OF TABLES

LIST OF FIGURES

LIST OF SYMBOLS

Symbol	Definition
C	Solute Concentration
C_o	Initial Solute Concentration
C(h)	Slope of the moisture characteristic curve θ(h)
D_{ij}	Dispersion coefficient tensor in HYDRUS-2D
D(θ)	Diffusivity
D	Hydrodynamic dispersion coefficient
D*	Molecular diffusion coefficient
D'	Mechanical dispersion coefficient
E	Maximum potential rate of infiltration or evaporation
F	Equation simplification term
G	Equation simplification term
h	Capillary or matric potential head
H	Hydraulic head
h_A	Minimum pressure head allowed during evaporative flux
h_o	Initial head distribution $h_o(x,z)$
h_s	Water head at $\theta = \theta_s$

J_H	Hydrodynamic dispersion flux
k	Adsorption isotherm rate constant
K	Hydraulic conductivity
K_s	Saturated hydraulic conductivity
K(h)	Hydraulic conductivity function
K_{iz}^A	Anisotropy tensor for (i,z)
K_{ij}^A	Anisotropy tensor for (i,j)
K_r	Relative hydraulic conductivity
L	Length
m	Curve fitting parameter (generally = 1-1/n)
n	Slope of θ(h), indicative of pore size distribution
q	Water flux (specific discharge)
R	Retardation factor
S	Sink term in water flow equation
Se	Reduced water content function (θ_s - θ / θ_s - θ_r)
t	Time
V	Pore water velocity
x	Length component in x direction
z	Length component in z direction
α	Curve fitting parameter, indicative of air-entry value (1/α)
γ_w	Zeroth order rate constant for liquid phase
γ_s	Zeroth order rate constant for solid phase

λ	Dispersivity
μ_w	First order rate constant for liquid phase
μ_s	First order rate constant for liquid phase
ρ	Bulk density
φ	Soil water potential
θ	Soil water content
θ_r	Residual water content
θ_s	Saturated water content
θ_v	Volumetric water content

CHAPTER 1

INTRODUCTION

Water quality research has rapidly gained stature as a critical need area in agricultural research. Agricultural activity is generally recognized as the largest contributor to non-point source water pollution in the United States (EPA, 1990a). Sediment and nutrient loading of surface water by runoff and agrichemical contamination of groundwater by leaching are the two most important pathways impacting groundwater quality in agricultural areas. Of the surface waters in the United States, not supporting designated use, agricultural runoff is identified as the source of impairment for about 60% of the area affected (EPA, 1990a). In a recent nationwide survey of groundwater quality (EPA, 1990b), EPA observed nitrate in over half of the 1300 wells sampled. EPA estimates that 1.2% of community wells and 2.4% of rural domestic wells contain nitrate in excess of 10 mg/l.

In as much as the application rates of agrichemicals continues to increase (for example, according to TVA statistics, fertilizer application rates in the Great Plains States have tripled since 1965), changes in agricultural management which reduce water quality degradation are required. Because of the complexity of processes governing the environmental fate and transport of agrichemicals

and the vast areas to which these chemicals are applied, transport models will necessarily play a key role in predicting the fate of agrichemicals and perhaps ultimately result in stricter regulation of their use. In general, a transport model selected for the task of predicting chemical fate and transport might yield unreasonable results because; (1) the model is an oversimplification of the dominant processes (mechanistically inaccurate) and/or, (2) the inputs required to run the model are not measured directly, and must be guessed (or estimated indirectly) and/or, (3) the inputs are measured, but the values are not representative of the media or of the scale the model is designed to simulate.

If models are to fulfill their role as a tool toward better managing agrichemicals, then clearly models need to be tested and validated using a multitude of approaches, including sensitivity to failures of the second and third types as listed above.

A key element in all unsaturated zone solute transport models is estimation of soil water flux. Except for the simplest case of steady-state flow, the depth and time dependence of the drainage flux is estimated using Richards' equation of a simplified drainage model (van Genuchten and Jury, 1987; Feddes et al., 1988). In the matric potential (h) form, Richards' equation in one-dimension is

$$C(h)\,\frac{\partial h}{\partial t} = \frac{\partial}{\partial z}\left[K(h)\left(\frac{\partial h}{\partial z} + 1\right)\right] \qquad (1.1)$$

where C(h) is the slope of the soil moisture retention curve (h(θ)) and K(h) is the hydraulic conductivity function of the soil. Of interest are the functions h(θ) and K(h). A large body of research suggests that K(h) and h(θ) are hysteretic and depend upon the method of estimation, the sample volume, and the number of representative samples used to measure these relationships. Curve fitting parameters determined from laboratory measured soil moisture retention for a draining soil sample may not be indicative of in-situ profiles, where potentials and moisture contents may differ due to the hysteretic nature of the soil and the wetting and draining history prior to measurement.

The goal of this research is to evaluate the influence of calibration (soil parameter estimation) method on the predictive accuracy of a main-stream numerical code for modeling water flow and transport of a conservative solute. Soil hydraulic parameters are estimated using field, laboratory, and indirect methods. Using these alternative parameter estimates as input to the model, simulated water content and solute concentration profiles are generated and then compared with observed water content and solute concentration profiles. Presumably, the alternative methods of hydraulic property characterization will influence the predictive accuracy of the numerical model. By comparing the models predictions, we hope to address several questions; 1) does the most rigorous, labor intense characterization of the hydraulic properties lead to the most accurate model simulations, 2) what loss of predictive accuracy is incurred using indirect estimation of the hydraulic properties, 3) to what extent does the

support scale of a hydraulic property measurement influence predictive accuracy and, 4) what combination of measurements maximizes predictive accuracy while minimizing experimental effort.

This dissertation is divided into five sections: 1) literature review, 2) experimental methods, 3) comparison of hydraulic property data obtained using field, lab, and indirect methods, 4) comparison of the predictive accuracy of the HYDRUS-2D code as affected by parameter estimation method, and 5) the conclusions drawn from the study.

CHAPTER 2

LITERATURE REVIEW

2.0 Introduction

This chapter focuses on past and present research performed in the areas of, 1) water flow and solute transport in soils, 2) hydraulic parameter estimation, and 3) effects of management on water and solute movement.

2.1 Water Flow and Solute Transport: Governing Equations

Water Movement in Soils

Darcy's law, first derived empirically in 1856, forms the basis for most efforts to describe flow through porous media (Swartzendruber, 1969; Nielsen et al., 1972)

$$q = -K \frac{dH}{dL} \qquad (2.1)$$

where q is water flux/unit area ($L^3L^{-2}t^{-1}$), also referred to as the specific discharge or Darcy velocity, K is hydraulic conductivity ($L\ t^{-1}$), H is hydraulic head (L), and L is length (L).

Combining the principal of mass conservation with Darcy's law results in the Laplace equation, which governs fluid flow under homogenous, isotropic,

saturated steady state conditions (Nielsen et al., 1972)

$$\frac{\partial^2 \phi}{\partial x^2} + \frac{\partial^2 \phi}{\partial y^2} + \frac{\partial^2 \phi}{\partial z^2} = 0 \qquad (2.2)$$

where ϕ is the total soil water potential (pressure + elevation head/water density) (L), and (x, y, z) are the direction coordinates.

Darcy's law can also be applied to unsaturated flow through porous media. The main difference for unsaturated flow is that the potential gradient term is usually dominated by capillary forces and secondly, hydraulic conductivity is a function of a soils' moisture content (Richards, 1931). Buckingham (1907) was the first to apply the concept of capillary potential as the driving force of water movement in unsaturated soils

$$q = -K(h) \left(\frac{\partial h}{\partial z} + 1\right) \qquad (2.3)$$

where K(h) is hydraulic conductivity as a function of pressure head ($L\ t^{-1}$), h is the capillary or matric potential head (L), and z is the gravitational component (L). The utility of Darcy's law to describe saturated and unsaturated flow is well established, especially when applied to homogenous soil columns in the laboratory, or in uniform soils (Philip, 1969b; Swartzendruber, 1969; Haverkamp et al., 1977; Bear and Verruijt, 1987). However, with increasing variations in flow velocity, under heterogenous soil conditions frequently found under field conditions, predictions of water movement based on Darcy's law become less

accurate (Elrick and French, 1966; Bouma and Anderson, 1973; McMahon and Thomas, 1974; Lewis, 1977; Philip, 1983).

Combining the continuity equation with Equation 2.3 results in Richards' equation

$$C(h)\frac{\partial h}{\partial t} = \frac{\partial}{\partial z}[K(h)(\frac{\partial h}{\partial z} + 1)] \qquad (2.4)$$

where C(h) is the soil water capacity dθ/dh. With defined initial and boundary conditions and known K(h) and C(h), Richards' equation describes spatial and temporal changes in soil water flux (q(z,t)) and soil water content (θ(z,t)).

A useful transform of Eq. 2. is found by introducing the soil water diffusivity (Kirkham and Powers, 1972)

$$D(\theta) = K(\theta)\frac{\partial h}{\partial \theta} \qquad (2.5)$$

For horizontal flow in homogeneous soil, Eq. 2.4 reduces to

$$\frac{\partial \theta}{\partial t} = \frac{\partial}{\partial x}(D(\theta)\frac{\partial \theta}{\partial x}) \qquad (2.6)$$

which, if D(θ) is constant, is mathematically identical to the heat transfer equation and may be solved analytically for a wide variety of boundary and initial conditions (Carslaw and Jeager, 1959; Nielsen et al., 1972).

Many commonly used infiltration equations are derived from a special case of Darcy's equation, the Hagen-Poiseuilles equation (Green and Ampt,

1911; Richards, 1931; Klute, 1952; Philip, 1957; Holtan, 1961; Bouwer, 1969; Mein and Larson, 1973). In the absence of simplifying assumptions regarding homogeneity or sharpness of the wetting front, Eq. 2.4 must be solved numerically to describe infiltration and redistribution.

Solute Transport Processes

Movement of solutes through a porous media is controlled by several different processes; advection, mechanical dispersion, and molecular diffusion. Advection is the component of solute transport attributed to the bulk motion of flowing fluid. Mechanical dispersion is the mixing that occurs during fluid advection. It is important on both microscopic and macroscopic levels. Collectively molecular diffusion and mechanical dispersion are generally referred to as hydrodynamic dispersion. Hydrodynamic dispersion is quantified by the coefficient of hydrodynamic dispersion, D, (Bear, 1972)

$$D = D' + D^* \qquad (2.7)$$

where D' is the mechanical dispersion coefficient and D* is the molecular diffusion coefficient. Under advective-dispersive solute transport, molecular diffusion is generally neglected since it is typically one or two orders of magnitude smaller than mechanical dispersion at velocities commonly seen in field and laboratory studies. Under this condition, the hydrodynamic dispersion flux is mathematically equivalent to the dispersion flux

$$J_H = -D(\theta)\ \frac{\partial C}{\partial x} \qquad (2.8)$$

where J_H is hydrodynamic dispersion flux, θ is volumetric water content, C is solute concentration, and x is distance in the x direction. This coefficient is a function of fluid velocity, degree of saturation, and dispersivity (λ) and can be related to the pore water velocity by (Bear, 1972)

$$D(\theta) = \lambda V \qquad (2.9)$$

where V is the pore water velocity described as (Bear, 1972)

$$V = \frac{q}{\theta} \qquad (2.10)$$

where q is specific flux and θ is volumetric water content.

Solute Transport in Soils

This section provides an overview of mathematical approaches to describe solute transport in soils. All of the models discussed address, in some manner, the variability of solute movement in a soil, either locally or on a field scale.

The most commonly used representation of solute movement is the advection-dispersion representation. Analytical and numerical solutions for the advection-dispersion equation have been developed for a variety of boundary conditions. The equation has been widely used to model solute movement through saturated media under uniform flow conditions (Danckwerts, 1953;

Ogata and Banks, 1961; Brenner, 1962; Nielsen and Biggar, 1962; Bear, 1972; Freeze and Cherry, 1979; Anderson, 1984; Parker, 1984; van Genuchten and Wierenga, 1986; and Wierenga, 1977). For one-dimensional steady state flow this differential equation becomes

$$\frac{\partial C}{\partial t} = D \frac{\partial^2 C}{\partial x^2} - V \frac{\partial C}{\partial x} \qquad (2.11)$$

where C is the flux averaged solute concentration C(x,t) ($M\ L^{-3}$), D is the apparent diffusion coefficient ($L^2\ t^{-1}$), V is the average pore water velocity ($L\ t^{-1}$), x is the distance from where solute is introduced (L), and t is the time after solution is applied to a column (t). Pore water velocity (V) used in Equation 2.11 is also described as the linear velocity and can be calculated as in Equation 2.10.

Equation 2.11 was derived from steady state flow conditions and the continuity equation. It assumes no interaction between solute and soil particles (Chu and Sposito, 1980; van Genuchten and Wierenga, 1986). The equation is a combination of three solute transport mechanisms: advection ($V\ \partial C/\partial x$), molecular diffusion, and mechanical dispersion ($D\ \partial^2 C/\partial x^2$). The apparent diffusion coefficient (D) is frequently assumed to be a linear combination of molecular diffusion and mechanical dispersion (Eq. 2.7) (Bear, 1972; Kirda et al. 1973; Hillel, 1980; Gillham and Cherry, 1982; van Genuchten and Wierenga, 1986). The apparent diffusion coefficient (D) is generally determined from empirical equations, by curve fitting, or estimated (Wierenga, 1977; De Smedt

and Wierenga, 1978; Bresler and Dagan, 1982; Gillham and Cherry, 1982;). van Genuchten and Wierenga (1986) review a number of methods for fitting a value for D to breakthrough curve data. Fried (1975) presents several approaches used for determining diffusion coefficients on a field scale.

For unsaturated conditions with non-steady state water flow, transport of non-interacting solutes can be described in one dimension by (Warrick et al., 1971)

$$\frac{\partial(\theta C)}{\partial t} = \frac{\partial}{\partial x}(\theta D \frac{\partial C}{\partial x}) - \frac{\partial(qC)}{\partial x} \qquad (2.12)$$

where the coefficients are as defined previously.

Solutions to Eq. 2.12 have relied on numerical methods or simplifying assumptions. De Smedt and Wierenga (1978) used an approximate analytical solution to solve Equation 2.12 for a steady-state water flux but nonuniform water content. They found their results agreed with an analytical solution for solute movement in soils having uniform water content. Bresler and Hanks (1969), Warrick et al. (1971), Kirda et al. (1973), and Jury et al. (1976) developed numerical solutions to the advection-dispersion equation for unsaturated non-steady flow conditions. The model of Bresler and Hanks makes the simplifying assumption of ignoring the diffusion term. Jury et al. (1976) solves the equation using constant moisture contents for individual layers. Warrick et al. (1971) assumed a constant value for velocity and diffusion coefficient. They found that fitting their model to field data required a diffusion

coefficient 10 to 100 times larger than the value of molecular diffusion alone.

Limitations on Using the ADE

Although the advection-dispersion approach is well suited for laboratory columns, the use of a single average soil pore velocity or dispersion value to represent what is actually a range of velocities, causes difficulties in a field situation (Green et al., 1986; Horton and Wierenga, 1986; and Wagenet, 1986). Gish and Jury (1982) found that plant roots lowered the fraction of wetted pore space compared to when no plants were present. With plant roots present, pore velocities calculated from the local water flux divided by the local water content, under-predicted velocity and over-estimated solute travel time. As a soil becomes increasingly unsaturated, larger flow paths are progressively eliminated, and the proportion of soil water not readily mobile increases (Biggar and Nielsen, 1967). Nielsen and Biggar (1962) suggest that the greater the range in velocity distribution, the less accurately Equation 2.12 represents the actual physical process. They also note that the apparent diffusion coefficient is dependent on the value used for the average velocity.

Pickens and Grisak (1981) and Molz et al. (1986) determined from studies of saturated flow that effective dispersion is scale dependent. Molz et al. (1986) conclude that ". . . combining local mixing and differential advection with a single dispersion term is not reasonable physically or possible mathematically." They point out that field scale models frequently use D as a fitted parameter. This results in a value generally several orders of magnitude

larger than those determined in a laboratory column.

An additional concern for describing solute transport by the advection equation is raised by Horton and Wierenga (1986). They point out that solutions based on differential equations must be differential functions. For many soils, water and solutes move irregularly in discontinuous steps. The greatest obstacle however, to extrapolating a advection-dispersion model to a field site is that a single-valued parameter cannot be used to describe field heterogeneities (Parker and van Genuchten, 1984; Wagenet, 1986).

Other Modeling Approaches

While the advection-dispersion equation (ADE) is the basic transport model, others have developed methods aimed at improving the predictive accuracy of the concept. Numerous models have been developed using the concept of a two-region or multiple-region model. This approach is a variation of the advection-dispersion equation that seeks to account for the variability in pore water velocity on an scale intermediate between a column and a field (Skopp and Warrick, 1974; Addiscott, 1977; De Smedt and Wierenga, 1979; Parker and van Genuchten, 1984; Crittenden et al., 1986; Rasmuson, 1986; van Genuchten and Dalton, 1986; Roberts et al., 1987; Seyfried and Rao, 1987). For example, the mobile-immobile water model (van Genuchten and Wierenga, 1976) divides water and solute flow in the soil into two or more flow regions. For this type of two-region model, water moving in the larger pores and between aggregates is considered mobile water. Water held close to soil particles or inside soil

aggregates is considered immobile water. Water infiltrating through the soil displaces only the mobile fraction of the soil solution. Solutes transfer between the mobile and immobile regions by diffusion. Parameters for the mobile-immobile model, especially the proportion of mobile and immobile pores, are determined primarily by curve fitting (Rao et al., 1979; Pandey and Gupta, 1984; Parker and van Genuchten, 1984). This requirement for calibration data is a limitation on the predictive utility of the model. It is of interest to note that the two-region model is identical mathematically to that of a two-site kinetic adsorption model (Nkedi-Kizza et al., 1982). In addition, the use of two regions is rather arbitrary and any number of regions can be employed. Hutson and Wagenet (1994) discuss the use of a multiregion model to describe water flow and solute transport. Their TRANSMIT model was easily adaptable to a range of multiregion and two-dimensional geometries.

Another approach to modeling field heterogeneities is to treat inputs to a deterministic model as stochastic variables. If it assumed that the soil and water parameters in a field vary at random, then solute concentration in the soil profile can be defined in statistical terms (Nielsen et al., 1973). However, it is generally impossible to completely characterize the random field for a soil property. As a result, the first and second statistical moments are often used to quantify field spatial variability.

Stochastic models can be used to predict the uncertainty of water transport and solute distribution in a field system, but require an accurate

understanding of the spatial variability of the soil and water parameters in the field (Wagenet, 1986). Van de Pol et al. (1977) showed that values of pore velocity and apparent diffusivity were normally log distributed. As a consequence, they note that determining solute flux by the product of an average soil water concentration and an average pore velocity resulted in substantial errors.

McBride (1985) used the mean and confidence limits of pore velocity to estimate the distribution variability of chloride concentrations in a soil profile. Ammozegar-Fard et al. (1982) used Monte Carlo simulation to generate individual values of pore velocity and apparent diffusion after previously determining their log normal distribution parameters. The resulting 2000 paired values were used as inputs to an analytical solution to Equation 2.11. The results were compiled into probability curves for solute concentration profiles in the soil. They found that variability of pore water velocity was more important to solute distribution than any variability caused by the apparent diffusivity. This result emphasizes, that for field scales, the dispersion term in the ADE is predominantly due to advective variability.

Dagan and Bresler (1979) and Bresler and Dagan (1979) developed transfer functions relating soil water content and soil solute concentration. Their results indicate that the average concentration profile differs completely from that predicted using average values for V and D with Equation 2.11. Transfer function models have been used with reasonable success to describe leaching

of chloride, bromide, tritiated water, and nitrate (Bresler and Dagan, 1979; Jury et al., 1982; Gish, 1987; Jennings and Martin, 1988; and Butters et al., 1989).

Unsaturated Flow and Transport: Numerical Solution using the HYDRUS-2D Model

The HYDRUS-2D model is one of many numerical codes developed and used to predict water and solute movement. Essentially all models of this type use Richard's equation to simulate water flow and some form of the ADE to predict solute movement. The HYDRUS-2D code (Simunek et al., 1996) is a Microsoft Windows based two-dimensional finite element model for simulating water flow and solute transport in variably saturated porous media. The program numerically solves Richards' equation for saturated-unsaturated water flow. The code can account for root water uptake, evapotranspiration (ET), and includes provisions for linear equilibrium adsorption, zero-order production, and first-order degradation. The flow region can be composed of a single homogeneous layer or multiple layers, each with different properties. The governing flow and transport equations are solved using either Gaussian elimination or the conjugate gradient method, depending upon the size of the grid.

The governing flow equation for two-dimensional Darcian flow of water in a variably saturated rigid porous media is given by a modified form of Richards' equation

$$\frac{\partial \theta}{\partial t} = \frac{\partial}{\partial x_i}[K(K_{ij}^A \frac{\partial h}{\partial x_j} + K_{iz}^A)] - S \qquad (2.13)$$

where S is the sink term, x_i (i=1,2) are the spatial coordinates, K_{ij}^A are components of a dimensionless anisotropy tensor K_A, and K is the unsaturated hydraulic conductivity function given by

$$K(h,x,z) = K_s(x,z)\, K_r(h,x,z) \qquad (2.14)$$

where K_r is the relative hydraulic conductivity and K_s is the saturated hydraulic conductivity.

In the absence of the extrapolated (θ_m and θ_a) terms used to specify anisotropy, the unsaturated soil properties are described by a set of equations resembling van Genuchten (1980) and Mualem (1976)

$$\theta(h) = \theta_r + \frac{(\theta_s - \theta_r)}{(1 + |\alpha h|^n)^m} \qquad h < h_s \qquad (2.15)$$

$$\theta(h) = \theta_s \qquad h \geq h_s \qquad (2.16)$$

and

$$K(h) = K_s\, K_r(h) \qquad h \leq h_k \qquad (2.17)$$

where

$$K(h) = K_s \qquad h \geq h_s \qquad (2.18)$$

Estimation of the parameters of Eqs. 2.15 through 2.19 and how that affects

$$K_r = S_e^{\frac{1}{2}} [1 - (1 - S_e)^m]^2 \qquad (2.19)$$

predictive accuracy of the model is the central focus of this dissertation.

Solution of equation 2.13 requires knowledge of the initial distribution of pressure head or water content

$$h(x,z,t) = h_0(x,z) \quad for\ t = 0 \qquad (2.20)$$

where h_0 is a prescribed function of x and z. Boundary conditions can be specified pressure heads (Dirichlet type), specified flux (Neumann type), or specified gradient.

In addition to the above mentioned boundary conditions, HYDRUS-2D considers three different types of system-dependent boundary conditions which cannot be defined directly by the user. One of these involves the soil-atmosphere interface. The potential fluid flux across the atmospheric boundary is controlled by external conditions, but the actual flux depends upon the transient soil moisture conditions. Thus, soil surface boundary conditions may change from prescribed flux to prescribed head and vice-versa. In the absence of surface ponding of water, the numerical solution of Eq. 2.13 is obtained by limiting the absolute value of the flux such that the following conditions are satisfied

$$|K\,(K_{ij}^{A}\,\frac{\partial h}{\partial x_j} + K_{iz}^{A})\,n_i| \le E \qquad (2.21)$$

and

$$h_A \le h \le h_s \qquad (2.22)$$

where E is the maximum potential rate of infiltration or evaporation under the atmospheric conditions, h is the pressure potential at the soil surface, and h_A and h_S are the minimum and maximum pressure heads allowed under the prevailing soil conditions. The value for h_A is determined from the equilibrium conditions between soil water and atmospheric water vapor, and h_S is usually set to zero.

For solute transport, HYDRUS-2D uses a Fickian-based advection-dispersion equation

$$-\theta R\,\frac{\partial c}{\partial t} - q_i\frac{\partial c}{\partial x_i} + \frac{\partial}{\partial x_i}(\theta D_{ij}\frac{\partial c}{\partial x_j}) + Fc + G = 0 \qquad (2.23)$$

where

$$F = \mu_w\,\theta + \mu_s\,\rho\,k + S \qquad (2.24)$$

$$G = \gamma_w + \gamma_s \rho - S c_s \qquad (2.25)$$

For equations 2.23 through 2.25, c is the solution concentration, q_i is the *i*-th component of the volumetric flux (LT^{-1}), μ_w and μ_s are the first-order rate constants for the liquid and solid phases ($1T^{-1}$), respectively, γ_w and γ_s are the zero-order rate constants for the liquid (MLT^{-1}) and solid phases (T^{-1}), respectively, ρ is the soil bulk density (ML^{-3}), S is the sink term in the water flow equation(Eq. 2.13), c_s is the concentration of the sink term (ML^{-3}), and D_{ij} is the dispersion coefficient tensor (L^2T^{-1}). To solve Eq. 2.23 it is necessary to know the water content and volumetric flux. Both of which are obtained from solutions of the Richards equation.

HYDRUS-2D assumes equilibrium interactions between the solution (c) and the adsorbed (s) concentrations of the solute in the soil. The adsorption isotherm relating *s* and *c* is described by a linear equation, *s=kc*. The retardation factor R is, thus defined as

$$R = 1 + \frac{\rho k}{\theta} \qquad (2.26)$$

where k is an empirical constant (L^3/M).

Solution of equation 2.23 requires the initial solute concentration within the flow region and specification of boundary conditions. Two types of boundary conditions, prescribed concentration or prescribed solute flux, can be used.

When an atmospheric boundary is applied on the flow region and there is water moving out of the flow region due to evaporation, the prescribed solute flux upper boundary condition reduces to a second-type or Neumann condition to prevent the model from moving solute across the atmospheric boundary.

2.2 Applying the Flow and Transport Model: The Calibration Challenge

Possibly the greatest challenge that faces anyone using a mathematical model to predict water and/or solute movement is collection of the necessary data needed to operate the model. The model can be simplistic and require only limited input data or it can be quite complex and require data that the researcher may have no knowledge of a priori. A variety of methods exist for determination of saturated and unsaturated flow parameters. Many of these methods have been used as tools for the prediction of fate and transport of solutes. This section discusses methods of measuring or obtaining soil hydraulic properties (Eqs. 2.15 - 2.19) and factors that may effect the collection or determination of those properties.

(a) <u>In-Situ Methods for Determining Soil Hydraulic Parameters</u>

In-situ estimates of K(h) and h(θ) can be obtained through the rigorous unsteady drainage flux or instantaneous profile method (Hillel et al., 1972; Green et al., 1986). The method was first developed by Richards et al. (1956) and improved upon by Watson (1966) who used instantaneous measurements of moisture content and water potential. The test allows determination of saturated

and unsaturated hydraulic conductivity for the vertical soil profile outlined by the test. The data can also be used to determine the unsaturated hydraulic parameters (α and n, Eq. 2.15) to be used as input for analytical and numerical models for prediction of water and solute movement.

Analysis is based on an equation describing one-dimensional, isothermal, non-hysteretic, unsaturated flow of water during drainage (Green et al., 1986)

$$\frac{\partial \theta(z,t)}{\partial t} = \frac{\partial}{\partial z}\left[K(\theta)\,\frac{\partial H(z,t)}{\partial z}\right] \qquad (2.27)$$

where $\theta(z,t)$ is the transient volumetric water content of the soil at any depth "z" and time "t", $H(z,t)$ is the soil-water potential, and $K(\theta)$ is the unsaturated hydraulic conductivity.

If the test plot is covered to prevent evaporation, the initial condition for Eq. 2.27 is the moisture-content profile at the start of the test and the upper boundary condition is zero flux at the surface (z=0). With these conditions we can integrate Eq. 2.27 with respect to z, between z=0 and some arbitrary depth $z=z_1$ for any given time

$$\frac{\partial}{\partial t}\int_0^{z_1} \theta(z,t)\,dz = K(\theta)\,\frac{\partial H(z,t)}{\partial z}\Big|_{z_1} \qquad (2.28)$$

The right and left sides of Equation 2.28 are evaluated at simultaneous times

using the θ and H profile data to determine $K(\theta)$ at any depth $z=z_1$.

The need for rapid methods for determining hydraulic conductivity of field soils has led investigators to develop a means of measuring infiltration under tension. Bouwer (1966) designed an air-entry permeameter for measuring in-situ saturated hydraulic conductivity. The method combines knowledge of the soil air-entry value, saturated infiltration rate, and wetting front advancement to calculate K_s. Topp and Binns (1976) modified the Bouwer design for an air-entry permeameter by adding a tensiometer to track the position of the wetting front. Their device also determined the air-entry value and saturated hydraulic conductivity. Topp and Zebchuk (1985) modified the air-entry permeameter to allow it to measure infiltration rate at a negative head of 5 cm. They reported their infiltrometer was easier to use than the air-entry permeameter that it replaced. Hillel and Gardner (1970) developed theory for determining unsaturated hydraulic conductivity by measuring infiltration through a layer of low conductivity material at the soil surface. Extending this theory, Clothier and White (1981) developed a disc permeameter for measuring infiltration under tension, which lead to the development of similar devices, such as the tension infiltrometer (Ankeny, 1988b). Tension infiltrometers (Ankeny et al., 1988a; Perroux and White, 1988) can be used for in-situ measurement of wet range K(h) (Perroux and White, 1988; Clothier and Smettem, 1990). Double or concentric ring tension infiltrometers have also been introduced which improve extrapolation of K(h) to lower than measured soil water potentials

(Smettem et al., 1994; Zhang et al., 1999). Casey et al. (1997) investigated the use of tension infiltrometers for determining the mobile-immobile water parameters and mass exchange coefficients.

Other recent methods include the borehole field method (Shan and Stephens, 1993) for determining unsaturated hydraulic conductivity. The method involves injecting water at a point and monitoring the steady state pressure distribution surrounding the source. The method is a adaption of the Guelph permeameter (Reynolds et al., 1984), used to measure hydraulic conductivity of near surface soils.

(b) Laboratory Methods for Determining Soil Hydraulic Parameters

A multitude of laboratory methods exist for determining hydraulic parameters of soils. Laboratory procedures for measuring saturated hydraulic conductivity are reviewed by Klute and Dirksen (1986). These methods include the constant head measurement, that is best suited for materials with relatively high permeability (1×10^{-4} cm/s or greater), and the falling head measurement that is best suited for low permeability materials. Conca and Wright (1992) recently tested the centrifuge method of Nimmo et al. (1987) for rapidly determining saturated hydraulic conductivity of soils.

Unsaturated hydraulic conductivity can be determined under steady-state conditions (Richards, 1931; Nielsen and Biggar, 1961) or under transient flow conditions (Gardner, 1956). Alternatively, diffusivity (Eq. 2.5) can be measured with horizontal infiltration experiments (Bruce and Klute, 1956;

Gardner, 1958; and Whisler and Watson, 1968) and converted to conductivity if $h(\theta)$ is known. Mualem (1976) presented an analytical method for determining unsaturated hydraulic conductivity using moisture retention data. The model has been adapted for use with the RETC code for determination of unsaturated flow parameters. Campbell (1974) also developed a method for determining unsaturated hydraulic conductivity from $h(\theta)$ data. Both the Mualem and Campbell models have been used extensively to predict $K(\theta)$ relationships.

Unsaturated flow parameters that describe the soils ability to retain water under tension can be obtained through moisture retention analysis. Klute (1986) gives a review of the methods for measuring moisture retention or capillary-pressure/saturation. Brooks and Corey (1964) suggested mathematical formulations to describe the moisture characteristics of soils. They described several parameters, bubbling pressure and pore size distribution index, as a means for describing the functional relationship. van Genuchten (1980) presented a new function to describe the moisture retention of soils (Eq. 2.15) which has been widely adopted in numerical modeling of unsaturated flow. A parameter estimation code RETC (van Genuchten et al., 1991) is a widely used tool to fit the van Genuchten retention and Mualem conductivity forms to experimental data.

The desire to obtain unsaturated hydraulic parameters in a more timely fashion has led to inverse approaches. Gardner (1962) first suggested calculating diffusivity from a one-step pressure increment. The analysis has also

been applied to pressure-membrane cell outflow experiments (Doering, 1965) and to evaporating columns (Rowse, 1975). Gupta and co-workers in Minnesota (1974) found that Gardner's method could be in error and proposed a more accurate method that has not been widely used because of the complexity. Passioura (1976) assumed that the rate of change of water content at a given time is constant over the length of the sample (L) and derived diffusivity as

$$D(\theta_L) = \frac{\partial q}{\partial \theta} \frac{L^2}{2} \qquad (2.29)$$

where θ_L is the volumetric water content at the core top and q is the outflow rate. Passioura's method was used by Jaynes and Tyler (1980) to calculate conductivities. Hydraulic conductivity results were favorable, except at saturation.

Several groups have tried to improve parameter estimates by using numerical inversion techniques on transient outflow experiments. Most have started with an initially saturated soil column and applied a one-step pressure while measuring water outflow. However, Hopmans et al. (1994) suggested that a unique solution is not likely to be obtained unless the one-step analysis begins with an initially unsaturated soil sample. They state that unless the sample is unsaturated, Richard's equation is violated and the analysis is flawed. Zachmann and coworkers (1981 and 1982) attempted to simultaneously estimate hydraulic conductivity and water capacity of a soil using a power function for $K(\theta)$ and exponential function for $h(\theta)$. Others (Kool et al., 1985;

Kool and Parker, 1988; van Dam et al., 1992) have also used so-called "inverse" methods to estimate van Genuchten moisture retention parameters. Numerical analysis by Toorman et al. (1992) suggest that unique parameter estimates are likely to be obtained using transient outflow experiments, but more information (boundary values) is needed to obtain a unique solution. Multistep experiments with simultaneous measurements of outflow and soil water potential (at a point within the soil sample) improve estimation of K(h) and reduce uniqueness problems. Prieksat et al. (1997) developed a one-step outflow cell to measure the required boundary conditions, and found a unique solution to the flow problem.

(c) Limited Data and Indirect Measurement of Hydraulic Parameters

Attempts have been made to relate saturated hydraulic conductivity to soil morphology by summing the capillary flow calculated from pores and cracks (Anderson and Bouma, 1973; Bouma and Anderson, 1973; Bouma and Denning, 1974; Bouma et al., 1979; Smettem and Collis-George, 1985b). The results have been variable and sensitive to errors in measuring pore sizes. Bouma and Anderson (1973) and Leeds-Harrison and Shipway (1984) found that hydraulic conductivity values calculated from pore size measurements were much higher than those obtained from actual measured conductivities.

Pore-size distribution models have also been used to predict the hydraulic conductivity from retention data (Millington and Quirk, 1961; Mualem, 1976). Other rapid field estimates of K(h) and $\theta(h)$, involving limited data, have

gained popularity in assessing soil hydraulic properties and spatial variability (Gupta and Larson, 1979; Ahuja et al., 1985; and Ahuja et al., 1988). Several other methods have been developed which approximate the hydraulic functions from soil textural data, bulk density, or other soil data (Rawls et al.,1982; Haverkamp and Parlange, 1986; Wosten and van Genuchten, 1988). Nimmo (1997) used a new model based on soil porosity and particle-size distribution to predict soil water retention curves. The model, though slated as a new method, was simply a rehash of previous attempts to predict hydraulic properties from limited physical data. Williams et al. (1992) compared indirect methods for estimating hydraulic functions. They concluded that methods that incorporated at least one measured value of $h(\theta)$ were much better than those using only textural data.

In addition to methods that use simplified analytical techniques, there are a growing number of publications that have compiled measured data for a number of soil textural classes (Rawls et al., 1982; Carsel and Parrish, 1988). The UNSODA database (Leij et al., 1996) has listings of soil hydraulic parameters and data for a multitude of soils from different regions. There are also many soils catalogs for specific regions such as those published by USDA/ARS research stations and universities (ARS-USDA Pub #41-144, 1968; Southern Cooperative Series Bulletin 303, 1985).

(d) <u>In-Situ Versus Laboratory Studies</u>

Historically, there has been poor correspondence between in-situ and

laboratory measurements of θ(h) and K(h) (Anderson and Bouma, 1973; Ahuja et al., 1980; Field et al., 1984). In the study by Anderson and Bouma (1973), in-situ measurement of K_s (double ring method) had a mean value of about 60 cm/d compared with 600 cm/d and 200 cm/d for 5 and 17 cm length cores, respectively, taken from the same site. Banton (1993) compared field and lab measured hydraulic conductivities. He found that statistical characteristics of K_s varied widely due to measurement method. Lab measured K_s values were ten times higher than field measured K_s values and five times more variable.

Field et al. (1984) reported poor agreement between field and laboratory θ(h) measurements and suggested that the cores taken to the lab (5.4 cm length) were too small or too disturbed to represent the macroporosity in the field. The authors also noted that the commonly used technique of predicting K(h) from laboratory θ(h) (Mualem, 1976; van Genuchten, 1980) produced significantly different values than the in-situ procedures. Hills et al. (1989) used several sets of parameters from field and lab measurements to model infiltration into a very dry soil. Both the Mualem and Campbell models were used to predict the K(θ) functions. They found that Campbell's model resulted in better agreement between observed and predicted infiltration. Also, redistribution parameter estimation methods results in better prediction of infiltration than lab-based methods. Their infiltration model was very sensitive to the method used to estimate the hydraulic parameters. van Wesenbeeck and Kachanoski (1995) compared in-situ hydraulic properties measured with the

Guelph permeameter to lab measured hydraulic properties. Lab K_s values were larger and more variable, but the α parameter values predicted from each method were similar.

Large scale field and laboratory efforts were conducted by Marion et al. (1994) which compared in-situ and laboratory measured soil-water retention and unsaturated hydraulic conductivity functions. A total of 36 field plots were instrumented with neutron access tubes and tensiometers to perform instantaneous profile tests (IPM). Water retention and conductivity results from the IPM were compared with results obtained from laboratory analysis of soil cores taken form the same field plots. Data from the IPM were used as the standard against which all other data was compared. Several laboratory methods produced results that correlated well with the field data from the IPM. Retention data, obtained using inverse methods or one-step methods, from shallow soil cores (less than 30 cm deep) showed favorable results. However, at deeper depths the correlation was less favorable possibly due to compaction of the cores during sampling. Poor correlation was seen in the conductivity data using the inverse method. Traditional multi-step experiments and subsequent data analysis using the RETC (van Genuchten et al., 1991) code showed good correlation in both retention and conductivity to field data, but failed to save time and expense when compared to field experiments. The authors suggest a scenario for parameter characterization: obtaining small cores from the field and using inverse or one-step tests to obtain the retention data, and using the IPM at

shallow depths and Libardi's method (Libardi et al., 1980) at deeper depths to obtain the conductivity function. The results suggest that there is no easy or inexpensive alternative to field experimentation.

Mallants et al. (1997) compared three hydraulic property measurement methods on soil cores of different sizes. The three methods used for the comparison were 1) the unsteady-drainage flux (IPM) using 30 cm-diameter by 1 m-long soil columns, 2) the combined crust test and hot-air methods applied to columns of 30 cm-diameter by 0.2 m-long, and 3) the standard moisture retention analysis using pressure plates and small 5 cm-diameter by 5.08 cm-long soil cores. The study found "considerable" differences between mean soil hydraulic properties as obtained using different measurement methods.

Only recently have there been any publications that investigated the impact of the hydraulic property estimation technique on the prediction of water flow. Wu et al. (1996) compared measured and estimated soil parameters and the effects of those parameter estimates on simulation of a field-water regime. The authors used the IPM as a comparison to laboratory methods. Parameter estimates were obtained by fitting field and lab data with the RETC code. Parameters were then input into the Root Zone Water Quality Model (RZWQM) and water content profiles that each parameter set generated were compared. The authors concluded that the method used to generate a set of hydraulic parameters did have a significant impact on the simulation of water content profiles.

In a related paper, Mallants et al. (1998) investigated the sensitivity of a one-dimensional drainage model to the description of the hydraulic properties. Hydraulic properties were determined using two different sizes of soil cores (5 cm diameter x 5.1 cm long, and 30 cm diameter x 100 cm long). Moisture retention data were obtained using traditional moisture retention analysis for the 5 cm diameter cores and using a gravity drainage experiment similar to an IPM test for the 30 cm diameter cores. The drainage data were analyzed using four different schemes; 1) normal van Genuchten retention model (RETC) to predict parameters for small 5cm diameter cores, 2) multimodal van Genuchten (SHYPFIT) model to predict parameters for small 5cm diameter cores, 3) normal van Genuchten model to predict parameters for the 30 cm diameter cores, and 4) scaled retention and conductivity data of method 3. The parameter data were input into a 1-D model called WAVE and the predicted drainage was compared to measured drainage data obtained from the gravity-drainage experiments. The smaller cores analyzed using RETC resulted in mean cumulative outflows that accounted for only 70% of the total measured outflow. Analysis of the 5 cm diameter core data using the multimodal model did not improve the drainage estimates. Hydraulic functions derived for the larger 30 cm diameter cores resulted in simulated outflow that only accounted for 79% of the total measured drainage. Despite using different analyses techniques, measurement methods, and core sizes to estimate the hydraulic properties, simulation using a single porosity model (WAVE) could not account for the drainage characteristics of the

soil. The authors suggest that increased predictive accuracy may be possible using a dual porosity model.

(e) Sample Size and Support

Statistical inferences can usually only be made when adequate sample size and support are maintained. However, it is generally not practical or economically feasible to conduct large scale projects to determine hydraulic properties. Several studies have investigated the effect of sample size and support on determination of hydraulic properties.

Bouma (1981) pointed out that only large undisturbed samples will be representative when measuring saturated hydraulic conductivity. Smettem and Collis-George (1985a) recommended a sample size of at least a 1000 cm^2 area to assure a normal distribution of pore sizes for measurement of hydraulic properties. Bouma (1981) recommended that sample size should be based on the size of the "elementary unit of structure", which for an unstructured soil would be the primary particle size. In a structured soil, this elementary unit of structure would be a soil aggregate. Bouma (1981) also noted that vertical large-pore continuity decreased with depth, indicating that the sample length taken in a structured soil is important. Bouma (1981) found that the value determined for saturated hydraulic conductivity decreased as the sample depth increased.

Parker and Albrecht (1987) reported measurements of the draining $\theta(h)$ and saturated hydraulic conductivity (K_s) using small, medium, and large

undisturbed soil cores. A statistically significant difference in the $h(\theta)$ profiles was not observed until the soil was quite dry (-6 bars), and they concluded that sample volume had little effect on water retention. However, mean K_s values decreased as sample volume decreased. The coefficient of variation of K_s decreased with increasing sample support, indicating that fewer large samples were needed to obtain a prescribed level of confidence. In addition, only small differences were observed between breakthrough curves for the varied core sizes.

Similarly, Anderson and Bouma (1973) measured K_s on 7.5 cm diameter undisturbed soil cores of different lengths (5 to 17 cm) and observed the same variance reduction with increasing support but a decrease in K_s with increasing length. The authors suggested that the decrease in K_s resulted from decreased continuity of macropores in the longer samples. The decrease in variance of K_s and infiltration rate with increasing sample support has also been reported by Sisson and Wierenga (1981), Bouma (1983), Young (1983), and Wagenet (1984).

Starr et al. (1995) evaluated the effect of sample size on soil physical, chemical, and biological properties. Comparisons were made on six different sizes of soil samples ranging from 1.7 cm-diameter soil cores to 20 x 30 cm soil blocks. Thirty six samples of each size were tested for bulk density, water content, phosphate content, pH, NO_3-N and denitrification rates. Results indicate that all soil parameters except bulk density exhibited spatial

dependence and the effect of sample size varied with physical property. Smaller size samples gave smaller means and higher variances. Thus, physical property data obtained using core samples may not readily represent field scale soil properties.

(f) Effects of Soil Management

Tillage has an obvious effect on soil structure and solute transport. Kanwar et al. (1985) noted the difference in nitrate losses between no-till and moldboard plowing. They found after 19 cm of simulated rainfall, no-till plots retained nearly one-third more nitrate in the top 150 cm than those plots which had been moldboard plowed. The increase in nitrate loss under moldboard plowing was suggested to be the result of more uniform soil conditions which allowed greater leaching by the applied rainfall.

Anderson and Bouma (1977a and b) compared two different soil structures on five different soil profiles each with a silty clay loam texture. Their data show that for a non-crusted condition, soil columns with subangular blocky structure had greater solute movement than did profiles having prismatic column structure. Under artificial soil crust conditions formed by an equal mixture of gypsum and sand however, the breakthrough curves were similar for the two soil structures. Anderson and Bouma noted that using a crust to reduce dispersion on soils with small peds was more effective than controlling water application rates to the surface.

Compaction also affects soil structure and solute transport. Moore et

al. (1986) found that when the surface of a forest soil was disturbed by logging operations, macropores were destroyed and hydraulic conductivity decreased. The identical effect was noted for an agricultural soil after compaction by wheel traffic during tillage (Ankeny et al. 1988a). Prieksat et al., (1994) indicated that infiltration within a corn field was affected, by position, by method of tillage, and by stage of plant growth. Tillage and traffic patterns also have dramatic effects on corn root and shoot growth (Kaspar et al., 1995), which in turn affects water infiltration and solute movement

CHAPTER 3

EXPERIMENTAL METHODS

3.0 Introduction

This study was part of a long term research initiative conducted near Waverly, Colorado that began in the Spring of 1992. During the initial phase of the study a solute transport experiment was conducted to investigate bromide movement in non-tilled (NT) and tilled (T) soil treatments under sprinkler irrigation. The second stage of the experiment, which began in the summer of 1993 and ended in the fall of 1994, was designed to measure, using a variety of techniques, the hydraulic properties of the field soil.

3.1 Field Site

An experimental field was established about 1 mile northeast of Waverly Colorado during the spring of 1992. The field site was a level rectangular plot with native grass vegetation and some interspersed alfalfa that had not been tilled for at least eight years. The soil was classified as a fine loamy mesic Ustollic Haplargid, predominantly a calcareous fine sandy clay loam with notable pockets of gravel. Some soil structure was noted in the upper 2 meters of the profile, but the soil was massive and structureless below 2 meters (Table 3.1).

3.2 Experimental Design: Overview

Table 3.1. Soil profile description for the Waverly Colorado experimental field site.

Depth (cm)	Horizon	Texture	Structure	Description
0-30	Ap	Sandy Clay Loam	Subangular Blocky	
30-55	Bt1	Sandy Clay Loam	Subangular Blocky	
55-87	Bt2	Sandy Clay Loam	Prismatic/Subangular Blocky	Less Sand than Ap and Bt1
87-123	Bk1	Sandy Clay Loam	Subangular Blocky	Notable pockets of gravel
123-163	BK2	Sandy Clay Loam	Subangular Blocky	
163-200	BK3	Clay Loam	Subangular Blocky	
200-254	2C1	Sandy Loam	Structureless	Fragments of Sandstone
254-293	2C2	Sandy Loam	Structureless	Fragments of Sandstone

Figure 3.1 shows the tilled half of the experimental field. Tillage to a depth of about 20 cm was accomplished using a rototiller with multiple passes at varying angles. To match the fallow condition, the NT plot was sprayed with Round-up herbicide to kill the native vegetation. Once established, the T and NT plots were subsequently accessed using the portable "catwalks" evident in Fig. 3.1. Each plot was then delineated into two regions; an inner 3m x 3m area devoted to the solute recovery experiment, and four 1.2m x 1.2m regions for hydraulic property measurements located on the outside corners of the solute recovery area. In each hydraulic property area, an instantaneous profile (IPM) setup (details to follow) was installed resulting in four repetitions of the IPM in both the T and NT treatments. IPM repetitions in the T treatment can be seen in the corners of the experimental plot shown in Figure 3.1. String lines, which can be seen in Figures 3.1 and 3.2, were stretched across the plots to form grid lines 1m apart. The solute recovery area between the IPM repetitions in the T plot is evident in the figures. A co-worker can be seen collecting soil samples from the solute recovery area in Figure 3.2. Identical irrigation systems were installed in the T and NT plots as shown in Figures 3.1 and 3.2. Each system had eight sprinkler heads providing good uniformity of water application (coeff. of uniformity >98%) to the study area. The sprinkler system delivered 7 cm/hr (plot average) and was operated intermittently, if necessary, to prevent ponding.

3.3 Solute Transport Experiment

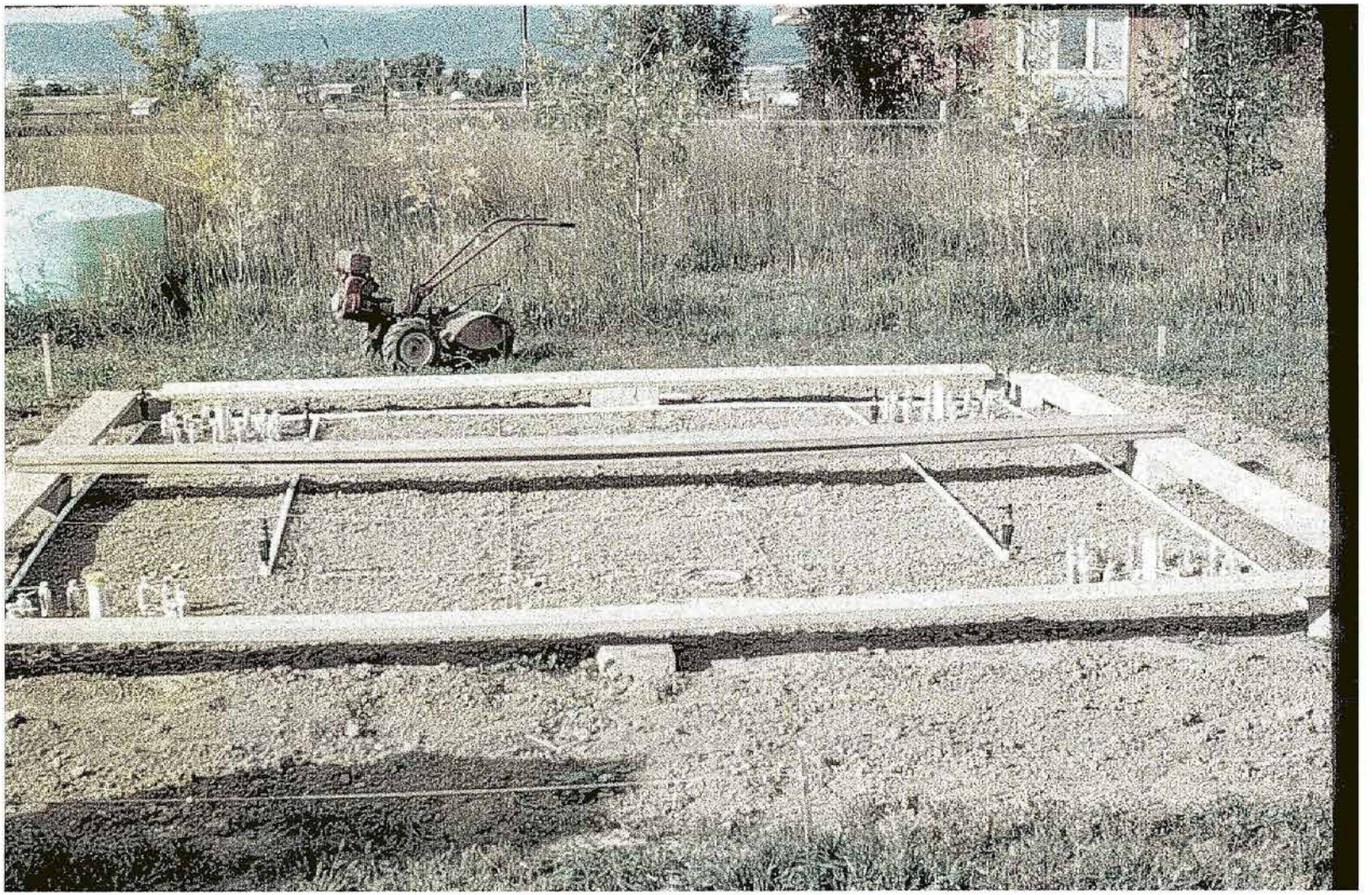

Figure 3.1. Experimental field design..

Figure 3.2. Soil samples being collected during the solute transport experiment.

After retrieval of soil cores to characterize the initial water content profile, the sprinkler system on each plot was used to deliver a narrow pulse of potassium bromide (KBr) solution. Potassium bromide was applied at a rate of 94 mmol Br/m^2 to the T plot and 105 mmol Br/m^2 to the NT plot in a 0.5 cm pulse. The bromide solution was then replaced with well water and an additional 0.5 cm pulse of "clean" well water was applied. The plots were irrigated with well water about every two weeks, but the irrigation schedule depended upon the timing of precipitation events. Meteorological data were obtained on site with a standard weather box recording rainfall, temperature, relative humidity, wind speed, and solar radiation. Additionally, in each plot a small (20 cm diameter by 20 cm long column) hanging-water-table lysimeter was monitored daily for change in weight and drainage (Fig. 3.2).

Soil bromide was sampled by collecting 2.54 cm-diameter soil samples to a depth of about 2 m from the solute recovery areas periodically during the experiment. Soil samples were collected at 8, 22, 36 and 117 days after bromide application for the T plots, and 9, 23, 37, and 118 days for the NT plots. Eighteen soil samples were collected from each recovery area on each collection date. The samples were taken back to the lab and sectioned into 5 cm increments. Samples from each 5 cm increment were combined to form a composite sample. The sample composites were sub-sampled for determination of gravimetric water content. A known mass of soil was then extracted with a known volume of distilled water as a saturation paste. Bromide

concentration of the extracts was determined using a Lachet auto-analyzer.

3.4 Measurement of Soil Hydraulic Properties

A combination of field and laboratory methods were employed to determine the saturated and unsaturated hydraulic parameters (k_s, θ_r, θ_s, α and n, (Eq. 2.15 - Eq. 2.19)) of the soil. The methods include the drainage flux or instantaneous profile method, tension infiltrometry, laboratory pressure plate and constant head flow measurements on soil cores, and indirect estimation based on soil texture. The details of these methods and the scale/sample support employed for each are discussed below.

Instantaneous Profile Method

An instantaneous profile or drainage flux experimental plot is essentially a large double-ring infiltrometer with instrumentation for h and θ monitoring in the inner ring. In this study, air-pocket tensiometers were used for soil water potential measurements and neutron attenuation was used for water content measurement. Figure 3.3 shows one IPM repetition with the tensiometers, borders, and access tubes in place. The photo in Figure 3.3 was taken after the IPM tests had been completed and prior to the plots being excavated for further investigation. The IPM plots were void of weeds during the drainage tests. Each IPM repetition had an outer 10 cm high plastic berm (installed after the solute recovery experiment) that measured 2.6 x 2.6 m square and an inner 10 cm high metal berm that measured 1.2 x 1.2 m square. The PVC tube in the center of the IPM rep of Figure 3.3 is a frequency domain response (FDR)

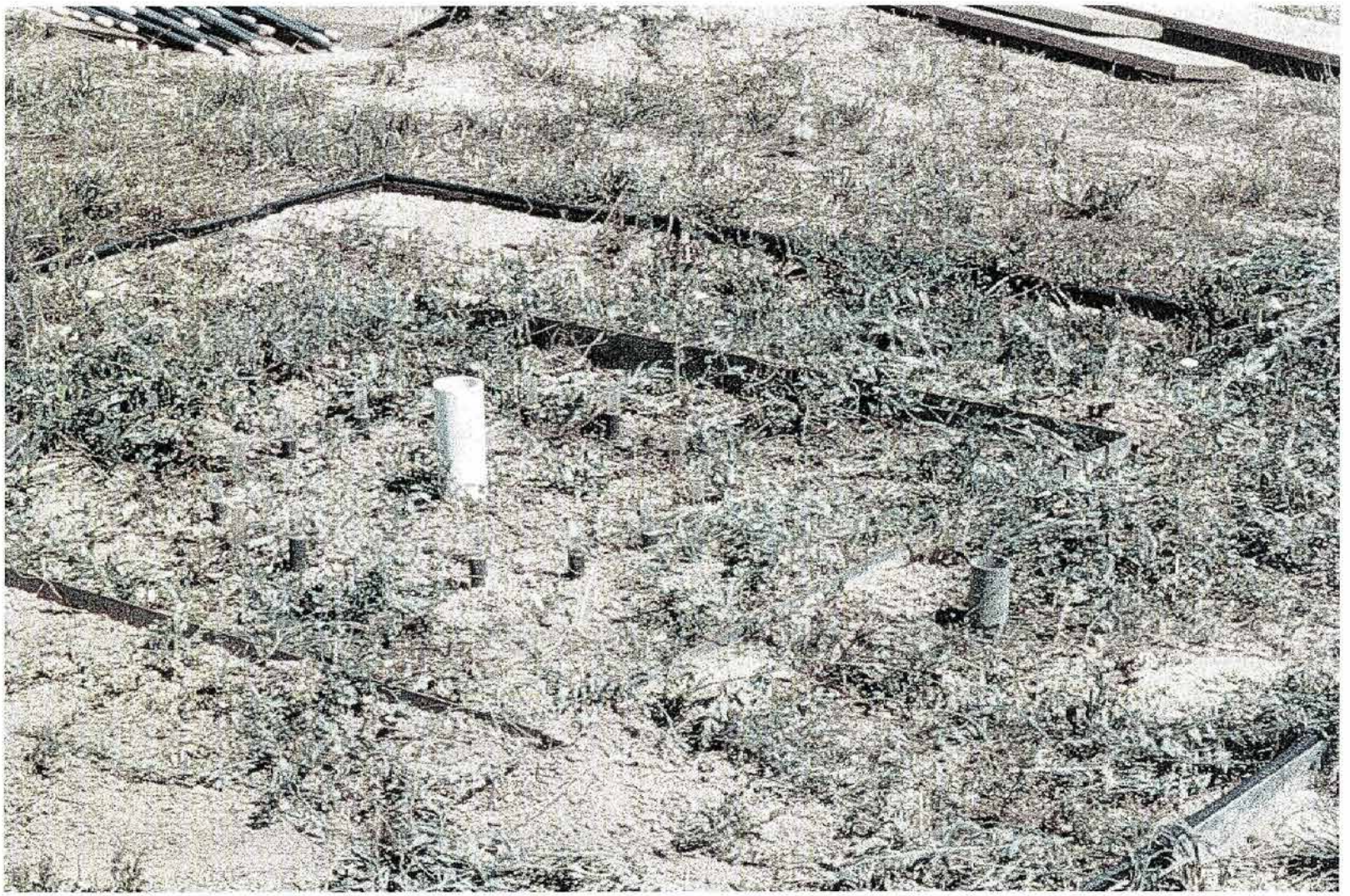

Figure 3.3. IPM plot with the borders and neutron access tube installed.

access tube and the metal tube just outside the inner berm is a neutron probe (NP) access tube. It was discovered, after calibration efforts failed, that the FDR probe was not a viable tool for use at this particular site. It is possible that air gaps between the access tube and the soil cause the device to indicate erroneous water content values.

Tensiometers (Soil Moisture Equipment Corp.) were assembled and installed in duplicate at 10, 20, 30, 60, 90, 120, 150 and 180 cm depths in a circular pattern around the center-point of the inner 1.2 x 1.2 m area. Tensiometers consisted of a porous ceramic cup epoxied onto one end of a PVC tube and a septa port epoxied onto the other end. Water potential was recorded by means of a needle gage pressure transducer connected to a tensimeter (Soil Moisture Equipment Corp.) that read a value of pressure in millibar. The needle was inserted through the rubber septa at the top of the tensiometer. Water level in the tensiometer was also recorded relative to the length of the tensiometer. Hydraulic head was calculated from the pressure and elevation heads.

A tensiometer installation tool was used to bore vertical holes, just large enough to insert the tensiometers, to the desired depth. Diatomacious earth was mixed with water into a thick slurry and then a small amount of the slurry was tremmied into the bottom of the bore hole. Immediately after pouring the slurry into the hole, the tensiometer was inserted and allowed to set. The soil around the top of the tensiometer was packed and sealed to prevent water from

flowing down the wall of the tensiometers.

Neutron probe access tubes were installed just outside of the inner berm in each plot. The 5.08 cm-diameter, thin walled steel access tubes were installed to a depth of 2 m. The neutron probe was calibrated to in-situ field soils by recording multiple neutron probe readings at each depth and then collecting soil cores to a depth of about 2 m during different stages of the experiment. Vertical soil cores, 2.54 cm in diameter, were removed from the area between the inner and outer berms area within 10 to 15 cm of the access tube. The cores were taken to the lab, sectioned (accounting for compaction), and oven dried to determine gravimetric moisture content. Soil cores were obtained at different degrees of soil saturation (wet, moist, dry) in order to construct calibration curves for each field repetition.

The instantaneous profile method (Green et al., 1986) uses Darcian analysis of soil water potential gradients and corresponding soil water fluxes in a draining soil profile to estimate unsaturated hydraulic conductivity. For this study, soil water content was monitored between 10 cm and 180 cm soil depth using a neutron attenuation probe. Hydraulic head profiles were determined using duplicate tensiometers installed at 10, 20, 30, 60, 90, 120, 150, and 180 cm depths. The experiment involves two phases; an initial steady-state, saturated flow phase that allows estimation of K_s at the soil surface and in the subsoil and, second, a drainage phase with zero flux upper boundary condition (e.g. plastic cover) lasting several weeks.

To initiate the first phase, water was ponded in both the inner and outer bermed areas, much like a double-ring infiltometer test. Water content and hydraulic head were measured periodically during the saturated infiltration experiment. Tensiometer readings near zero or positive are indicative of saturation. When the profile was deemed to be saturated, depth of surface ponded water was recorded, tensiometer and neutron probe data were recorded, and a downward water flux was calculated for each plot. Water flux was calculated by measuring the volume of water applied to the inner bermed area of the plot over time and dividing by the area of infiltration inside the inner berm.

After the saturated infiltration experiment had been completed, the plots were covered with 60 mil plastic sheeting and insulation to prevent evaporation. The plots were allowed to drain freely. Water pressure head and moisture content were recorded often during the first several days of drainage, but data recording tapered off during the later stages of the experiment as the rate of drainage slowed. Moisture content and pressure head data were collected from each plot over a period of about 35 to 45 days. Figures 3.4 and 3.5 show moisture content and hydraulic head profiles measured on one of the IPM repetitions during the drainage cycle.

Unsaturated hydraulic conductivity profiles were determined using the protocol of Green et al.(1986). Hydraulic heads were determined from the tensiometer data recorded at the different depths and times from each field

repetition. Pressure heads (h) were determined by converting the tensiometer readings from mbars to cm and adding the length (cm) of the water column in the tensiometer. Hydraulic heads (H) were determined by adding the gravitational head to the pressure head. Figures 3.5 and 3.6 show drainage data used to determine the hydraulic properties.

Hydraulic head vs. time for each depth were plotted and a smooth curve was fit through the data. Gradients ($\partial H/\partial z$) were determined at each depth position in the plots.

$$\frac{\partial \int \theta\,(z,t)\,dz}{\partial t} \qquad (3.1)$$

Moisture content vs. time was plotted for each depth and a smooth curve was fit through the data. The integral

$$\int_0^{z_1} \theta(z,t)\,dz \qquad (3.2)$$

was estimated using a curve fitting program (Table Curve) and these integrals were plotted against time. Derivatives of the integral versus time plots were evaluated at different times to determine the fluxes at fixed depths and times.

Unsaturated hydraulic conductivity was determined by dividing the fluxes by the gradients at the same times and depths. Field saturated hydraulic conductivities were determined by dividing the steady-state infiltration rates by

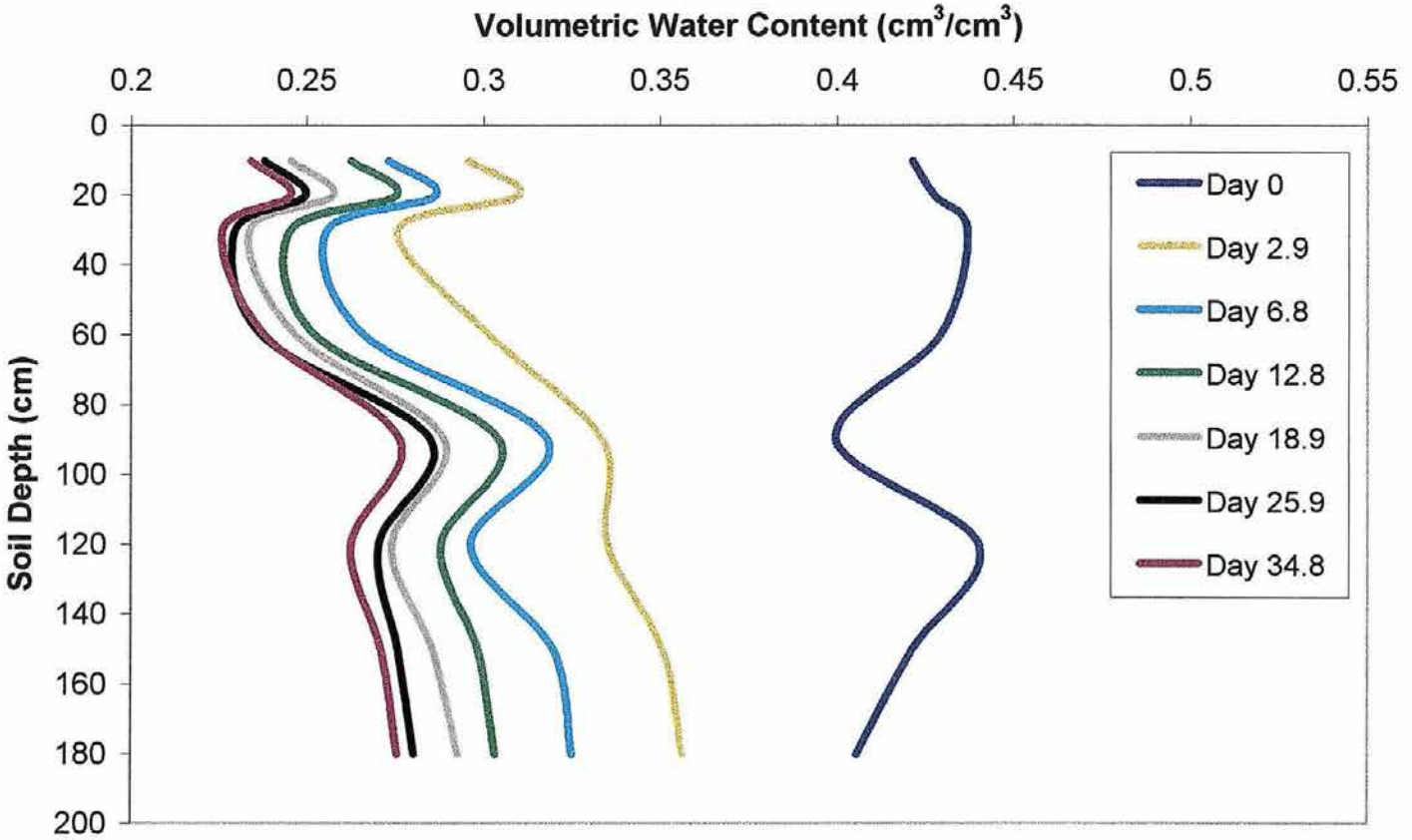

Figure 3.4. Water content profiles from one IPM repetition measured during the drainage experiment.

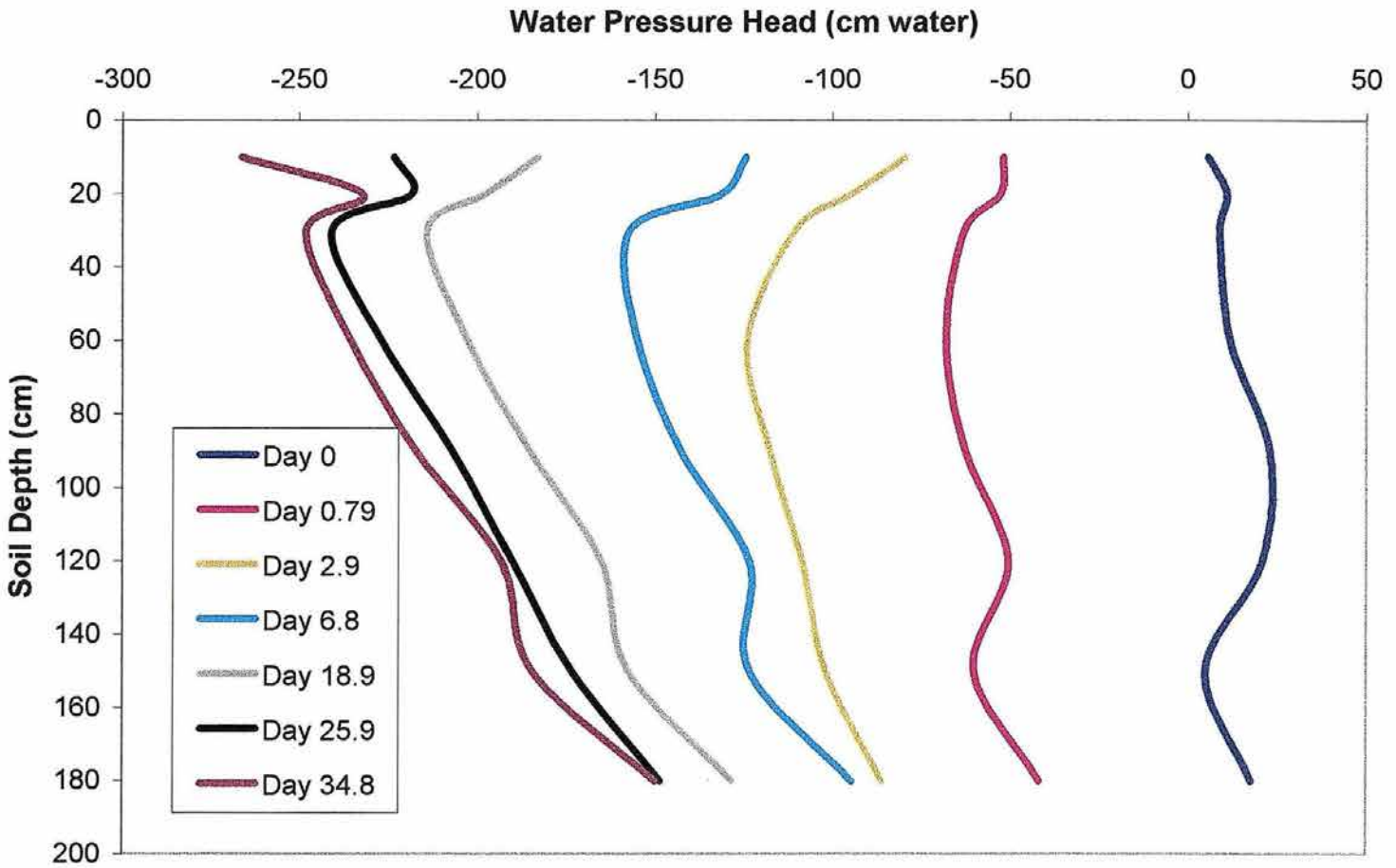

Figure 3.5. Pressure head profiles from one IPM repetition measured during the drainage experiment.

the hydraulic gradients determined from tensiometric data recorded at the time when the soil was still saturated water.

The unsaturated flow parameters (Eq. 2.15 - 2.19) were determined from the K(h) and h(θ) data using the RETC code (van Genucthen et al., 1991) for determining the unsaturated hydraulic parameters of soils. The code was used to determine the α and n parameter values. The θ_r value was selected as the 15 bar point on the predicted h(θ) curve, and θ_s was determined from the measured data.

Permeameters or Infiltrometers

After completion of the IPM drainage studies, the inner 1.2 m x 1.2 m region of each IPM repetition was used for all subsequent measurements. Saturated and unsaturated hydraulic conductivity were measured using disk permeameters at depths of 0, 10, 20, 30, 60, 90, 120, 150 and 180 cm in each plot. The subsurface depths were reached by careful excavation. Infiltration measurements were made in duplicate and at two scales using 20.8 cm-diameter disc permeameters (Perroux and White, 1988) and 7.6 cm-diameter infiltrometers (Ankeny et al. 1988b; Prieksat et al., 1992). Figure 3.6 shows infiltration measurements being made at the soil surface using two different size permeameters. Saturated infiltration measurements were made at a slight positive head of 0.5 cm, while unsaturated infiltration was measured at supply pressure heads of -3 cm, -6 cm, and -12 cm. Figure 3.7 shows infiltration measurements at one of the sites that had been excavated by hand to a depth of

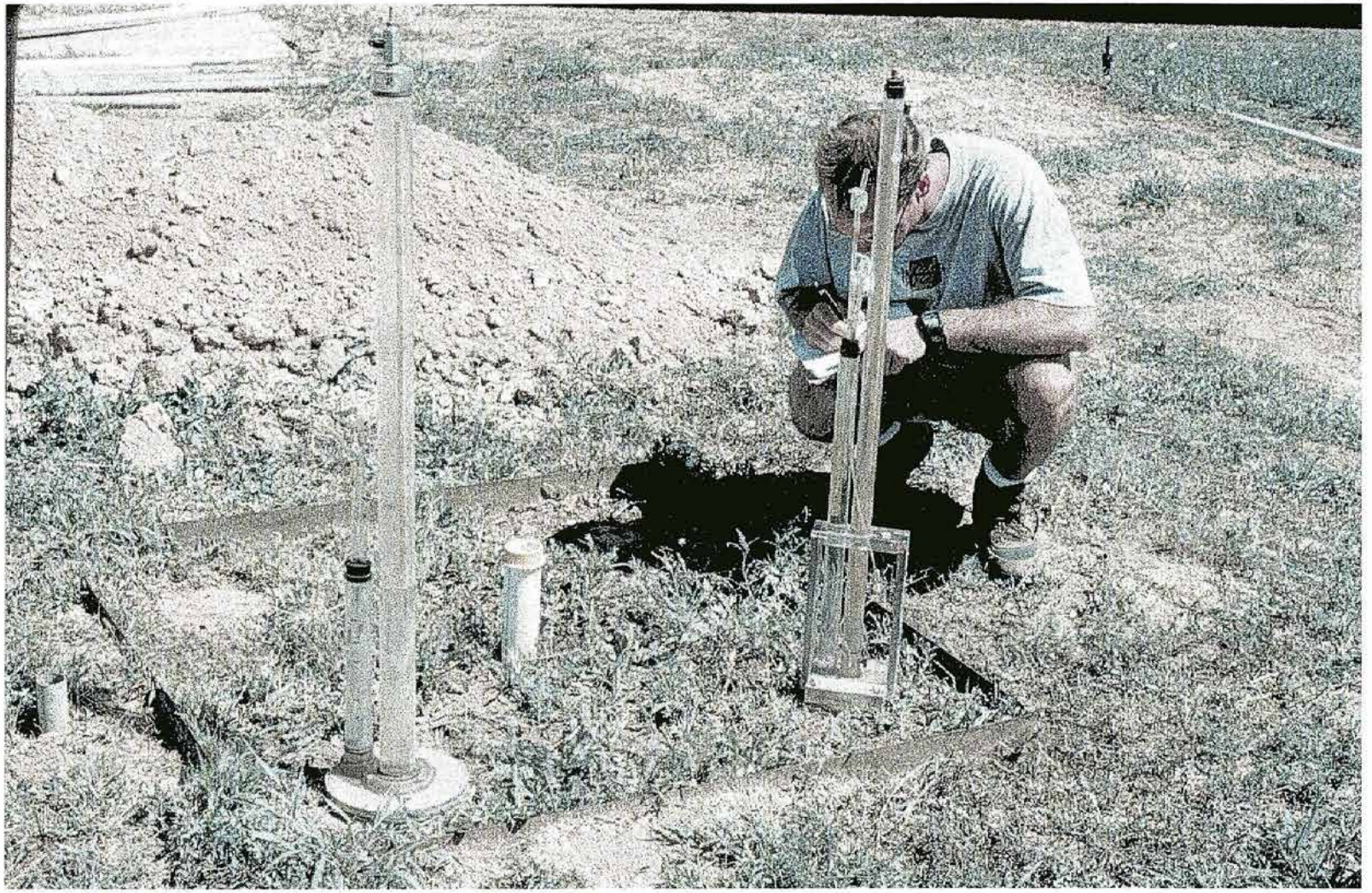

Figure 3.6. Infiltration measurements being made with the 8TI and 4TI methods.

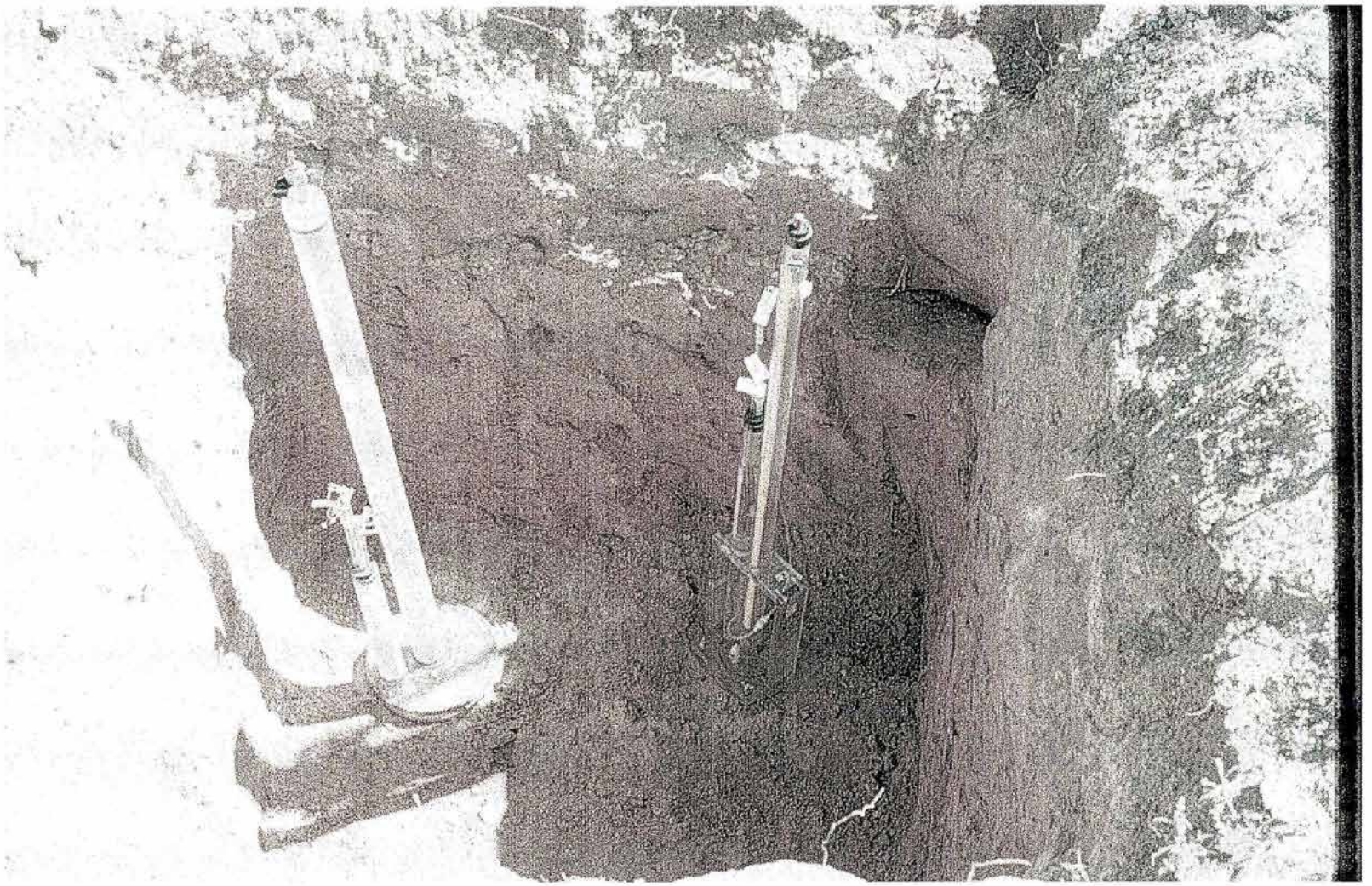

Figure 3.7. Infiltration measurements being made at about 1 meter soil depth.

about one meter. Figures 3.6 and 3.7 are demonstration photographs; during the actual measurements, the permeameters were shaded to minimize temperature effects of solar heating. Saturated and unsaturated hydraulic conductivity profiles were determined using the protocol of Ankeny et al., (1991). Saturated and unsaturated infiltration data from each measurement site was used to determine the saturated and unsaturated hydraulic conductivities. Four hydraulic conductivity values at pressure heads of +0.5 cm, -3 cm, -6 cm, and -12 cm were determined for each size infiltrometer, treatment repetition, and depth.

The unsaturated flow parameters were determined from analysis of the K(h) data combined with 15 bar equilibrium pressure step data from the 5.08 cm-diameter cores. Because no moisture content data was measured, θ_s values determined for the 5.08 cm-diameter soil cores were used to complete the parameter data sets for the infiltrometers.

Soil Core Samples

Four 5.08 cm-diameter by 5.08 cm-long soil cores and two 10.16 cm-diameter by 5.08 cm-long soil cores were collected at each depth where infiltration was measured. After the pits had been excavated to the 180 cm depth and all other measurements were finished, a Giddings soil probe (Giddings Machine Company) was used to obtain 5.08 cm-diameter soil cores to a depth of about 3 m. These cores were sectioned and subsamples were obtained at 2, 2.5, and 3 m depths.

The soil cores were taken to the lab for determination of K_s and $h(\theta)$. Saturated hydraulic conductivity was determined using the falling head method (Klute and Dirksen, 1986). Moisture retention characteristics were determined using pressure plate analysis (Klute, 1986). The soil cores were saturated by placing them in a pan and slowly raising the water level until it was even with the top of the sample. After saturating the samples, they were weighed to determine saturated water contents. These values were later compared with porosity values calculated from bulk density measurements as a quality control check on the data. Samples were then placed on pressure plates inside pressure extraction cells and subjected to a series of equilibrium pressure steps ranging from 0 to 15 bar pressure potential. During each pressure step, the soil samples were removed periodically from the extraction cells and weighed. When the samples had reached a consistent weight at a pressure step, the sample weights were recorded, the samples were placed back in the extraction cells, and the pressure was increased to the next level. A total of 12 to 14 equilibrium pressure steps were used during moisture retention analysis.

The $h(\theta)$ relationship was measured directly using the protocol of Klute (1986). Volumetric water content values were determined from the moist and oven-dry weights, and the volume of the sample. Pressure head was recorded as the directly applied air-pressure in bar. The $h(\theta)$ data and the saturated hydraulic conductivity values were used to predict the $K(\theta)$ relationships for each soil sample using the RETC code (van Genucthen et al., 1991).

Indirect Measurement

By far the most convenient method of obtaining soil hydraulic parameters is to get them from published literature. Several sources are available that provide van Genuchten parameters (Eq. 2.15 - Eq. 2.19) and saturated hydraulic conductivity for a range of soil textural classes. Three sources were selected and used as input into the HYDRUS-2D model. Data from the UNSODA soils catalog (Liej, 1996) are available as default values within the HYDRUS-2D model. The model allows you to select hydraulic parameters based on a specific soil type, such as clay loam. The two other sources that were used to select input hydraulic parameters are those of Carsel and Parrish (1988) and Rawls et al., (1982).

3.5 Data Analysis

Moisture content data, pressure head data, and hydraulic conductivity data ($h(\theta)$ and $K(\theta)$) from each individual method, with the exception of the indirect method, were analyzed using the RETC code (van Genuchten et al., 1991) for determining the unsaturated hydraulic parameters of soils. In all analysis using the RETC code, the code was used to predict the α and n parameters. Saturated water contents and the saturated hydraulic conductivities determined from each method were not fit by using the code. Residual water contents were determined as the water content at the -15 bar pressure point from the predicted curves.

It is probably worth noting at this time, the physical significance of the individual parameters. The measured and predicted parameters are α, n, θ_r, θ_s, and K. The α parameter is inversely equivalent to the air-entry value of the soil. The air-entry value is the pressure head where the wetting fluid, usually water, is first displaced by the non-wetting fluid, usually air. The n parameter is the slope of the moisture content vs. pressure head relationship. This value is indicative of the pore size distribution of the soil. The larger the n, the narrower the pore size distribution (i.e. most of the pores are of the same diameter/size). A practical range for n is between 1.0 and 2.5. The θ_r and θ_s parameters are the residual or irreducible water content and the saturated water content, respectively. The residual water content is described as the point where large changes in applied pressure result in small changes in water content. This does not mean that water will no longer flow, but the contribution to flow is very small. Some researchers set θ_r at h=-15 bar, while others use even lower potentials or simply treat θ_r as an adjustable curve fitting parameter. The saturated water content is described as the point at which all pore space in the sample is filled with water. Since this is rarely achieved, generally we will see differences between porosity calculated from bulk density data and the saturated water content. The K parameter is hydraulic conductivity or the ability of the soil to transmit water.

After the individual parameters had been determined using the RETC

code they were compiled and analyzed for statistical inference using SAS for Windows (SAS Institute, Inc.). The parameters were compared, at each depth for differences between methods, for differences between depths and tillage treatments within each method, and between methods using the entire profile data. Simulated water content and solute concentration profiles generated using the HYDRUS-2D model were compared to the measured profiles by calculating the correlation between the output and the measured data.

3.6 Summary of Methods - Abbreviations

Even though the preceding sections presented details of the sampling methods, the following section gives abbreviations used for each method with a brief description.

2C

Soil core samples, 5.08 cm diameter by 5.08 cm long, collected with a core barrel sampler using brass sleeves. Saturated hydraulic conductivities measured using the falling head method and the moisture retention analysis using traditional pressure plate analysis were analyzed using the RETC code.

4C

Soil core samples, 10.16 cm diameter by 5.08 cm long, collected using PVC cylinders. Soil columns, slightly larger than the PVC cylinders, were excavated and PVC rings were pushed down around the soil column and sectioned at the bottom. These samples were analyzed using the same techniques as were

used for the 2C method.

4TI

Infiltrometers, 10.16 cm in diameter, were used to measure water infiltration into the soil. Water infiltration was measured at four different heads (+0.5 cm, -3 cm, -6 cm, -12 cm). The infiltration data were used to calculate saturated and unsaturated hydraulic conductivities. The hydraulic conductivity data was analyzed using the RETC code. However, analysis only provided the α and n values, so it was necessary to use the θ_s and θ_r data from the 2 inch cores to complete the data sets. For consistency, only data from corresponding repetitions were combined.

8TI

This method is the same as the 4TI, but at a scale that is 20.32 cm in diameter.

IND

This method used published data from three different sources to determine the soil hydraulic properties. After we had characterized the soil texture, we used the texture data to select hydraulic properties from the literature.

IPM

Saturated and unsaturated hydraulic conductivity data $K(\theta)$ and $h(\theta)$ data obtained from a gravity drainage experiment were analyzed simultaneously using the RETC code.

3.7 Prediction of Water and Solute Movement Using the HYDRUS-2D Model

The hydraulic properties estimated by each method were used as input to the HYDRUS-2D numerical code for simulating water flow and solute transport in 2-D variably saturated media. In addition to the hydraulic property data, measured atmospheric and irrigation data were also used in the simulations. For the 2C, 4C, 4TI, and 8TI methods, the soil profile was divided into nine layers; 0-5, 5-15, 15-25, 25-45, 45-75, 75-105, 105-135, 135-165, and 165-180 cm soil depths. The soil profile for the IPM method had eight layers corresponding to 0-10, 10-20, 20-30- 30-60, 60-90, 90-120, 120-150, and 150-180 cm soil depths. Because the textural data (Table 3.1) showed limited textural change, the IND simulations had only two soil layers; 0-160, and 160-180 cm depths. Initial conditions (pressure heads) for each layer were calculated from measured water contents using the van Genuchten equation (1980) and the hydraulic properties of each soil layer and method. Bulk density values, obtained from 5.08 cm-diameter soil cores, were input for each layer and remained constant during all simulations. For solute transport, no attempts were made to calibrate the dispersion parameters using the bromide concentration profiles. Instead, longitudinal and transverse dispersivity values of 5 cm and 0 cm, respectively, were assumed for all depths in both treatments. An ionic diffusion coefficient of 1.5 cm^2/d was assumed for bromide. Numerical simulations were carried out over a length of time corresponding to the length of

the field solute transport experiment; 117 days for the T treatment and 118 days for the NT treatment. The predicted profiles were compared to water content and solute concentration profiles measured during the solute transport experiment.

CHAPTER 4

COMPARISON OF HYDRAULIC PARAMETER ESTIMATION METHODS

4.0 Introduction

Two basic approaches were taken to describe the hydraulic parameter data sets. The initial approach was to statistically analyze the parameters as independent variables, comparing the hydraulic parameters determined by the various methods from the different soil depths. Secondly, the hydraulic functions (Eq. 2.15 - Eq. 2.19) which utilize a combination of the measured parameters were compared and contrasted visually. The following sections describe trends and observations gleaned from the data.

4.1 Bulk Density

Table 4.1 lists soil bulk density (ρ_b) values (mean ± 95% confidence limits, CL) obtained from analysis of the 5.08 cm-diameter by 5.08 cm-long soil cores removed from the field site. The ρ_b of the tillage zone (0-15 cm) is less than that of the non-tilled soil. This is expected since the purpose of tillage is to reduce the density and increase the porosity to promote better plant growth. Below the tillage zone, no significant differences in ρ_b between tillage treatments were observed nor are there differences in ρ_b between depths. There is no

Table 4.1. Soil bulk density as a function of depth below soil surface and tillage treatment.
*** Rows with the same letter are not significantly different from one another.

Depth	Treatment	Bulk Density	+/- 95%	***
(cm)		(g/cm^3)		
0-5	NT	1.508	0.043	ac
	T	1.355	0.041	b
10-15	NT	1.553	0.031	ac
	T	1.433	0.044	bc
20-25	NT	1.523	0.105	ac
	T	1.470	0.073	ac
30-35	NT	1.510	0.126	ac
	T	1.525	0.076	ac
60-65	NT	1.510	0.054	ac
	T	1.528	0.041	a
90-95	NT	1.533	0.116	ac
	T	1.560	0.074	a
120-125	NT	1.535	0.046	a
	T	1.580	0.112	ac
150-155	NT	1.538	0.141	ac
	T	1.593	0.144	ac
180-185	NT	1.555	0.065	a
	T	1.580	0.057	a

justification for separating ρ_b by tillage treatment below the 15 cm depth and any differences between the NT and T plots below the tillage zone would have to be attributed to spatial variability.

4.2 Soil Hydraulic Properties

Tables 4.2 through 4.5 list the measured hydraulic property parameters (α, n, θ_s, K) obtained using the six methods described in chapter two. All of the measured data from each repetition are contained in Appendix A. Each table has two parts (a and b): part "a" shows mean and variance values for each parameter and t-test comparisons made between methods for each depth; part "b" repeats part "a" but shows t-test comparisons between depths and tillage for each method. Letter comparisons indicate whether the parameters are significantly different from one another and the triangles at the top of the column indicate the direction of the comparison. Like letters, even when appearing in combination with other letters, are not significantly different. For example, the letter "ac" indicates that the mean value is not statistically different than a mean with the designation "a" or "ac", but it is different from a mean designated as "b" or "bd".

<u>α (curve fitting parameter indicative of air-entry value)</u>

Tables 4.2(a and b) list the mean and confidence limits for each depth,

Table 4.2(a). Mean, variance, and **t-test comparisons between methods** for each depth and tillage for the α parameter.

Depth	α – Curve Fitting Parameter (cm^{-1}) by Method of Measurement																	
Treatment	2C			4C			4TI			8TI			IND			IPM		
	Mean	+/- 95%	▶	MEAN	+/- 95%	▶	MEAN	+/- 95%	▶	MEAN	+/- 95%	▶	MEAN	+/- 95%	▶	MEAN	+/- 95%	▶
0-NT	0.0130	0.0054	a	0.0110	0.0150	a	0.0480	0.0039	b	0.0575	0.0582	ab	0.0383	0.0360	ab	-	-	-
0-T	0.0409	0.0022	a	0.0400	0.0190	a	0.0800	0.0600	a	0.1513	0.0301	b	0.0383	0.0360	a	-	-	-
10-NT	0.0226	0.0095	a	0.0212	0.0340	ab	0.0384	0.0103	b	0.0451	0.0246	ab	0.0383	0.0360	ab	0.0263	0.0026	a
10-T	0.0180	0.0167	a	0.0218	0.0060	a	0.0500	0.0402	abc	0.0750	0.0137	b	0.0383	0.0360	abc	0.0450	0.0196	c
20-NT	0.0107	0.0028	a	0.0214	0.0620	ab	0.0325	0.0220	ab	0.0243	0.0311	ab	0.0383	0.0360	ab	0.0275	0.0042	b
20-T	0.0171	0.0121	a	0.0168	0.0160	a	0.0314	0.0121	a	0.0501	0.0100	b	0.0383	0.0360	ab	0.0495	0.0303	ab
30-NT	0.0192	0.0126	a	0.0155	0.0340	a	0.1008	0.0373	b	0.0365	0.0180	a	0.0383	0.0360	a	0.0275	0.0077	a
30-T	0.0152	0.0193	ab	0.0128	0.0010	a	0.0195	0.0194	ab	0.0341	0.0128	b	0.0383	0.0360	ab	0.0383	0.0259	ab
60-NT	0.0158	0.0063	a	0.0209	0.1080	ab	0.0270	0.0083	b	0.0315	0.0139	b	0.0383	0.0360	ab	0.0140	0.0034	a
60-T	0.0158	0.0100	a	0.0149	0.0150	a	0.0370	0.0054	b	0.0372	0.0174	bc	0.0383	0.0360	abc	0.0253	0.0062	a
90-NT	0.0142	0.0013	a	0.0117	0.0230	a	0.0265	0.0242	a	0.0303	0.0225	a	0.0383	0.0360	a	0.0140	0.0034	a
90-T	0.0128	0.0113	ac	0.0129	0.0220	abc	0.0366	0.0211	b	0.0366	0.0126	b	0.0383	0.0360	abc	0.0200	0.0061	c
120-NT	0.0069	0.0079	ab	0.0070	0.0002	a	0.0228	0.0240	ab	0.0365	0.0326	ab	0.0383	0.0360	ab	0.0140	0.0046	b
120-T	0.0064	0.0015	a	0.0087	0.0780	abc	0.0643	0.0312	b	0.0559	0.0274	b	0.0383	0.0360	abc	0.0143	0.0060	c
150-NT	0.0084	0.0030	a	0.0070	0.0130	ac	0.0491	0.0247	b	0.0390	0.0479	abc	0.0383	0.0360	abc	0.0165	0.0054	c
150-T	0.0025	0.0024	a	0.0104	0.0940	abcd	0.0392	0.0038	bc	0.0644	0.0290	c	0.0383	0.0360	abcd	0.0125	0.0033	d
180-NT	0.0089	0.0022	ac	0.0080	0.0130	ac	0.0490	0.0330	bc	0.0375	0.0190	b	0.0390	0.0367	abc	0.0155	0.0067	c
180-T	0.0070	0.0041	a	0.0082	0.0720	b	0.0393	0.0181	b	0.0642	0.0368	b	0.0390	0.0367	abc	0.0150	0.0034	c

Table 4.2(b). Mean, variance, and **t-test comparisons between depths and tillage treatments** within methods for the a parameter.

Depth	α – Curve Fitting Parameter (cm^{-1}) by Method of Measurement																	
Treatment	2C			4C			4TI			8TI			IND			IPM		
	Mean	+/- 95%	▼	MEAN	+/- 95%	▼	MEAN	+/- 95%	▼	MEAN	+/- 95%	▼	MEAN	+/- 95%	▼	MEAN	+/- 95%	▼
0-NT	0.0130	0.0054	bcde	0.0110	0.0150	abc	0.0480	0.0039	cd	0.0575	0.0582	bcd	0.0383	0.0360	a	-	-	-
0-T	0.0409	0.0022	a	0.0400	0.0190	ab	0.0800	0.0600	ab	0.1513	0.0301	a	0.0383	0.0360	a	-	-	-
10-NT	0.0226	0.0095	b	0.0212	0.0340	abc	0.0384	0.0103	cd	0.0451	0.0246	bcd	0.0383	0.0360	a	0.0263	0.0026	bc
10-T	0.0180	0.0167	bc	0.0218	0.0060	a	0.0500	0.0402	cd	0.0750	0.0137	b	0.0383	0.0360	a	0.0450	0.0196	a
20-NT	0.0107	0.0028	cde	0.0214	0.0620	abc	0.0325	0.0220	cd	0.0243	0.0311	d	0.0383	0.0360	a	0.0275	0.0042	bc
20-T	0.0171	0.0121	bcd	0.0168	0.0160	abc	0.0314	0.0121	d	0.0501	0.0100	bcd	0.0383	0.0360	a	0.0495	0.0303	a
30-NT	0.0192	0.0126	bc	0.0155	0.0340	abc	0.1008	0.0373	a	0.0365	0.0180	cd	0.0383	0.0360	a	0.0275	0.0077	bc
30-T	0.0152	0.0193	bcd	0.0128	0.0010	b	0.0195	0.0194	d	0.0341	0.0128	cd	0.0383	0.0360	a	0.0383	0.0259	ab
60-NT	0.0158	0.0063	bcd	0.0209	0.1080	abc	0.0270	0.0083	d	0.0315	0.0139	cd	0.0383	0.0360	a	0.0140	0.0034	cd
60-T	0.0158	0.0100	bcd	0.0149	0.0150	abc	0.0370	0.0054	cd	0.0372	0.0174	cd	0.0383	0.0360	a	0.0253	0.0062	cd
90-NT	0.0142	0.0013	bcd	0.0117	0.0230	ab	0.0265	0.0242	d	0.0303	0.0225	cd	0.0383	0.0360	a	0.0140	0.0034	cd
90-T	0.0128	0.0113	bcde	0.0129	0.0220	ab	0.0366	0.0211	cd	0.0366	0.0126	cd	0.0383	0.0360	a	0.0200	0.0061	cd
120-NT	0.0069	0.0079	de	0.0070	0.0002	c	0.0228	0.0240	d	0.0365	0.0326	cd	0.0383	0.0360	a	0.0140	0.0046	cd
120-T	0.0064	0.0015	de	0.0087	0.0780	abc	0.0643	0.0312	bc	0.0559	0.0274	bcd	0.0383	0.0360	a	0.0143	0.0060	cd
150-NT	0.0084	0.0030	cde	0.0070	0.0130	abc	0.0491	0.0247	cd	0.0390	0.0479	cd	0.0383	0.0360	a	0.0165	0.0054	cd
150-T	0.0025	0.0024	e	0.0104	0.0940	abc	0.0392	0.0038	cd	0.0644	0.0290	bc	0.0383	0.0360	a	0.0125	0.0033	d
180-NT	0.0089	0.0022	cde	0.0080	0.0130	ac	0.0490	0.0330	cd	0.0375	0.0190	cd	0.0390	0.0367	a	0.0155	0.0067	cd
180-T	0.0070	0.0041	de	0.0082	0.0720	abc	0.0393	0.0181	cd	0.0642	0.0368	bc	0.0390	0.0367	a	0.0150	0.0034	cd

treatment, and method combination of the α parameter. There is no data for the IPM method at the 0 cm depth because instrumentation could not be installed at the surface.

In comparing the methods (Table 4.2a), from 0 to 60 cm depth, the 4TI and 8TI methods appear to produce similar results, while the 2C, 4C, and IPM methods are more similar. For 60 to 180 cm depth range, the 2C and 4C methods produce similar results, the 4TI and 8TI methods are similar, but the IPM shows no specific trend. The IND has consistently large α values and CL's. Because of the large CL's, the IND tends to not be significantly different from the other methods. Alpha values for the 2C and 4C methods tend to be the smallest, and the α values from the 4TI, 8TI, and IND tend to be the largest. The IPM tends to produce intermediate α values. Coefficient of variation (CV) (Appendix B) calculations indicate that the IPM α values are overall less variable than those determined from other methods. The IND method is highly variable. Even though the IND data were obtained from soils in the same textural class, differences in density and structure would undoubtedly cause differences in the parameters. The CV tables also indicate that for the α parameter, variation between methods is greater than spatial variability.

It is clear from Table 4.2b that there are tillage effects at the surface for all the methods except the IND. The IND method should not show tillage effects, because the data were selected based on texture and therefore the same data were used for the T and NT treatments. Only the IPM method shows

tillage effects at either of the 10 or 20 cm depths. Within the tillage zone, the T treatment has larger α values than the NT treatment, indicating a lower air-entry value. This is expected since part of the purpose of tillage is to break up the structure of the soil and increase porosity. The 2C, 4C and IPM methods (Table 4.2b) show a slight trend towards α decreasing in value with increase in depth. The changes in α are small and do not coincide with soil textural changes. For example, for the soil between 120 and 180 cm depth, the 2C α's on the order of 0.0025 to 0.0089 cm^{-1}. These values are smaller than those found near the surface that range from 0.0107 to 0.0409 cm^{-1}. In contrast, the 4TI and 8TI methods show little change in α with depth below about 10 cm depth. The IND method show no change in α because the value is based on soil texture and there is only one textural change and that occurs at about 160 cm depth. In addition, the soil texture change is slight going from sandy clay loam to clay loam.

n (curve fitting parameter indicative of pore size distribution)

Tables 4.3(a and b) show results of analysis of the "n" parameter. The n values range from about 1.4 to 2.0 and are well within the normal values from these soil types. Examining Table 4.3a, differences between methods are inconsistent and in general it appears that n is less method dependent than was α. The only exception appears to be the IND with an typically small n value. As we can see from Table 4.3b, there are no tillage effects on n within any of the methods. In addition, there are no trends or changes in the parameter with

Table 4.2(a). Mean, variance, and **t-test comparisons between methods** for each depth and tillage for the n parameter.

Depth	n - Curve Fitting Parameter (dimensionless) by Method of Measurement																	
Treatment	2C			4C			4TI			8TI			IND			IPM		
	Mean	+/- 95%	▶	MEAN	+/- 95%	▶	MEAN	+/- 95%	▶	MEAN	+/- 95%	▶	MEAN	+/- 95%	▶	MEAN	+/- 95%	▶
0-NT	1.6500	0.4269	ab	1.8640	1.1440	ab	1.7500	0.1812	a	1.7661	0.1686	a	1.3800	0.2166	b	-	-	-
0-T	1.7968	0.7125	ab	1.8637	3.7230	ab	1.6250	0.3156	ab	1.7277	0.2178	a	1.3800	0.2166	b	-	-	-
10-NT	1.7110	0.1880	ac	1.7170	1.7410	abc	1.7829	0.1457	a	1.7156	0.1728	ac	1.3800	0.2166	b	1.5600	0.1355	bc
10-T	1.6364	0.3137	ab	1.7167	3.8570	ab	1.7440	0.2261	b	1.7403	0.2250	b	1.3800	0.2166	a	1.4625	0.0664	a
20-NT	1.7360	0.6800	abc	1.6730	2.3640	abc	1.7200	0.1989	bc	1.7424	0.2263	bc	1.3800	0.2166	a	1.5075	0.0957	ac
20-T	1.6678	0.3056	ab	1.6731	2.6930	ab	1.5532	0.1127	a	1.7730	0.1082	b	1.3800	0.2166	a	1.5225	0.1217	a
30-NT	1.6620	0.3277	ab	1.4660	2.4530	ab	1.6658	0.2509	ab	1.8708	0.1316	b	1.3800	0.2166	a	1.5300	0.0975	a
30-T	1.7804	0.2348	a	1.4190	2.0970	abc	1.5085	0.1654	bc	1.6667	0.1619	ab	1.3800	0.2166	c	1.5250	0.1329	bc
60-NT	1.9240	0.6044	abc	1.3050	0.2670	abc	1.6800	0.0579	b	1.6451	0.2340	bc	1.3800	0.2166	c	1.7650	0.2023	b
60-T	1.6663	0.2954	ab	1.3425	1.6210	ab	1.5400	0.1576	ab	1.6015	0.0731	a	1.3800	0.2166	a	1.7000	0.0801	b
90-NT	1.8390	0.3860	a	1.5040	3.1900	ab	1.6759	0.3479	ab	1.6370	0.2506	ab	1.3800	0.2166	b	1.7225	0.2723	ab
90-T	1.7657	0.4470	ab	1.5125	0.4380	ab	1.5361	0.3211	ab	1.6033	0.2208	ab	1.3800	0.2166	a	1.7075	0.1003	b
120-NT	1.4140	0.8443	abc	1.9950	0.0380	a	1.6399	0.3296	abc	1.6542	0.1785	b	1.3800	0.2166	c	1.6525	0.2035	b
120-T	1.8291	0.5717	abc	1.9935	0.0830	a	1.7210	0.1895	b	1.6129	0.2180	bc	1.3800	0.2166	c	1.7150	0.0703	b
150-NT	1.7530	0.3680	ab	1.4780	1.1440	ab	1.6320	0.2137	ab	1.7944	0.1737	a	1.3800	0.2166	b	1.5275	0.1484	b
150-T	1.6545	0.1616	a	1.5110	1.0550	ab	1.6586	0.2425	ab	1.7077	0.2083	a	1.3800	0.2166	b	1.7100	0.0631	a
180-NT	1.6020	0.3506	abc	1.6510	0.0380	ab	1.6300	0.1561	ac	1.7748	0.1739	a	1.3280	0.2643	bc	1.5575	0.0347	c
180-T	1.6923	0.4270	ab	1.6855	0.7940	ab	1.6600	0.3073	ab	1.7125	0.1718	a	1.3280	0.2643	b	1.5650	0.0416	ab

Table 4.2(b). Mean, variance, and **t-test comparisons between depths and tillage treatments** within methods for the n parameter.

Depth	n - Curve Fitting Parameter (dimensionless) by Method of Measurement																	
Treatment	2C			4C			4TI			8TI			IND			IPM		
	Mean	+/- 95%	▼	MEAN	+/- 95%	▼	MEAN	+/- 95%	▼	MEAN	+/- 95%	▼	MEAN	+/- 95%	▼	MEAN	+/- 95%	▼
0-NT	1.6500	0.4269	a	1.8640	1.1440	ab	1.7500	0.1812	a	1.7661	0.1686	ab	1.3800	0.2166	a	-	-	-
0-T	1.7968	0.7125	a	1.8637	3.7230	ab	1.6250	0.3156	a	1.7277	0.2178	ab	1.3800	0.2166	a	-	-	-
10-NT	1.7110	0.1880	a	1.7170	1.7410	ab	1.7829	0.1457	a	1.7156	0.1728	ab	1.3800	0.2166	a	1.5600	0.1355	bc
10-T	1.6364	0.3137	a	1.7167	3.8570	ab	1.7440	0.2261	a	1.7403	0.2250	ab	1.3800	0.2166	a	1.4625	0.0664	c
20-NT	1.7360	0.6800	a	1.6730	2.3640	ab	1.7200	0.1989	a	1.7424	0.2263	ab	1.3800	0.2166	a	1.5075	0.0957	bc
20-T	1.6678	0.3056	a	1.6731	2.6930	ab	1.5532	0.1127	a	1.7730	0.1082	ab	1.3800	0.2166	a	1.5225	0.1217	bc
30-NT	1.6620	0.3277	a	1.4660	2.4530	ab	1.6658	0.2509	a	1.8708	0.1316	a	1.3800	0.2166	a	1.5300	0.0975	bc
30-T	1.7804	0.2348	a	1.4190	2.0970	ab	1.5085	0.1654	a	1.6667	0.1619	ab	1.3800	0.2166	a	1.5250	0.1329	bc
60-NT	1.9240	0.6044	a	1.3050	0.2670	a	1.6800	0.0579	a	1.6451	0.2340	ab	1.3800	0.2166	a	1.7650	0.2023	a
60-T	1.6663	0.2954	a	1.3425	1.6210	ab	1.5400	0.1576	a	1.6015	0.0731	b	1.3800	0.2166	a	1.7000	0.0801	a
90-NT	1.8390	0.3860	a	1.5040	3.1900	a	1.6759	0.3479	a	1.6370	0.2506	b	1.3800	0.2166	a	1.7225	0.2723	a
90-T	1.7657	0.4470	a	1.5125	0.4380	a	1.5361	0.3211	a	1.6033	0.2208	b	1.3800	0.2166	a	1.7075	0.1003	a
120-NT	1.4140	1.8443	a	1.9950	0.0380	b	1.6399	0.3296	a	1.6542	0.1785	ab	1.3800	0.2166	a	1.6525	0.2035	ab
120-T	1.8291	0.5717	a	1.9935	0.0830	b	1.7210	0.1895	a	1.6129	0.2180	b	1.3800	0.2166	a	1.7150	0.0703	a
150-NT	1.7530	0.3680	a	1.4780	1.1440	ab	1.6320	0.2137	a	1.7944	0.1737	ab	1.3800	0.2166	a	1.5275	0.1484	bc
150-T	1.6545	0.1616	a	1.5110	1.0550	ab	1.6586	0.2425	a	1.7077	0.2083	ab	1.3800	0.2166	a	1.7100	0.0631	a
180-NT	1.6020	0.3506	a	1.6510	0.0380	a	1.6300	0.1561	a	1.7748	0.1739	ab	1.3280	0.2643	a	1.5575	0.0347	bc
180-T	1.6923	0.4270	a	1.6855	0.7940	ab	1.6600	0.3073	a	1.7125	0.1718	ab	1.3280	0.2643	a	1.5650	0.0416	bc

change in depth. Tillage should generally result in smaller predicted n values (Klute, 1982). This is a result of increased porosity and macroporosity. Non-significant differences in the hydraulic properties between the T and NT treatments could be due to soil settling between tillage events. In addition, variability within the measurement method could overshadow any differences present between the treatments. For example, the n values measured using the IPM method at the 10 cm depth show the trend noted by Klute (1982), but the differences are not significant. As was seen for α, the IPM data is less variable overall than the data from the other methods. However, calculated CV values (Appendix B) indicate that both method and spatial variability are quite high for the n parameter.

θ_s (saturated water content)

Compiled results of the saturated water content values are recorded in Tables 4.4(a and b). There are no comparisons for the 4TI and 8TI methods because θ_s values from the 2C method were used during the analysis of the permeameter data. Thus the 2C, 4TI, and 8TI methods all have the same θ_s values. Again, as with the n data, there are no apparent trends in the data comparing depths and tillage treatments. There are differences between θ_s values as predicted by method, but that depends upon which depth is compared. As a quality control check of the data, total porosity values for the 2C method, calculated from bulk density and a particle density of 2.65 g/cm^3, were compared with θ_s values obtained from the RETC fit of the moisture retention data for the

Table 4.4(a). Mean, variance, and **t-test comparisons between methods** for each depth and tillage for the θ_s parameter.

Depth	Saturated Water Content (%, cm^3/cm^3) by Method of Measurement																	
Treatment	2C			4C			4TI			8TI			IND			IPM		
	Mean	+/- 95%	▶	MEAN	+/- 95%	▶	MEAN	+/- 95%	▶	MEAN	+/- 95%	▶	MEAN	+/- 95%	▶	MEAN	+/- 95%	▶
0-NT	0.4600	0.0174	a	0.3314	0.0610	b	0.4600	0.0000	-	0.4600	0.0000	-	0.3900	0.1102	ab	-	-	-
0-T	0.4888	0.1215	a	0.4085	1.0460	a	0.4888	0.0000	-	0.4888	0.0000	-	0.3900	0.1102	a	-	-	-
10-NT	0.4823	0.0128	a	0.3258	0.2460	ab	0.4820	0.0000	-	0.4820	0.0000	-	0.3900	0.1102	ab	0.4124	0.0177	b
10-T	0.4699	0.0943	a	0.4007	0.5830	a	0.4699	0.0000	-	0.4699	0.0000	-	0.3900	0.1102	a	0.4244	0.0099	a
20-NT	0.4433	0.0508	a	0.3068	0.0670	b	0.4430	0.0000	-	0.4430	0.0000	-	0.3900	0.1102	ab	0.4211	0.0178	a
20-T	0.4088	0.0443	a	0.3708	0.9370	a	0.4088	0.0000	-	0.4088	0.0000	-	0.3900	0.1102	a	0.4196	0.0244	a
30-NT	0.4390	0.0523	a	0.3527	0.0840	b	0.4390	0.0000	-	0.4390	0.0000	-	0.3900	0.1102	ab	0.4227	0.0189	a
30-T	0.4260	0.1024	a	0.3414	0.2970	a	0.4260	0.0000	-	0.4260	0.0000	-	0.3900	0.1102	a	0.4404	0.0158	a
60-NT	0.4178	0.0279	a	0.3365	0.2620	a	0.4180	0.0000	-	0.4180	0.0000	-	0.3900	0.1102	a	0.4012	0.0326	a
60-T	0.3859	0.0876	ab	0.3562	0.1020	ab	0.3859	0.0000	-	0.3859	0.0000	-	0.3900	0.1102	ab	0.4168	0.0379	b
90-NT	0.4371	0.0103	a	0.3533	0.0300	b	0.4370	0.0000	-	0.4370	0.0000	-	0.3900	0.1102	ab	0.4193	0.0316	a
90-T	0.3669	0.0951	a	0.3348	0.1420	a	0.3669	0.0000	-	0.3669	0.0000	-	0.3900	0.1102	a	0.4357	0.0164	a
120-NT	0.4251	0.0820	a	0.3181	0.0200	b	0.4250	0.0000	-	0.4250	0.0000	-	0.3900	0.1102	ab	0.4050	0.0417	a
120-T	0.3985	0.0801	a	0.3673	0.6960	a	0.3985	0.0000	-	0.3985	0.0000	-	0.3900	0.1102	a	0.4314	0.0041	a
150-NT	0.4534	0.0539	a	0.3376	0.1040	a	0.4530	0.0000	-	0.4530	0.0000	-	0.3900	0.1102	a	0.4207	0.0133	a
150-T	0.4180	0.1515	a	0.3608	0.5780	a	0.4180	0.0000	-	0.4180	0.0000	-	0.3900	0.1102	a	0.4276	0.0121	a
180-NT	0.3849	0.0391	a	0.3596	0.1840	a	0.3850	0.0000	-	0.3850	0.0000	-	0.3967	0.0212	a	0.4089	0.0276	a
180-T	0.3987	0.0999	a	0.3907	0.0830	a	0.3987	0.0000	-	0.3987	0.0000	-	0.3967	0.0212	a	0.4198	0.0149	a

Table 4.4(b). Mean, variance, and **t-test comparisons between depths and tillage treatments** within methods for the qs parameter.

Depth	Saturated Water Content (%, cm^3/cm^3) by Method of Measurement																	
Treatment	2C			4C			4TI			8TI			IND			IPM		
	Mean	+/- 95%	▼	MEAN	+/- 95%	▼	MEAN	+/- 95%	▼	MEAN	+/- 95%	▼	MEAN	+/- 95%	▼	MEAN	+/- 95%	▼
0-NT	0.4600	0.0174	abc	0.3314	0.0610	a	0.4600	0.0000	-	0.4600	0.0000	-	0.3900	0.1102	a	-	-	-
0-T	0.4888	0.1215	a	0.4085	1.0460	a	0.4888	0.0000	-	0.4888	0.0000	-	0.3900	0.1102	a	-	-	-
10-NT	0.4823	0.0128	a	0.3258	0.2460	a	0.4820	0.0000	-	0.4820	0.0000	-	0.3900	0.1102	a	0.4124	0.0177	bcd
10-T	0.4699	0.0943	ab	0.4007	0.5830	a	0.4699	0.0000	-	0.4699	0.0000	-	0.3900	0.1102	a	0.4244	0.0099	abcd
20-NT	0.4433	0.0508	abc	0.3068	0.0670	a	0.4430	0.0000	-	0.4430	0.0000	-	0.3900	0.1102	a	0.4211	0.0178	abcd
20-T	0.4088	0.0443	abc	0.3708	0.9370	a	0.4088	0.0000	-	0.4088	0.0000	-	0.3900	0.1102	a	0.4196	0.0244	abcd
30-NT	0.4390	0.0523	abc	0.3527	0.0840	a	0.4390	0.0000	-	0.4390	0.0000	-	0.3900	0.1102	a	0.4227	0.0189	abcd
30-T	0.4260	0.1024	abc	0.3414	0.2970	a	0.4260	0.0000	-	0.4260	0.0000	-	0.3900	0.1102	a	0.4404	0.0158	a
60-NT	0.4178	0.0279	abc	0.3365	0.2620	a	0.4180	0.0000	-	0.4180	0.0000	-	0.3900	0.1102	a	0.4012	0.0326	d
60-T	0.3859	0.0876	bc	0.3562	0.1020	a	0.3859	0.0000	-	0.3859	0.0000	-	0.3900	0.1102	a	0.4168	0.0379	abcd
90-NT	0.4371	0.0103	abc	0.3533	0.0300	a	0.4370	0.0000	-	0.4370	0.0000	-	0.3900	0.1102	a	0.4193	0.0316	abcd
90-T	0.3669	0.0951	c	0.3348	0.1420	a	0.3669	0.0000	-	0.3669	0.0000	-	0.3900	0.1102	a	0.4357	0.0164	ab
120-NT	0.4251	0.0820	abc	0.3181	0.0200	a	0.4250	0.0000	-	0.4250	0.0000	-	0.3900	0.1102	a	0.4050	0.0417	cd
120-T	0.3985	0.0801	abc	0.3673	0.6960	a	0.3985	0.0000	-	0.3985	0.0000	-	0.3900	0.1102	a	0.4314	0.0041	abc
150-NT	0.4534	0.0539	abc	0.3376	0.1040	a	0.4530	0.0000	-	0.4530	0.0000	-	0.3900	0.1102	a	0.4207	0.0133	abcd
150-T	0.4180	0.1515	abc	0.3608	0.5780	a	0.4180	0.0000	-	0.4180	0.0000	-	0.3900	0.1102	a	0.4276	0.0121	abcd
180-NT	0.3849	0.0391	bc	0.3596	0.1840	a	0.3850	0.0000	-	0.3850	0.0000	-	0.3967	0.0212	a	0.4089	0.0276	bcd
180-T	0.3987	0.0999	abc	0.3907	0.0830	a	0.3987	0.0000	-	0.3987	0.0000	-	0.3967	0.0212	a	0.4198	0.0149	abcd

Table 4.5(a). Mean, variance, and **t-test comparisons between methods** for each depth and tillage for the K_s parameter.

Depth	Saturated Hydraulic Conductivity (cm/s) by Method of Measurement																	
Treatment	2C			4C			4TI			8TI			IND			IPM		
	Mean	+/- 95%	▶	MEAN	+/- 95%	▶	MEAN	+/- 95%	▶	MEAN	+/- 95%	▶	MEAN	+/- 95%	▶	MEAN	+/- 95%	▶
0-NT	0.0007	0.0002	a	0.0010	0.0008	a	0.0048	0.0012	b	0.0062	0.0019	b	0.0002	0.0003	c	0.0016	0.0002	d
0-T	0.0010	0.0002	a	0.0015	0.0119	abc	0.0045	0.0014	b	0.0054	0.0019	b	0.0002	0.0003	c	0.0030	0.0007	ac
10-NT	0.0005	0.0002	a	0.0009	0.0005	b	0.0061	0.0025	c	0.0058	0.0023	c	0.0002	0.0003	d	0.0017	0.0006	e
10-T	0.0008	0.0004	a	0.0014	0.0085	abc	0.0061	0.0011	b	0.0058	0.0010	b	0.0002	0.0003	c	0.0031	0.0007	a
20-NT	0.0007	0.0002	a	0.0009	0.0009	a	0.0061	0.0017	b	0.0063	0.0023	b	0.0002	0.0003	c	0.0016	0.0005	d
20-T	0.0008	0.0003	a	0.0013	0.0090	abc	0.0055	0.0014	b	0.0053	0.0016	b	0.0002	0.0003	c	0.0030	0.0005	a
30-NT	0.0006	0.0002	a	0.0007	0.0010	a	0.0045	0.0022	b	0.0051	0.0015	b	0.0002	0.0003	c	0.0015	0.0004	d
30-T	0.0007	0.0008	a	0.0011	0.0095	abc	0.0051	0.0033	b	0.0056	0.0040	b	0.0002	0.0003	a	0.0027	0.0005	bc
60-NT	0.0007	0.0002	a	0.0006	0.0006	a	0.0055	0.0023	b	0.0066	0.0029	b	0.0002	0.0003	c	0.0014	0.0003	d
60-T	0.0008	0.0001	a	0.0010	0.0022	acd	0.0062	0.0010	b	0.0064	0.0025	b	0.0002	0.0003	c	0.0024	0.0009	d
90-NT	0.0007	0.0002	a	0.0011	0.0008	abd	0.0055	0.0023	c	0.0066	0.0029	c	0.0002	0.0003	d	0.0013	0.0002	b
90-T	0.0005	0.0005	a	0.0012	0.0028	ab	0.0062	0.0010	c	0.0064	0.0025	c	0.0002	0.0003	a	0.0023	0.0011	b
120-NT	0.0006	0.0001	a	0.0008	0.0005	acd	0.0065	0.0010	b	0.0071	0.0008	b	0.0002	0.0003	c	0.0013	0.0002	d
120-T	0.0006	0.0002	a	0.0009	0.0005	a	0.0053	0.0013	b	0.0062	0.0026	b	0.0002	0.0003	c	0.0022	0.0012	d
150-NT	0.0006	0.0001	a	0.0007	0.0025	acd	0.0067	0.0026	b	0.0063	0.0023	b	0.0002	0.0003	c	0.0012	0.0002	d
150-T	0.0006	0.0004	ad	0.0011	0.0036	abcd	0.0045	0.0021	bd	0.0053	0.0022	b	0.0002	0.0003	c	0.0021	0.0012	d
180-NT	0.0006	0.0005	a	0.0009	0.0005	a	0.0067	0.0026	b	0.0063	0.0023	b	0.0002	0.0003	a	0.0012	0.0002	a
180-T	0.0005	0.0001	a	0.0009	0.0008	acd	0.0045	0.0021	b	0.0053	0.0022	b	0.0002	0.0003	c	0.0021	0.0014	d

Table 4.5(b). Mean, variance, and **t-test comparisons between depths and tillage treatments** within methods for the Ks parameter.

Depth	Saturated Hydraulic Conductivity (cm/s) by Method of Measurement																	
Treatment	2C			4C			4TI			8TI			IND			IPM		
	Mean	+/- 95%	▼	MEAN	+/- 95%	▼	MEAN	+/- 95%	▼	MEAN	+/- 95%	▼	MEAN	+/- 95%	▼	MEAN	+/- 95%	▼
0-NT	0.0007	0.0002	ab	0.0010	0.0008	a	0.0048	0.0012	a	0.0062	0.0019	a	0.0002	0.0003	a	0.0016	0.0002	b
0-T	0.0010	0.0002	a	0.0015	0.0119	a	0.0045	0.0014	a	0.0054	0.0019	a	0.0002	0.0003	a	0.0030	0.0070	a
10-NT	0.0005	0.0002	b	0.0009	0.0005	a	0.0061	0.0025	a	0.0058	0.0023	a	0.0002	0.0003	a	0.0017	0.0006	b
10-T	0.0008	0.0004	ab	0.0014	0.0085	a	0.0061	0.0011	a	0.0058	0.0010	a	0.0002	0.0003	a	0.0031	0.0007	b
20-NT	0.0007	0.0002	ab	0.0009	0.0009	a	0.0061	0.0017	a	0.0063	0.0023	a	0.0002	0.0003	a	0.0016	0.0005	b
20-T	0.0008	0.0003	ab	0.0013	0.0090	a	0.0055	0.0014	a	0.0053	0.0016	a	0.0002	0.0003	a	0.0030	0.0005	b
30-NT	0.0006	0.0002	b	0.0007	0.0010	a	0.0045	0.0022	a	0.0051	0.0015	a	0.0002	0.0003	a	0.0015	0.0004	b
30-T	0.0007	0.0008	ab	0.0011	0.0095	a	0.0051	0.0033	a	0.0056	0.0040	a	0.0002	0.0003	a	0.0027	0.0005	b
60-NT	0.0007	0.0002	ab	0.0006	0.0006	a	0.0055	0.0023	a	0.0066	0.0029	a	0.0002	0.0003	a	0.0014	0.0003	b
60-T	0.0008	0.0001	ab	0.0010	0.0022	a	0.0062	0.0010	a	0.0064	0.0025	a	0.0002	0.0003	a	0.0024	0.0009	b
90-NT	0.0007	0.0002	ab	0.0011	0.0008	a	0.0055	0.0023	a	0.0066	0.0029	a	0.0002	0.0003	a	0.0013	0.0002	b
90-T	0.0005	0.0005	b	0.0012	0.0028	a	0.0062	0.0010	a	0.0064	0.0025	a	0.0002	0.0003	a	0.0023	0.0011	b
120-NT	0.0006	0.0001	ab	0.0008	0.0005	a	0.0065	0.0010	a	0.0071	0.0008	a	0.0002	0.0003	a	0.0013	0.0002	b
120-T	0.0006	0.0002	b	0.0009	0.0005	a	0.0053	0.0013	a	0.0062	0.0026	a	0.0002	0.0003	a	0.0022	0.0012	b
150-NT	0.0006	0.0001	ab	0.0007	0.0025	a	0.0067	0.0026	a	0.0063	0.0023	a	0.0002	0.0003	a	0.0012	0.0002	b
150-T	0.0006	0.0004	b	0.0011	0.0036	a	0.0045	0.0021	a	0.0053	0.0022	a	0.0002	0.0003	a	0.0021	0.0012	b
180-NT	0.0006	0.0005	ab	0.0009	0.0005	a	0.0067	0.0026	a	0.0063	0.0023	a	0.0002	0.0003	a	0.0012	0.0002	b
180-T	0.0005	0.0001	b	0.0009	0.0008	a	0.0045	0.0021	a	0.0053	0.0022	a	0.0002	0.0003	a	0.0021	0.0014	b

2C method. All of the predicted θ_s values agree quite well with the calculated porosity values..

K_s (saturated hydraulic conductivity)

Tables 4.5(a and b) list K_s values for each method, tillage, and depth. Inspection of Table 4.5(a) reveals that methods 2C and 4C and methods 4TI and 8TI are similar for most of the depths and tillage treatments. The IND and IPM values show no trends and overall seem to be significantly different from the other methods. The 4TI and 8TI K_s values tend to be larger than the K_s values obtained from the soil cores. The IND values are consistently low and the IPM values are intermediate between the permeameter and the soil core K_s values. It is interesting that the 4C data is less variable than the other methods and could be due to stricter measurement control in the lab. As was seen for α, the IPM K_s has a low CV (Appendix B) and method variability is greater than spatial variability for the K_s parameter. Also, IND K_s values are several times more variable than K_s values from any of the other methods.

In Table 4.5(b), only the IPM method shows a tillage effect. The T treatment K_s value is about two times greater than the K_s value for the NT treatment for the surface soil. Klute (1982) noted that if tillage increased the total porosity of the soil, then the K_s of the soil will be increased. None of the methods show any significant differences in K_s with depth below the tillage zone. The IND method doesn't show any differences with depth because the K_s values from the 3 data sets are very similar for the sandy clay loam and clay loam soils.

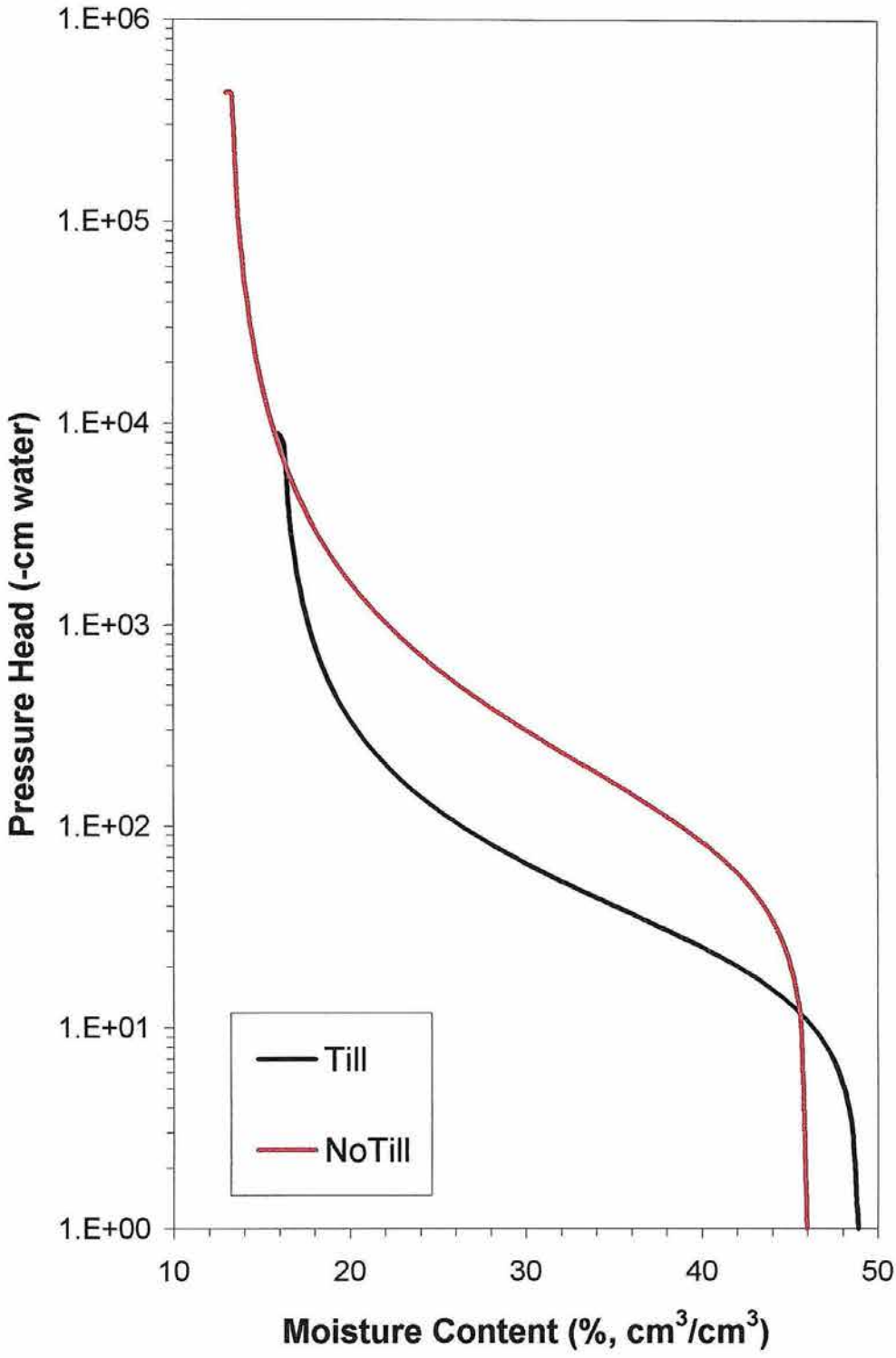

Figure 4.1. Hydraulic head versus moisture content plots constructed using data obtained at the 0 cm depth.

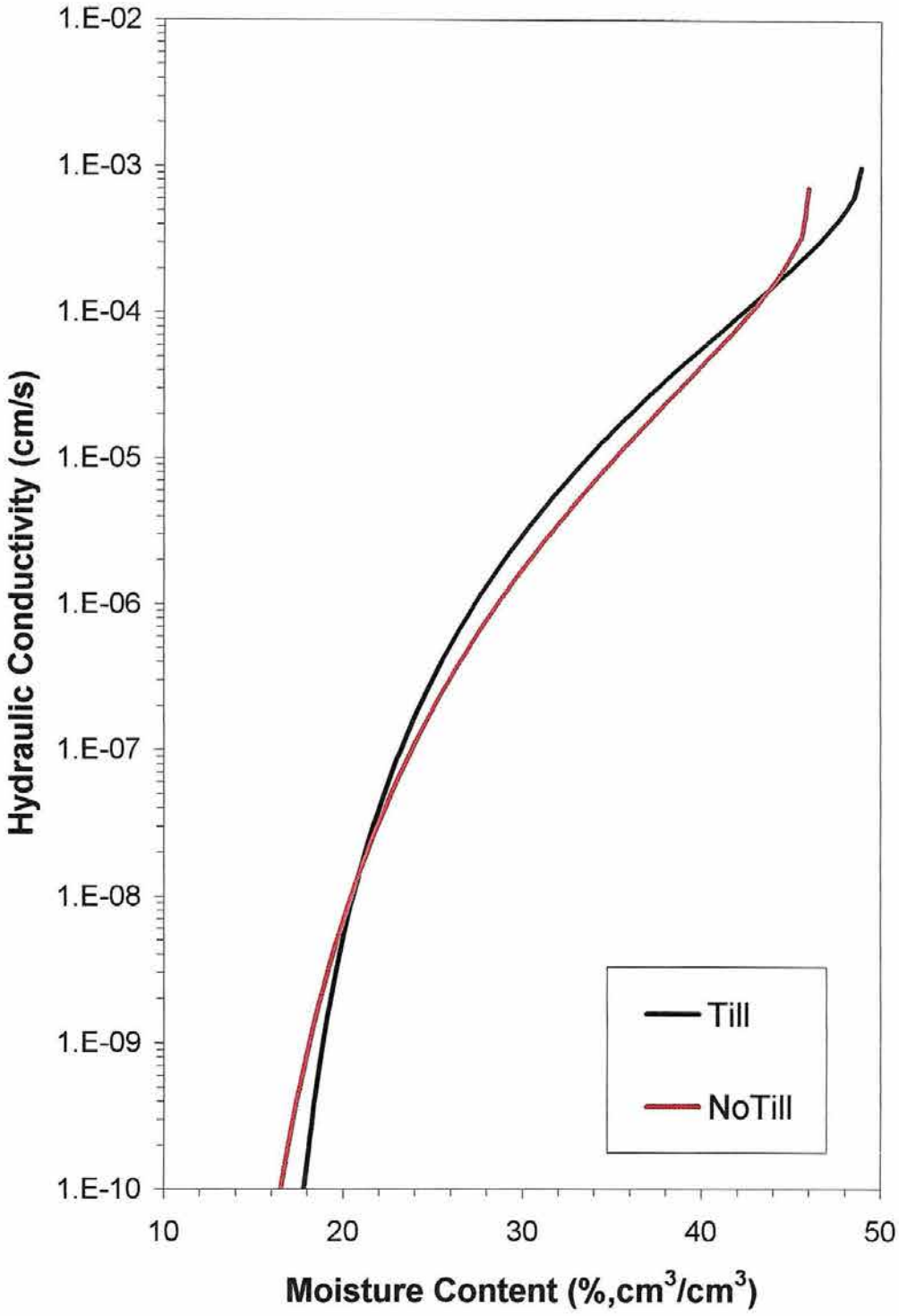

Figure 4.2. Hydraulic conductivity versus moisture content plots constructed using data obtained at the 0 cm depth.

Functional Forms of the Parameters

Because the hydraulic parameters discussed above are not independent of one another, it is important to investigate how the functional forms of the hydraulic properties (Eqs. 2.15 - 2.19) vary based on method of measurement, tillage treatment, and depth. Comparing the parameter functions yields more complete understanding of the differences between the methods. As an example, Figure 4.1 shows the h(θ) relationship for T and NT reps at the 0 cm depth, generated using data from the 2C method. In Figure 4.1 the difference in the shape of these two curves is clear. However, data from Tables 4.2 through 4.5 suggest that the only significant difference between the T and NT curves is between their α parameter values. In order to compare α values we have to compare the air-entry values, which are proportional to 1/α. The T treatment has an air-entry value of about 10 cm and the NT treatment has an air-entry value of about 30 cm. The difference in the α shifts the entire curve, not just the height of the toe, and θ over the range of h from 0 to 10,000 cm is greatly affected. For instance, at a pressure head of 100 cm the volumetric water content of the T treatment would be about 25 % compared to about 37% in the NT soil. Slight changes in even one parameter can have a profound effect on the soil's drainage or water transport properties.

Figure 4.2 shows the hydraulic conductivity profiles for the same two soils as shown in Figure 4.1. The curves appear to be quite similar, again with the exception of the α parameter, which controls the point where the moisture

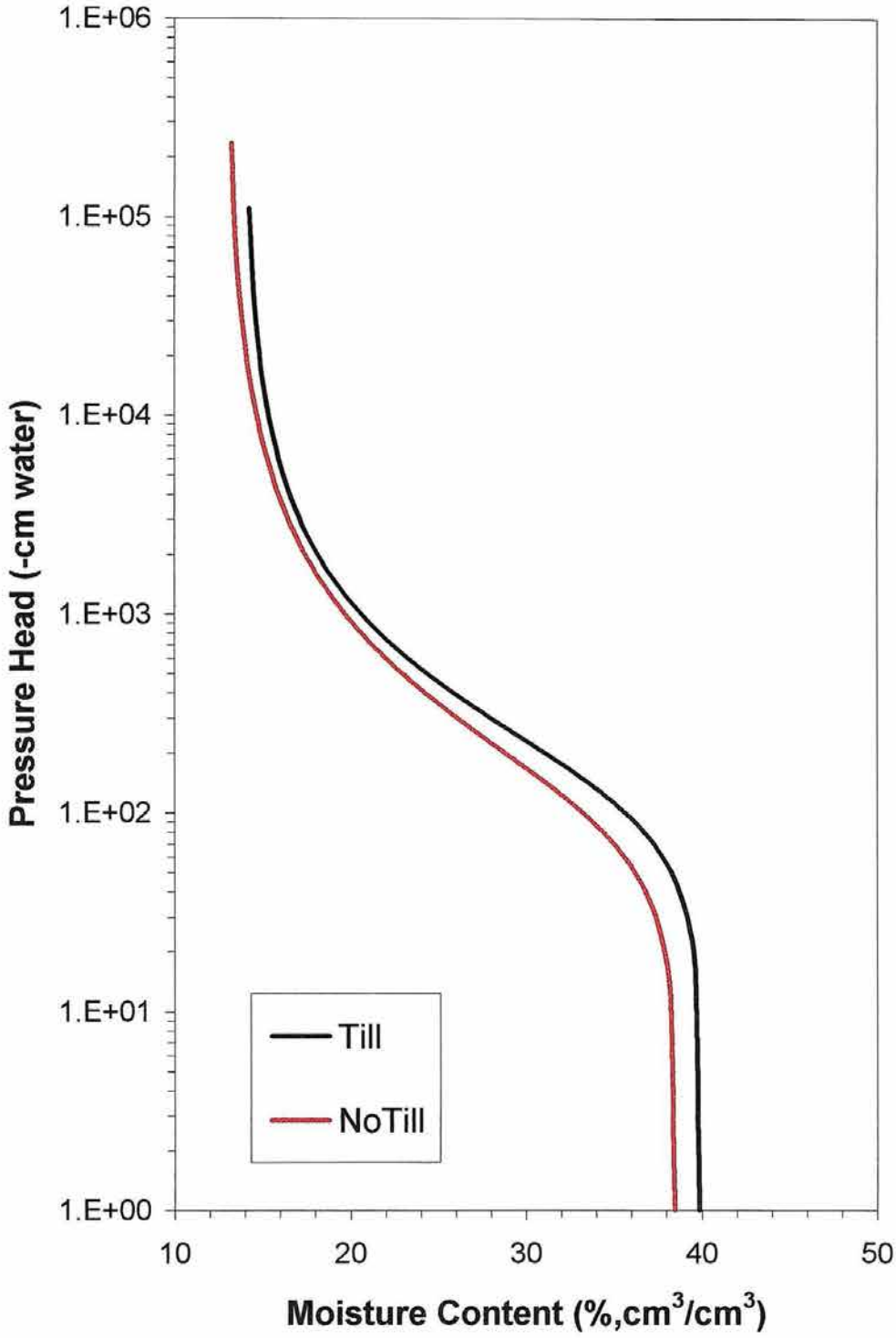

Figure 4.3. Hydraulic head versus moisture content plots constructed using data obtained at the 180 cm depth.

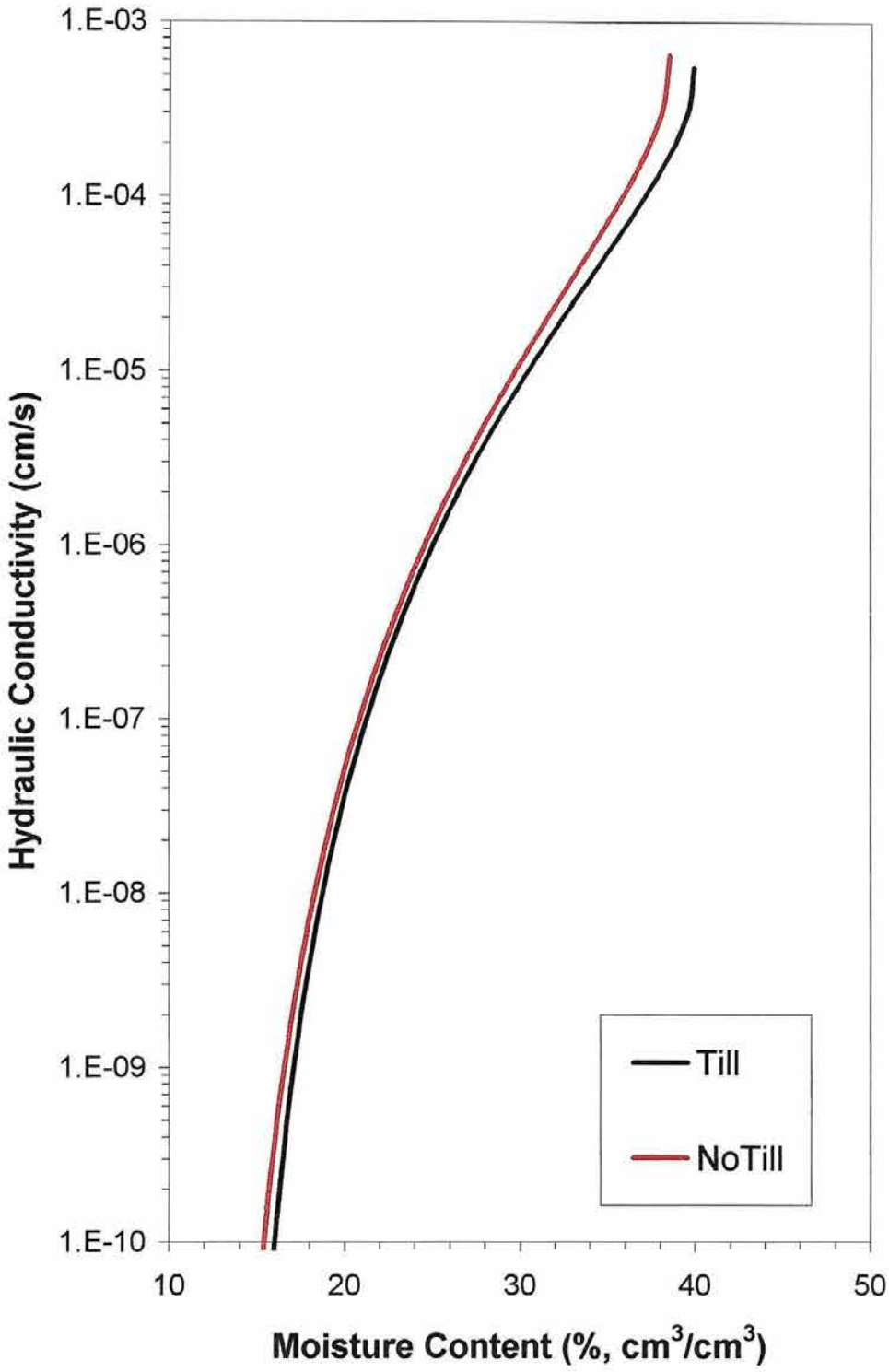

Figure 4.4. Hydraulic conductivity versus moisture content plots constructed using data obtained at the 180 cm depth.

content starts to drop off with respect to changes in conductivity. The differences in the curves appear small because the scale over which the conductivity ranges is quite large. For instance, at $\theta_v = 0.3$, the K_s values differ by about 40%.

Figures 4.3 and 4.4 show the same T and NT treatment soils as in Figures 4.1 and 4.2, but at the 180 cm depth. At this depth, differences between treatments are very small which is consistent with Tables 4.2 through 4.5, indicating no significant differences in the 2C parameters at this depth. The curves have very similar shapes as well as starting and ending points. Tillage differences are confined to the surface soil and differences that do occur between treatments below the tillage zone can be attributed to spatial variability.

For a visual comparison of all the methods, Figs. 4.5 - 4.8 show the method dependent $\theta(h)$ and $K(\theta)$ at 10 cm and 180 cm depths. The suite of methods employed yield widely varying estimates of the hydraulic properties for the same soil. For example, at the 180 cm depth (Figs. 4.7 and 4.8), θ at about h=-100 cm ranges from about 15% to 35% depending on the method, while K at θ=25% ranges over about three orders of magnitude. The 4C method appears to consistently have lower θ_s values and higher θ_r values. The 2C and IPM favor larger θ (at any h) than the other methods. Hysteresis may also be a factor when comparing draining methods (2C, 4C, IPM) with wetting methods (4TI, 8TI), but a consistent bias toward larger θ (at any h) for the draining methods is not discernable. Noteworthy is that the IND method appears within the variability

represented by the direct methods in nearly all the plots. Appendix A contains plots of all the method comparisons by depth and treatment. Finally, notice that the IPM $\theta(h)$ and $K(\theta)$, except near saturation, are typically in the middle of the group, i.e. representing the mean result.

4.3 Measurement Scale

One objective of this research was to investigate the affect of scale or sample support size on the determination of hydraulic properties. The measurements were not only split into in-situ and laboratory, but made at contrasting scales. Sample support size ranges from 5.08 cm diameter for the 2C method to about 100 cm diameter for the IPM.

Inspection of Tables 4.2 through 4.5 reveals no consistent or significant scale dependence within soil core sampling methods for any of the parameters. However, θ_s values measured by the 2C and 4C methods appear consistently different when looking at the hydraulic functions (Fig. 4.5 and Appendix A). The 2C appears to have larger θ_s values than the 4C method. In addition, the depth averaged K_s value for the 4C method is over two times larger than the 2C value. The 4TI and 8TI produce very similar results for all of the parameters, indicating no scale dependence within the permeameter method (Table 4.2 - 4.5, and Appendix A). However, scale affects, over the range of measurement scales (2C to IPM) may also be important. Some apparent scale dependence can be seen in the conductivity data. The IPM data tends to be different than the other

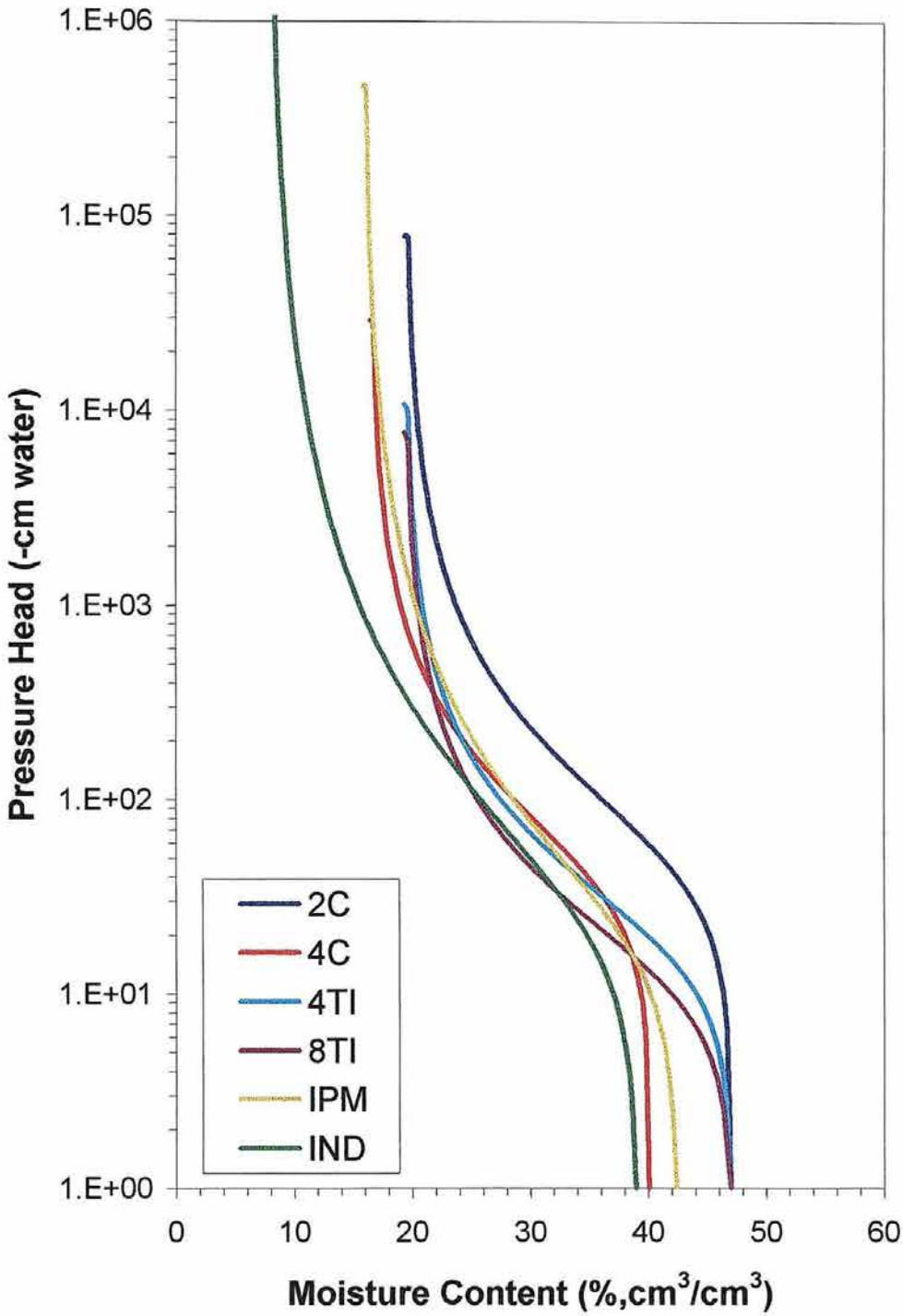

Figure 4.5. Hydraulic head versus moisture content plots constructed using data obtained at the 10 cm depth in the tilled treatment.

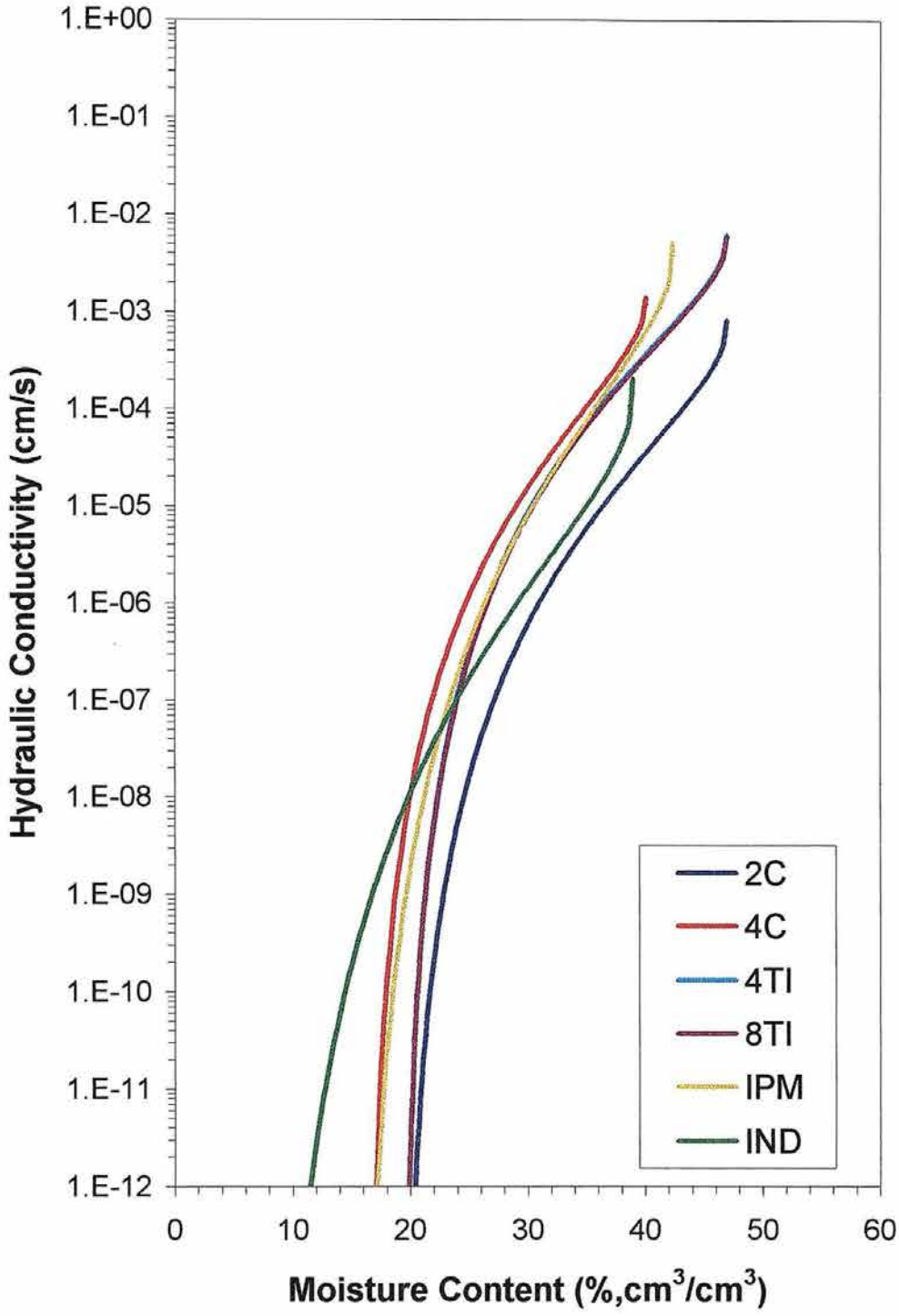

Figure 4.6. Hydraulic conductivity versus moisture content plots constructed using data obtained at the 10 cm depth in the tilled treatment.

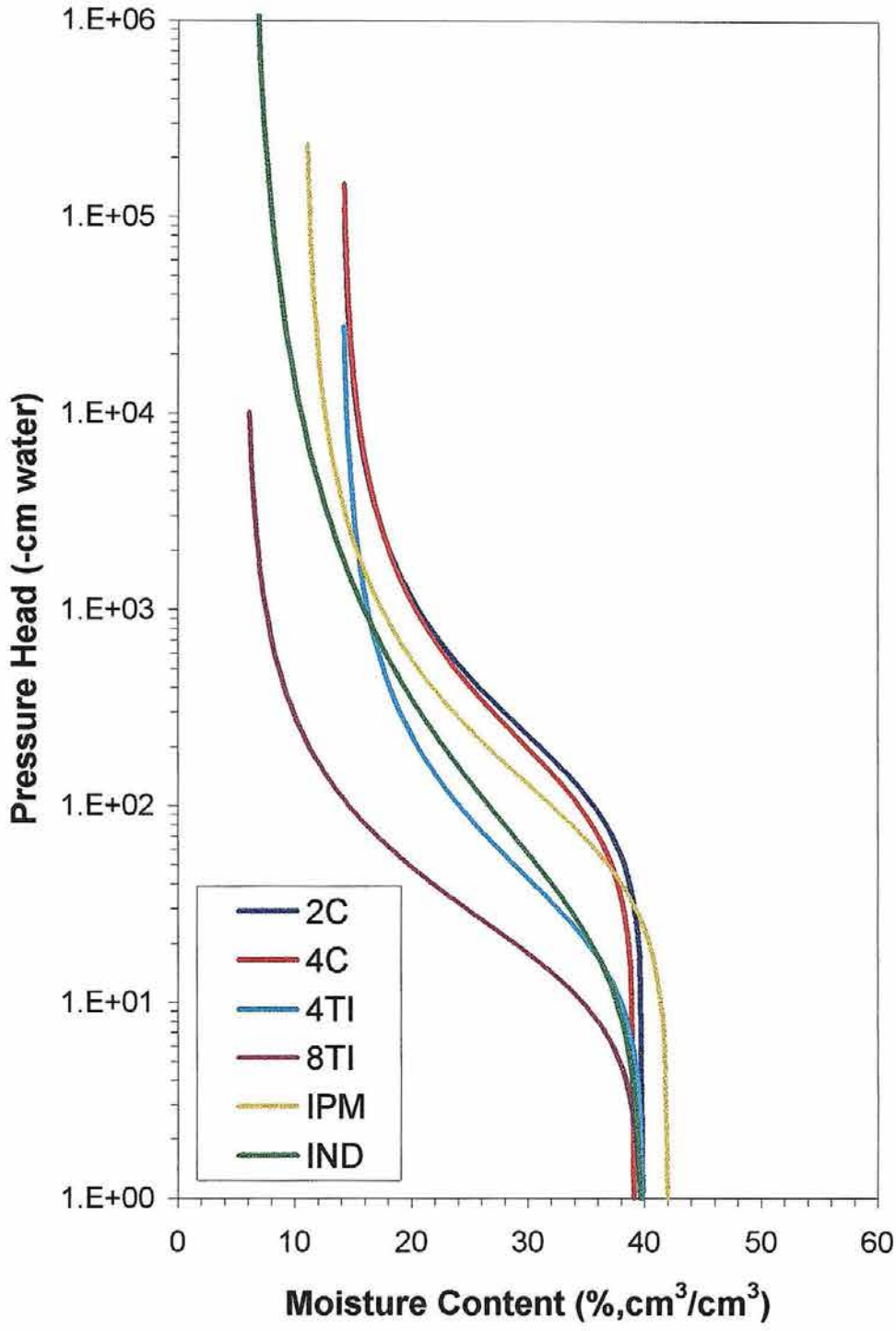

Figure 4.7. Hydraulic head versus moisture content plots constructed using data obtained at the 180 cm depth in the tilled treatment.

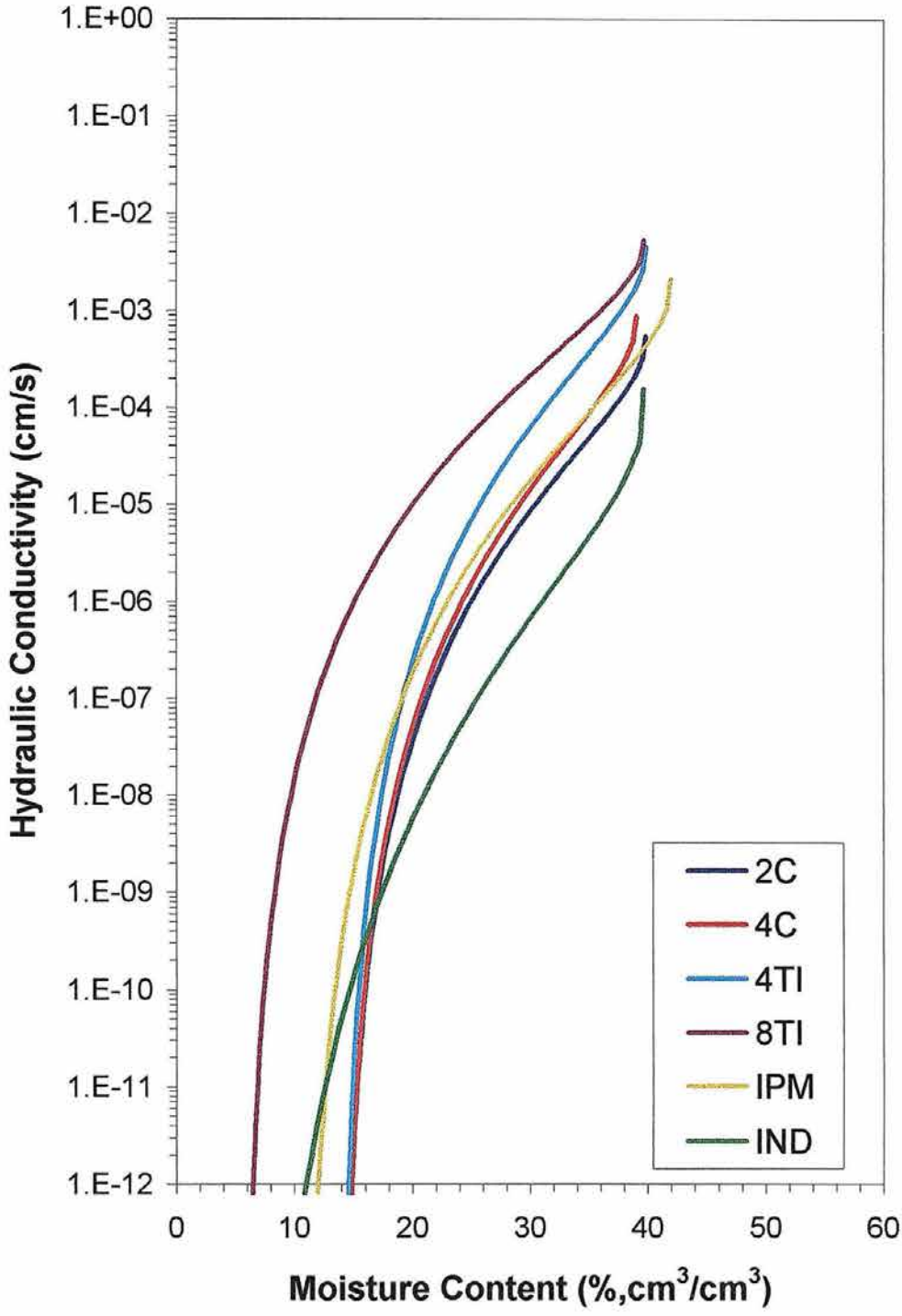

Figure 4.8. Hydraulic conductivity versus moisture content plots constructed using data obtained at the 180 cm depth in the tilled treatment.

methods, but the measured values are between the values measured for the cores and permeameters. The larger scale IPM method results in K_s values that are more similar to the smaller scale core values. The K_s values measured using the permeameters are higher than those measured using the soil cores and using the IPM method. There seems to be some intermediate scale of measurement where the variability tends to increase before decreasing due to the scale of the measurement. For instance, the 2C which has a measurement scale of about 5 cm diameter and the IPM, which has a scale of about 100 cm diameter, are both slightly less variable than the 20.32 cm diameter permeameter (8TI). Since the "real" value of K_s isn't known, it is impossible to say which method produces better results. Small variability in the K_s values for the IPM is consistent with results obtained by other researchers as noted in section 2.4.6. However, the lack of variability noted in the smaller scale soil core data is not consistent with other findings.

4.4 Summary

Estimation of soil hydraulic properties is sensitive to the measurement method selected. In this study, widely varying $\theta(h)$ and $K(\theta)$ were observed in a side-by-side comparison of methods. Comparisons of individual parameters of the estimated $\theta(h)$ and $K(\theta)$ functions found statistically significant differences between methods but these differences were not consistent over all depths. The key findings of this evaluation of soil hydraulic properties are:

1) The differences in $\theta(h)$ and $K(\theta)$ parameters between methods are comparable or larger than spatial variability in the parameters for a given method.

2) Estimation of α and K_s was more sensitive to method and scale selection than was estimation of n and θ_s.

3) The largest scale measurement, the IPM, had the least spatial variability in the $\theta(h)$ and $K(\theta)$ and tended to represent the mean $\theta(h)$ and $K(\theta)$ of all methods.

4) Tillage introduced a statistically significant change in the hydraulic properties and increased the spatial variability of the hydraulic parameters (regardless of method).

5) Comparing sample support (2C vs. 4C, and 4TI vs. 8TI), α and n showed little scale dependence. Saturated K was twice as large for 4C than for 2C, but nearly equal for 4TI and 8TI. 2C showed larger θ_s values than 4C.

Finally it is important to emphasize that the relevance of the differences in the $\theta(h)$ and $K(\theta)$ by method can only be assessed in the context of an application. In a transient, unsaturated flow simulation, for example, even apparently "small" or statistically insignificant differences in $K(\theta)$ may lead to significant differences in a desired output (e.g. q(z,t). The effect of the method dependent hydraulic properties on the prediction of unsaturated flow and transport is the subject of the next chapter.

CHAPTER 5

COMPARISON OF THE PREDICTIVE ACCURACY OF THE HYDRUS-2D CODE AS AFFECTED BY PARAMETER ESTIMATION METHOD

5.0 Overview

In this chapter, hydraulic properties estimated from each of the six methods listed in Chapter 2 are used as input to HYDRUS-2D to predict the movement of water and bromide tracer. The predicted water and bromide concentration profiles at selected times are compared to measured water and bromide concentration profiles obtained during solute transport experiments. Model predictions are obtained by two contrasting approaches; first by using the average hydraulic parameters for a given estimation method (Tables 4.2 - 4.5) as input to HYDRUS-2D, and second, by using the method dependent parameters from each specific replicate as input to HYDRUS-2D followed by averaging of the model output. In addition, comparisons are made comparing the tilled and non-tilled treatments. Finally, in an effort to optimize predictive accuracy while minimizing experimental effort, some logical combinations of the hydraulic property estimation methods are investigated.

Table 5.1. Average absolute difference in water content between predicted and observed data.

	Till Soil Treatment					
	Average Absolute Deviation in Water Content by Method (cm^3/cm^3)					
Day	2C	4C	4TI	8TI	IPM	IND
8	0.0254	0.0279	0.0261	0.0280	0.0211	0.0358
22	0.0238	0.0190	0.0234	0.0239	0.0192	0.0452
36	0.0222	0.0187	0.0485	0.0564	0.0170	0.0772
117	0.0301	0.0223	0.0342	0.0384	0.0130	0.0485
	No-Till Soil Treatment					
	Average Absolute Deviation in Water Content by Method (cm^3/cm^3)					
Day	2C	4C	4TI	8TI	IPM	IND
9	0.0438	0.0260	0.0397	0.0364	0.0380	0.0432
23	0.0616	0.0618	0.0489	0.0583	0.0618	0.0660
37	0.0437	0.0548	0.0485	0.0348	0.0467	0.0935
118	0.0218	0.0502	0.0251	0.0198	0.0216	0.0487

5.1 Comparison of Water Content Profiles as Predicted by Parameter Estimation Method

Using the mean values of the parameters to form hydraulic property input data, Figs. 5.1 - 5.4 show the HYDRUS-2D predicted $\theta(z)$ profiles against the observed $\theta(z)$ profiles. Figure 5.1(a) shows predicted and measured water content profiles for the T treatment at eight days after the start of the experiment. Essentially all of the methods do a good job of estimating the water content profile early in the study. The largest deviations in θ ($\Delta\theta$ = |observed θ - predicted θ|) are about $\Delta\theta = 0.5$, and all in all the profiles look good. The average absolute deviation (AAD, average of $\Delta\theta$ in volumetric water content) for each method and time was also calculated (Table 5.1). AAD values range from about 2 to 3.6 percent, indicating that the predicted profiles fit the observed water content profile well. Calculated correlation coefficients (CC) were used to estimate goodness of fit of the model predicted profiles to the measured data. The Other methods such as sum of squared residuals were explored, but they are more difficult to calculate and can weight certain parts of the curve based on the magnitude of the dependent variable. Correlation values between the observed and predicted water content profiles for both the T and NT treatments are listed in Table 5.2. For the tilled soil at t=8 days, the CC values range from about 0.8 to 0.95. Similar results are found for the early time NT treatment as illustrated by Figure 5.2(a). The CC values (Table 5.2) range from about 0.8 to 0.87. AAD values are slightly larger for the NT t=day 8 simulation and range

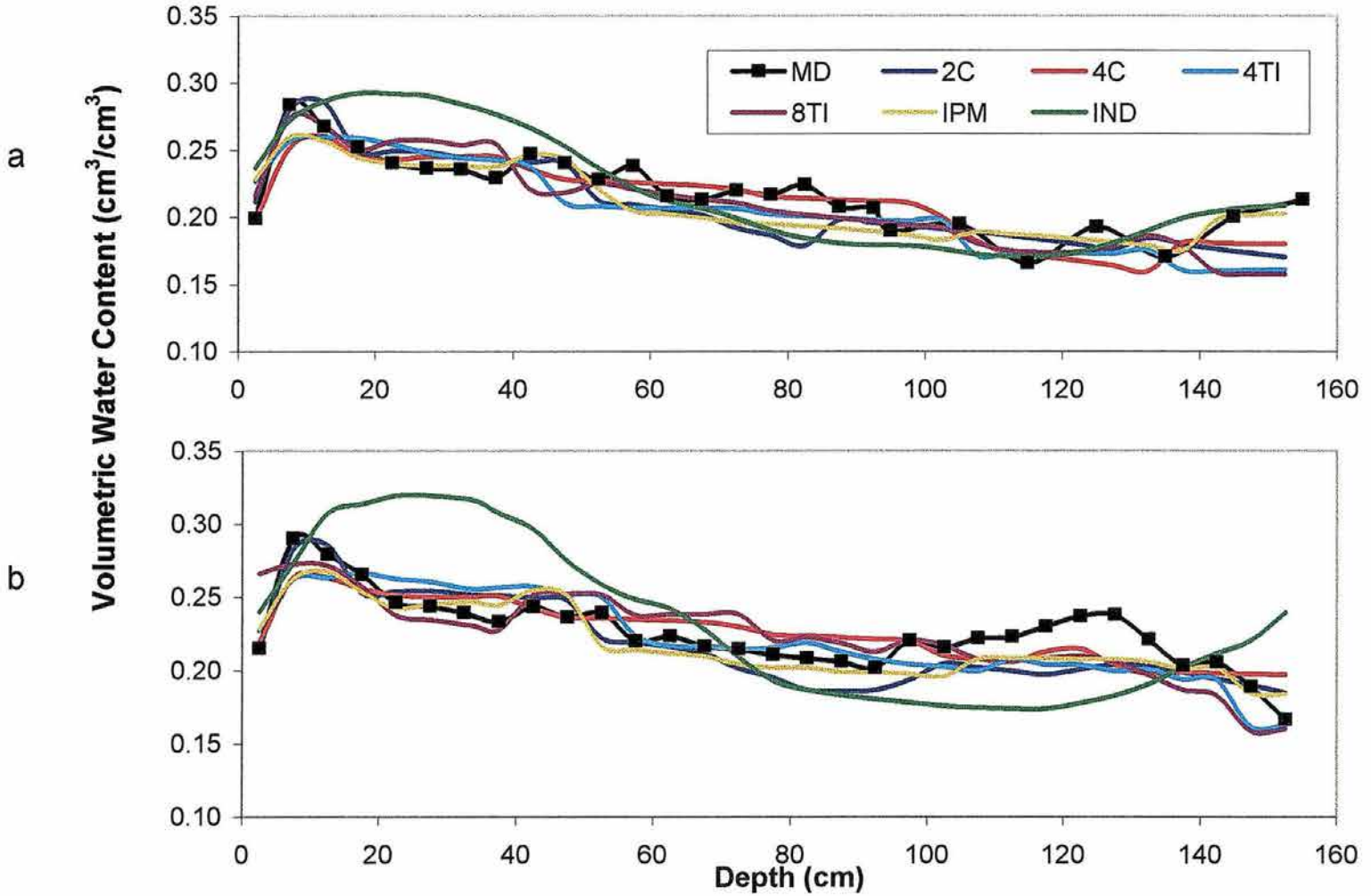

Figure 5.1. Observed and predicted volumetric water content profiles for tilled treatment at 8 days after application (a) and 22 days after application (b).

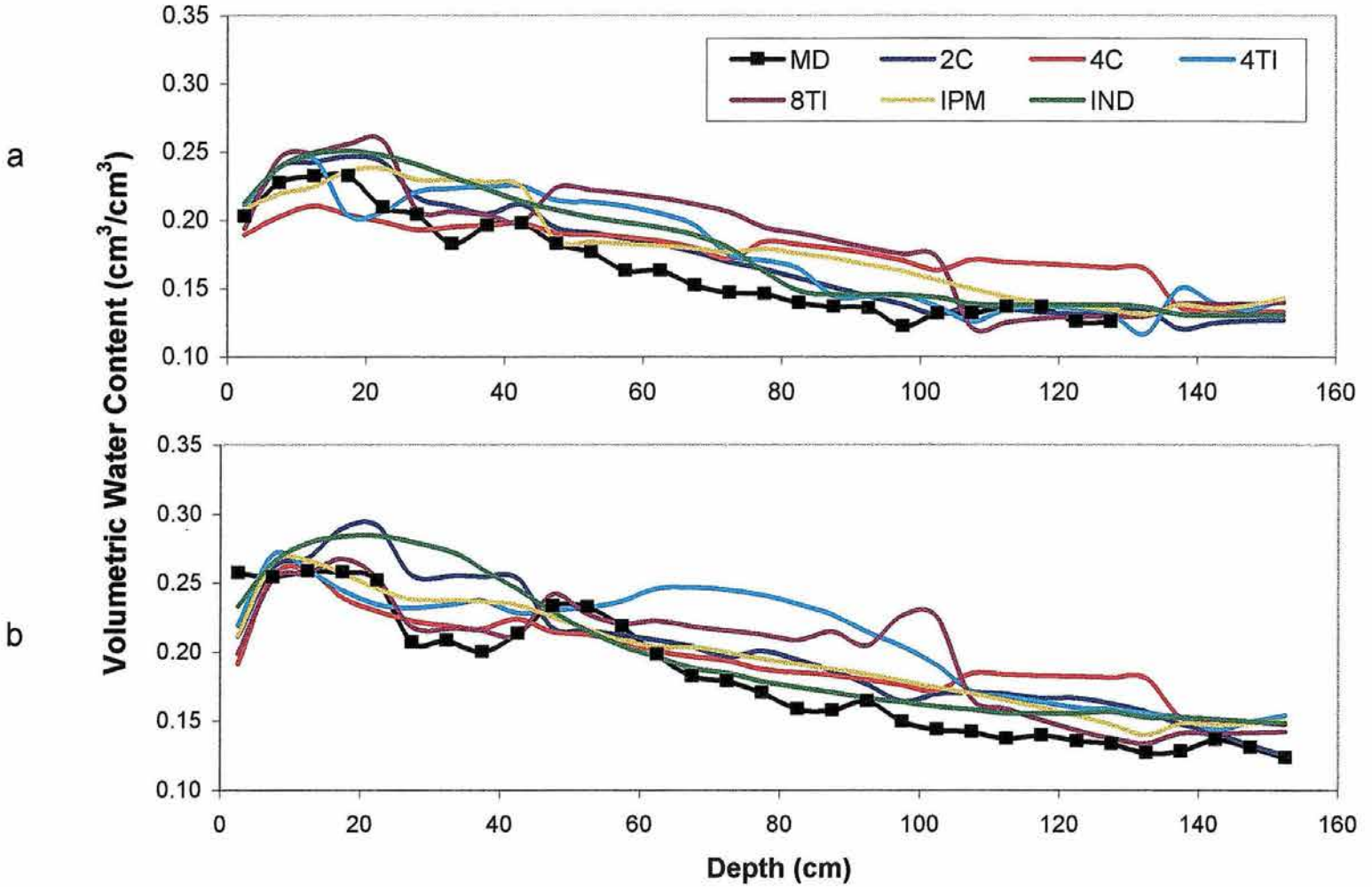

Figure 5.2. Observed and predicted volumetric water content profiles for No-Till Treatment at 9 days after application (a) and 23 days after application (b).

from 2.6 to 4.4 percent volumetric water content. All of the simulations over-predict θ_v from 50 to 100 cm soil depth. The IND input simulates the measured data quite well and has a correlation value of 0.84.

Water content profiles generated for the simulated times 21 and 22 days (T and NT treatments, respectively) after the start of the experiment are shown by Figures 5.1(b) and 5.2(b). The IND simulation for the T treatment is starting to deviate from the measured profile ($\Delta\theta$=0.10) and the correlation has dropped off to about 0.63. However, AAD values from Table 5.1 indicate that the IND simulated profile is predicting water contents that on average are within about 4.5 percent of the observed data. In addition, correlation between the IND simulation for the NT treatment and the observed NT data is still around 0.8. The remainder of the methods in the T simulation are predicting water contents within several percent of the measured values and their CC values range from about 08 to 0.93 percent. Correlation coefficients from the NT simulations at day 23 are slightly lower than those of the T treatment and range from about 0.76 to 0.86 percent. Data from Table 5.1 also indicates that the AAD values are greater for the NT simulations than the T simulations, ranging from 4.9 to 6.6 percent. We can see from the figures that the IND data produces much smoother curves, due to minimal changes in the parameter values with soil depth.

As the simulation time increased to 36 and 37 days (time for T and NT simulations, respectively) correlation between the simulated water content

Table 5.2. Correlation Coefficients (R^2) for comparisons of water content and solute concentration. MD corresponds to the measured data.

No-Till Treatment							
Concentration Correlation							
Measured Data		**Method**					
Date	MD	2C	4C	4TI	8TI	IPM	IND
9	1.000	0.995	0.997	0.992	0.992	0.992	0.976
23	1.000	0.921	0.933	0.946	0.877	0.966	0.907
37	1.000	0.911	0.957	0.952	0.971	0.922	0.498
118	1.000	0.694	0.685	0.734	0.933	0.632	0.239
Water Content Correlation							
Measured Data		**Method**					
Date	MD	2C	4C	4TI	8TI	IPM	IND
9	1.000	0.834	0.823	0.867	0.803	0.822	0.835
23	1.000	0.802	0.816	0.756	0.765	0.855	0.805
37	1.000	0.774	0.526	0.542	0.598	0.642	0.289
118	1.000	0.673	0.572	0.721	0.621	0.631	0.474

Till Treatment							
Concentration Correlation							
Measured Data		**Method**					
Date	MD	2C	4C	4TI	8TI	IPM	IND
8	1.000	0.995	0.991	0.988	0.994	0.998	0.991
22	1.000	0.857	0.843	0.867	0.832	0.809	0.947
36	1.000	0.833	0.831	0.812	0.802	0.748	0.506
117	1.000	0.928	0.913	0.947	0.807	0.843	0.223
Water Content Correlation							
Measured Data		**Method**					
Date	MD	2C	4C	4TI	8TI	IPM	IND
8	1.000	0.946	0.839	0.875	0.835	0.886	0.801
22	1.000	0.893	0.874	0.810	0.824	0.931	0.624
36	1.000	0.754	0.779	0.575	0.547	0.786	0.235
117	1.000	0.793	0.814	0.778	0.682	0.864	0.455

profiles and the measured profiles for both T and NT treatments dropped off dramatically, especially for the IND simulation. Figures 5.3(a) and 5.4(a) show the drastic change in simulation accuracy for the day 36 and 37 simulations. Correlation coefficients for the T soil range from 0.24 to 0.79, with the IND giving the lowest CC and the IPM giving the highest CC. This is consistent with AAD values (Table 5.1) that range from 0.077 for the IND to 0.017 for the IPM. Thus, on average, there is less than 2 percent difference in volumetric water content between the IPM predicted data and the observed data (T soil). The 4TI and 8TI CC values dropped substantially to 0.58 and 0.55, respectively and their AAD values have increased from about 2.5 percent to around 5 percent. The same trend is seen for the NT soil. Correlation values for the 4C, 4TI, and 8TI methods dropped below 0.6 and the IND CC plummeted to 0.29. The AAD values range from about 4 percent for the 2C method, to over 9 percent for the IND method. The 2C simulation predicts the water content profile fairly well, with a CC of 0.77. Overall, the IPM and core data (2C and 4C) better simulate the observed data than the 4TI, 8TI, and IND data for both the T and NT soils. The IND simulation looked promising through the first 22 to 23 days, but fails miserably at simulating the day 36 data.

By simulation day 117 and 118 simulations for the T and NT soils, respectively, the simulated water content profiles come back into line with measured profiles (Figs. 5.3(b) and 5.4(b)). The CC values for the T treatment range from a low of 0.46 for the IND method to a high of 0.86 for the IPM

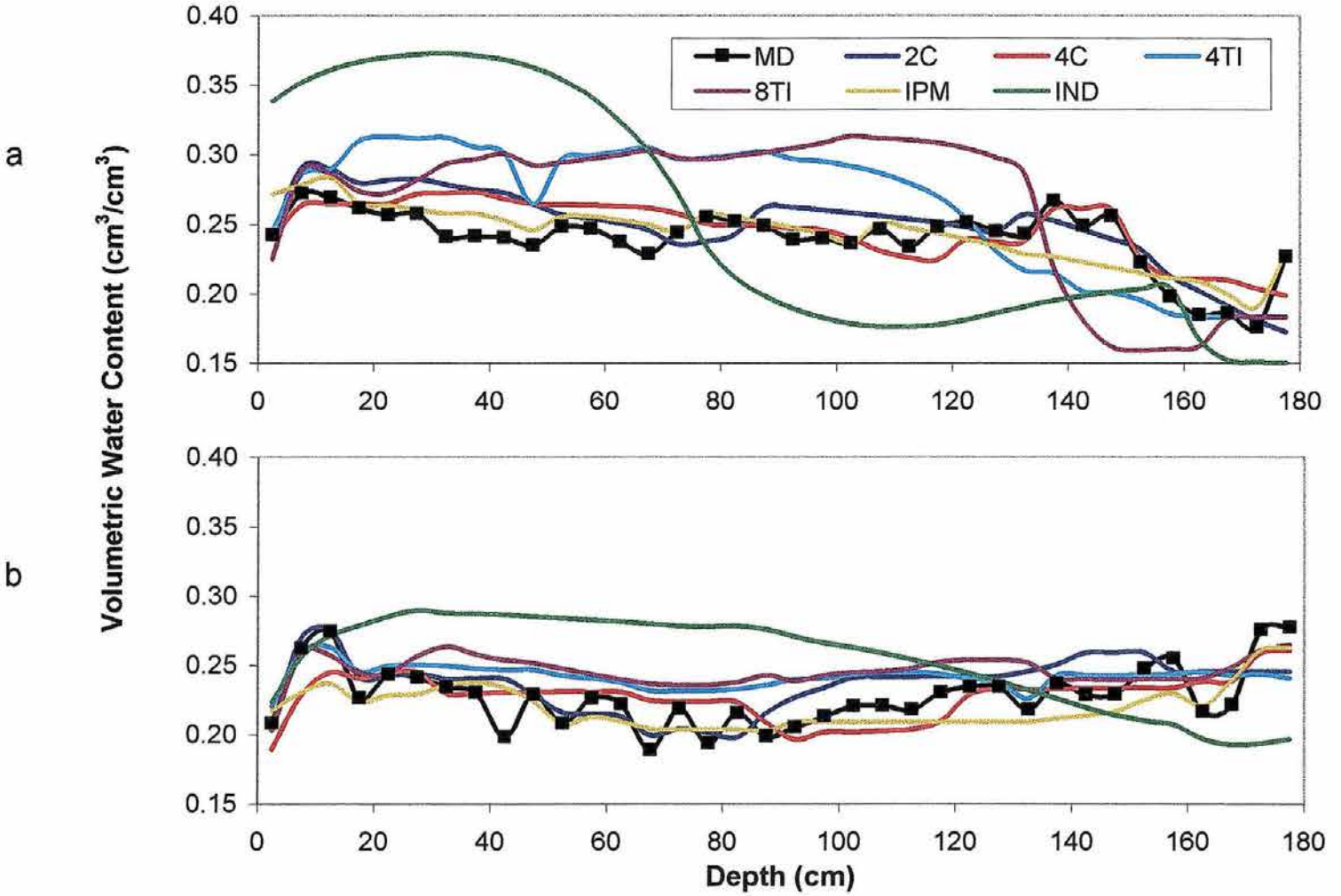

Figure 5.3. Observed and predicted volumetric water content profiles for tilled treatment at 36 days after application (a) and 117 days after application (b).

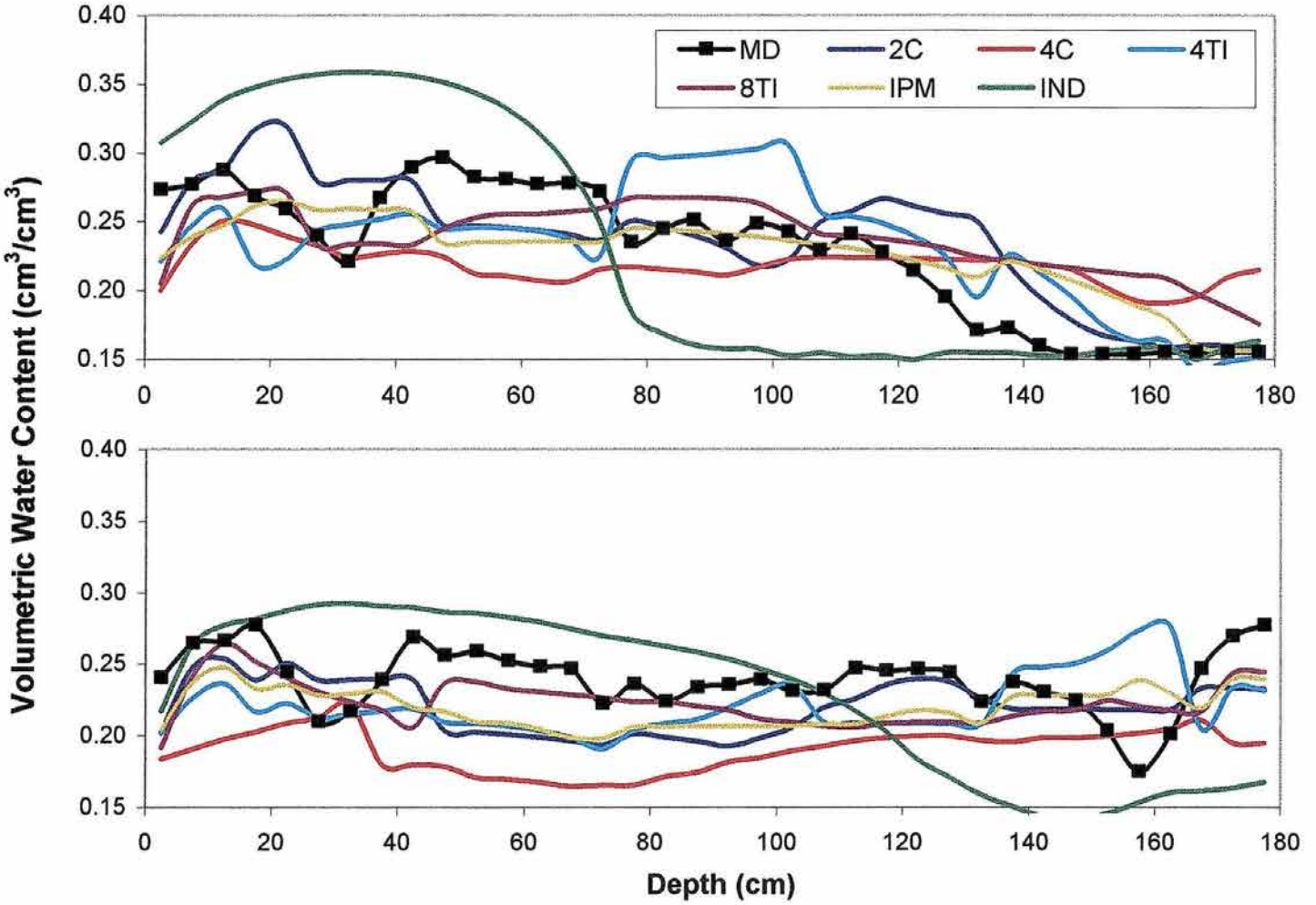

Figure 5.4. Observed and predicted volumetric water content profiles for No-Till Treatment at 37 days after application (a) and 118 days after application (b).

method. Even though the correlation for the IND data is low, overall the simulated water content profile is not drastically different from the measured profile and the AAD value for the IND is only about 0.05. Large deviations in water contents ($\Delta\theta$=0.1) remain in the IND, but the profile no longer has the sharp changes in θ near 70 cm soil depth evident in the day 36 simulation. Correlation coefficients for the NT data are lower than those of the T treatment; CC values range from 0.47 for the IND to 0.72 for the 4TI method. The AAD values for both the T and NT simulations are smaller than for the t=day 36/37 AAD values; values range from 0.01 to about 0.05. The correlation data suggests that the simulated profiles fit the observed data poorly for both the T and NT treatments. The deviations ($\Delta\theta$) are typically 0.05 or less except for the IND and 4TI where larger deviations are observed.

The questions again rise as to how different is "different" and what limits are we willing to accept given the amount of effort required to obtain the data. General indications from the water content data reviewed in this section, are that the most rigorous and time consuming method, meaning the IPM method, does not always provide the best or most accurate prediction of water content. With the exception of the day 36 and 37 data, most of the methods do a fair to good job of simulating the measured water content profiles throughout the given time periods. Even the IND simulations, that have low correlation values may be accurate enough to provide useful information about the movement of water under certain circumstances. Given the amount of effort required, the IND

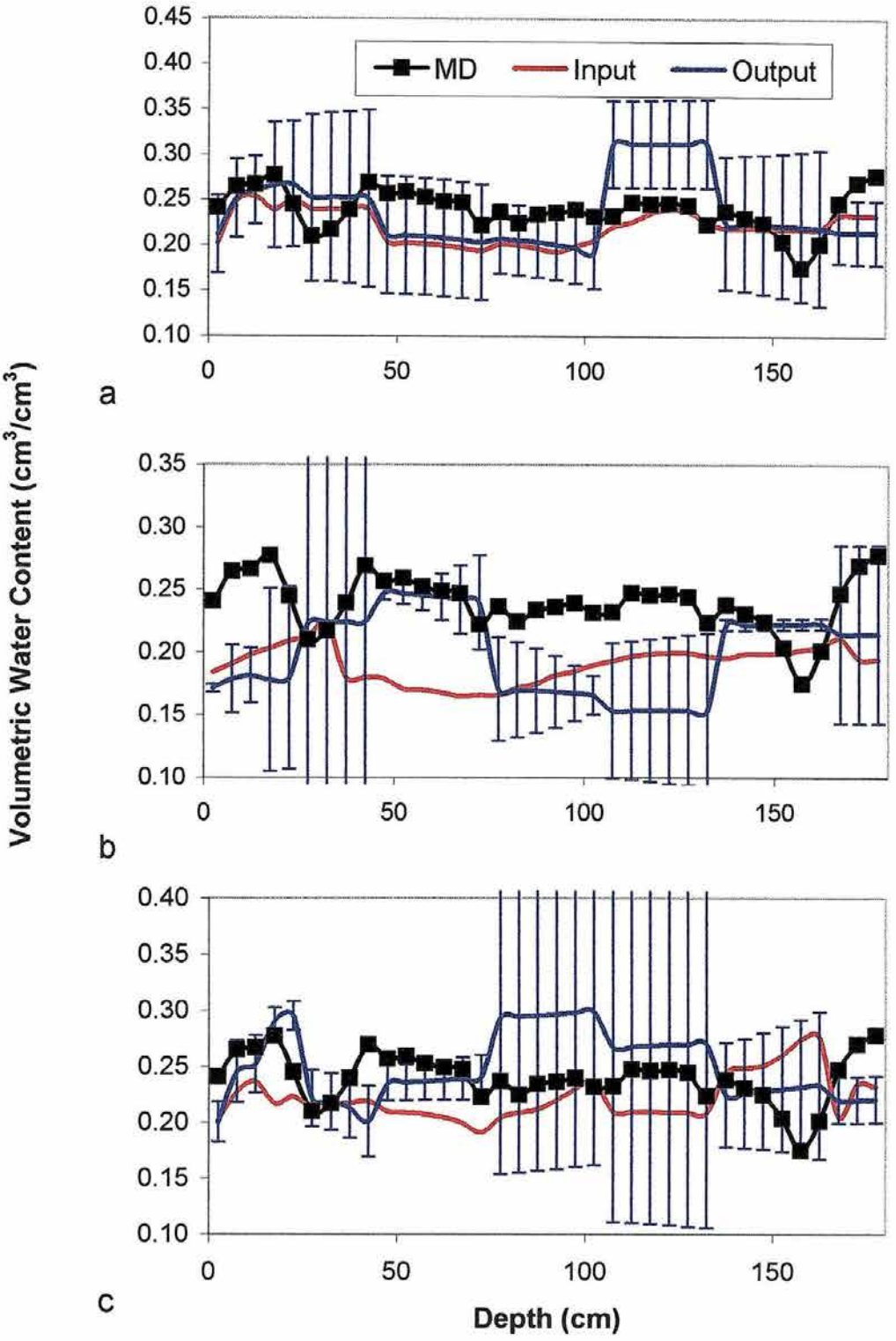

Figure 5.5. Water content profiles produced using averaged input parameters and averaged output water content profiles for NT soil at day 118. (a=2C, b=4C, c=4TI)

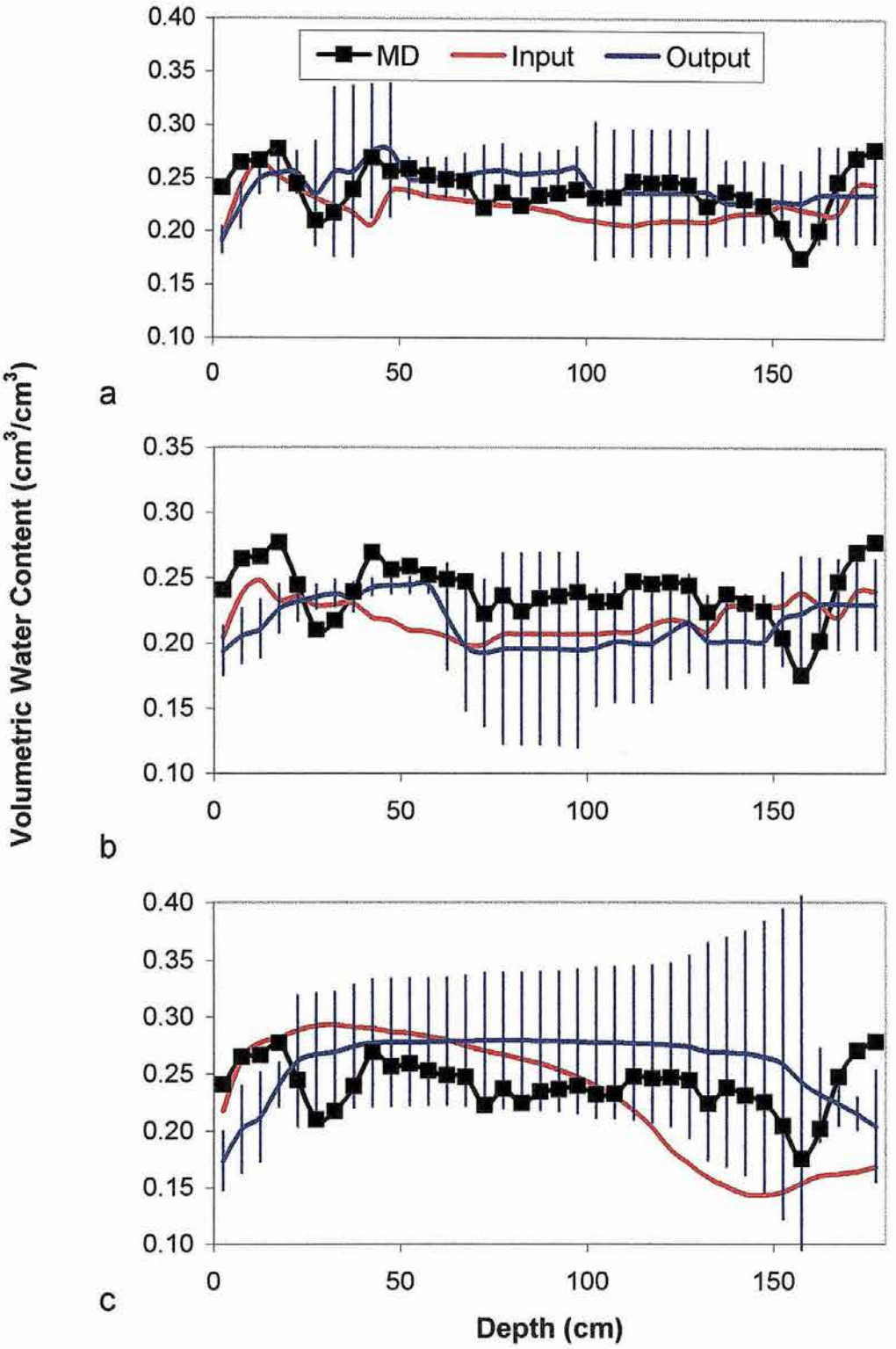

Figure 5.6. Water content profiles produced using averaged input parameters and averaged output water content profiles for NT soil at day 118. (a=8TI, b=IPM, c=IND)

method may be good as a first approximation and can be setup in hours instead of days or weeks. The focus of this dissertation is the effect if hydraulic property estimation on the predictive accuracy of solute movement. The sometimes poor prediction of water movement should make us somewhat skeptical about our prospects for successfully predicting solute movement.

In addition, water content profiles generated using average (representative) values were contrasted with water content profiles generated by averaging the output profiles of the individual repetition data (Figs. 5.5 and 5.6). The figures only show the profiles for the NT treatment, but the trends are similar for both tillage treatments. The output data has associated confidence limits, shown in the figures, that indicate the degree of variability in the predictions. The 2C, 8TI and IPM data show the least amount of predictive variability (Fig. 5.6) and the 4C, 4TI and IND tend to show the greatest variability. The likelihood of predicting very poorly fit water content data using a single measured properties data set from the 4C, 4TI, or IND is very high. It is clear that the averaging methods do not produce the same results, and that the averaged curves differ more for those methods exhibiting more variability (4C, 4TI, and IND).

5.2 Comparison of Bromide Concentration Profiles as Predicted by Parameter Estimation Method

There have been virtually no publications investigating the effect of the method of parameter estimation of hydraulic properties on model predictive

accuracy in terms of solute transport. While the previous section discussed simulating water movement, this section will focus on simulation of solute movement. Comparisons between simulated and measured concentration profiles are ranked or judged using some additional criteria including center of mass calculations, and the amount of chemical mass in the system. Keep in mind when looking at the concentration profiles, that they are linked to the water content profiles discussed in the previous section by the mass of chemical in the system (i.e. mass = concentration x water content).

Figures 5.7 through 5.10 show bromide concentration profiles for both T and NT treatments over 117 and 118 days, respectively. Solute concentration profiles were generated for the same times as the water content profiles. Figures 5.7(a) and 5.8(a) show predicted and measured Br- profiles for day 8 and 9 for the T and NT treatments, respectively. All of the simulations are similar and predict the measured profile well for the T treatment. Again, for the NT treatment, all of the methods give similar results, but the simulations do not fit the data as well in the upper 20 cm of the soil profile. However, all the simulations are highly correlated , 90 percent or higher, to the measured data. This is because the correlation is over the entire soil profile and the simulations fit very well below about 30 cm depth where the concentration is essentially zero.

The center of mass (CM) of the measured Br- plume (Table 5.3) is at 9.3 cm and at 11.5 cm for the T and NT treatments, respectively. All of the

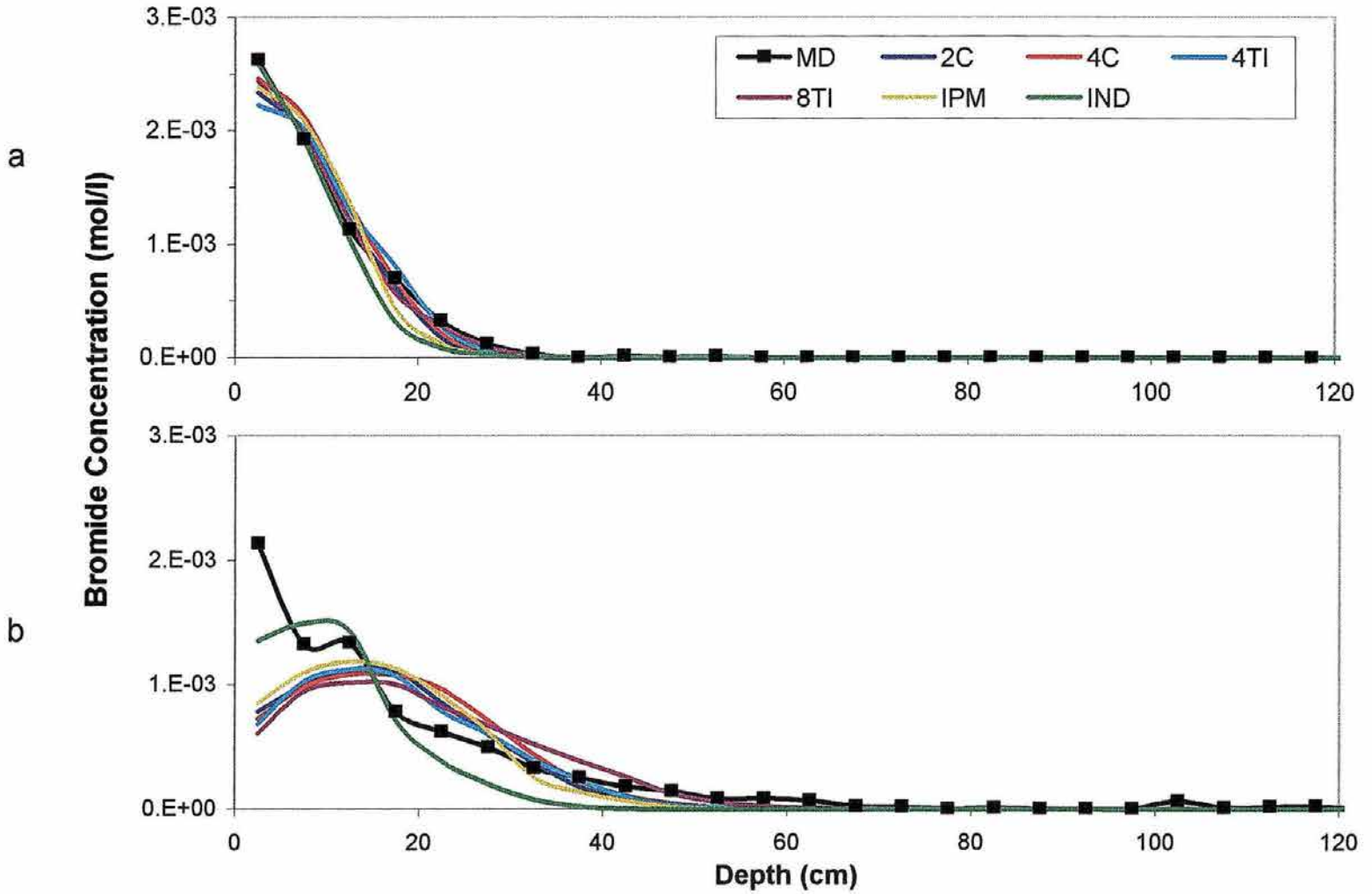

Figure 5.7. Observed and predicted Bromide concentration profiles for tilled treatment at 8 days after application (a) and 22 days after application (b).

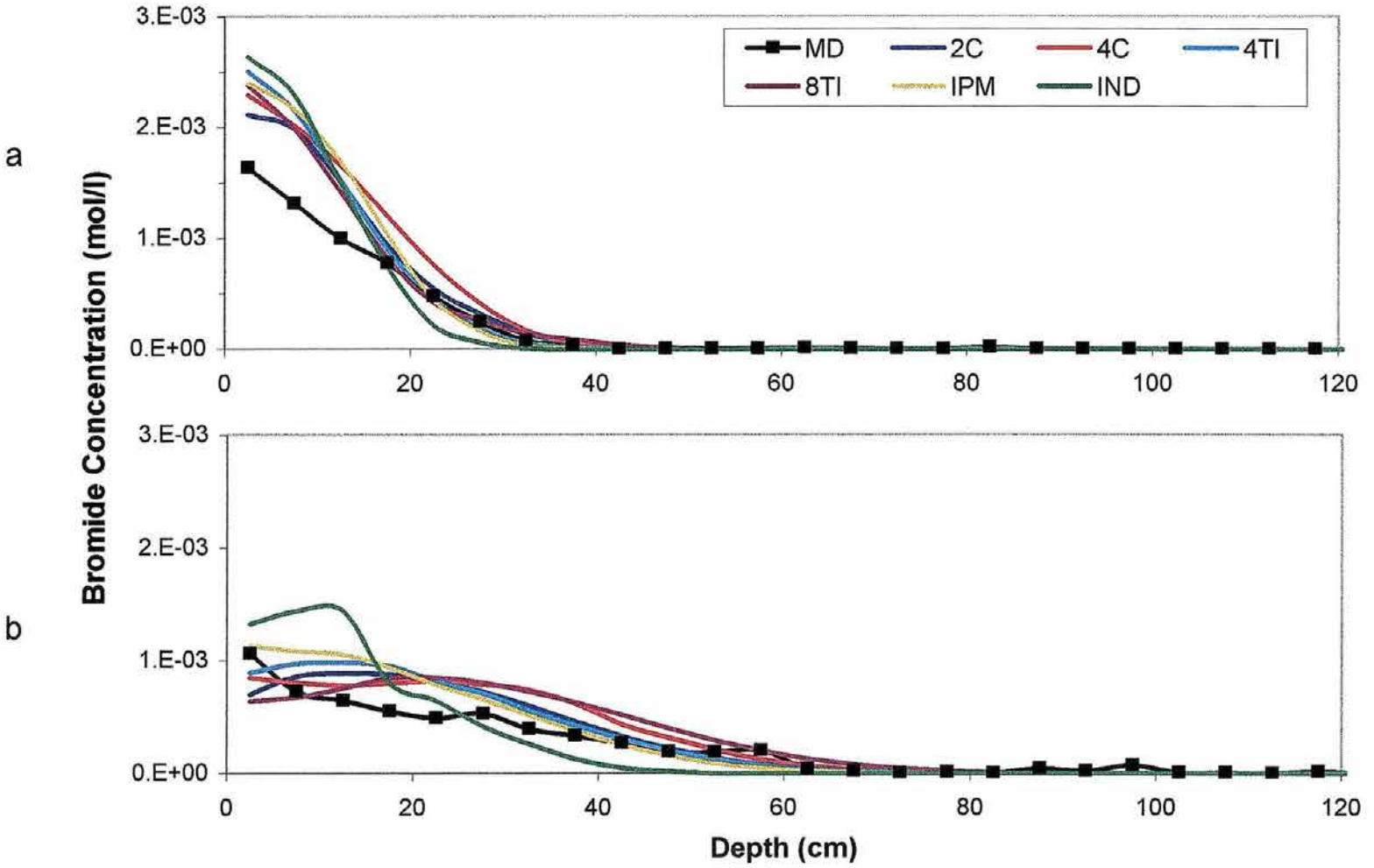

Figure 5.8. Observed and predicted Bromide concentration profiles for No-Till Treatment at 9 days after application (a) and 23 days after application (b).

simulations for the T treatment predict the center of mass to be within about 2 cm of the measured center of mass. The IND method shows the most lag at 7.3 cm and the 4TI method over-predicts the CM slightly at 9.4 cm. Deviations in the calculated CM's are greater for the NT simulations than for the T simulations. The IND simulation predicts the CM to be 8.7 cm, but the 2C and 4C methods are very close at 11.2 cm and 11.5 cm, respectively.

Mass calculations (Table 5.3) for all the simulations are equal to the actual mass of the applied Br- solute. The calculated mass from the simulations are different from the calculated mass of the measured data, due to incomplete recovery of bromide during the solute transport experiments. Mass recovery of bromide changes from date to date during the experiment. Mass recovery percentage was lowest, at about 78 percent, for day 8 in the NT soil. The remainder of the measurement dates have good mass recovery between 85 and 110 percent. Masses are slightly higher in the NT treatment due to the application of more bromide during that experiment.

Figures 5.7(b) and 5.8(b) show the day 22 and 23 simulations for the T and NT soils, respectively. It is evident from these plots that Br- has moved deeper for the NT soil than the T soil. A more detailed comparison of the bromide movement in the tilled and non-tilled soil will be presented later in this chapter. With the exception of the IND method, the simulations predict relatively smooth, gaussian like concentration profiles. The IND simulation matches the T measured Br- profile fairly well in the upper 20 cm (even emulating the solute

Table 5.3. Calculated mass (MASS, mmol/cm^2), center of mass (CM, cm), and variance (VAR, cm2) for each method and treatment. MD corresponds to the measured data.

No-Till Soil								
Measured Data			**Method**					
	Date	MD	2C	4C	4TI	8TI	IPM	IND
MASS	9	0.006	0.009	0.009	0.009	0.009	0.009	0.009
CM	9	11.48	11.24	11.51	9.73	10.94	10.11	8.68
VAR	9	81.86	61.25	69.06	48.13	69.82	46.27	34.05
MASS	23	0.008	0.009	0.008	0.009	0.009	0.009	0.009
CM	23	23.15	22.11	22.90	20.33	27.18	18.67	13.83
VAR	23	501.65	186.37	244.46	203.69	266.16	172.55	88.62
MASS	37	0.009	0.009	0.009	0.009	0.009	0.009	0.008
CM	37	55.05	47.20	57.57	52.92	58.28	47.80	29.72
VAR	37	550.56	730.34	789.44	753.31	758.70	659.85	279.95
MASS	118	0.009	0.009	0.009	0.009	0.009	0.009	0.008
CM	118	106.11	86.35	88.52	92.04	103.55	77.48	45.79
VAR	118	1276.83	1580.38	1490.83	1100.82	1559.67	1342.44	745.26
Till Soil								
Measured Data			**Method**					
	Date	MD	2C	4C	4TI	8TI	IPM	IND
MASS	8	0.008	0.008	0.008	0.008	0.008	0.008	0.008
CM	8	9.27	8.58	8.83	9.42	8.98	7.84	7.29
VAR	8	47.95	30.83	33.40	35.43	38.13	28.32	28.29
MASS	22	0.010	0.008	0.008	0.008	0.008	0.008	0.008
CM	22	16.95	16.74	18.10	17.25	20.10	15.84	11.98
VAR	22	293.01	97.62	104.80	108.12	143.86	89.62	54.02
MASS	36	0.008	0.008	0.008	0.008	0.008	0.008	0.008
CM	36	40.34	40.50	43.78	44.48	47.74	35.63	26.51
VAR	36	780.68	361.45	393.67	545.19	379.18	463.38	182.75
MASS	117	0.007	0.008	0.008	0.008	0.008	0.008	0.008
CM	117	77.07	70.54	72.91	74.09	89.52	74.04	37.60
VAR	117	1371.85	859.83	785.71	895.81	900.18	718.46	316.96

being held up near the surface), but is a poor representation below 20 cm. The other methods predict that the solute should have moved away from the surface. As a consequence, the IND data are highly correlated to the measured T data at 0.95. The other simulations are have CC values ranging from 0.8 to 0.9. Even though the CC values look good, Table 5.3 shows that the center of mass of the IND simulation is lagging the CM of the measured T data by about 5 cm. The 8TI simulation has over-predicted mass movement to put the CM at 20.1 cm, almost 3 cm past the measured value. All other simulations are within about 1 cm of the measured CM value. The CC values remain high because the simulations predict the nearly zero bromide concentration values fairly well at depths below 40 cm in the soil profile.

The IND simulation of the NT treatment again predicts that the solute has not moved from the near surface soil zones (Figure 5.8(b)). The CM of the IND simulation is at 13.8 cm, almost 10 cm behind the CM of the measured NT data. Despite the overall poor representation provided by the IND, the correlation value for the IND simulation is 0.90. This result indicates that correlation alone is not a reliable indices for comparing predictive accuracy of the methods. The IPM simulation under-predicts CM by about 4 cm while 8TI over-predicts CM by about 4 cm. The 2C, 4C, and 4TI simulations are within about 2 cm of the measured CM. The correlation values for the methods are all about 0.90. With the exception of IND, all the hydraulic property sets are resulting in similar and fairly accurate predictions of the br- profile in the T and NT soil.

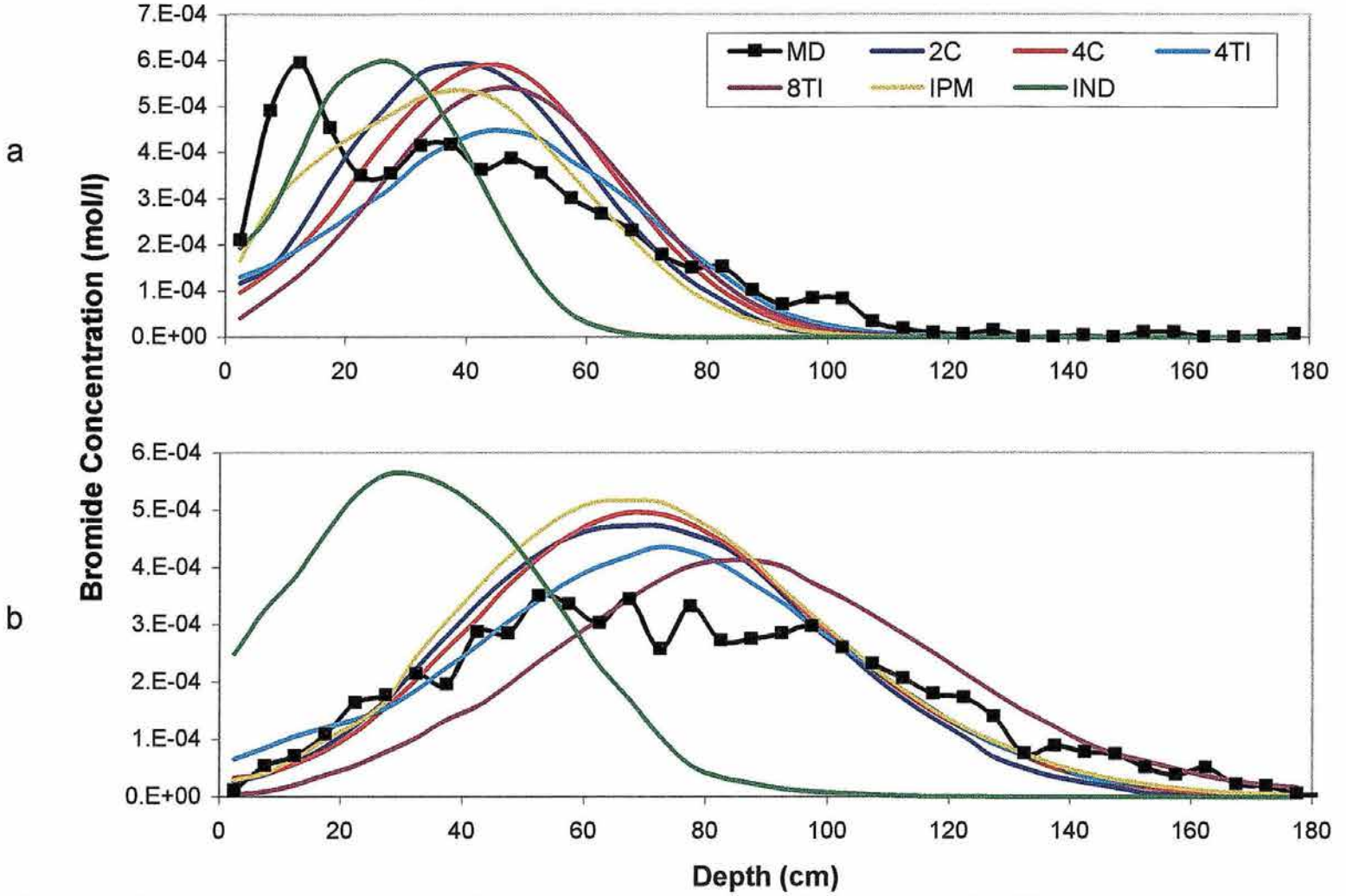

Figure 5.9. Observed and predicted Bromide concentration profiles for tilled treatment at 36 days after application (a) and 117 days after application (b).

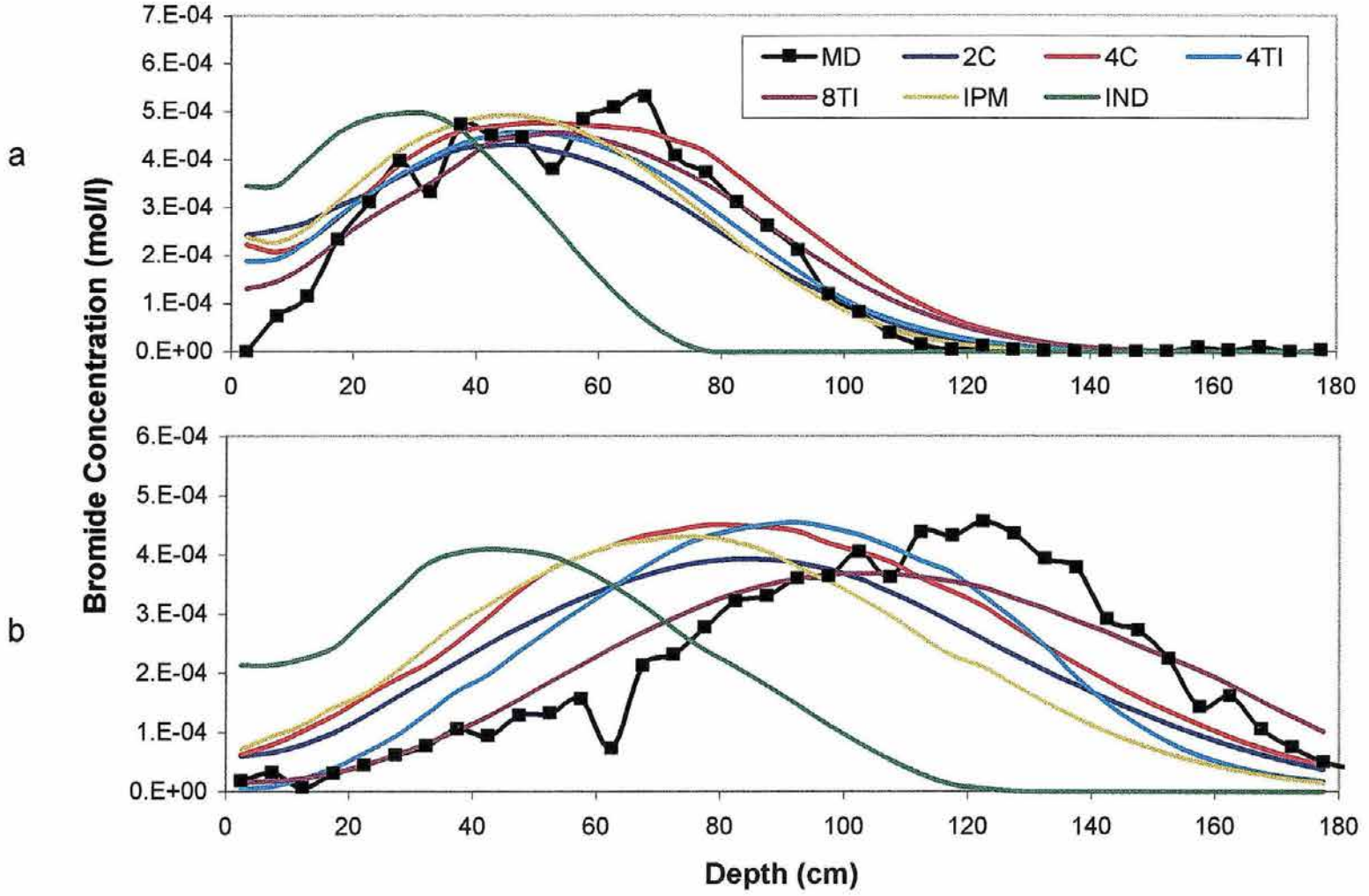

Figure 5.10. Observed and predicted Bromide concentration profiles for No-Till Treatment at 37 days after application (a) and 118 days after application (b).

Simulated and measured Br- concentrations for days 36 and 37 are shown in Figures 5.9(a) and 5.10(a), respectively. There are some dramatic differences in the movement of the Br- solute between the T and NT treatments. The solute has been held up in the tillage zone and there is almost a split in the solute plume at the 25 cm soil depth. None of the simulations match the measured Br- profile for the T soil very well, as each ignores the high bromide concentration in the tillage zone. The correlation values have dropped to around 0.8, except for the IND which dropped to around 0.5. The CM of the measured data (Table 5.3) is 40.3 cm. The 2C simulation is almost dead-on the mark with a predicted CM of 40.5 cm. The 4C, 4TI, and 8TI simulations over-predict the CM with values at 43.8, 44.5, and 47.7 cm, respectively. The IPM and IND simulations are under-predicting the CM with values at 35.6 and 26.5 cm, respectively. All of the simulations underestimate the dispersion (variance).

Figure 5.10(a) shows the NT simulations at day 37. Each method, except the IND, appear to simulate the measured data well. It is apparent that the IND CM is well short of the measured CM and that is confirmed by inspection of Table 5.3. The CM of the measured data is at 55.1 cm and the CM of the IND simulation is at 29.7 cm, well below the measured value. The 2C, 4TI, and IPM simulations have under-predicted the CM by about 7, 2, and 6 cm, respectively. The 4C, and 8TI simulations have over predicted the measured CM by about 3 cm. Correlation values for the NT simulations remain above 0.9, except for the IND method which dropped to about 0.5. Through the first 36 to 37 days of

simulation, most of the methods, with the exception of the IND, have predicted the Br- movement well. The trend has been that the predictive accuracy of the IND method gets progressively worse with time.

Moving forward in the simulation to days 117 and 118, the results do not get any better for the IND simulation. The CM of the IND method is almost 40 cm behind the CM of the T soil and 60 cm behind for the NT soil. The poor predictive fits of the IND simulations can be clearly seen in Figures 5.9(b) and 5.10(b). The CC values for the IND fits have dropped to 0.24 and 0.22 for the NT and T treatments, respectively. The 8TI simulation for the NT treatment fits quite well and predicts a CM (103) close to the measured CM of 106 cm. As would be expected the 8TI data correlates very well to the measured NT data. In the tilled plots, the 8TI simulation over-predicts the CM by about 12 cm, but still correlates with the measured data at 0.8. The 2C and 4C simulations are very similar and predict CM's of 86.4 and 88.5 cm for the NT simulation. These values are about 20 cm short of the measured CM. The 2C and 4C methods have better predictions of the CM of the T treatment and are only about 7 and 4.5 cm short of the measured CM. The simulations for the 2C and 4C methods fit the T data quite well and are highly correlated to the measured data. Overall, the 4TI simulation fits the measured data of the T treatment the best. The CM is only 3 cm short of the measured CM, and the simulated concentration profile correlates highly with the measured data. The CM of the IPM is also very close

to the CM of the measured data, but the concentration data isn't as highly correlated as the 4TI data.

In summary, when considering all sampling times in both plots, the method of hydraulic property estimation did affect predictive accuracy, but the differences were sometimes subtle. With the exception of the IND method, the alternative approaches yielded similar predictions with no method distinguished as consistently superior. Importantly, the most rigorous method (IPM) for determining the hydraulic properties did not result in the best prediction of solute movement. The results for the IPM are not bad, but the other methods, with the exception of the IND method, result in simulations that are as accurate, if not more accurate, than those of the IPM. While the IND method gives favorable results for the prediction of water movement, the same cannot be said for solute movement. If the simulation were only over about 20 days, the IND method may be appropriate, but as the simulation time increased so did the error. Finally, irrespective of the method employed, the model failed to simulated the bromide profile in the two cases; first, the model underestimated early-time bromide hold-up in the tillage zone, and second, the model underestimated long-time advection in the non-tilled soil.

5.3 Tillage Treatment Effects

Obvious differences in the movement of the bromide tracer were observed between the T and NT treatments. Figures 5.11 and 5.12 show the

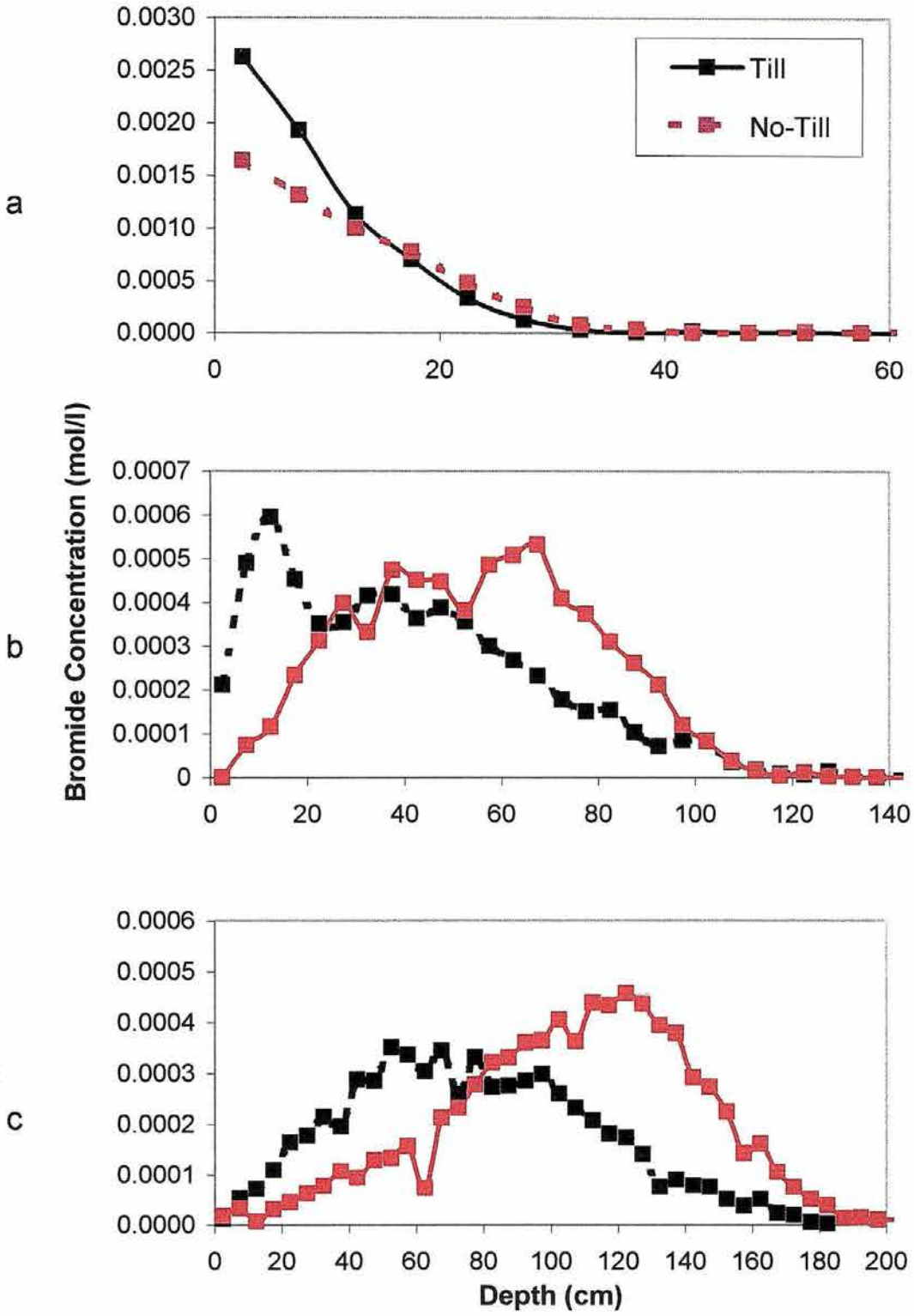

Figure 5.11. Measured Bromide concentration profiles for the T and NT treatments at 8and 9 days (a), 22 and 23 days (b) , and 117 and 118 days (c), respectively.

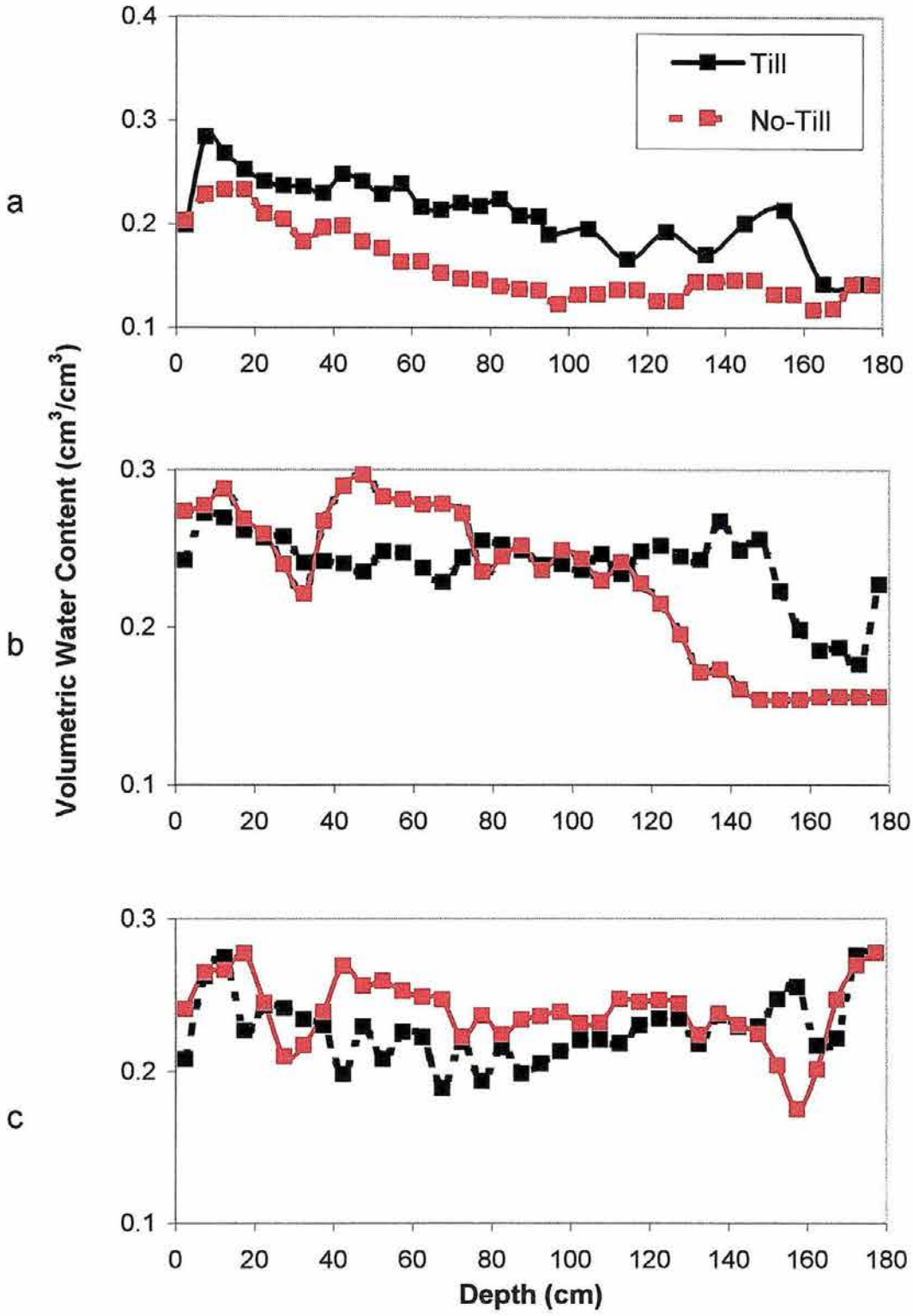

Figure 5.12. Measured water content profiles for the T and NT treatments at 8 and 9 days (a), at 22 and 23 days (b) , and at 117 and 118 days (c), respectively.

measured water content and bromide concentration profiles for the two treatments. Inspection of Figure 5.11 shows that the tillage zone appears to be retarding the movement of the tracer. By day 118, the CM of the bromide plume in the NT plot is 106 cm versus 77 cm in the tilled soil. Retardation of bromide movement through the tillage zone may be due to the loss of structure and the creation of dead-end or unconnected pore space by tillage. The same effect was seen by Bandaranayake et al., (1998) where tillage reduced the leaching of chemigated bromide. The chemigated solute was retained in the tillage zone and subsequent leaching moved the solute, but not as deep as seen in the non-tilled soil. Inspection of the plots in Figure 5.12 reveals that the water content profiles of the T and NT treatments were very different near the beginning of the experiment 5.12(a) but similar near the end of the experiment 5.12(c). The initial water content profiles (Fig. 5.13) between 60 and 160 cm were quite different for the two tillage treatments. The T plot was initially wetter over the 60 to 160 cm depth. This may have been due to pre-study irrigation of the area to be tilled for the tillage treatment. The expected effect of the difference in the initial $\theta(z)$ would be to slow downward movement of bromide in the NT plot (relative to the T plot) since a larger portion of infiltered water would go toward increasing storage at the expense of drainage.

Examining the water balance for the T and NT treatments (Table 5.4), the net applied water (NAW) for the T and NT were 15.7 cm and 17.1 cm, respectively. Despite the slightly larger water input to the NT treatment, the

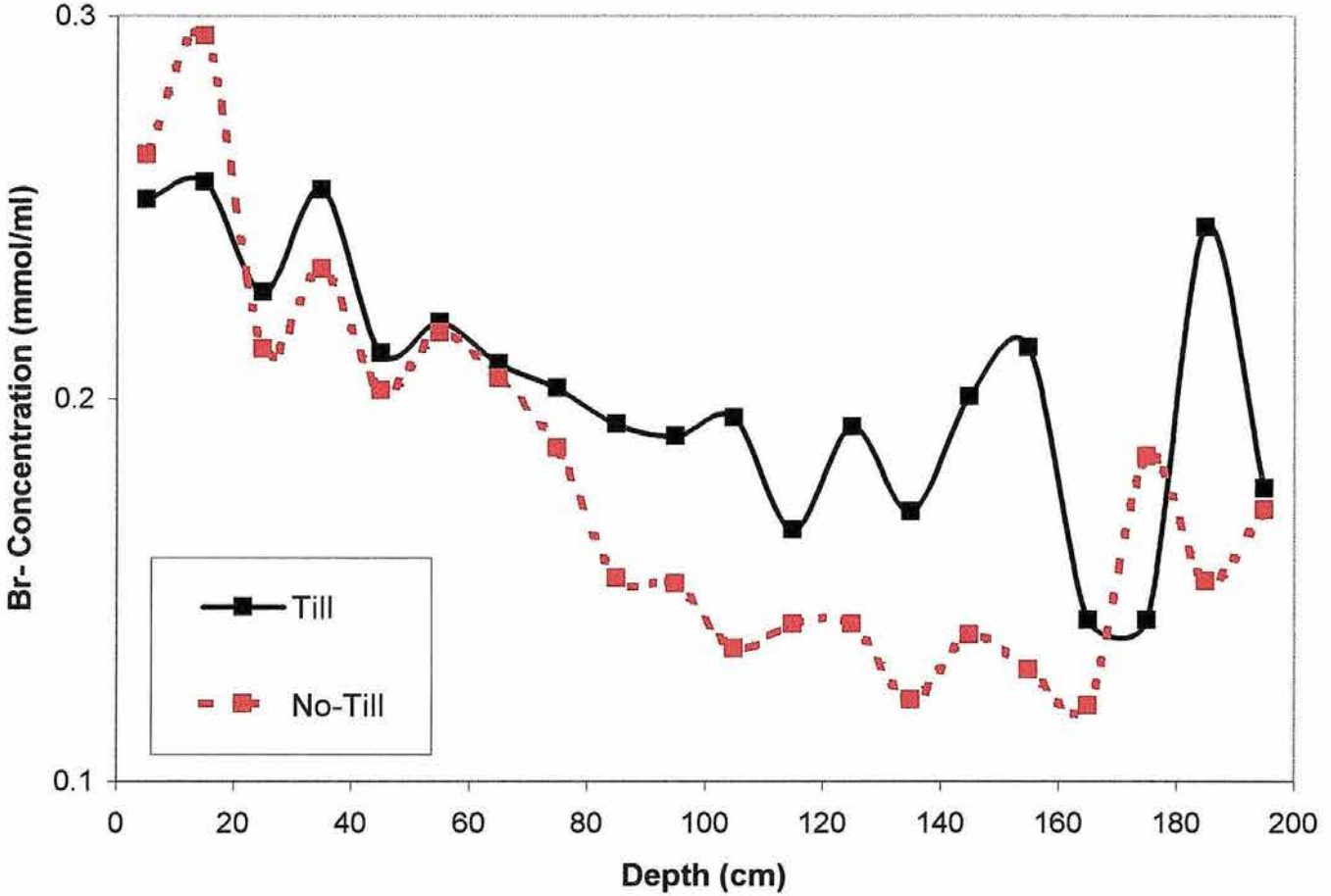

Figure 5.13. Water content profiles for the T and NT treatments at the beginning of the solute transport experiment (Day 0).

Table 5.4. Net applied water (NAW) and net drainage (ND) values predicted for each simulation run. Change in storge is NAW minus ND. NAW and ND for the measured data (MD) were calculated using atmospheric data and data from weighing lysimeters.

* Total volume of water (irrigation and precipitation) was 36.57 cm
** Total volume of water (irrigation and precipitation) was 39 cm
*** Estimated from (NAW-Change in Storage)

Simulation Method	Treatment	NAW (cm)	ND (Past 180 cm) (cm)	Change in Storage (cm)
MD	T	15.72 *	11.37 ***	4.35
2C	T	14.70	6.09	8.61
4C	T	13.70	10.01	3.69
4TI	T	19.00	7.36	11.64
8TI	T	21.90	11.2	10.7
IPM	T	13.20	10.4	2.8
IND	T	6.35	0.004	6.35
2C/IPM	T	15.10	2.61	12.49
4TI/IPM	T	20.90	6.4	14.5
8TI/IPM	T	17.30	3.97	13.33
2C/IND	T	16.10	2.84	13.26
2C-1 LAYER	T	9.30	1.03	8.27
2C-2 LAYERS	T	9.10	0.81	8.29
MD	NT	17.11 **	6.22 ***	10.89
2C	NT	16.70	0.985	15.72
4C	NT	10.80	6.49	4.31
4TI	NT	17.40	4.38	13.02
8TI	NT	17.50	11.10	6.40
IPM	NT	12.60	1.73	10.87
IND	NT	8.70	0.030	8.67
2C/IPM	NT	17.30	3.36	13.94
4TI/IPM	NT	24.70	8.67	16.03
8TI/IPM	NT	23.60	7.91	15.69
2C/IND	NT	17.60	3.01	14.59
2C-1 LAYER	NT	11.51	0.021	11.49
2C-2 LAYERS	NT	11.02	0.39	10.63

estimated net drainage (ND) below 180 cm depth was 11.4 cm for the T soil and only 6.2 cm for the NT soil. The seemingly contradicting result of greater drainage in the tilled soil than in the non-tilled soil, but with less resulting bromide displacement is consistent with; 1) tillage zone chemical retention, perhaps by bromide diffusion into dead-end pores, or 2) bypass chemical movement in the NT soil. Bypass flow has been discussed by several researchers to explain advanced chemical movement in NT soils. HYDRUS-2D uses a single region advection-dispersion model to describe solute transport. For comparing tillage systems, a mobile-immobile water model may be more appropriate. However, use of a two-region approach introduces new problems, particularly estimation of the immobile water fraction which can range from 0.25 to 0.952 (Jaynes et al., 1995, Casey et al., 1997). Angulo-Jaramillo et al. (1996) infer that the mobile water content may depend upon both the dynamics of water movement and the connectivity of pores. Thus, since the T system has less pore connectivity the immobile water content would appear to increase. Liwang and Selim (1997) used several non-equilibrium models to predict Atrazine transport and concluded that a second-order mobile-immobile model worked best to describe Atrazine transport. Another approach that might be used is to adjust the dispersivity to account for the solute being held-up in the tillage layer. However, that would require calibration to determine dispersivity values for each soil, something that was avoided during this study.

5.4 Factors Affecting the Predictive Accuracy of the HYDRUS-2D Model

Because of observed differences in the solute transport simulations, it is desirable to explore possible reasons for those differences and thereby identify possible improvements for the methods. Short of simply saying that there are differences in the hydraulic properties, how do those differences make one set of data a better predictor than the other for a given scenario.

Soil Surface Affects

It became apparent through trial and error that the hydraulic properties of the soil at the atmospheric boundary are critical in the prediction of water and solute movement. The amount of water that is infiltrated into the soil is controlled by the upper boundary condition (atmospheric), that in turn is controlled by the hydraulic properties of the surface soil. Atmospheric scientists have discovered the importance of surface soil hydraulic properties in modeling hydrological balances. This is evident by the increased focus on remote sensing of surface water content and evaporative flux. Saturated hydraulic conductivity is one the parameters that most effects mesoscale atmospheric models (Kim and Stricker, 1995).

One reason why the various simulations result in different center of mass displacement of bromide can be appreciated in Figures 5.14 and 5.15. Given that the amount of water applied (rainfall and irrigation) during each simulation is the same, we might expect that the net applied water would be similar. Net applied water (NAW) is defined as the applied water (cumulative rainfall and

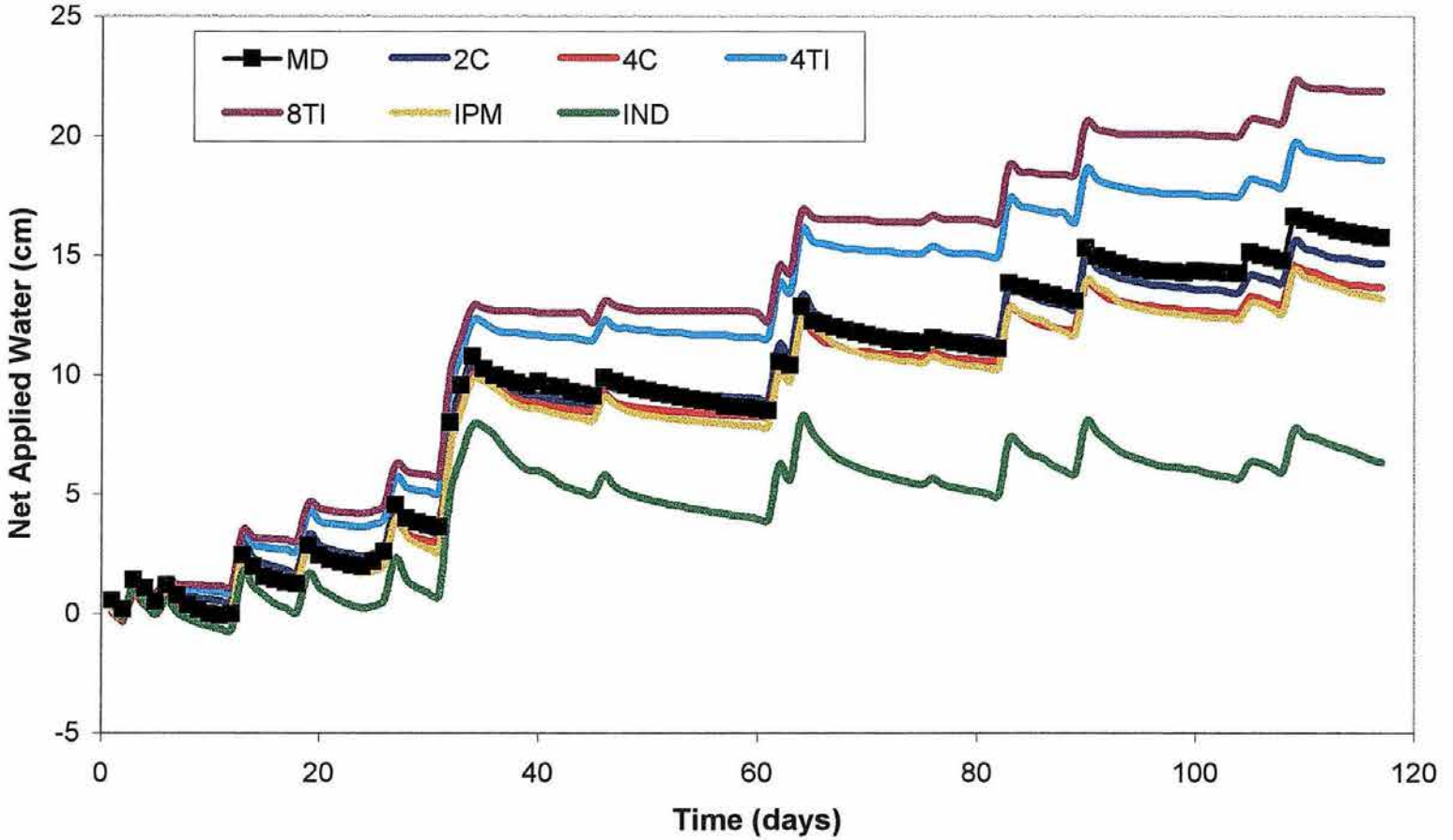

Figure 5.14. Water flux at the atmospheric boundary for the T treatment.

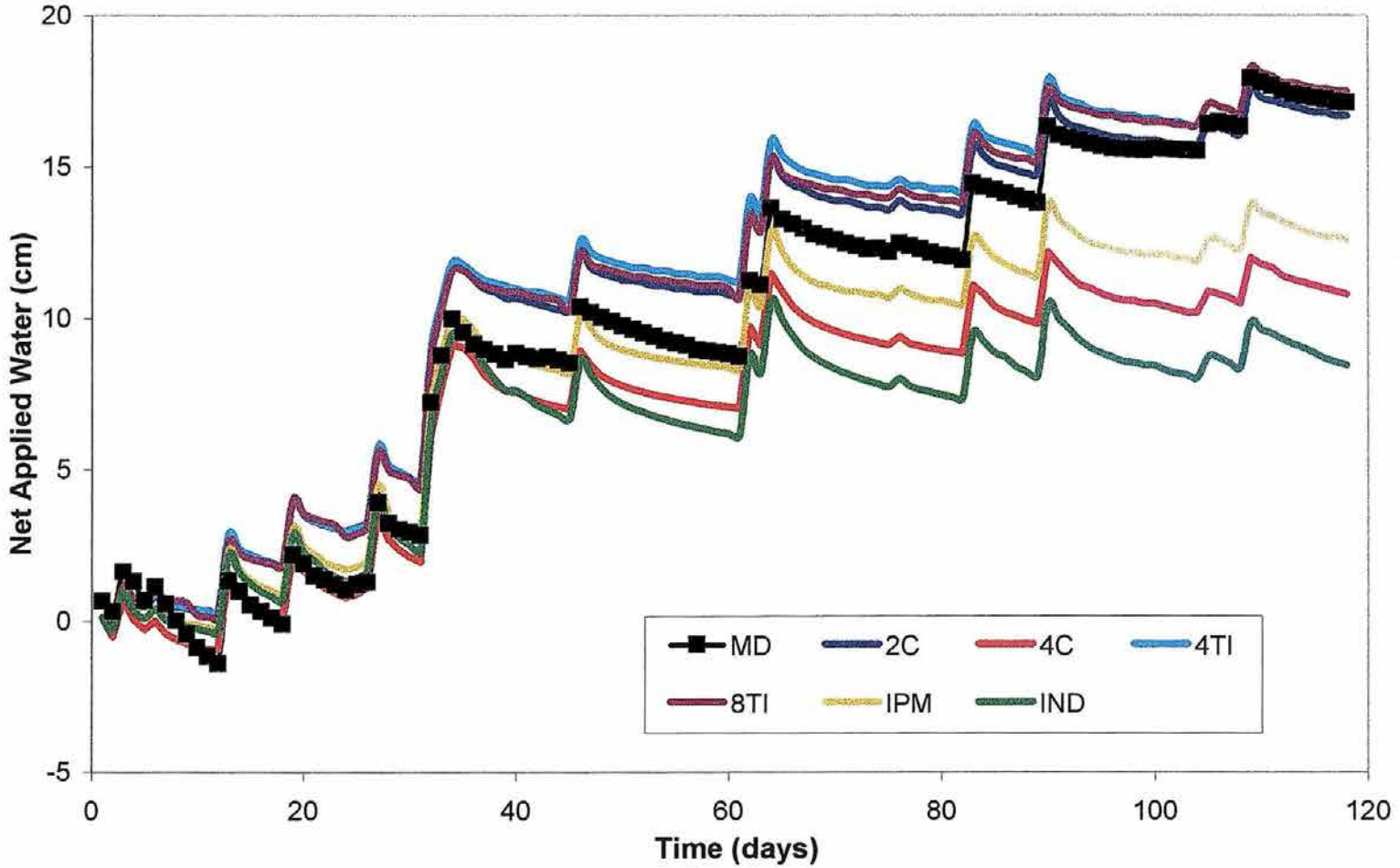

Figure 5.15. Water flux at the atmospheric boundary for the NT treatment.

irrigation water) minus the cumulative atmospheric water flux. From Figure 5.14, the amounts of NAW differ dramatically between methods. During the IND simulation for the T soil, only about 6 cm of water was infiltrated and is a plausible explanation as to why the IND underestimated bromide leaching. The NAW determined from the transport experiment using atmospheric data and irrigation data was 15.8 cm of water for the T soil. The NAW's of the 2C, 4C, and IPM simulations are just slightly less than the measured NAW of the T soil, and their predicted CM's are very close to the measured CM. The 4TI and 8TI apply more water than the actual experiment. The 4TI simulation predicts a CM very close to the measured CM, but the 8TI simulation moves the solute 12 cm further than the measured CM. The atypically large evaporative water loss from the IND method of calibration is a result of it's homogeneity and it's atypically high K at low θ values. The broader pore-size distribution of the IND soil (indicated by the lowest n value in Table 4.3) maintains the highest evaporative flux as the soil drains. Also, since the IND soil drains slowest at medium to high θ, the IND soil remains at a higher water content which facilitates evaporative water loss.

Figure 5.15 shows NAW for the NT treatment. The 2C, 4TI, and 8TI simulations predict NAW very close to the NAW calculated from the measured data. The 4C, IPM, and IND simulations underestimate NAW by 7.2, 5.1 and 9.5 cm of water, respectively. However, the IND simulation is affected most dramatically by the underestimate of NAW. The other simulations, with the

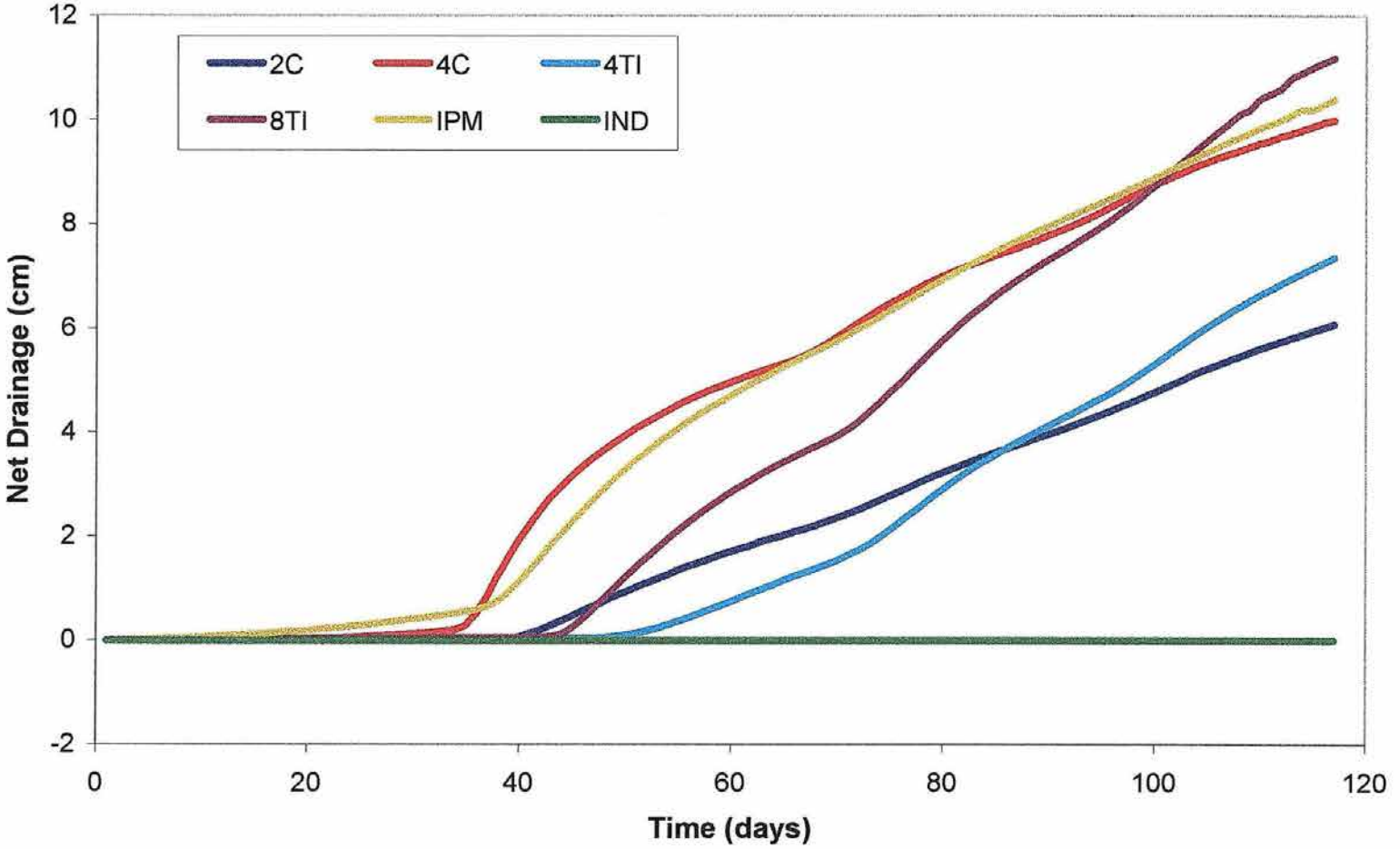

Figure 5.16. Water flux at the 180 cm depth for the T treatment.

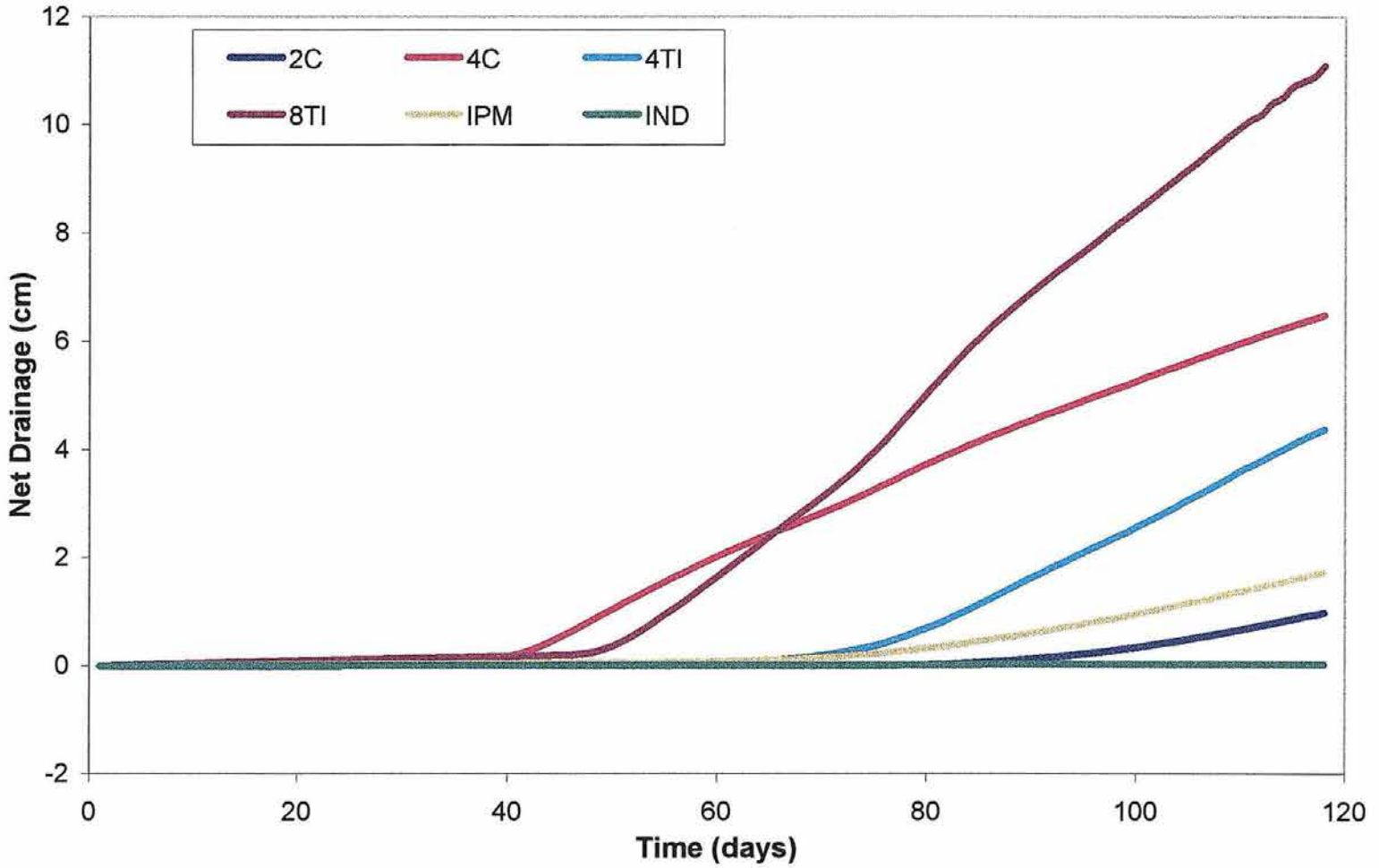

Figure 5.17. Water flux at the 180 cm depth for the NT treatment.

exception of the 8TI, under predict the CM of the NT soil as well.

Drainage

Another important factor controlling solute movement is the amount of drainage through the soil profile. The difference between the NAW and the ND is the amount of water storage in the system. Table 5.4 lists all of the NAW, ND, and storage values for most of the numerical simulations and measured data. Even though the initial conditions for each simulation were the same (based on measured water contents), the alternative hydraulic property sets naturally lead to different amounts of storage. Notice that for the IND case, although it doesn't produce the greatest change in storage, all of the NAW goes into storage between 0-180 cm soil depth.

Figures 5.16 and 5.17 show net drainage (ND) of water at the 180 cm depth for all the simulations in the T and NT soils. The 8TI simulation predicts more drainage for the T soil than the other methods and that is one reason the Br- is moved farther into the soil profile than in the other simulations. The more water that flows through the system, typically the farther the solute is moved. The 4C and IPM methods have about 10 cm of ND and about the same NAW. As a result, the predicted CM's from those simulations are about the same and the simulated Bromide concentration profiles closely match the measured data. The 4TI simulation predicts about 19 cm of NAW but predicts only about 7 cm of ND. However, the 4TI simulation still results in a good representation of the T data. Even though the ND predicted by the 4TI simulation is small, water

redistributes within the soil profile moving solute within the system. The till 4C and IPM simulations have only about 3 or 4 cm of storage change and thus have fairly large ND values. Even though they have lower NAW values than the measured data, a substantial amount of water is moved through the soil system due to smaller storage values. Bromide is moved deep into the profile, resulting in model simulations that fit the measured data well.

The same results seen above are evident when inspecting Figure 5.17. The 8TI simulation predicts the largest amount of ND, and results in the deepest movement of the CM of the Br- solute. The IND simulation has the least NAW and ND and results in very little movement of the solute mass. The basic story is that more NAW water and less storage, results in more drainage and deeper movement of solute mass. However, redistribution of water within the soil profile accounts for substantial chemical movement. For example, notice in the IPM data the radically different ND values between T and NT despite similar NAW to the two plots. The six times greater drainage in the IPM tilled plot occurs because of higher initial θ in the tilled soil compared to the non-tilled soil, The predicted chemical movement in these two IPM cases is nearly identical, however.

Supplementation of Soil Surface Properties

It is not entirely clear what parameter values or combinations of parameters most affect the NAW and ND. Under normal circumstances, it would be expected that a homogeneous soil profile would infiltrate more water

than a layered profile. Jury et al. (1991), states that any soil layering, whether fine or coarse, will ultimately reduce water infiltration. However, just as layering can prohibit infiltration of water, it can also inhibit evaporation of water. Capillary barriers are based on this principle and so are mulches. A homogeneous profile will evaporate more water because the evaporative front can remove water from deeper depths due to a lack of layering. It is important to note that layering is not always due to changes in soil texture, but rather, due to changes in the hydraulic properties, however slight, with depth. This trend is seen when contrasting the difference between the IND soil profile and the 2C soil profile. The IND profile is homogeneous (same hydraulic properties) to a depth of about 160 cm, but the 2C profile is layered (8 layers with different hydraulic properties) throughout the profile. Elrick et al. (1997) discuss the upward movement and accumulation of solute due to evaporative flux of water. Solute does not have to be moved upward but can be retained near the surface due to gradients that cause water to move upward.

Given the importance of the soil hydraulic properties at the atmospheric boundary, the IND data were supplemented with the 2C data at the soil surface (0 to 10 cm). This represents the case where a researcher uses a direct method for the soil surface only and relies on the indirect estimation for the sub-surface properties. Figures 5.18 and 5.19 show results of the simulations for the T and NT soils. In both instances, supplementing the IND data with measured surface soil properties resulted in greater water infiltration (reduced evaporative loss)

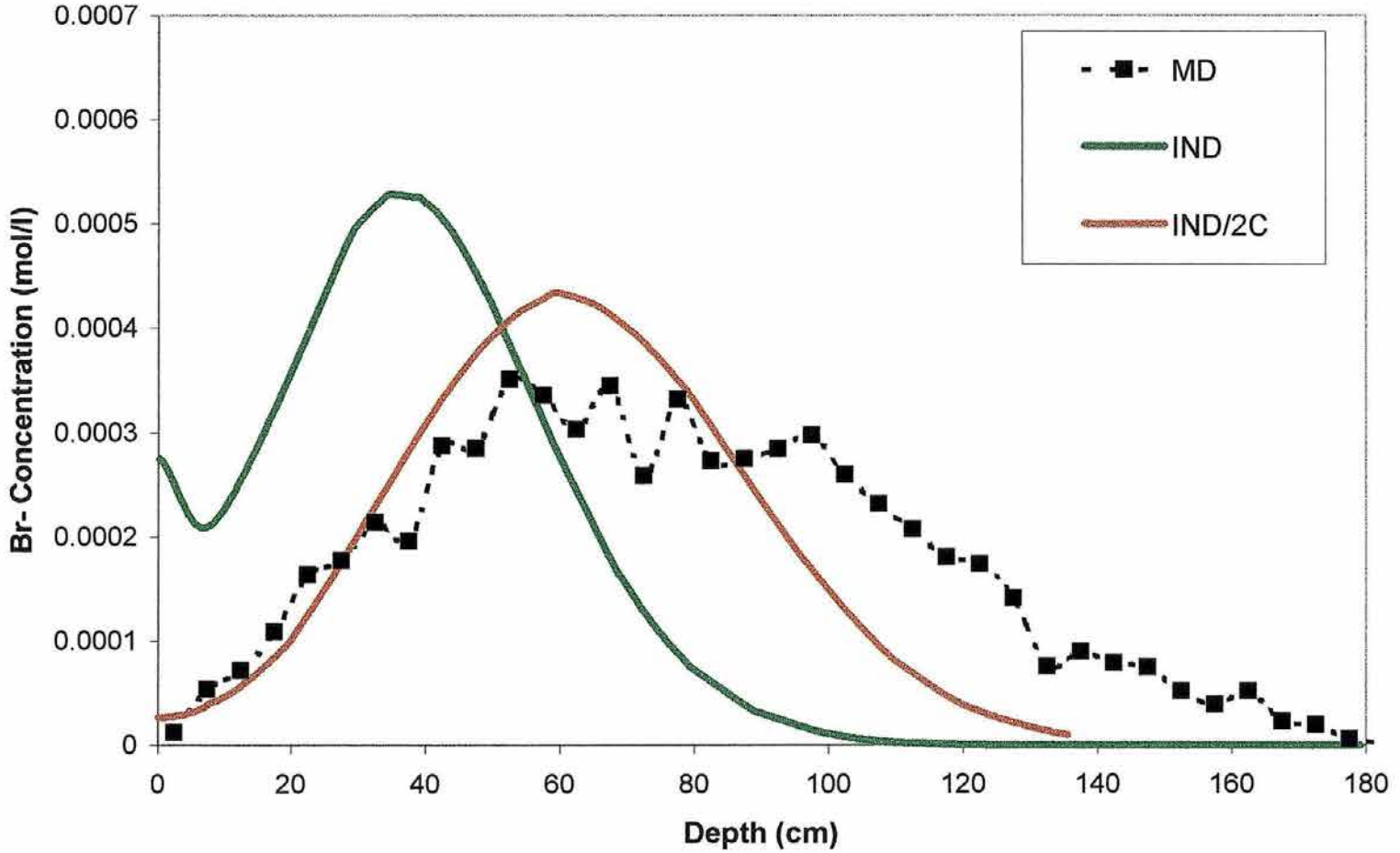

Figure 5.18. Bromide profiles for the T soil at day 117 simulated using IND data for the entire profile (IND) and IND data supplemented with 2C at the soil surface (IND/2C)

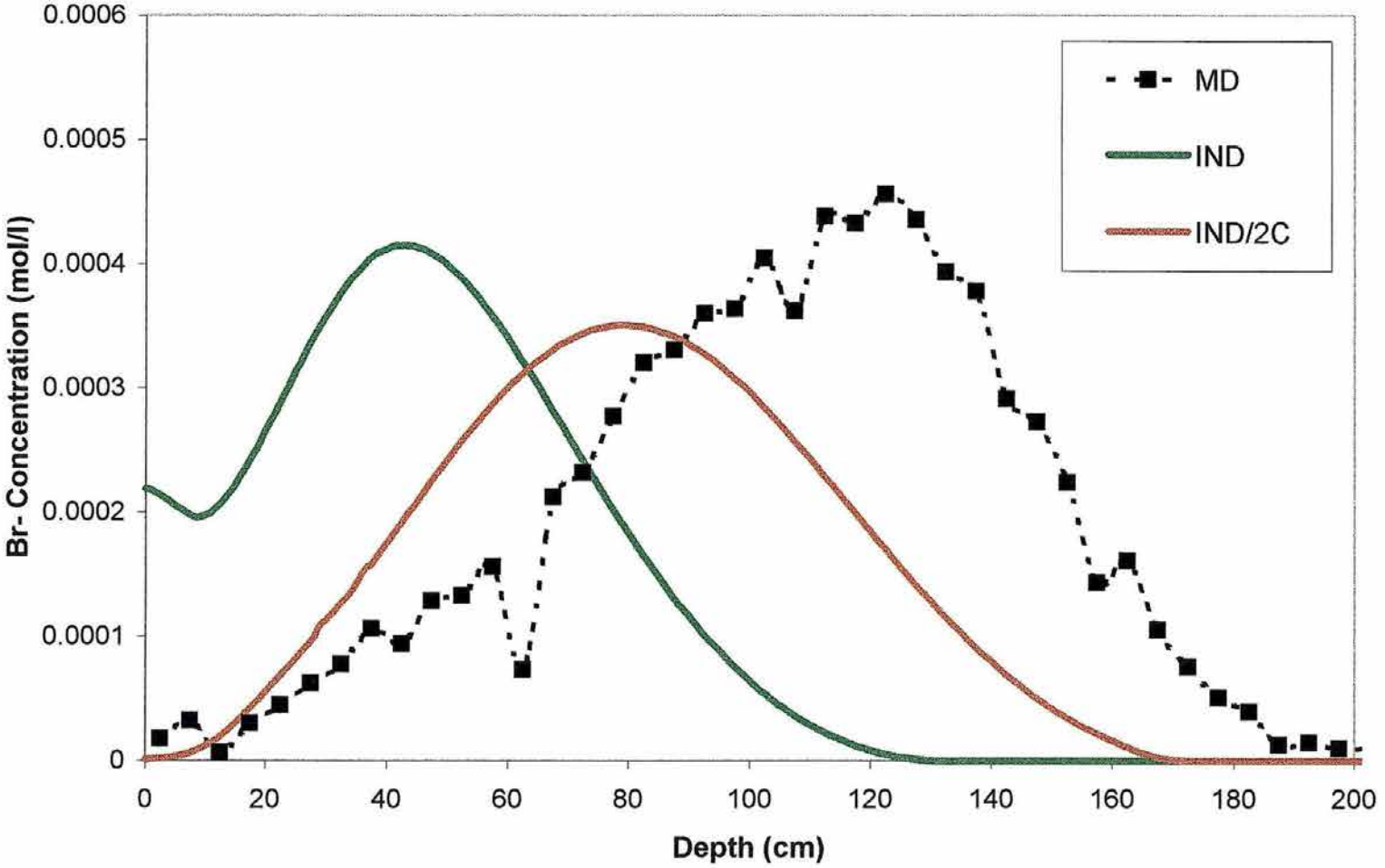

Figure 5.19. Bromide profiles for the NT soil at day 118 simulated using IND data and IND data supplemented with 2C surface data.

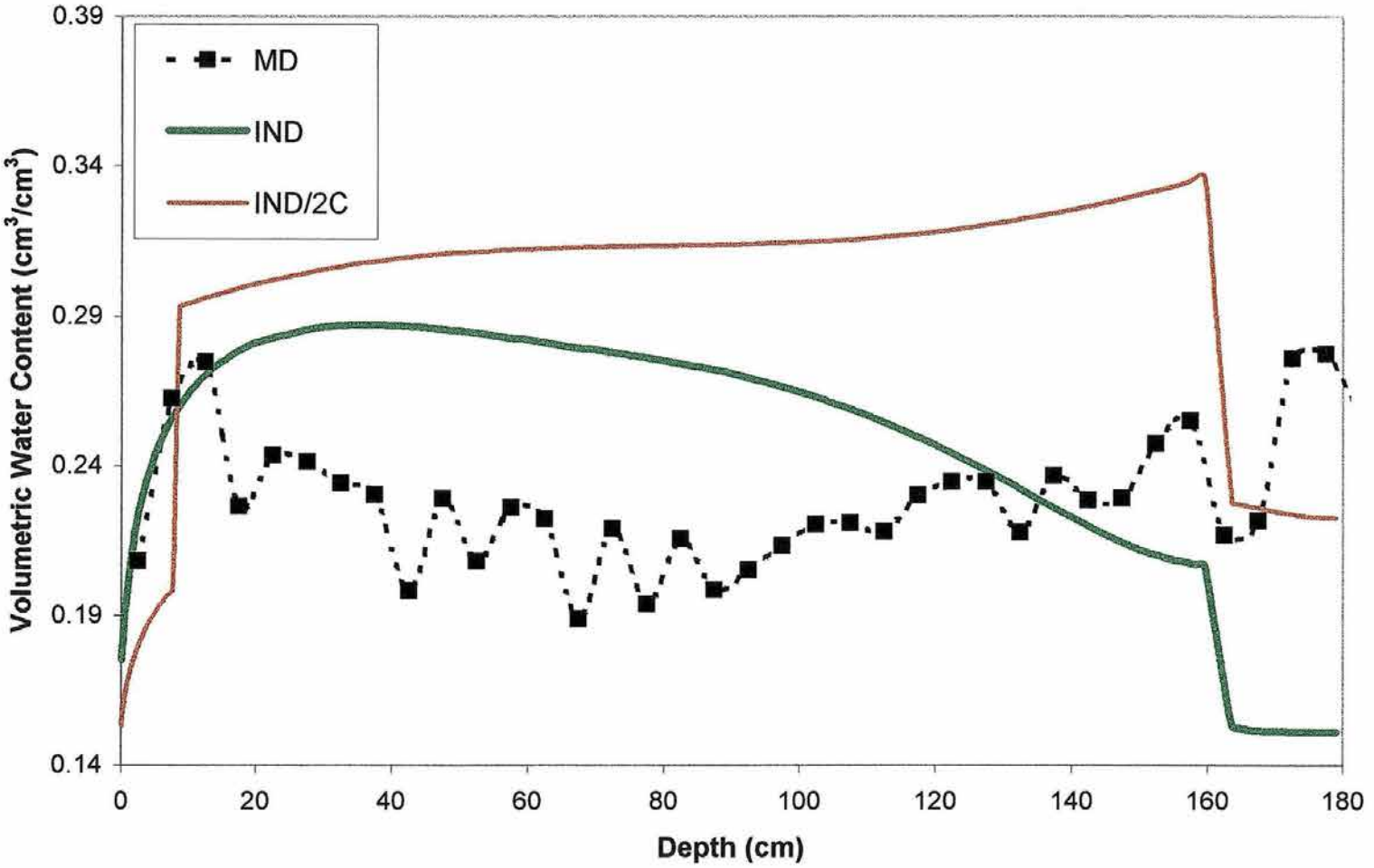

Figure 5.20. Water content profiles for the T soil at day 117 simulated using IND data for the entire profile (IND) and IND data supplemented with 2C at the soil surface (IND/2C).

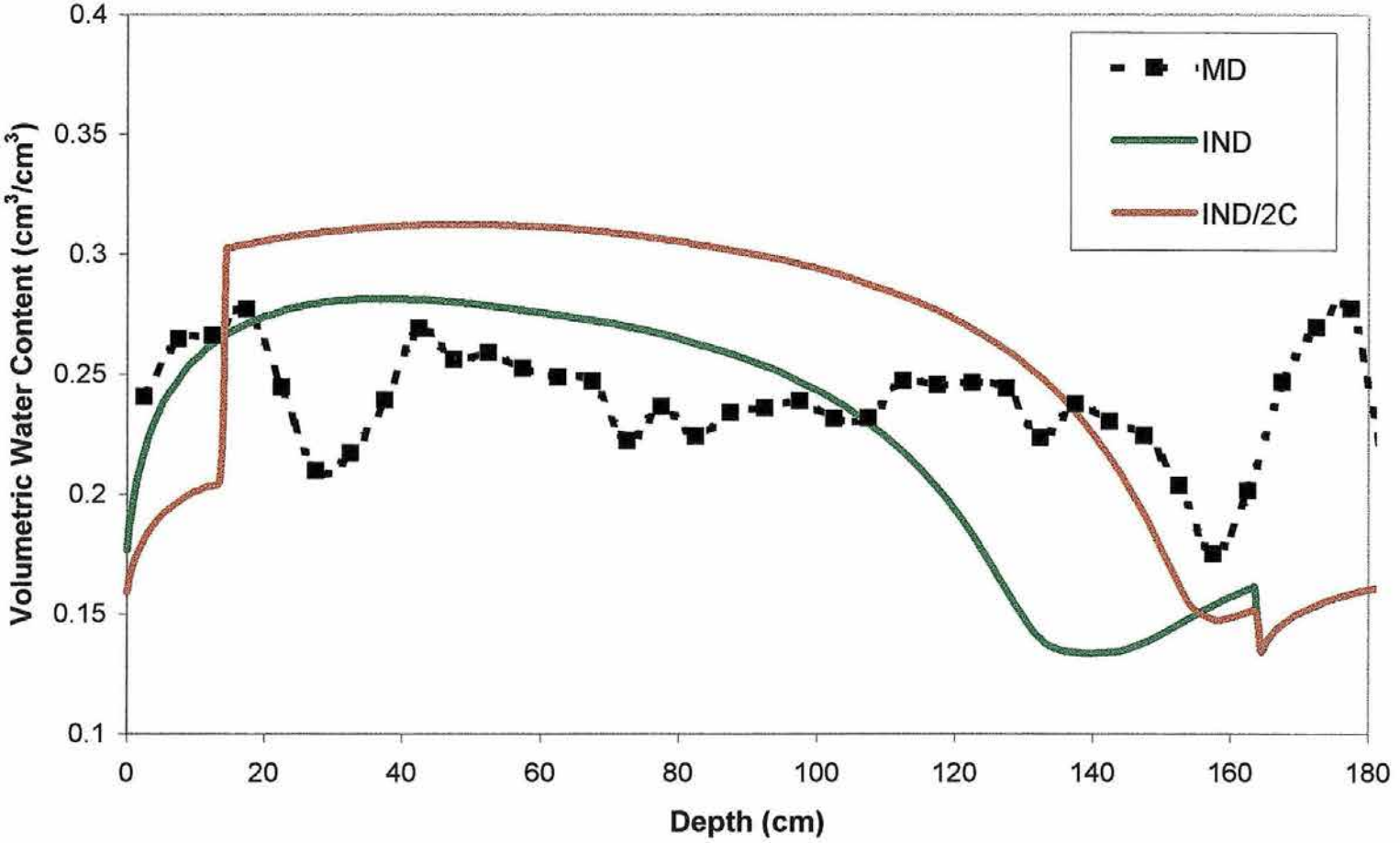

Figure 5.21. Water content profiles for the NT soil at day 118 simulated using IND data and IND data supplemented with 2C surface data.

and deeper solute movement. The NAW for the T soil went from 6.6 cm to 16.1 cm and from 8.7 cm to 17.6 cm for the NT soil treatment. The simulated profiles still do not fit the measured data extremely well, but we have improved the prediction of bromide movement significantly by adding measured surface soil properties. The downside of increasing infiltration is that the predicted water content profiles are now greatly disturbed as shown in Figures 5.20 and 5.21. Even though the simulation results in a better fit of the measured bromide profiles, the fit to the measured water content profiles is significantly worse. The addition of the 2C surface soil data increased water infiltration, but drainage increased only slightly. Thus, more water went into storage and dramatically changed the water content profiles. If more water had drained through the profile, the simulations would have been better for both the water and solute. The conductivity values for the IND soil at $\theta > \sim 0.2$ are less than those of the other soils and, as a result, not as much water is moved through the soil profile. So, by increasing infiltration we have improved the solute movement prediction, but worsened the water movement prediction.

Because it became evident that the hydraulic parameters of the surface soil critically affect the simulations, the IPM simulations were supplemented with surface soil data from several other methods to see if predictive accuracy could be improved. The only hydraulic property that was measured at the soil surface by the IPM method was K_s. The other hydraulic parameters were averaged over the upper 0.15 cm of the profile because the most shallow placement of the

measurement instrumentation (tensiometers and neutron probe readings) was at 10 cm depth.

The IPM data set was supplemented with hydraulic parameter data from the 4TI, 8TI, and 2C methods. Since the 4TI and 8TI methods measure hydraulic conductivity directly, the data were used as they were originally analyzed. However, the 2C data were re-analyzed using K_s from the IPM because the in-situ K_s value was thought to be more reliable than the laboratory measured K_s value, due to the scale. Figures 5.22 and 5.23 show the results of supplementing the IPM method with surface soil hydraulic properties. Supplementing the IPM data resulted in decreased evaporative water loss and, as illustrated in the figures, deeper movement of solute. The 4TI and 8TI supplements resulted in deeper solute movement than the 2C supplement. The K_s values are not significantly different between the 4TI, 8TI, and IPM for the NT soil, but are for the T soil. In addition, the 2C data tends to be more similar overall to the IPM than does the permeameter data. Thus, the increased infiltration is due primarily to changes in the hydraulic properties of the surface soil. Supplementing the IPM with permeameter data resulted in increased infiltration and over-prediction of the bromide solute movement for the T treatment. However, for the NT treatment, supplementing the IPM data with the permeameter data resulted in better fit between simulated and measured data profiles. The 2C data supplement results in better simulation of the data for both T and NT treatments. Figures 5.24 and 5.25 show the measured water content

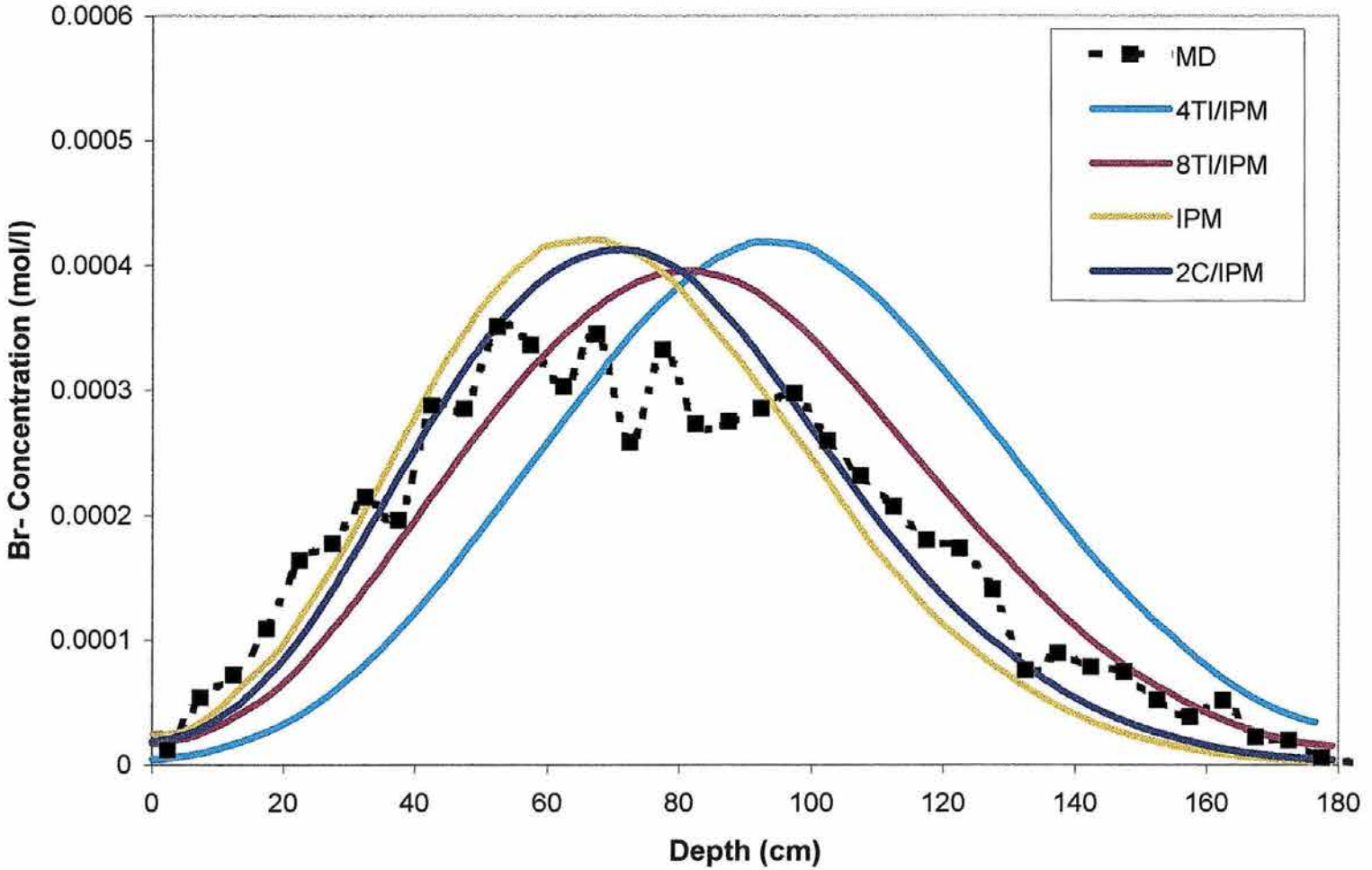

Figure 5.22. Simulations of Bromide transport in the T soil and 117 days using IPM data supplemented with surface soil data from 2C, 4TI, and 8TI methods.

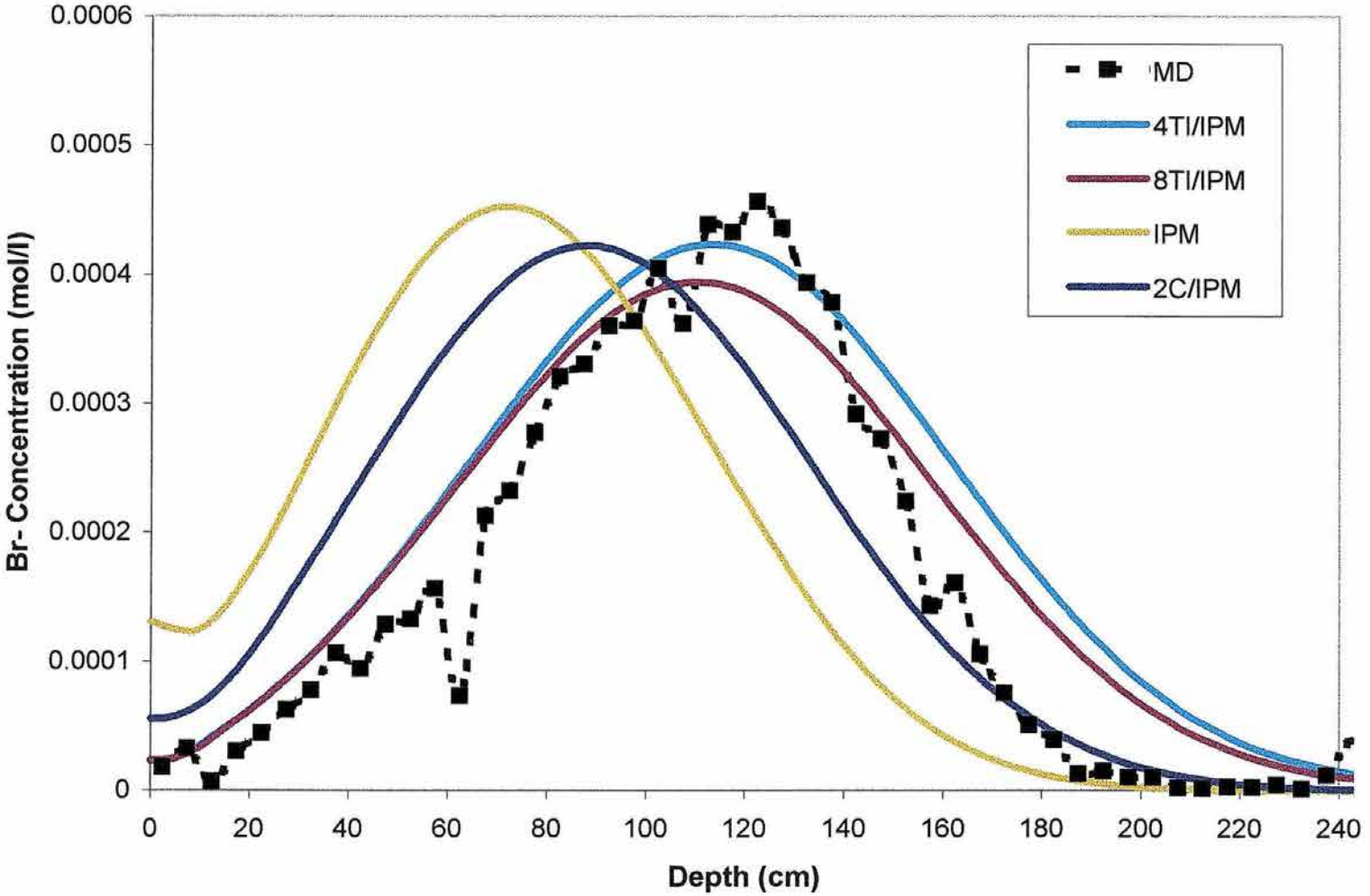

Figure 5.23. Simulations of Bromide transport in the NT soil and 118 days using IPM data supplemented with surface soil data from 2C, 4TI, and 8TI methods.

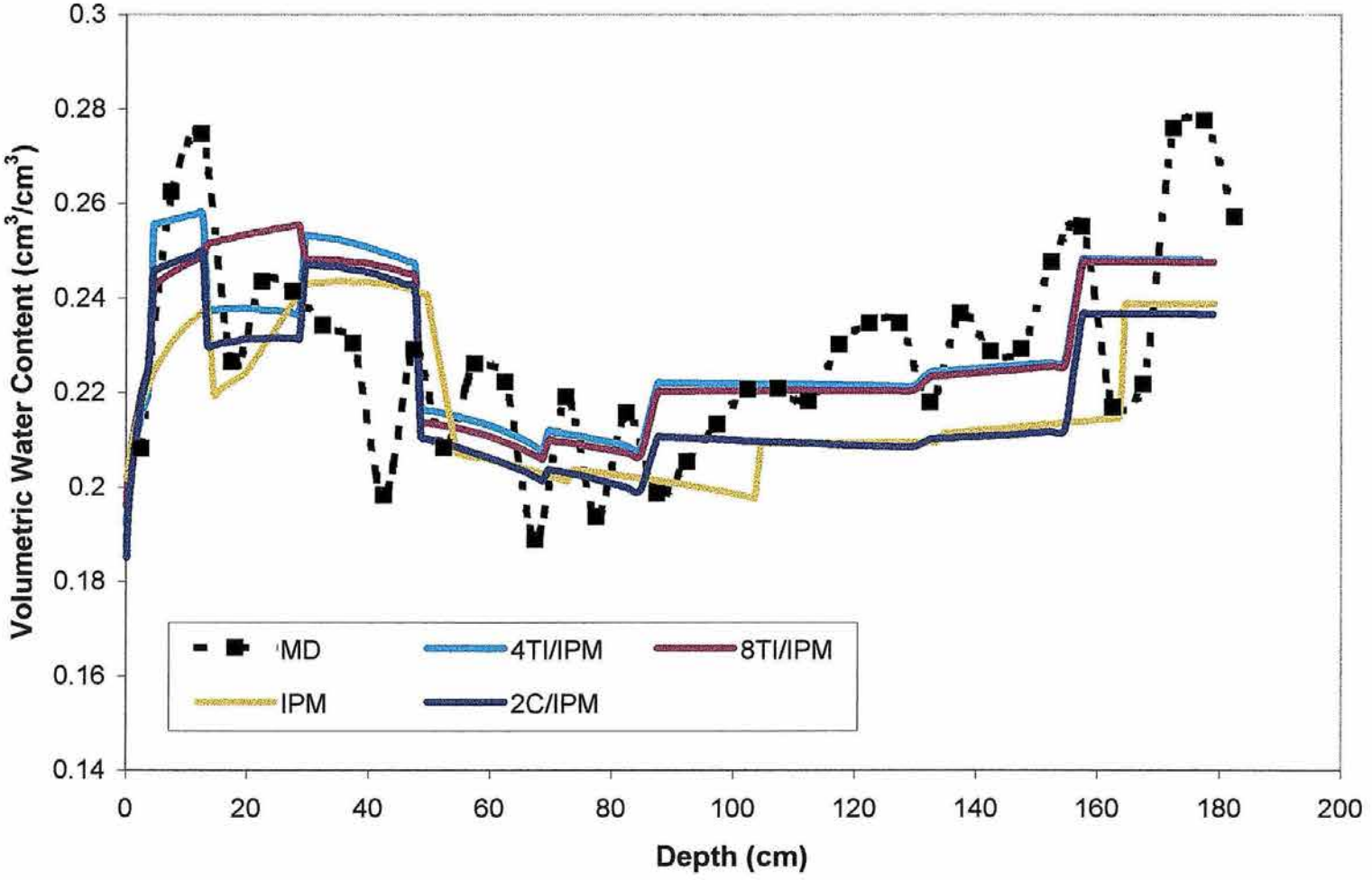

Figure 5.24. Simulated water content profiles in the T soil and 117 days using IPM data supplemented with surface soil data from 2C, 4TI, and 8TI methods.

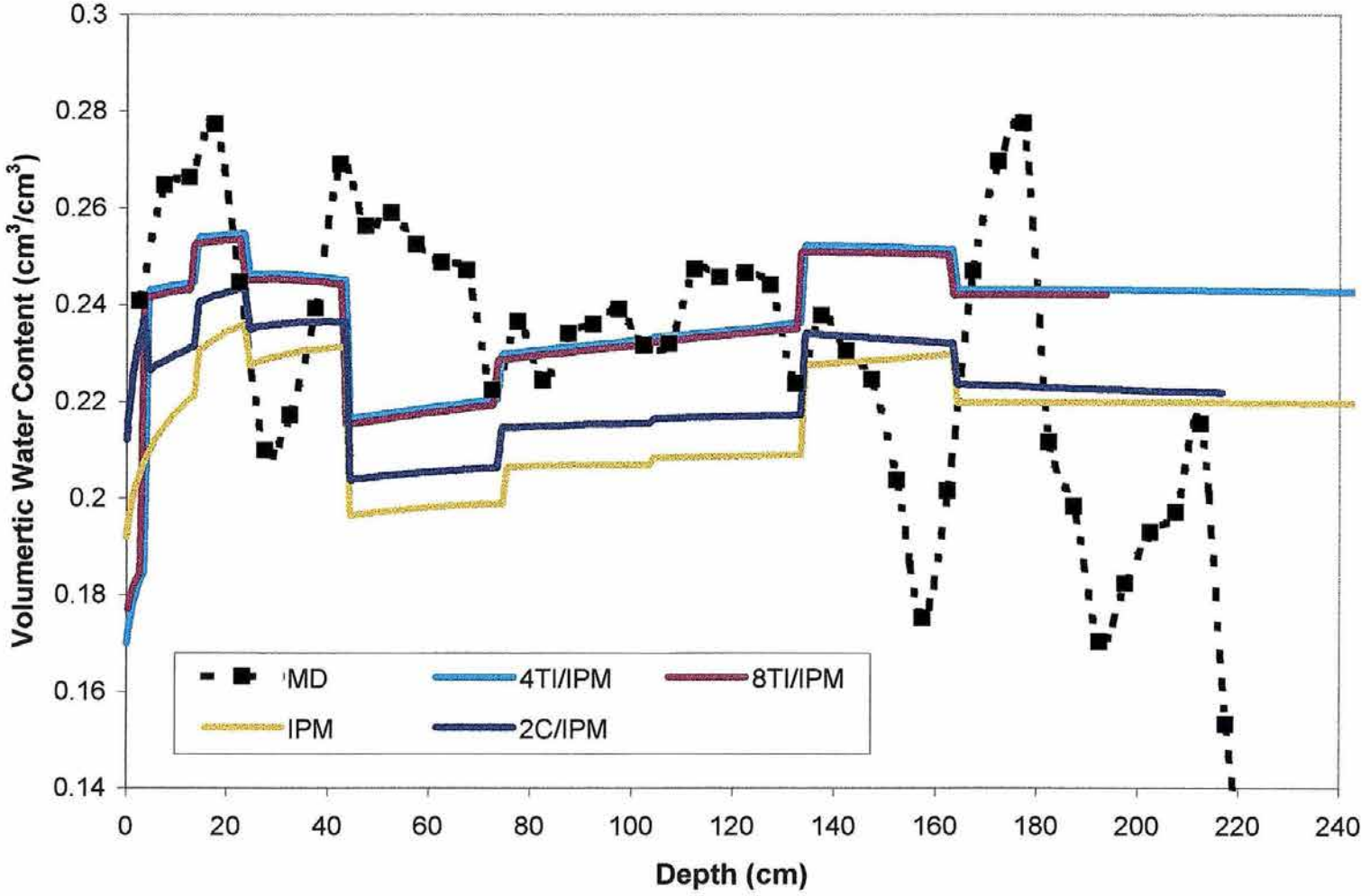

Figure 5.25. Simulated water content profiles in the NT soil and 118 days using IPM data supplemented with surface soil data from 2C, 4TI, and 8TI methods.

profile and predicted water content profiles from the IPM and the supplemented IPM simulations. Supplementing the IPM data has not significantly impacted the prediction of water content in the system. Because it is unclear what impacts supplementing the IPM data will have due to the nature of the system, it is not recommended that the IPM data be supplemented. The results could make the prediction better or worse, depending upon conditions.

Minimization of Data

In addition to supplementing the IPM and IND data sets with surface data, a test was conducted to explore what amount of measured data was necessary to predict the solute and water movement observed in the T and NT systems. Because soil core sampling is a standard practice for many researchers and consultants, data from the 2C method were used for all the simulations in this section.

The first set of simulations used only data collected from the soil surface layer to represent the entire soil profile (one layer). As can be seen from Figures 5.26 and 5.27 the resulting simulations are poor representations of the measured bromide profiles. Both the T and NT simulations under-predicted bromide movement when only surface soil data were used. On a good note, the simulated water content profiles shown by Figures 5.28 and 5.29 are still good representations of the measured data.

The second set of simulations were setup as a two layer system, using data from the soil surface and data from the 10 cm depth. Hydraulic properties

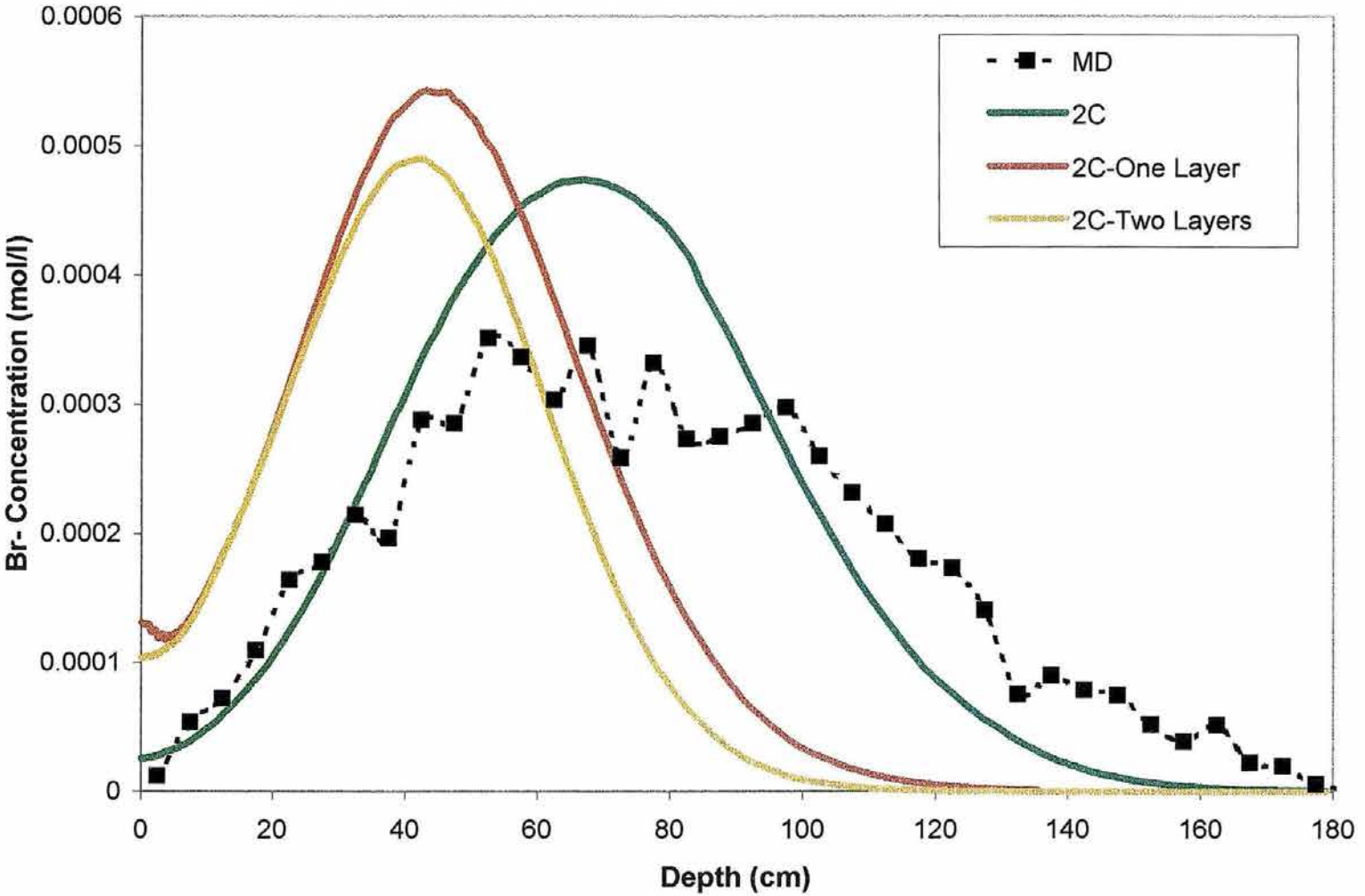

Figure 5.26. Simulated Bromide movement using 2C data for the T soil at day 117.

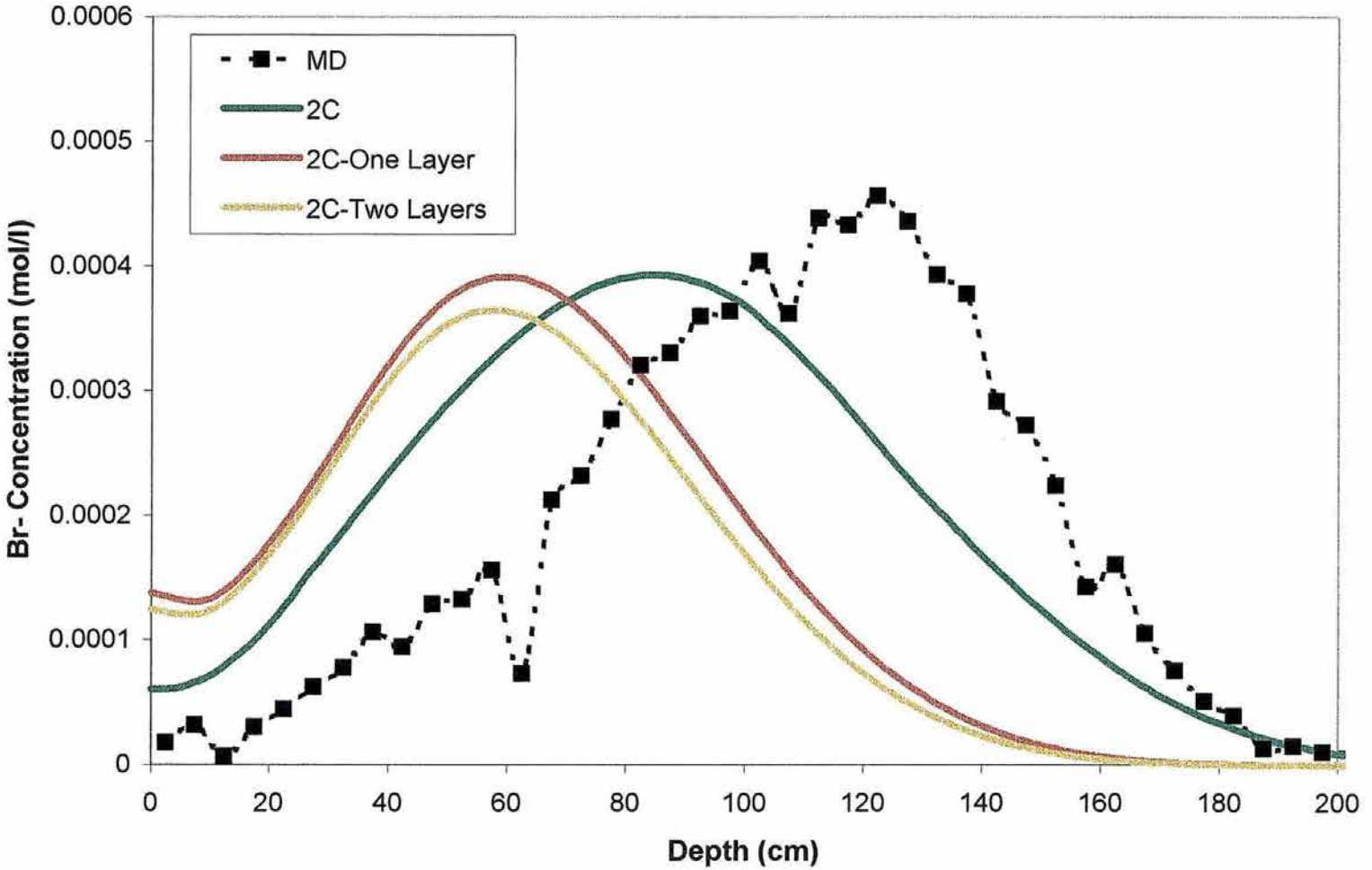

Figure 5.27. Simulated Bromide movement using 2C data for the NT soil at day 118.

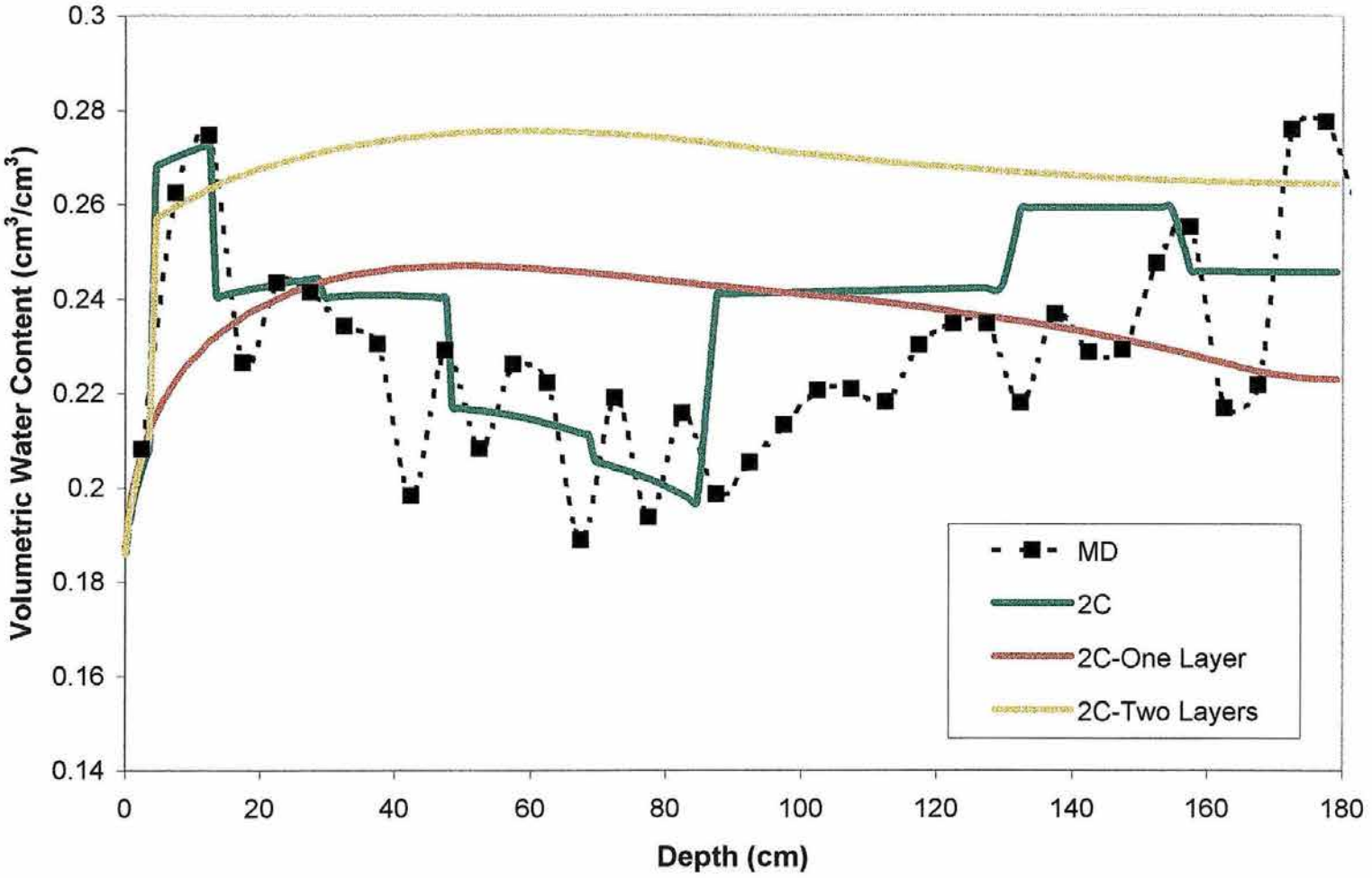

Figure 5.28. Simulated water content profiles using 2C data for the T soil at day 117.

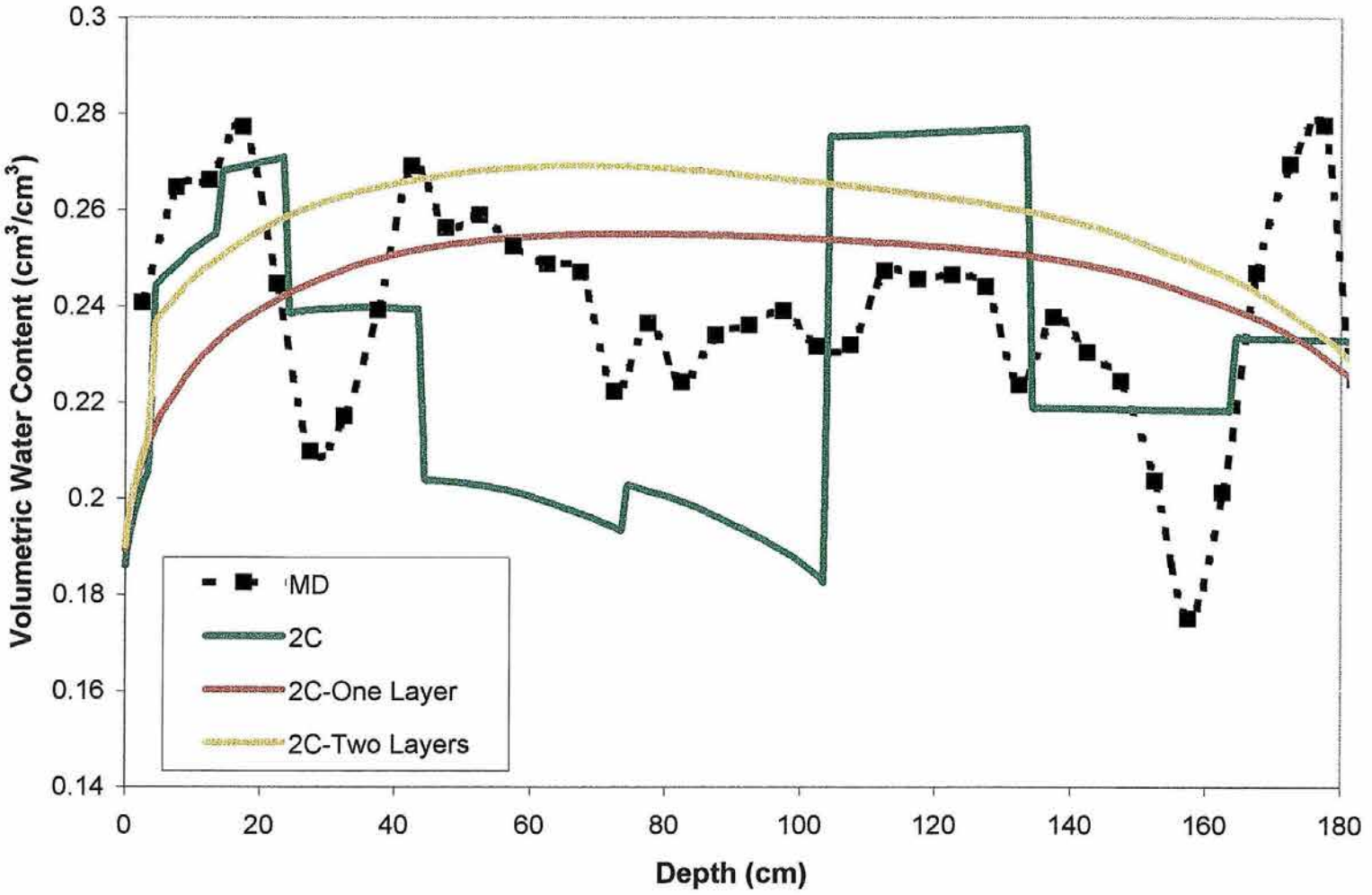

Figure 5.29. Simulated water content profiles using 2C data for the NT soil at day 118.

from the 10 cm soil layer was used to represent hydraulic properties of the soil profile below 10 cm meter depth. From Figures 5.26 and 5.27, the two layer system did not improve prediction solute movement over the one layer simulation. In addition, the two layer simulation resulted in poorer prediction of water content profiles as compared to the one layer simulation and the regular 2C method (Figures 5.28 and 5.29).

The net result is that water and solute movement cannot be accurately predicted simply using limited amount of measured data from near the soil surface. The simulations are no more accurate than the IND method, where no direct measurements were performed.

5.5 Methods of Averaging

Typically, when an experiment is designed, repetitions are used so that statistical information about the data can be inferred. However, the averaging method used to obtain the simulated water content and concentration profiles may itself affect model predictive accuracy. The question becomes, is it more valid to use the spatially averaged parameter values of a particular method as input into the numerical model, or is it more appropriate to use the individual repetitions of the parameters to independently predict water content and concentration profiles and then average these output profiles. It is clear that information about the variance of the predicted output data can only be obtained using the latter method. The former method provides information about the

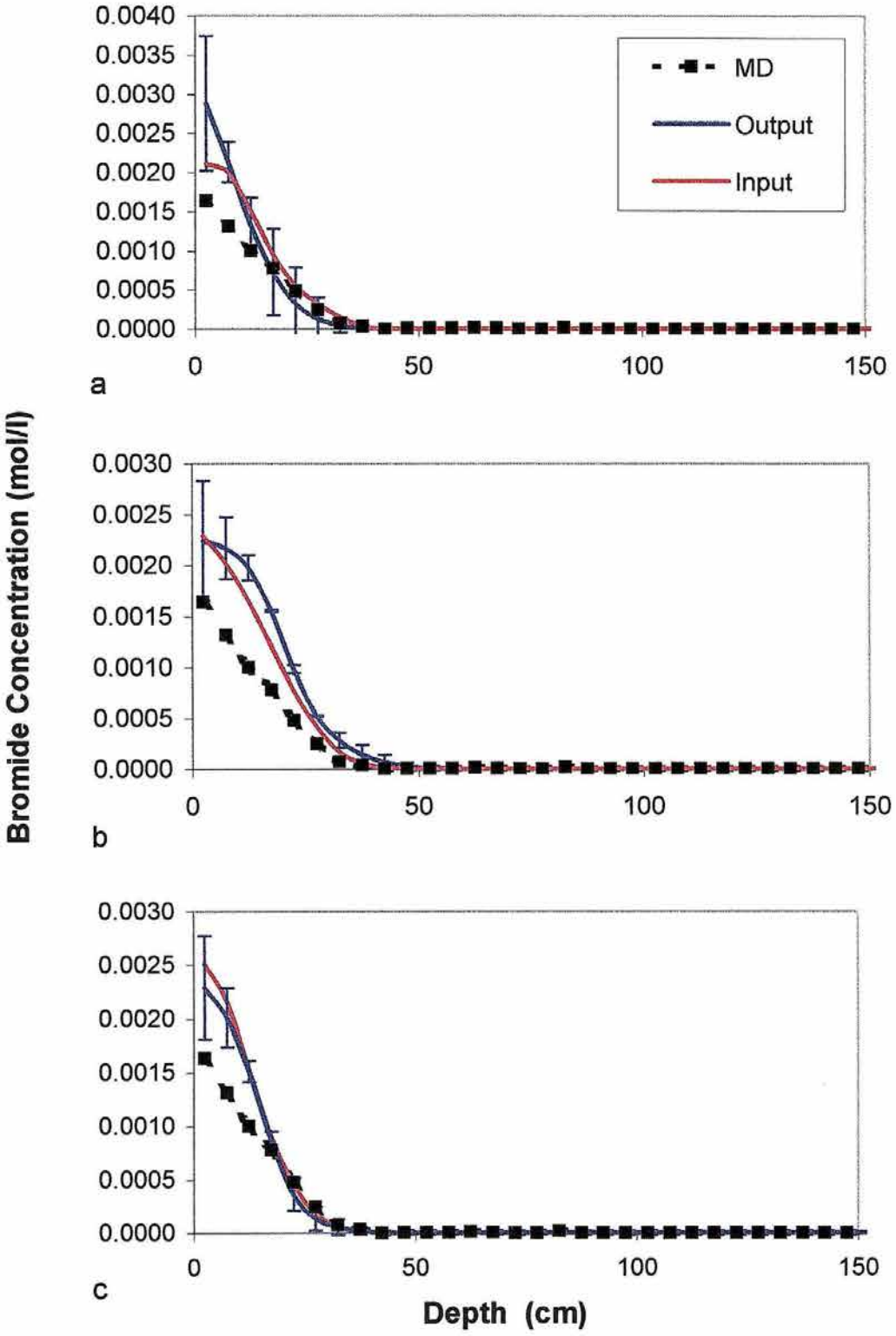

Figure 5.30. Concentration vs. soil depth simulations produced using averaged input parameters and averaged output concentration profiles. NT soil day 9 simulations. (a=2C, b=4C, c=4TI)

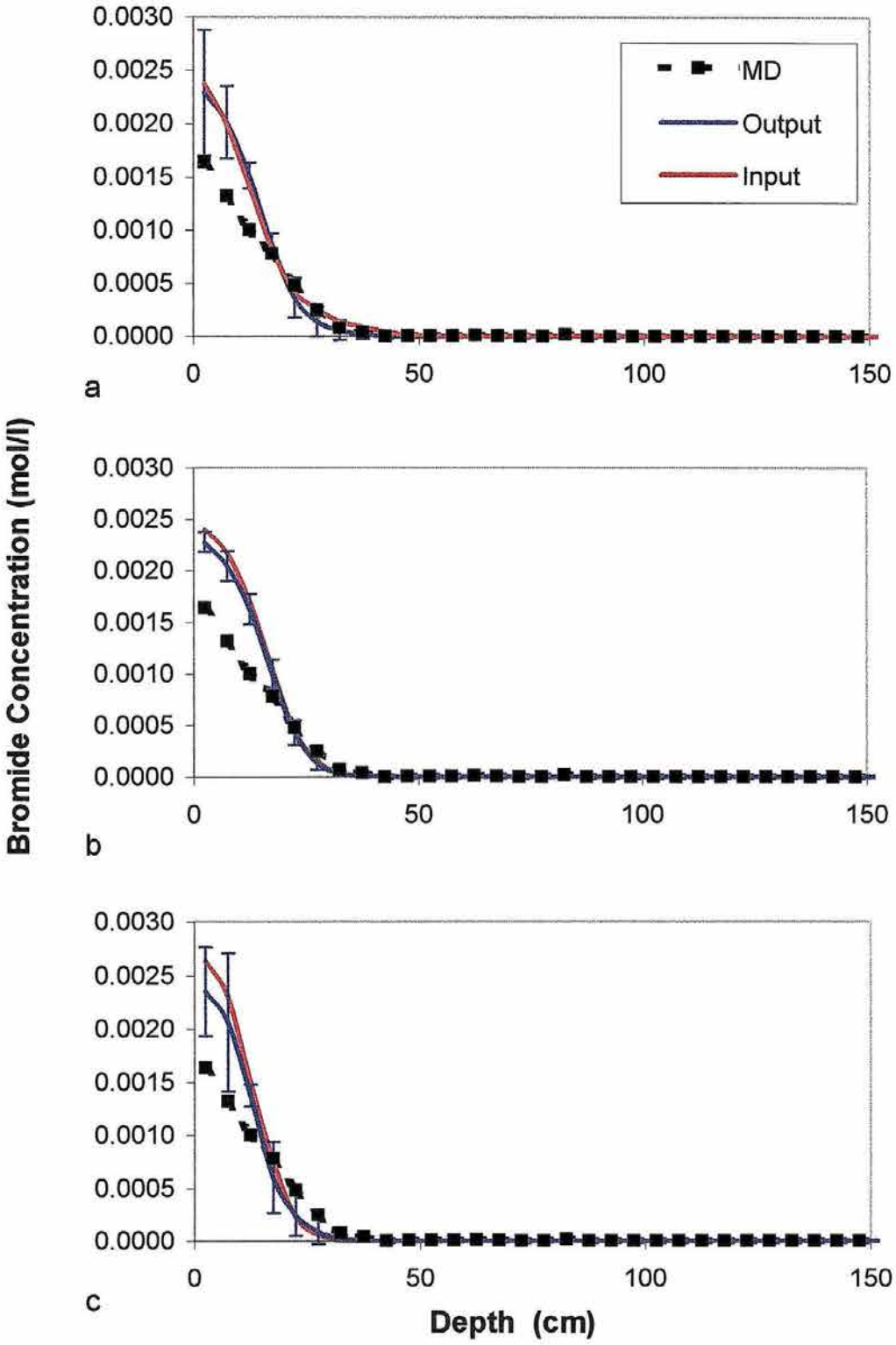

Figure 5.31. Concentration vs. soil depth simulations produced using averaged input parameters and averaged output concentration profiles. NT soil day 9 simulations. (a=8TI, b=IPM, c=IND)

variance of the input parameters, but not about the variance of the predicted data.

Figures 5.30 through 5.31 show results of averaged input and averaged output bromide concentration simulations for day 9, 37, and 118 on the NT soil, respectively. Data for the T treatment is contained in Appendix C. The averaged output data were generated by averaging the concentration values from the four output simulations at each depth. Each averaged output simulation has 95 percent confidence bars around each point to indicate the variance in the predicted output values. The two predicted data sets are very similar during the early stages of the simulation as shown by Figures 5.30 and 5.31. In general, the averaged input simulations fall within the confidence limits of the averaged output simulations. The exception is the 4C simulation that shows only small variance in the middle part of the predicted curve.

As the simulation time increased to 37 days (Figures 5.32 and 5.33) so did the uncertainty in the predicted bromide concentration profile. The variability of the averaged output data increased for all the methods, but the increase was most dramatic for the 8TI and IND simulations. The IPM simulations show the least amount of variability and this coincides with small variability in the hydraulic properties. For this simulation time there was also an increase in incidence where the averaged input profile did not fall within the confidence limits of the averaged output data. It is clear from the figures that the two averaging schemes result in different predicted profiles.

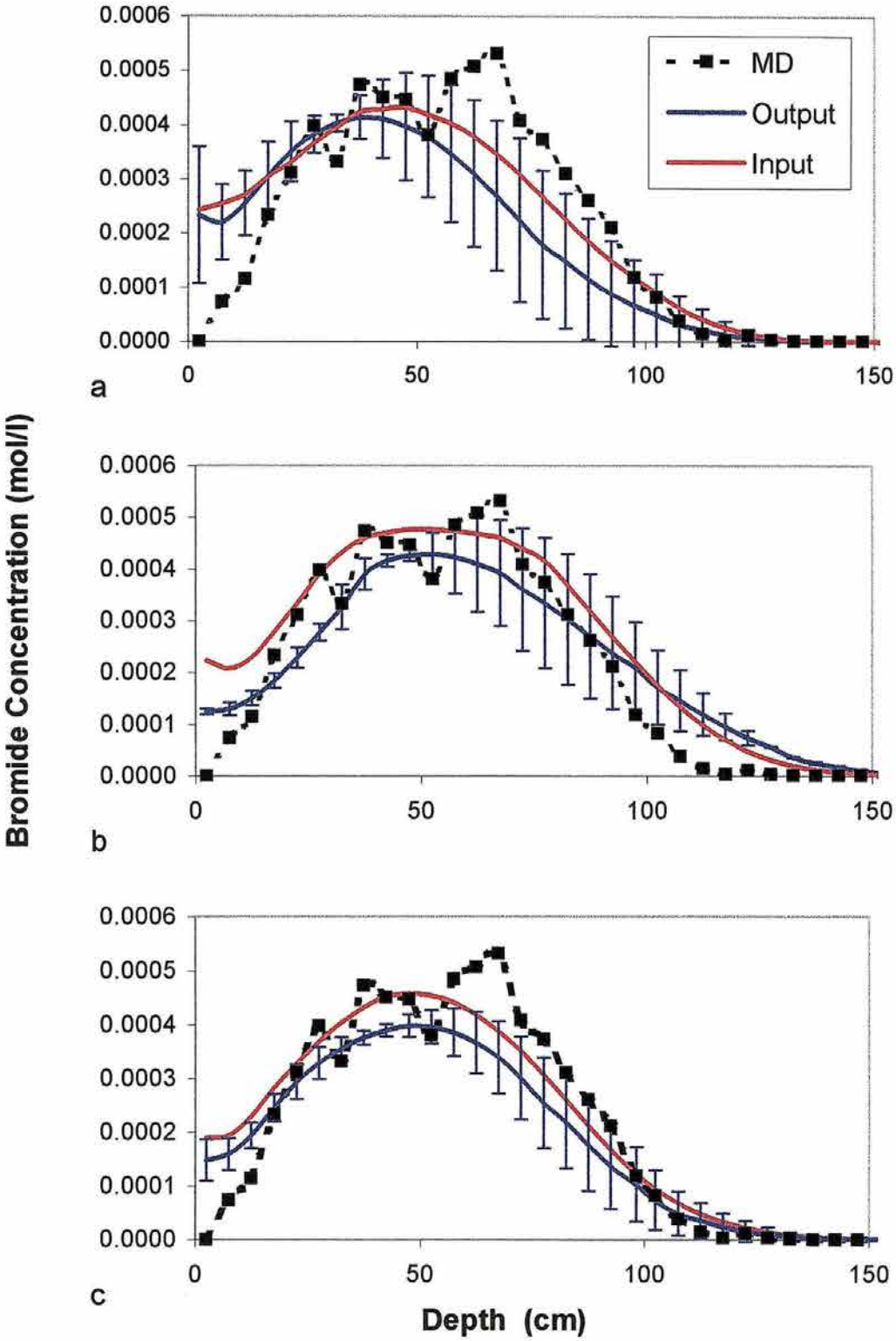

Figure 5.32. Concentration vs. soil depth simulations produced using averaged input parameters and averaged output concentration profiles. NT soil day 37 simulations. (a=2C, b=4C, c=4TI)

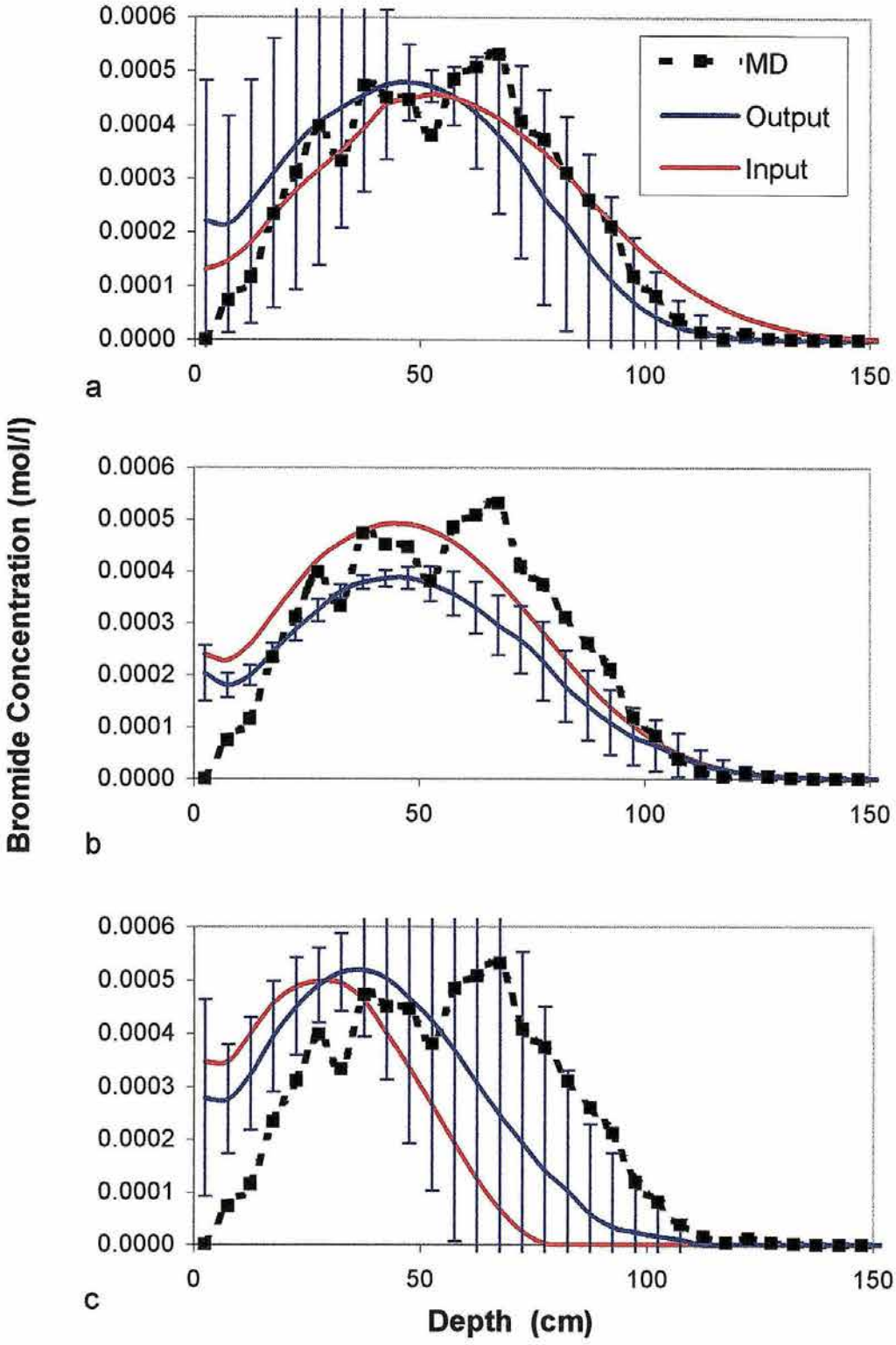

Figure 5.33. Concentration vs. soil depth simulations produced using averaged input parameters and averaged output concentration profiles. NT soil day 37 simulations. (a=8TI, b=IPM, c=IND)

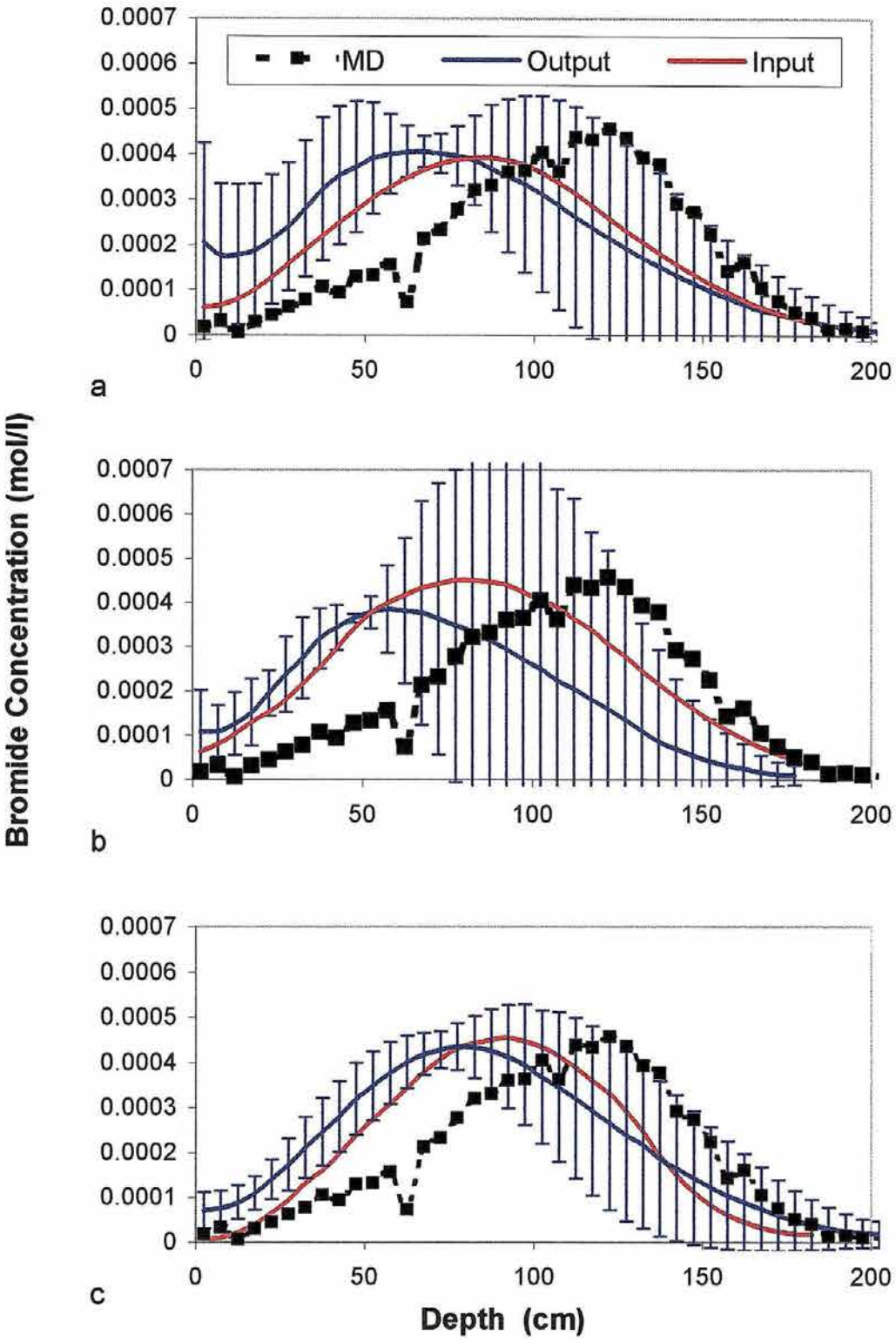

Figure 5.34. Concentration vs. soil depth simulations produced using averaged input parameters and averaged output concentration profiles. NT soil day 118 simulations. (a=2C, b=4C, c=4TI)

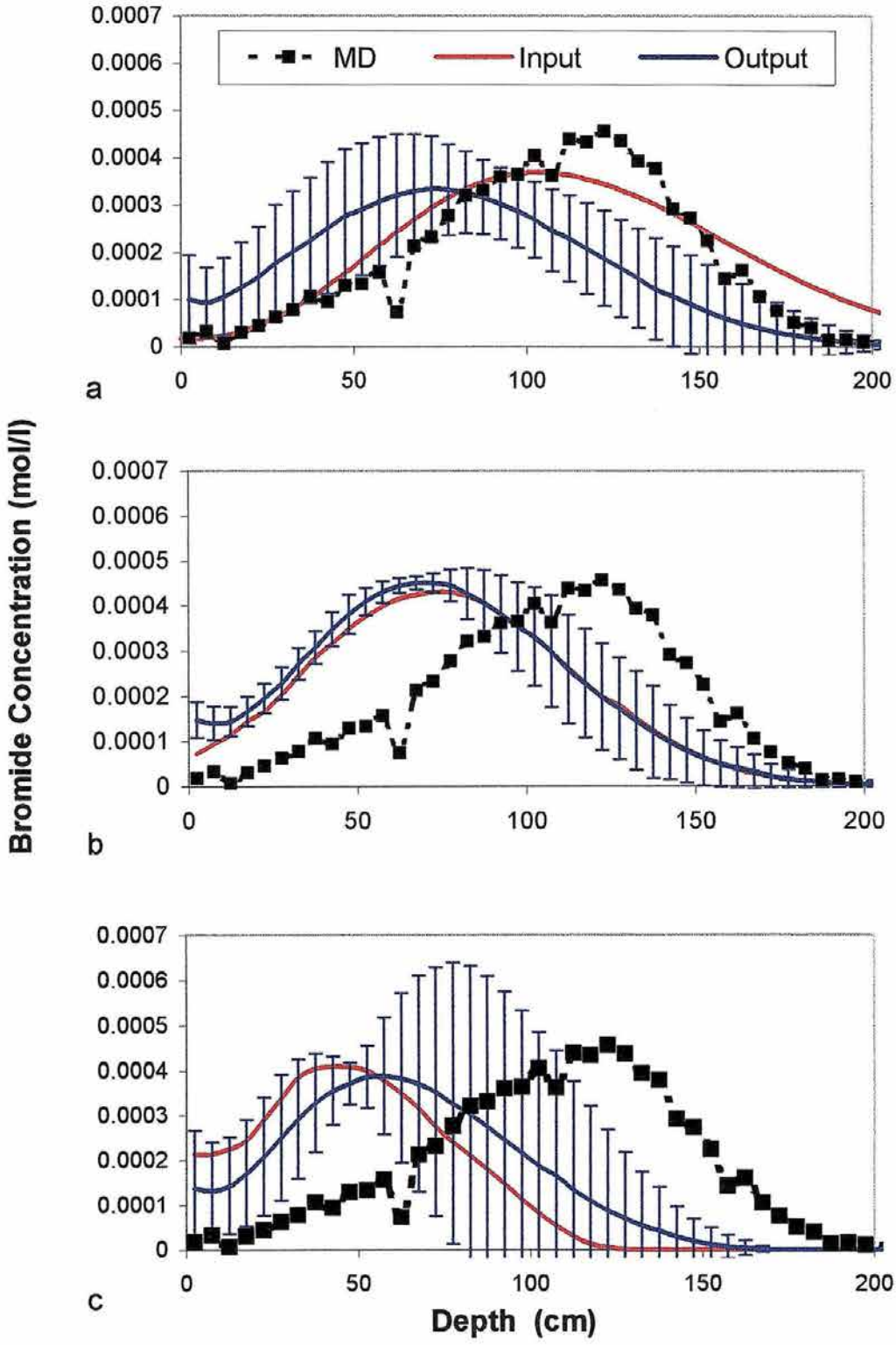

Figure 5.35. Concentration vs. soil depth simulations produced using averaged input parameters and averaged output concentration profiles. NT soil day 118 simulations. (a=8TI, b=IPM, c=IND)

Figures 5.34 and 5.35 shows the day 118 simulations for all the methods. There is a great deal of variability in the individual simulations, except in the IPM. The variability in the IPM simulations has remained quite small, indicating that the IPM is a more repeatable and consistent method of determining the hydraulic properties at this site. The soil profile at this site is fairly homogeneous and the same results may not be obtained in a heterogeneous soil profile. The IPM simulations are very similar and appear not to be affected by the averaging scheme. Variability, whether spatial or within the method, causes deviation between simulations. Increased variability means that the use of a specific method to estimate the hydraulic properties will increase the likelihood of producing an erroneous prediction if only one test is performed (i.e. one set of soil cores to estimate the properties of the soil profile). This idea is made clearer through inspection of Figures 5.36, 5.37, and 5.38. The IPM simulations, shown in Figure 5.36, are tightly grouped. It wouldn't matter whether the data sets were averaged or used individually, the resulting simulation would be almost the same. However, from Figures 5.37 and 5.38 it is apparent that the individual data sets from the 2C and IND methods result in dramatically different simulated output profiles. The methods are result in highly variable predictions and when taken individually, may not be very accurate. One conclusion is that if only one repetition of an experimental method were to be used to estimate the hydraulic properties, the IPM would be the best choice because of the small variability in the hydraulic properties and the predicted solute profiles. Nofziger

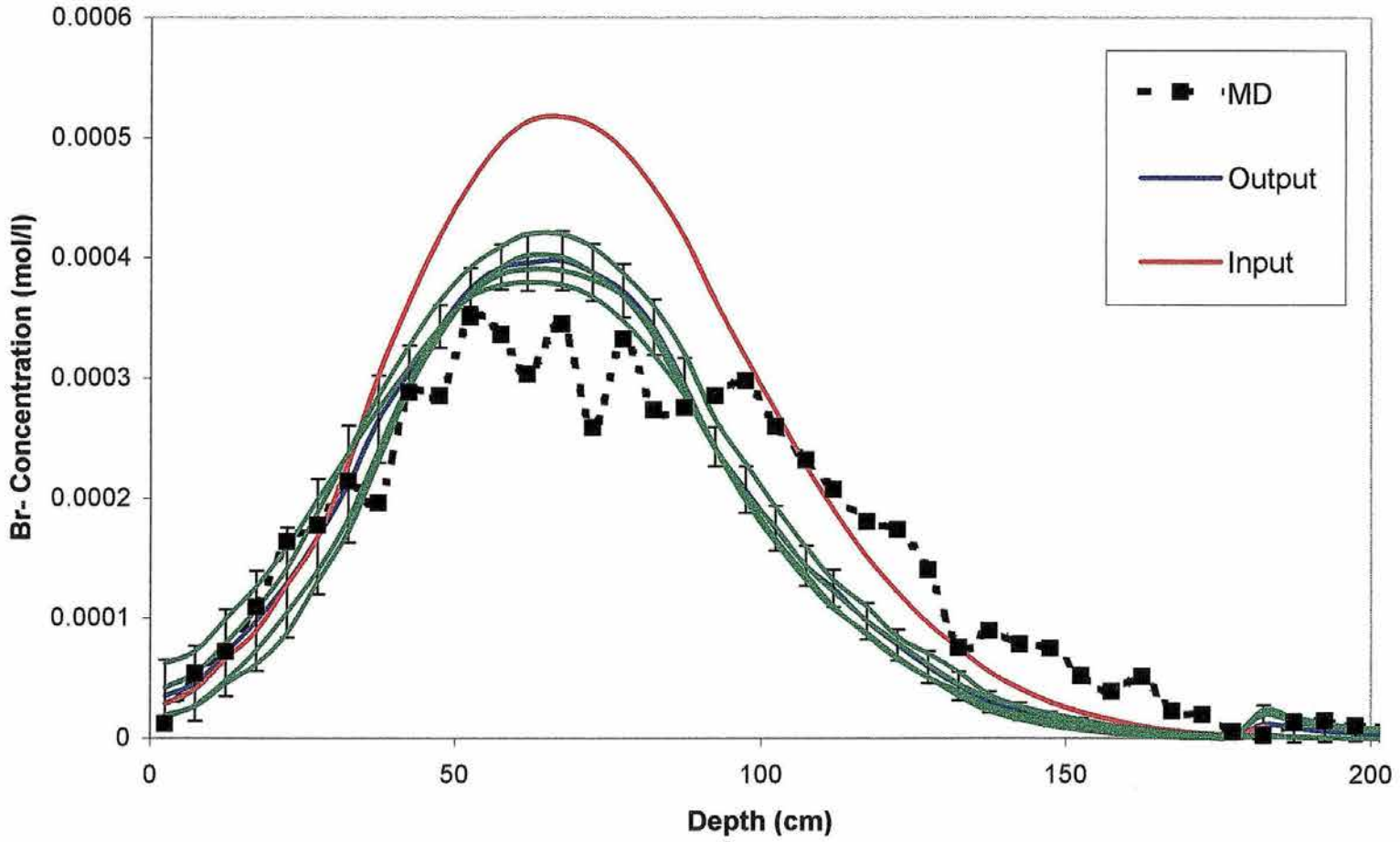

Figure 5.36. Simulated Bromide Concentration Profiles of the T soil at day 117 produced using data from the IPM method. Green colored curves are the individual output simulations, blue the average of the outputs, and red the ouput from average parameter inputs.

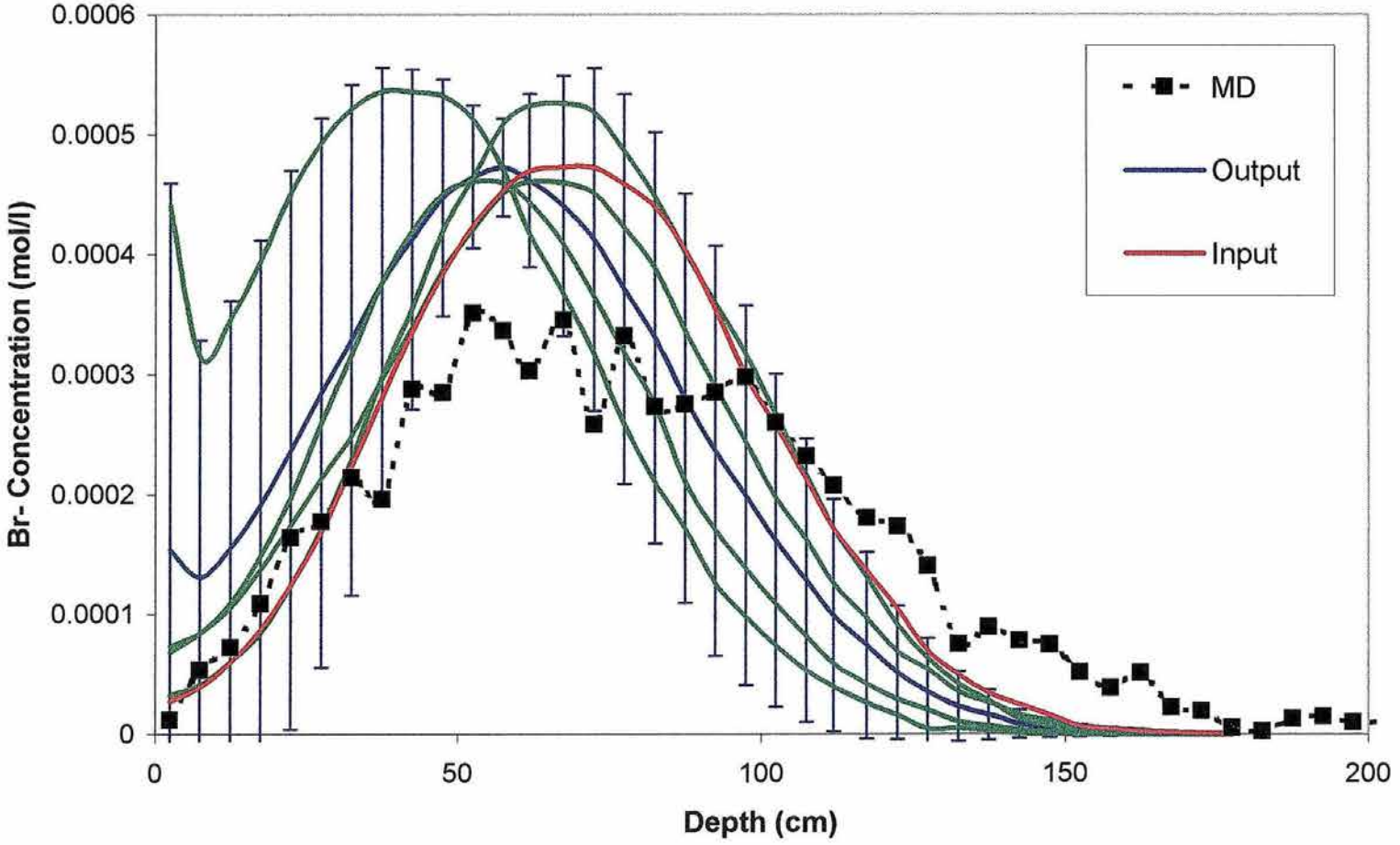

Figure 5.37. Simulated Bromide Concentration Profiles of the T soil at day 117 produced using data from the 2C method. Green colored curves are the individual output simulations, blue the average of the outputs, and red the ouput from average parameter inputs.

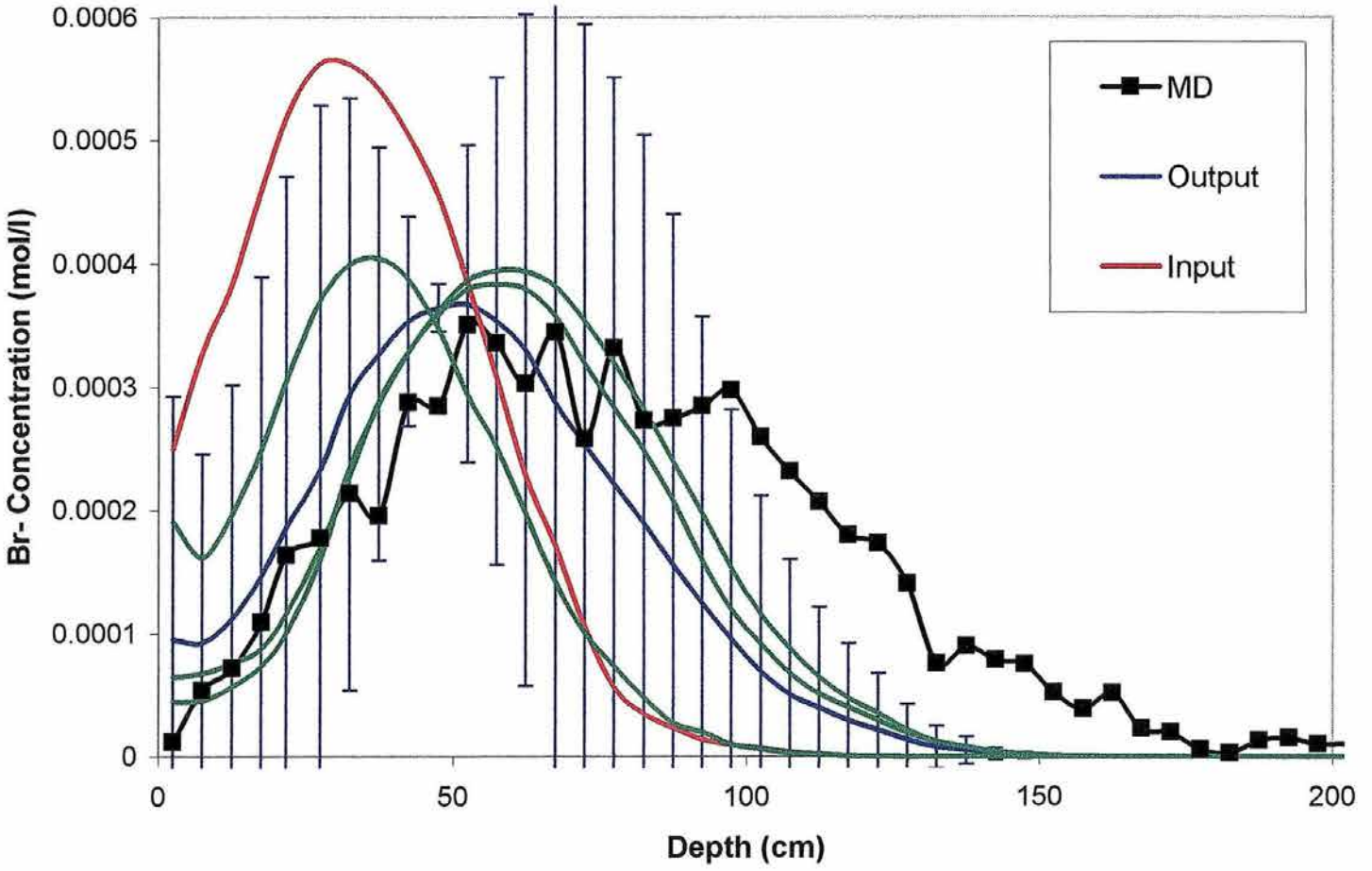

Figure 5.38. Simulated Bromide Concentration Profiles of the T soil at day 117 produced using data from the IND method. Green colored curves are the individual output simulations using three different references for the hydraulic properties

et al. (1994) also concluded that it is better to simulate solute movement using individual parameter data sets and to summarize the model predictions, than to use one single "representative" set of parameters. The knowledge gained using all the data sets can provide insight into possible uncertainties in predicting solute movement for a particular site.

5.6 Affect of Sample Support Scale on Model Predictive Accuracy

Support scale affects on hydraulic property determinations were discussed in Chapter 4, with the conclusion that no solid connection could be found between support scale and parameter value. The same conclusion can also be drawn when inspecting the solute simulation data. The 2C and 4C methods produce similar simulation results for both the T and NT treatments as seen in Figures 5.7 through 5.10. However, the 4TI and 8TI methods do not produce similar simulations. The 8TI method results in simulated bromide movement deeper into the profile than any other methods in both the T and NT. Thus, some support scale effects are seen between the permeameters, but not between the core samples. The IPM data produces results that are similar to the 2C, 4C, and 4TI methods for the T simulations, but lags behind those methods for the NT simulations. The IPM simulations are much less variable (Figures 5.34 and 5.35) than the other simulations. Thus, the larger scale measurement produces the desirable outcome of less variability, a result consistent with observations found by others (Parker and Albrecht, 1987).

5.7 Ranking of Methods

The discussion thus far in this chapter has focused on comparing the methods to the measured data or the accuracy of the methodologies. Now an effort is made to rank the methods in terms of accuracy, representativeness, ease of use, and cost. Since there is no ground truth value for the hydraulic properties, accuracy is judged in terms of the HYDRUS-2D model simulations relative to the observed $\theta(z)$ and $C(z)$. Representativeness refers to the uncertainty in the hydraulic properties: this uncertainty may arise from spatial variability of the hydraulic properties (a scale of measurement issue) and/or from the intrinsic variability of the method used to measure the hydraulic properties (a repeatability of measurement issue). The final categories, ease of use and cost, are the easiest to judge and the assignments are made based on personal experience in research and consulting.

The ratings are in qualitative rather than numerical ranking due to the subjective nature of the ranking. The ranking results are summarized in Table 5.5. In terms of accuracy, the IPM method resulted in the best overall simulation of the T data, but the 8TI method simulated the NT data better. This is evident from inspection Tables 5.2 and 5.3. The IPM has the best overall correlation to the water content and concentration data for the T treatment and minimizes deviation (Table 5.1). The IPM simulation also predicted the center of mass well for the T soil. Similarly, the 8TI method resulted in the best overall data fit for the NT soil. Thus the IPM and 8TI were deemed to be the most accurate

Table 5.5. Relative ranking of each method.

METHOD	PREDICTIVE ACCURACY	REPRESENTATIVENESS	EASE OF USE	COST
2C	MEDIUM	MEDIUM to LOW	EASY	MEDIUM
4C	MEDIUM	MEDIUM	HARD	HIGH
4TI	MEDIUM	MEDIUM	HARD	HIGH
8TI	HIGH (ESP FOR NT)	MEDIUM	HARD	HIGH
IND	LOW	LOW to VERY LOW	VERY EASY	NONE
IPM	HIGH (ESP FOR T)	HIGH	HARDEST	VERY HIGH

methods. The 2C, 4C, and 4TI methods resulted in simulations that were somewhat less accurate than the IPM and 8TI methods. The IND method produced, by far, the poorest simulations of the measured data for both the T and NT treatments.

To examine the representativeness of a method, it is necessary to examine the variability of the numerical simulations. The IPM method showed the least variability in both the measured parameter data and the simulated data profiles. This can be seen in Tables 4.2 through 4.5 and by inspection of Figures 5.30 through 5.35. The IND method resulted in the most variable simulated concentration profiles even though the "data" (literature sources) were not extremely variable. In a sense, the IND data may be the most repeatable method depending upon which sources are used, but the danger lies in selection of the data set. The 2C, 4C, 4TI and 8TI have similar variability in the parameter estimates. The saturated hydraulic conductivity values determined using the permeameters seemed atypically large for the soil we investigated. The 2C and 4C methods probably produce more repeatable estimates than the 4TI and 8TI, but because of the fairly small scale of these measurements, the hydraulic parameter estimates reflect spatial variability. The 2C and 4C methods also produce highly variable simulations as shown in Figures 5.34 and 5.35.

Ease of use describes the amount of time and effort required to obtain the parameter estimates. This is a very easy, no pun intended, category to rate. By far the IPM is the most time and labor intensive method. The IND is the easiest

method, because all that is required is to find a suitable reference and the task is finished. The 2C is the next easiest because it is fairly simple to remove soil core samples with depth if the right equipment is available. The 4TI and 8TI methods are next in ease of use, since they require essentially the same amount of effort. The 4C was rated next to last due the lack of equipment readily available to collect four inch diameter soil samples and the difficulty in handling the samples.

Cost is also simple to evaluate. The IND requires little cost, except the time taken to obtain a reference. The 2C method is the next least expensive, due to the low cost of obtaining and analyzing 2 inch diameter core samples. The 4TI and 8TI methods involve about the same cost and most of that is in terms of time. The 4C method would probably cost much more than the 2C method due to the need for larger equipment to obtain the samples. The alternative is to excavate by hand as was done during this experiment and that would require quite a bit of time as well. The IPM method is the most expensive to perform. Not only is the equipment expensive, but the time involved to perform the test and analyze the data is large relative to the other methods.

Given the criteria listed above, it appears that the 2C method gives a reasonably good combination of predictive accuracy, repeatability, ease of use, and cost. Supplementing IND estimates with measured conductivity data may be an attractive alternative. It is apparent that the IND method by itself would be a poor choice, probably due to the lack of reliable conductivity data. The IPM,

while the most representative method, did not always produce the best simulation results. It may be difficult to justify the added time and expense of the IPM method, when simpler methods applied at multiple locations may perform equally well.

CHAPTER 6

SUMMARY AND CONCLUSIONS

Statistical analysis of the hydraulic parameters in $K(\theta)$ and $\theta(h)$ revealed significant differences between parameters as estimated by method of measurement. However, the relationships are not consistent from parameter to parameter and often the parameters show no significant difference. In general, few significant differences in method, tillage, or depth were found for the n and θ_s parameters. The α and K_s parameters were the most sensitive to the method of measurement and had the greatest lateral variability. Below the tillage zone few significant differences in K_s between depths were noted for any of the methods. Alpha parameter values in the tilled soil tend to be larger than those in the no-till soil. The largest scale measurement, the IPM, had the least variability in the parameter estimates of all the methods. The soil core methods (2C and 4C) and the tension infiltrometer methods (4TI and 8TI) yielded similarly variable parameter estimates with no obvious differences between scales of like measurements. Systematic differences in the hydraulic properties from the alternative estimation methods were observed. The permeameters result in larger measured K_s values than the IPM, which has larger values than the cores. The permeameters seem to be overestimating the K_s value for this soil type.

The K_s are on the order of 300 to 400 cm/day, which are larger than any reported data for this soil type and several hundred cm/day more than the IPM. It is quite possible that this is why the permeameter simulations allow more NAW than the other simulations. Specific method types (i.e. 2C and 4C, core sampling) tend to result in similar estimates of the parameters. The IND method was distinguished by an atypically small K_s (an order of magnitude smaller than the direct measurements) and atypically small n.

There are obvious differences in solute movement between the tillage systems. Despite similar NAW, bromide was carried about 30 cm deeper in the NT treatment than in the T treatment after 118 days of transport. Solute was retained in the tillage zone and subsequent leaching did not move bromide as deep as in the NT soil. It was speculated that the bromide retention in the tillage zone was a result of diffusion into dead-end pore space created by tillage.

Numerical simulations carried out with the HYDRUS-2D code predicted varied movement of water and bromide, depending upon tillage and method of parameter estimation. Most of the parameter estimation methods resulted in simulated water content profiles that were quite similar to the measured profiles. Average absolute deviation (AAD) between the predicted and observed water content profiles were on the order of 2 to 5 percent, except for the IND simulation on days 36 and 37, where deviations were as high as 10 percent. The correlation values were highest during the early stages of simulation, but dropped for the later time stages. One reason the correlation values dropped

was because the measured water content profiles became less uniform as the drainage experiment progressed. It was not possible for the numerical simulation to predict the intricate and rather abrupt changes in water content seen in the day 117 and 118 data shown in Figures 5.3(b) and 5.4(b).

The quality of the bromide simulations relative to the measured data also tended to deteriorate with time, especially for the IND method. During the first 20 to 30 days of simulation the IND method gave good results and the simulated data was well correlated to the measured data. By day 36, the correlation values had dropped significantly and the simulated data matched the measured data poorly. By the end of the simulation, the center of mass of the predicted solute plume was about 60 cm behind the measured CM in the NT system and about 40 cm behind in the T system. The other methods, with the exception of the 8TI method, also under-predicted the center of mass movement in the NT system, but typically by about 20 cm. For the T soil, all of the methods (except the IND) predicted bromide movement well and the simulated data were well correlated with the measured data at all times throughout the simulations. Supplementing the IND data with measured surface soil hydraulic properties from the 2C method increased the depth of solute movement (Figures 5.18 and 5.19) . The CM still lags the measured CM by about 30 cm in the NT soil and about 20 cm in the T soil, but the finding is encouraging. One consideration is that the soil at the experimental site was relatively homogeneous and the results determined here may not apply in a more layered soil.

Analysis of the simulations revealed that the hydraulic properties of the surface soil are extremely important in controlling the amount of net applied water (NAW). Changing the surface properties of the IND to those measured using the 2C method, increased NAW by about 10 cm for both the T and NT treatments. The basic trend is that more NAW equals deeper movement of solute. Supplementing the IPM data with surface soil properties did not result in improved prediction of solute or water movement. Also, the profiles cannot simply be estimated using surface soil properties as shown by Figures 5.26 and 5.27. Simulations using 2C surface data to represent the entire soil profile failed to predict accurate solute movement.

Additional information about the variability of the solute predictions was gained by using individual non-averaged data sets as shown in Figures 5.36, 5.37, and 5.38. In addition, there are observed differences between predicted concentration profiles that are generated using statistically averaged parameters as input and individual non-averaged parameter data sets. It is not possible to say that one averaging method is better than the other, but more information can be gained by running individual simulations.

The answer to the question, "does the most rigorous, labor intensive method result in the most accurate prediction of solute transport?", is simply "no". The IPM method does not result in the most accurate prediction of solute transport. For the NT soil, the 8TI clearly gives better simulation results and for the T soil many of the other methods give similar results. The time and expense

of the IPM may be difficult to justified given the results shown by this study. The IPM, however, is probably the most reliable and repeatable method as is indicated by the small variability in the data. If only one test were to be made, the IPM would be the most highly recommended. The variability shown in Figures 5.34 and 5.35 indicate that the chance of obtaining a data set that results in poor simulation of solute movement is greatly increased with any other method. Thus, if the IPM is not used, then it is recommended that multiple parameter estimates be made to get a good statistically sound parameter estimates.

REFERENCES

Addiscott, T. M. 1977. A simple computer model for leaching in structured soils. J. Soil Sci. 28:554-563.

Ahuja, L.R., R.E. Green, S.K. Chong, and D.R. Nielsen. 1980. A simplified functions approach for determining soil hydraulic conductivities and water characteristics in-situ. Water Resour. Res. 16:947-953.

Ahuja, L.R., J.W. Naney, and R.D. Williams. 1985. Estimating soil water characteristics from simpler properties or limited data. Soil Sci. Soc. Am. J. 49:1100-1105.

Ahuja, L.R., J.D. Ross, R.R. Bruce, and D.K. Cassel. 1988. Determining unsaturated hydraulic conductivity from tensiometric data alone. Soil Sci. Soc. Am. J. 52:27-34.

Ammozegar-Fard, A., D. R. Nielsen, and A. W. Warrick. 1982. Soil solute concentration distributions for spatially varying pore water velocities and apparent diffusion coefficients. Soil Sci. Soc. Am. J. 46:3-9.

Anderson, J. L. and J. Bouma. 1973. Relationships between saturated hydraulic conductivity and morphometric data of an argillic horizon. Soil Sci. Soc. Am. Proc. 37:408-413.

Anderson, J. L. and J. Bouma. 1977a. Water movement through pedal soils: I. Saturated flow. J. Soil Sci. Soc. Am. 41:413-418.

Anderson, J. L. and J. Bouma. 1977b. Water movement through pedal soils: II. Unsaturated flow. J. Soil Sci. Soc. Am. 41:419-423.

Anderson, M. P. 1984. Movement of contaminants in groundwater: Groundwater transport-advection and dispersion. p. 37-45. In Groundwater contamination: Studies in geophysics. National Academy Press, Washington, D.C.

Angula-Jaramillo, R., J.P. Gaudet, J.L. Thony, and M. Vauclin. 1996. Measurement of hydraulic properties and mobile water content of a field soil. Soil Sci. Soc. Am. J. 60:710-715.

Ankeny, M. D., T. C. Kaspar, and R. Horton. 1988a. Field measurements of unconfined infiltration using a tension infiltrometer. Agronomy Abstracts.

Ankeny, M. D., T. C. Kasper, and R. Horton. 1988b. Design for an automated tension infiltrometer. Soil Sci. Soc. of Am. J. 52:893-896.

Ankeny, M.D., M. Ahmed, T.C. Kaspar, and R. Horton. 1991. Simple field method for determining unsaturated hydraulic conductivity. Soil Sci. Soc. Am. J. 55:467-470.

ARS-USDA Publication #41-144. 1968. Moisture-tension data for selected soils on experimental watersheds.

Bandaranayake, W.M., G.L. Butters, M. Hamdi, M. Prieksat, and T.R. Ellsworth. 1998. Irrigation and tillage management effects on solute movement. Soil and Tillage Research 46:165-173.

Banton, O. 1993. Field- and laboratory-determined hydraulic conductivities considering anisotropy and core surface area. Soil Sci. Soc. Am. J. 57:10-15.

Bear, J. 1972. Dynamics of fluids in porous media. American Elsevier Pub. Co., New York, N. Y.

Bear, J., and A. Verruijt. 1987. Modeling groundwater flow and pollution. D. Reidel Publishing Co., Dordrecht, Holland.

Biggar, S. W. and D. R. Nielsen. 1967. Miscible displacement and leaching phenomenon. In R. M. Hagan, H. R. Haise, and T. W. Edmister (eds.) Irrigation of Agricultural Lands. Agronomy 11:254-274.

Bouma, J. 1981. Soil morphology and preferential flow along macropores Agric. Water Management 3:235-250.

Bouma, J. 1983. Use of soil survey data to select measurement techniques for hydraulic conductivity. Agric. Water Manag. 6:177-190.

Bouma, J. and J. L. Anderson. 1973. Relationships between soil structure characteristics and hydraulic conductivity. In R. R. Bruce et al. (eds.) Field soil water regime. Soil Sci. Soc. Am. Special Publ. 5:77-105. Soil Sci. Soc. Am., Madison, WI.

Bouma, J. and J. L. Denning. 1974. A comparison of hydraulic conductivities calculated with morphometric and physical methods. Soil Sci. Soc. Am. Proc. 38:124-127.

Bouma, J., A. Jongerius, and D. Schoonderbeek. 1979. Calculations of saturated hydraulic conductivity of some pedal clay soils using micromorphometric data. Soil Sci. Soc. Am. J. 43:261-264.

Bouwer, H. 1966. Rapid field measurement of air entry value and hydraulic conductivity of soil as significant parameters in flow system analysis. Water Resour. Res. 2:729-738.

Bouwer, H. 1969. Infiltration of water into non-uniform soil. J. Irrig. Drain. Div. Am. Soc. Civil Eng. 95(IR4):451-462.

Brenner, H. 1962. The diffusion model of longitudinal mixing in beds of finite length. Numerical Values. Chem. Eng. Sci. 17:229-243.

Bresler, E. and G. Dagan. 1979. Solute dispersion in unsaturated soil at field scale: II. Application. Soil Sci. Soc. Am. J. 43:467-472.

Bresler, E. and G. Dagan. 1982. Modeling of water flow and solute transport in unsaturated heterogeneous fields. p. 159-176. In E. M. Arnold, G. W. Gee, and R. W. Nelson (eds.) Proceedings of the symposium on unsaturated flow and transport modeling. Office of Nuclear Material Safety and Safeguards. U. S. Nuclear Regulatory Commission, Washington, D. C. NUREG/CP-0030.

Bresler, E. and R. J. Hanks. 1969. Numerical method for estimating simultaneous flow of water and salt in unsaturated soils. Soil Sci. Soc. Am. Proc. 33:827-832.

Brooks, R.H. and A.T. Corey. 1964. Hydraulic properties of porous media. Hydrology Papers, Colorado State University No. 3.

Bruce, R.R., and A. Klute. 1956. The measurement of soil moisture diffusivity. Soil Sci. Soc. Am. Proc. 20:458-462.

Buckingham, E. 1907. Studies on the movement of soil moisture. U.S. Department of Agriculture Bulletin No. 38.

Butters, G.L., W.A. Jury, and F.F. Ernst. 1989. Field scale transport of bromide in an unsaturated soil 1. Experimental methodology and results. Water Resour. Res. 25:1575-1581.

Campbell, G.S. 1974. A simple method for determining unsaturated hydraulic conductivity from moisture retention data. Soil Sci. 117:311-314.

Carsel, R.F., and R.S. Parrish. 1988. Developing joint probability distributions of soil water retention characteristics. Water Resour. Res. 24:755-769.

Carslaw, H.S., and J.C. Jaeger. 1959. Conduction of heat in solids. Clarendon Press, Oxford.

Casey, F.X.M., S.D. Logsdon, R. Horton, and D.B. Jaynes. 1997. Immobile water content and mass exchange coefficient of a field soil. Soil Sci. Soc. Am. J. 61:1030-1036.

Chu, S.-Y. and G. Sposito. 1980. A derivation of the macroscopic solute transport equation for homogenous, saturated porous media. Water Resour. Res. 16:542-546.

Clothier, B.E., and I. White. 1981. Measurement of sorptivity and soil water diffusivity in the field. Soil Sci. Soc. Am. J. 45:241-245.

Clothier, B.E., and K.R. Smettem. 1990. Combining laboratory and field measurements to define the hydraulic properties of soil. Soil Sci. Soc. Am. J. 54:299-304.

Conca, J.L., and J.V. Wright. 1992. Diffusion and flow in gravel, soil, and whole rock. Appl. Hydrogeol. 1:5-24.

Crittenden, J. C., N. J. Hutzler, D. G. Geyer, J. L. Oravitz, and G. Friedman. 1986. Transport of organic compounds with saturated groundwater flow: Model development and parameter sensitivity. Water Resour. Res. 22:271-284.

Dagan, G. and E. Bresler. 1979. Solute dispersion in unsaturated heterogeneous soils at field scale: I. Theory. Soil Sci. Soc. Am. J. 43:461-466.

Danckwerts, P. V. 1953. Continuous flow systems: Distribution of residence times. Chem. Eng. Sci. 2:1-13.

De Smedt, F. and P. J. Wierenga. 1978. Solute transport through soil with nonuniform water content. Soil Sci. Soc. Am. J. 42:7-10.

De Smedt, F. and P. J. Wierenga. 1979. Mass transfer in porous media with immobile water. J. Hydrol. 41:59-67.

Doering, E.J. 1965. Soil-water diffusivity by the one-step method. Soil Sci. 99:322-326.

Elrick, D. E. and L. K. French. 1966. Miscible displacement patterns on disturbed and undisturbed soil cores. Soil Sci. Soc. Am. Proc. 30:153-156.

Elrick, D.E., M.I. Sheppard, A. Mermoud, and T. Monnier. 1997. An analysis of surface accumulation of previously distributed chemical during steady-state evaporation. J. Environ. Qual. 26:883-888.

Feddes, R.A., P. Kabat, P.J.T. Van Bakel, J.J.B. Bronswijk, and J. Halbertsma. 1988. Modeling soil water dynamics in the unsaturated zone - state of the art. J. Hydrol. 100:69-111.

Field, J.A., J.C. Parker, and N.L. Powell. 1984. Comparison of field and laboratory measured and predicted hydraulic properties of a soil with macropores. Soil Sci. 138:385-396.

Freeze, R. A. and J. A. Cherry. 1979. Groundwater. Prentice-Hall, Inc., Englewood Cliffs, N. J.

Fried, J. J. 1975. Groundwater pollution: Theory, methodology, modelling and practical rules. Elsevier Scientific Publishing Co., New York.

Gardner, W.R. 1956. Calculation of capillary conductivity from pressure plate and flow data. Soil Sci. Soc. Am. Proc. 20:317-320.

Gardner, W.R. 1958. Some steady-state solutions of the unsaturated moisture flow equation with application to evaporation from a water table. Soil Sci. 85:228-232.

Gardner, W.R. 1962. Approximate solutions of a non-steady-state drainage problem. Soil Sci. Soc. Am. Proc. 26:129-132.

Giddings Machine Company, Fort Collins, CO.

Gillham, R. W. and J. A. Cherry. 1982. Contaminant migration in saturated unconsolidated geologic deposits. In T. N. Narasimhan (ed.) Recent trends in hydrogeology. Spec. paper 189. Geol. Soc. Am. Boulder, Co.

Gish, T. J. 1987. Bromide transport in structured soils. Am. Soc. Agric. Eng. meeting paper no. 87-2625. St. Joseph, Mich.

Gish, T. J. and W. A. Jury. 1982. Estimating solute travel times through a crop root zone. Soil Sci. 133:124-130.

Green, W. H. and G. A. Ampt. 1911. Studies on soil physics, 1. The flow of air and water through soils. J. Agric. Sci. 4:1:1-24.

Green. R.E., L.R. Ahuja, and S.K. Chong. 1986. Hydraulic conductivity, diffusivity, and sorptivity of unsaturated soils: Field methods. In Methods of Soils Analysis, Part 1. Physical and Mineralogical Methods. Agronomy Monograph no. 9 (2nd Ed.).

Gupta, S.C., D.A. Farrell, and W.E. Larson. 1974. Determining effective soil water diffusivities from one-step outflow experiments. Soil Sci. Soc. Am. Proc. 38:710-716.

Gupta, S.C., and W.E. Larson. 1979. Estimating soil water retention characteristics from particle size distribution, organic matter percent, and bulk density. Water Resour. Res. 15:1633-1635.

Haverkamp, R., M. Vauclin, J. Touma, P. J. Wierenga, and G. Vachaud. 1977. A comparison of numerical simulation models for one-dimensional infiltration. Soil Sci. Soc. Am. J. 41:285-294.

Haverkamp, R., and J.Y. Parlange. 1986. Predicting the soil-water-retention curve from particle-size distribution: Sandy soils without organic matter. Soil Sci. 142:325-339.

Hillel, D. and W. R. Gardner. 1970. Measurement of unsaturated conductivity and diffusivity by infiltration through an impeding layer. Soil Sci. 109:149-153.

Hillel, D., V.D. Krentos, and Y.Stylianou. 1972. Procedure and test of an internal drainage method for measuring soil hydraulic characteristics in situ. Soil Sci. 114:395-400.

Hillel, D. 1980. Fundamentals of Soil Physics. Academic Press, New York.

Hills, R.G., D.B. Hudson, I. Porro, and P.J. Wierenga. 1989. Modeling one-dimensional infiltration into very dry soils 2. Estimation of the soil water parameters and model predictions. Water Resour. Res. 25(6):1271-1282.

Holtan, H. N. 1961. A concept for infiltration estimates in watershed engineering. U. S. Dept. Agric. ARS-41-51. 25pp.

Hopmans, J.W., J.C. van Dam, S.O. Eching, and J.N.M. Stricker. 1994. Parameter estimation of soil hydraulic functions using inverse modeling of transient outflow experiments. Trends in Hydrology.

Horton, R. and P. J. Wierenga. 1986. Preferential flow of water and solutes in structured soils. SSSA Workshop Paper no. 11.

Hutson, J.L. and R.J. Wagenet. 1994. A multiregion model describing water flow and solute transport in heterogeneous soils. Soil Sci. Soc. Am. J. 59:743-751.

Jaynes, D.B., and E.J. Tyler. 1980. Comparison of one-step outflow laboratory method to an in situ method for measuring hydraulic conductivity. Soil Sci. Soc. Am. J. 44:903-907.

Jaynes, D.B., S.D. Logsdon, and R. Horton. 1995. Field method for measuring mobile.immobile water content and solute transfer coefficient. Sci. Soc. Am. J. 59:352-356.

Jennings, G. D. and D. L. Martin. 1988. A transfer function model to predict field nitrogen leaching. Am. Soc. Agric. Eng. paper no. 88-2636. St. Josephs, Mich.

Jury, W. A., W. R. Gardner, P. G. Saffigna, and C. B. Tanner. 1976. Model for predicting simultaneous movement of nitrate and water through a loamy sand. Soil Sci. 122:36-43.

Jury, W. A., L. H. Stolzy, and P. Shouse. 1982. A field test of the transfer function model for predicting solute transport. Water Resour. Res. 18:369-375.

Jury, W.A., W.R. Gardner, and W.H. Gardner. 1991. Soil Physics. 5Th Ed. John Wiley and Sons, Inc. USA.

Kanwar, R. S., J. L. Baker, and J. M. Laflen. 1985. Nitrate movement through the soil profile in relation to tillage system and fertilizer application method. Trans. ASAE 28:1731-1735.

Kaspar, T. C., S.D. Laosdon, and M.A. Prieksat. 1995. Traffic pattern and tillage system effects on corn root and shoot growth. Agron. J. 87:1046-1051.

Kim, C.P., and J.N.M. Stricker. 1995. Consistency of modeling the water budget over long time series: comparison of simple parameterizations and a physically based model. J. of Applied Meter. 35:749-758.

Kirda, C., D. R. Nielsen, and J. W. Biggar. 1973. Simultaneous transport of chloride and water during infiltration. Soil Sci. Soc. Am. Proc. 37:339-345.

Kirkham, D. and W. L. Powers. 1972. Advanced Soil Physics. Wiley-Intersciences, New York.

Klute, A. 1952. A numerical method for solving the flow equation for water in unsaturated materials. Soil Sci. 73:105-116.

Klute, A. 1982. Tillage effects on the hydraulic properties of soil: A review. *In* Predicting Tillage Effects on Soil Phyical Properties and Processes. ASA, SSSA Publications.

Klute, A. 1986. Water Retention: Laboratory methods. *In* Methods of Soils Analysis, Part 1. Physical and Mineralogical Methods. Agronomy Monograph no. 9 (2nd Ed.).

Klute, A., and C. Dirksen. 1986. Hydraulic conductivity and diffusivity: Laboratory methods. *In* Methods of Soils Analysis, Part 1. Physical and Mineralogical Methods. Agronomy Monograph no. 9 (2nd Ed.).

Kool, J.B., J.C. Parker, and M.T. van Genuchten. 1985. Determining soil hydraulic properties from one-step outflow experiments by parameter estimation: I. Theory and numerical studies. Soil Sci. Soc. Am. J. 49:1348-1359.

Kool, J.B., and J.C. Parker. 1988. Analysis of the inverse problem for transient unsaturated flow. Water Resour. Res. 24:817-830.

Leeds-Harrison, P. B. and C. J. P. Shipway. 1984. Variations in hydraulic conductivity under different wetting regimes. In J. Bouma and P. A. C. Raatz (ed.) Proceedings of the ISSS Symposium on Water and Solute Movement in Heavy Clay Soils. Inter. Inst. for Land Reclamation and Improvement, The Netherlands.

Leij, F.J., W.J. Alves, and M.T. van Genuchten. 1996. The UNSODA unsaturated soil hydraulic database: Users Manual Version 1.0. U.S. Salinity Laboratory, Riverside California.

Lewis, D. T. 1977. Subgroup designation of three Udolls in southeastern Nebraska. Soil Sci. Am. J. 41:940-945.

Libardi, P.L., K. Reichardt, D.R. Nielsen, and J.W. Bigger. 1980. Simple field methods for estimating soil hydraulic conductivity. Soil Sci. Soc. Am.J. 44:3-7.

Liwang Ma, and H.M. Selim. 1997. Evaluation of nonequilibrium models for predicting atrazine transport in soils. Soil Sci. Soc. Am. J. 61:1299-1307.

Mallants, D., D. Jacques, P.H. Tseng, M.T. van Genuchten, and J. Feyen. 1997. Comparison of three hydraulic property measurement methods. J. Hydrol. 199:295-318.

Mallants, D., P.H. Tseng, M. Vanclooster, and J. Feyen. 1998. Predicted drainage for a sandy loam soil: sensitivity to hydraulic property description. J. Hydrol. 206:136-148.

Marion, J.M., D.E. Rolston, M.L. Kavvas, and J.W. Biggar. 1994. Evaluation of methods for determining soil-water retentivity and unsaturated hydraulic conductivity. Soil Sci. 158(1):1-13.

McBride, J. F. 1985. Measured and predicted anion movement in an Iowa soil. M. S. thesis. Iowa State University, Ames, Iowa.

McMahon, M. A. and G. W. Thomas. 1974. Chloride and tritiated water flow in disturbed soil cores. Soil Sci. Soc. Am. Proc. 38:727-732.

Mein, R. G. and C. L. Larson. 1973. Modeling infiltration during a steady rain. Water Resour. Res. 9:384-394.

Millington, R.J., and J.M. Quirk. 1961. Permeability of porous solids. Trans. Faraday Soc. 57:1200-1207.

Molz, F. J., O. Guven, J. G. Melville, and J. F. Keely. 1986. Performance and analysis of aquifer tracer tests with implications for contaminant transport modeling. Robert S. Kerr Environmental Research Laboratory office of Research and Development. U. S. Environ. Protect. Agency, Ada, Okla.

Moore, I. D., G. J. Burch, and P. J. Wallbrink. 1986. Preferential flow and hydraulic conductivity of forest soils. Soil Sci. Soc. Am. J. 50:876-881.

Mualem, Y. 1976. A new model for predicting the hydraulic conductivity of unsaturated porous media. Water Resour. Res. 12(3):513-522.

Nielsen, D. R. and J. W. Biggar. 1961. Miscible Displacement in Soils: I. Experimental Information. Soil Sci. Soc. Am. Proc. 25:1-5.

Nielsen, D. R. and J. W. Biggar. 1962. Miscible Displacement in soils. III. Theoretical considerations. Soil Sci. Soc. of Am. 26:216-221.

Nielsen, D. R., R. D. Jackson, J. W. Cary, and D. D. Evan (eds.) 1972. Soil Water. Am. Soc. Agron. and Soil Sci. Soc. Am., Madison, Wisc.

Nielsen, D. R., J. W. Biggar, and K. T. Erh. 1973. Spatial variability of field-measured soil water properties. Hilgardia 42:215-259.

Nimmo, J.R., J. Rubin, and D.P. Hammermeister. 1987. Unsaturated flow in a centrifugal field: Measurement of hydraulic conductivity and testing of Darcy's law. Water Resour. Res. 23:124-134.

Nimmo, J.R. 1997. Modeling structural influences on soil water retention. Soil Sci. Soc. Am. J. 61:712-719.

Nkedi-Kizza, P., P. S. C. Rao, and R. E. Jessup, and J. M. Davidson. 1982. Ion exchange and diffusive mass transfer during miscible displacement through an aggregated Oxisol. Soil Sci. Soc. Am. J. 46:471-476.

Nofziger, D.L., Jin-Song Chen, and C.T. Haan. 1994. Evaluation of unsaturated/vadose zone models for superfund sites. Report No. EPA/600/SR-93/184.

Ogata, A. and R. B. Banks. 1961. A solution of the differential equation of longitudinal dispersion in porous media. U. S. G. S. Prof. Paper 411 A.

Pandey, R. S. and S. K. Gupta. 1984. Analysis of breakthrough curves: Effect of mobile and immobile pore volumes. Aust. J. Soil Res. 22:23-30.

Parker, J. C. 1984. Analysis of solute transport in column tracer studies. Soil Sci. Soc. Am. J. 48:719-724.

Parker, J. C. and M. Th. van Genuchten. 1984. Determining transport parameters from laboratory and field tracer experiments. Va. Agric. Exp. Stn. Bull. 84-3.

Parker, J.C., and K.A. Albrecht. 1987. Sample volume affects on solute transport predictions. Water Resour. Res. 23:2293-2301.

Passioura, J.B. 1976. Determining soil water diffusivities from one-step outflow experiments. Aust. J. Soil Res. 15:1-8.

Perroux, K. M. and I. White. 1988. Designs for disc permeameters. 1988. Soil Sci. Soc. Am. J. 52:1205-1215.

Philip, J. R. 1957. The theory of infiltration: 4. Sorptivity and algebraic infiltration equations. Soil Sci. 84:257-264.

Philip, J. R. 1969. Theory of infiltration. Adv. Hydro-Sci. 5:215-296.

Philip, J. R. 1983. Infiltration in one, two, and three dimensions. p. 1-13. In Advances in infiltration: Proceedings of the National Conference on Advances in Infiltration. Am. Soc. of Agric. Eng., St. Joseph, Mich.

Pickens, J. F. and G. E. Grisak. 1981. Scale-dependent dispersion in a stratified granular aquifer. Water Resour. Res. 17:1191-1211.

Prieksat, M. A., M.D. Ankeny, and T.C. Kaspar. 1992. Design for an automated, self-regulating, single-ring infiltrometer. Soil Sci. Soc. Am. J. 56:1409-1411.

Prieksat, M.A., T.C. Kaspar, and M.D. Ankeny. 1994. Positional and temporal changes in ponded infiltration in a corn field. Soil Sci. Soc. Am. J. 58:181-184.

Prieksat, M.A., M.D. Ankeny, J.C. Kelsey, and M.T. Thurgood. 1997. A one-step outflow cell for the determination of soil hydraulic properties. SBIR Report No. 97-19834-25.

Rao, P. S. C., J. M. Davidson, R. E. Jessup, and H. M. Selim. 1979. Evaluation of conceptual models for describing nonequilibrium adsorption-desorption of pesticides during stead-flow in soils. Soil Sci. Soc. Am. J. 43:22-28.

Rasmuson, A. 1986. Modeling of solute transport in aggregated / fractured media including diffusion into the bulk matrix. Geoderma 38:41-60.

Rawls, W.J., D.L. Brakensiek, and K.E. Saxton. 1982. Estimating soil water properties. Trans. ASAE. 25(5):1316-1320.

Reynolds, W.D., D.E. Elrick, N. Baumgartner, and B.E. Clothier. 1984. The "Guelph Permeameter" for measuring the field-saturated soil hydraulic conductivity above the water table: 2. The apparatus. Proc. Canadian Hydrology Symposium, Quebec City, Quebec.

Richards, L. A. 1931. Capillary conduction of liquids through porous mediums. Physics 1:318-333.

Richards, L.A., W.R. Gardner, and G. Ogata. 1956. Physical processes determining water loss from soil. Soil Sci. Soc. Am. Proc. 20:310-314.

Roberts, P. V., M. N. Goltz, R. S. Summers, J. C. Crittenden, and P. Nkedi-Kizza. 1987. The influence of mass transfer on solute transporting column experiments with an aggregated soil. J. Contaminant Hydrol. 1:375-393.

Rowse, H.R. 1975. Simulations of the water balance of soil columns and fallow soils. J. Soil Sci. 26(4):337-349.

SAS Institute, Inc., Cary, NC.

Seyfried, M. S. and P. S. C. Rao. 1987. Solute transport in undisturbed columns of an aggregated tropical soil: preferential flow effects. Soil Sci. Am. J. 51:1434-1444.

Shan, C., and D.B. Stephens. 1993. A borehole field method to determine unsaturated hydraulic conductivity. Water Resour. Res., 29(8):2763-2769.

Simunek, J., M. Sejna, and M.T. van Genuchten. 1996. HYDRUS-2D: Simulating water flow and solute transport in two-dimensional variably saturated media. IGWMC, Colorado School of MInes.

Sisson, J.B., and P.J. Sierenga. 1981. Spatial variability of steady-state infiltration rates as a stochastic process. Soil Sci. Soc. Am. J. 45:699-704.

Skopp, J. and A. W. Warrick. 1974. A two-phase model for the miscible displacement of reactive solutes in soils. Soil Sci. Am. Proc. 38:545-550.

Smettem, K. R. J. and N. Collis-George. 1985a. Prediction of steady-state ponded infiltration distributions in a soil with vertical macropores. J. Hydrol. 79:115-122.

Smettem, K. R. J. and N. Collis-George. 1985b. Statistical characterization of soil biopores using a soil peel method. Geoderma 36:27-36.

Smettem, K.R.J., J.Y. Parlange, P.J. Ross, and R. Haverkamp. 1994. Three-dimensional analysis of infiltration from the disc infiltrometer, 1, Theoretical capillary approach. Water Resour. Res. 30:2925-2929.

Soil Moisture Equipment Corp. Santa Barbara, California.

Southern Cooperative Series Bulletin 303. 1985. Physical characteristics of soils of the southern region-summary of in-situ unsaturated hydraulic conductivity. North Carolina State University.

Starr, J.L., T.B. Parkin, and J.J. Meisinger. 1995. Influence of sample size on chemical and physical soil measurements. Soil Sci. Soc. Am. J. 59:713-719.

Swartzendruber, D. 1969. The flow of water in unsaturated soils. p. 215-292. In R. J. M. DeWiest (ed.) Flow through porous media. Academic Press, New York.

Toorman, A.F., P.J. Wierenga, and R.G. Hills. 1992. Parameter estimation of hydraulic properties from one-step outflow data. Water Resour. Res. 28:3021-3028.

Topp, G. C. and M. R. Binns. 1976. Field measurement of hydraulic conductivity with a modified air-entry permeameter. Canadian J. Soil Sci. 56:139-147.

Topp, G. C. and W. D. Zebchuk. 1985. A closed adjustable head infiltrometer. Canadian Agric. Eng. 27:99-104.

U.S. Environmental Protection Agency. 1990a. National Water Quality Inventory, 1988 Report to Congress. Office of Water. EPA 440-4-9-003.

U.S. Environmental Protection Agency. 1990b. National Pesticide Survey, Phase I Report. Office of Water. EPA 440-5-7-012.

van Dam, J.C., J.N.M. Stricker, and P. Droogers. 1992. Inverse method for determining soil hydraulic functions from one-step outflow experiments. Soil Sci. Soc. Am. J. 56:1042-1050.

Van De Pol, R. M., P. J. Wierenga, and D. R. Nielsen. 1977. Solute movement in a field soil. Soil Sci. Soc. Am. J. 41:10-13.

van Genuchten, M. Th. 1980. A closed-form equation for predicting the hydraulic conductivity of unsaturated soils. Soil Sci. Soc. Am. J. 44:892-898.13

van Genuchten, M. Th. and F. N. Dalton. 1986. Models for simulating salt movement in aggregated field soils. Geoderma 38:165-183.

van Genuchten, M. Th. and P. J. Wierenga. 1976. Mass transfer studies in sorbing porous media. 1. Analytical solutions. Soil Sci. Soc. Am. J. 40:472-480.

van Genuchten, M. Th. and P. J. Wierenga. 1986. Solute dispersion coefficients and retardation factors. In Methods of soil analysis Part I: Physical and mineralogical methods. Agronomy (2nd ed.) 9:1025-1054.

van Genuchten, M.T., and W.A. Jury. 1987. Progress in unsaturated flow and transport modeling. Reviews of Geophys. 25:135-140.

van Genuchten, M.T., F.J. Leij, and S.R. Yates. 1991. The RETC code for quantifying the hydraulic functions of unsaturated soils. U.S. Salinity Laboratory. Riverside, California.

van Wesenbeeck, I.J., and R.G. Kachanoski. 1995. Predicting field-scale solute transport using in situ measurements of soil hydraulic properties. Soil Sci. Soc. Am. J. 59:734-742.

Wagenet, R.J. 1984. Measurement and interpretation of spatially variable leaching processes. In Soil Spatial Variability, Proc. Of Workshop (Nielsen and Bouma, eds) Pudoc Wageningen, The Netherlands.

Wagenet, R. J. 1986. Principles of modeling pesticide movement in the unsaturated zone. p. 330-341. In Evaluation of pesticides in ground water. Am. Chem. Soc., Washington, D. C.

Warrick, A. W., J. W. Biggar, and D. R. Nielsen. 1971. Simultaneous solute and water transfer for unsaturated soil. Water Resour. Res. 7:1216-1225.

Watson, K.K. 1966. An instantaneous profile method for determining the hydraulic conductivity of unsaturated porous materials. Water Resour. Res. 2:709-715.

Wierenga, P. J. 1977. Solute distribution soil profiles computed with steady-state and transient water movement models. Soil Sci. Soc. Am. J. 41:1050-1055.

Whisler, F.D., and K.K. Watson. 1968. One-dimensional gravity drainage of uniform columns of porous materials. J. Hydrol. 6:277-296.

Williams, R.D, L.R. Ahuja, and J.W. Naney. 1992. Comparison of methods to estimate soil water characteristics from soil texture, bulk density, and limited data. Soil Sci. 153(3):172184.

Wosten, J.H.M., and M.T. van Genuchten. 1988. Using texture and other soil properties to predict soil hydraulic functions. Soil Sci. Soc. Am. J. 52:1762-1770.

Wu, L., R.R. Allmaras, J.B. Lamb, and K.E. Johnsen. 1996. Model sensitivity to measured and estimated hydraulic properties of a Zimmerman fine sand. Soil Sci. Soc. Am. J. 60:1283-1290.

Young, E.G. 1983. Soil physical theory and heterogeneity. Agric. Water Manag. 6:145-159.

Zachmann, D.W., P.C. Duchateau, and A. Klute. 1981. The calibration of Richards flow equation for a draining column by parameter identification. Soil Sci. Soc. Am. J. 44:892-898.

Zachmann, D.W., P.C. Duchateau, and A. Klute. 1982. Simultaneous approximation of water capacity and soil hydraulic conductivity by parameter identification. Soil Sci. 134:157-163.

Zhang, Y., R.E. Smith, G.L. Butters, and G.E. Cardon. 1999. Analysis and testing of a concentric-disk tension infiltrometer. (In Press).

APPENDIX A

Till Treatment, 2 Inch Diameter Core Samples						
Depth (cm)	Plot	α (cm^{-1})	n	θ_s (%)	θ_r (%)	K (cm/s)
0	Till1	0.039	1.697	0.551	0.147	1.22E-03
0	Till2	0.041	1.451	0.488	0.163	8.70E-04
0	Till3	0.034	1.489	0.365	0.148	9.50E-04
0	Till4	0.051	2.550	0.551	0.185	9.09E-04
		0.041	1.797	0.489	0.160	9.87E-04
10	Till1	0.014	1.551	0.520	0.187	6.50E-04
10	Till2	0.036	1.457	0.457	0.178	5.50E-04
10	Till3	0.013	1.570	0.379	0.195	9.80E-04
10	Till4	0.010	1.967	0.524	0.218	1.08E-03
		0.018	1.636	0.470	0.194	8.16E-04
20	Till1	0.026	1.447	0.422	0.199	7.70E-04
20	Till2	0.022	1.550	0.430	0.179	9.80E-04
20	Till3	0.006	1.725	0.361	0.186	8.40E-04
20	Till4	0.015	1.949	0.422	0.146	4.68E-04
		0.017	1.668	0.409	0.178	7.65E-04
30	Till1	0.013	1.773	0.479	0.158	9.60E-05
30	Till2	0.035	1.559	0.408	0.175	6.50E-04
30	Till3	0.004	1.967	0.329	0.180	4.70E-04
30	Till4	0.009	1.823	0.488	0.175	1.44E-03
		0.015	1.780	0.426	0.172	6.64E-04
60	Till1	0.016	1.632	0.377	0.152	7.70E-04
60	Till2	0.022	1.503	0.451	0.137	8.20E-04
60	Till3	0.020	1.555	0.303	0.127	6.30E-04
60	Till4	0.006	1.976	0.413	0.145	8.27E-04
		0.016	1.666	0.386	0.141	7.62E-04
90	Till1	0.006	1.737	0.355	0.155	4.50E-04
90	Till2	0.017	1.659	0.451	0.130	8.80E-05
90	Till3	0.022	1.453	0.285	0.149	6.80E-04
90	Till4	0.006	2.214	0.377	0.143	9.14E-04
		0.013	1.766	0.367	0.144	5.33E-04
120	Till1	0.006	2.361	0.465	0.166	5.90E-04
120	Till2	0.007	1.599	0.428	0.136	6.20E-04
120	Till3	0.005	1.426	0.346	0.110	7.40E-04
120	Till4	0.007	1.932	0.355	0.166	3.23E-04
		0.006	1.829	0.398	0.144	5.68E-04
150	Till1	0.002	1.751	0.530	0.174	5.58E-04
150	Till2	0.005	1.565	0.403	0.148	9.85E-04
150	Till3	0.002	1.543	0.274	0.125	4.26E-04
150	Till4	0.001	1.759	0.465	0.117	4.11E-04
		0.003	1.655	0.418	0.141	5.95E-04
180	Till1	0.007	2.110	0.479	0.140	4.70E-04
180	Till2	0.011	1.607	0.382	0.135	6.80E-04
180	Till3	0.004	1.373	0.309	0.166	5.20E-04
180	Till4	0.006	1.680	0.426	0.121	5.13E-04
		0.007	1.692	0.399	0.140	5.46E-04

Appendix A. Table of measured data.

No-Till Treatment, 2 Inch Diameter Core Samples						
Depth (cm)	Plot	α (cm^{-1})	n	θ_s (%)	θ_r (%)	K (cm/s)
0	NoTill1	0.014	1.472	0.464	0.166	7.24E-04
0	NoTill2	0.016	1.619	0.475	0.144	6.97E-04
0	NoTill3	0.007	2.093	0.447	0.141	5.56E-04
0	NoTill4	0.014	1.416	0.454	0.150	8.62E-04
		0.013	1.650	0.460	0.150	7.10E-04
10	NoTill1	0.028	1.663	0.487	0.178	5.56E-04
10	NoTill2	0.019	1.896	0.469	0.191	6.87E-04
10	NoTill3	0.029	1.709	0.490	0.188	4.26E-04
10	NoTill4	0.015	1.575	0.483	0.157	4.96E-04
		0.023	1.711	0.482	0.178	5.41E-04
20	NoTill1	0.010	1.515	0.474	0.164	7.58E-04
20	NoTill2	0.009	2.227	0.469	0.142	6.59E-04
20	NoTill3	0.011	2.045	0.434	0.168	7.19E-04
20	NoTill4	0.014	1.157	0.395	0.126	4.74E-04
		0.011	1.736	0.443	0.150	6.53E-04
30	NoTill1	0.029	1.969	0.435	0.155	4.25E-04
30	NoTill2	0.025	1.709	0.459	0.168	5.56E-04
30	NoTill3	0.014	1.547	0.388	0.120	7.26E-04
30	NoTill4	0.010	1.423	0.474	0.129	6.92E-04
		0.019	1.662	0.439	0.143	6.00E-04
60	NoTill1	0.017	1.888	0.406	0.112	8.84E-04
60	NoTill2	0.014	2.548	0.403	0.140	7.35E-04
60	NoTill3	0.011	1.685	0.415	0.148	7.67E-04
60	NoTill4	0.021	1.576	0.447	0.136	4.59E-04
		0.016	1.924	0.418	0.134	7.11E-04
90	NoTill1	0.014	2.016	0.430	0.157	5.58E-04
90	NoTill2	0.014	2.136	0.441	0.131	8.47E-04
90	NoTill3	0.015	1.615	0.432	0.086	7.14E-04
90	NoTill4	0.013	1.589	0.445	0.108	6.80E-04
		0.014	1.839	0.437	0.120	7.00E-04
120	NoTill1	0.010	3.344	0.440	0.079	6.87E-04
120	NoTill2	0.014	1.234	0.500	0.075	6.62E-04
120	NoTill3	0.002	0.471	0.364	0.070	5.78E-04
120	NoTill4	0.002	0.607	0.396	0.058	6.36E-04
		0.007	1.414	0.425	0.070	6.41E-04
150	NoTill1	0.009	2.010	0.481	0.104	6.63E-04
150	NoTill2	0.010	1.945	0.472	0.127	6.25E-04
150	NoTill3	0.005	1.590	0.465	0.095	6.98E-04
150	NoTill4	0.010	1.467	0.396	0.076	4.91E-04
		0.008	1.753	0.453	0.100	6.19E-04
180	NoTill1	0.007	1.590	0.409	0.119	9.98E-04
180	NoTill2	0.011	1.875	0.398	0.136	4.12E-04
180	NoTill3	0.009	1.268	0.388	0.145	8.75E-04
180	NoTill4	0.009	1.674	0.345	0.118	2.99E-04
		0.009	1.602	0.385	0.130	6.46E-04

Appendix A. Table of measured data.

Till Treatment, 4 Inch Diameter Core Samples						
Depth (cm)	Plot	α (cm^{-1})	n	θ_s (%)	θ_r (%)	K (cm/s)
0	Till1	0.038	1.571	0.491	0.186	5.70E-04
0	Till2	0.041	2.157	0.326	0.160	1.10E-03
0	Till3	-	-	-	-	8.50E-04
0	Till4	-	-	-	-	3.46E-03
		0.040	1.864	0.409	0.173	1.50E-03
10	Till1	0.021	1.413	0.447	0.190	8.80E-04
10	Till2	0.022	2.020	0.355	0.141	2.50E-03
10	Till3	-	-	-	-	1.80E-03
10	Till4	-	-	-	-	3.67E-04
		0.022	1.717	0.401	0.165	1.39E-03
20	Till1	0.018	1.461	0.445	0.176	1.15E-03
20	Till2	0.016	1.885	0.297	0.126	2.78E-03
20	Till3	-	-	-	-	5.80E-04
20	Till4	-	-	-	-	7.90E-04
		0.017	1.673	0.371	0.151	1.33E-03
30	Till1	0.013	1.584	0.365	0.187	2.70E-03
30	Till2	0.013	1.254	0.318	0.162	9.00E-04
30	Till3	-	-	-	-	5.10E-04
30	Till4	-	-	-	-	4.55E-04
		0.013	1.419	0.341	0.175	1.14E-03
60	Till1	0.016	1.470	0.364	0.132	1.40E-03
60	Till2	0.014	1.215	0.348	0.146	8.60E-04
60	Till3	-	-	-	-	9.20E-04
60	Till4	-	-	-	-	1.00E-03
		0.015	1.343	0.356	0.139	1.05E-03
90	Till1	0.011	1.547	0.346	0.125	1.10E-03
90	Till2	0.015	1.478	0.324	0.172	1.60E-03
90	Till3	-	-	-	-	8.90E-04
90	Till4	-	-	-	-	1.02E-03
		0.013	1.513	0.335	0.149	1.15E-03
120	Till1	0.003	2.000	0.422	0.178	9.20E-04
120	Till2	0.015	1.987	0.313	0.152	8.60E-04
120	Till3	-	-	-	-	9.60E-04
120	Till4	-	-	-	-	8.40E-04
		0.009	1.994	0.367	0.165	8.95E-04
150	Till1	0.003	1.594	0.406	0.146	9.60E-04
150	Till2	0.018	1.428	0.315	0.155	1.00E-03
150	Till3	-	-	-	-	8.70E-04
150	Till4	-	-	-	-	1.73E-03
		0.010	1.511	0.361	0.150	1.14E-03
180	Till1	0.003	1.748	0.397	0.149	9.20E-04
180	Till2	0.014	1.623	0.384	0.132	8.10E-04
180	Till3	-	-	-	-	8.00E-04
180	Till4	-	-	-	-	9.83E-04
		0.008	1.686	0.391	0.140	8.78E-04

Appendix A. Table of measured data.

No-Till Treatment, 4 Inch Diameter Core Samples						
Depth (cm)	Plot	α (cm^{-1})	n	θ_s (%)	θ_r (%)	K (cm/s)
0	NoTill1	0.010	1.954	0.336	0.148	9.50E-04
0	NoTill2	0.012	1.774	0.327	0.152	1.01E-03
0	NoTill3	-	-	-	-	1.16E-03
0	NoTill4	-	-	-	-	1.07E-03
		0.011	1.864	0.331	0.150	1.05E-03
10	NoTill1	0.024	1.580	0.306	0.128	8.74E-04
10	NoTill2	0.019	1.854	0.345	0.147	8.86E-04
10	NoTill3	-	-	-	-	9.81E-04
10	NoTill4	-	-	-	-	8.72E-04
		0.021	1.717	0.326	0.138	9.03E-04
20	NoTill1	0.026	1.487	0.302	0.127	7.49E-04
20	NoTill2	0.017	1.859	0.312	0.130	9.87E-04
20	NoTill3	-	-	-	-	8.43E-04
20	NoTill4	-	-	-	-	8.30E-04
		0.021	1.673	0.307	0.129	8.52E-04
30	NoTill1	0.018	1.273	0.359	0.120	6.68E-04
30	NoTill2	0.013	1.659	0.346	0.088	6.23E-04
30	NoTill3	-	-	-	-	7.68E-04
30	NoTill4	-	-	-	-	8.71E-04
		0.016	1.466	0.353	0.104	7.33E-04
60	NoTill1	0.029	1.326	0.357	0.124	6.51E-04
60	NoTill2	0.012	1.284	0.316	0.138	6.67E-04
60	NoTill3	-	-	-	-	5.38E-04
60	NoTill4	-	-	-	-	6.71E-04
		0.021	1.305	0.336	0.131	6.32E-04
90	NoTill1	0.014	1.755	0.356	0.114	1.16E-03
90	NoTill2	0.010	1.253	0.351	0.129	9.67E-04
90	NoTill3	-	-	-	-	1.09E-03
90	NoTill4	-	-	-	-	1.00E-03
		0.012	1.504	0.353	0.122	1.05E-03
120	NoTill1	0.007	1.998	0.320	0.075	7.84E-04
120	NoTill2	0.007	1.992	0.317	0.088	7.76E-04
120	NoTill3	-	-	-	-	8.24E-04
120	NoTill4	-	-	-	-	9.01E-04
		0.007	1.995	0.318	0.082	8.21E-04
150	NoTill1	0.006	1.568	0.346	0.099	5.26E-04
150	NoTill2	0.008	1.388	0.329	0.097	9.95E-04
150	NoTill3	-	-	-	-	9.38E-04
150	NoTill4	-	-	-	-	4.61E-04
		0.007	1.478	0.338	0.098	7.30E-04
180	NoTill1	0.007	1.648	0.374	0.128	8.87E-04
180	NoTill2	0.009	1.654	0.345	0.091	8.25E-04
180	NoTill3	-	-	-	-	8.46E-04
180	NoTill4	-	-	-	-	9.55E-04
		0.008	1.651	0.360	0.110	8.78E-04

Appendix A. Table of measured data.

Till Treatment, 4 Inch Diameter TI						
Depth (cm)	Plot	α (cm^{-1})	n	θ_s (%)	θ_r (%)	K (cm/s)
0	Till1	0.140	1.944	0.489	0.160	3.13E-03
0	Till2	0.065	1.422	0.489	0.160	4.25E-03
0	Till3	0.076	1.618	0.489	0.160	5.15E-03
0	Till4	0.039	1.517	0.489	0.160	5.34E-03
		0.080	1.625	0.489	0.160	4.46E-03
10	Till1	0.088	1.856	0.470	0.194	5.45E-03
10	Till2	0.056	1.559	0.470	0.194	6.10E-03
10	Till3	0.025	1.658	0.470	0.194	5.79E-03
10	Till4	0.030	1.903	0.470	0.194	7.24E-03
		0.050	1.744	0.470	0.194	6.15E-03
20	Till1	0.026	1.511	0.409	0.178	6.00E-03
20	Till2	0.037	1.485	0.409	0.178	6.30E-03
20	Till3	0.022	1.548	0.409	0.178	4.02E-03
20	Till4	0.041	1.669	0.409	0.178	5.87E-03
		0.031	1.553	0.409	0.178	5.55E-03
30	Till1	0.016	1.422	0.426	0.172	1.55E-03
30	Till2	0.023	1.552	0.426	0.172	5.58E-03
30	Till3	0.003	1.657	0.426	0.172	6.45E-03
30	Till4	0.037	1.403	0.426	0.172	6.65E-03
		0.019	1.508	0.426	0.172	5.06E-03
60	Till1	0.033	1.692	0.386	0.141	5.29E-03
60	Till2	0.035	1.554	0.386	0.141	5.84E-03
60	Till3	0.037	1.487	0.386	0.141	6.54E-03
60	Till4	0.042	1.428	0.386	0.141	6.97E-03
		0.037	1.540	0.386	0.141	6.16E-03
90	Till1	0.059	1.487	0.367	0.144	5.29E-03
90	Till2	0.026	1.874	0.367	0.144	5.84E-03
90	Till3	0.035	1.358	0.367	0.144	6.54E-03
90	Till4	0.028	1.425	0.367	0.144	6.97E-03
		0.037	1.536	0.367	0.144	6.16E-03
120	Till1	0.093	1.874	0.398	0.144	3.88E-03
120	Till2	0.055	1.688	0.398	0.144	5.72E-03
120	Till3	0.040	1.551	0.398	0.144	5.44E-03
120	Till4	0.070	1.771	0.398	0.144	6.00E-03
		0.064	1.721	0.398	0.144	5.26E-03
150	Till1	0.042	1.420	0.418	0.141	3.62E-03
150	Till2	0.036	1.655	0.418	0.141	3.35E-03
150	Till3	0.040	1.729	0.418	0.141	4.45E-03
150	Till4	0.040	1.831	0.418	0.141	6.65E-03
		0.039	1.659	0.418	0.141	4.52E-03
180	Till1	0.023	1.373	0.399	0.140	3.62E-03
180	Till2	0.043	1.885	0.399	0.140	3.35E-03
180	Till3	0.054	1.768	0.399	0.140	4.45E-03
180	Till4	0.038	1.614	0.399	0.140	6.65E-03
		0.039	1.660	0.399	0.140	4.52E-03

Appendix A. Table of measured data.

No-Till Treatment, 4 Inch Diameter TI						
Depth (cm)	Plot	α (cm^{-1})	n	θ_s (%)	θ_r (%)	K (cm/s)
0	NoTill1	0.047	1.889	0.460	0.150	5.12E-03
0	NoTill2	0.048	1.579	0.460	0.150	3.49E-03
0	NoTill3	0.047	1.732	0.460	0.150	5.02E-03
0	NoTill4	0.050	1.800	0.460	0.150	5.46E-03
		0.048	1.750	0.460	0.150	4.77E-03
10	NoTill1	0.084	1.895	0.482	0.178	5.49E-03
10	NoTill2	0.049	1.667	0.482	0.178	6.37E-03
10	NoTill3	0.056	1.725	0.482	0.178	4.18E-03
10	NoTill4	0.085	1.844	0.482	0.178	8.46E-03
		0.068	1.783	0.482	0.178	6.12E-03
20	NoTill1	0.054	1.521	0.443	0.150	4.41E-03
20	NoTill2	0.023	1.715	0.443	0.150	6.63E-03
20	NoTill3	0.019	1.847	0.443	0.150	6.23E-03
20	NoTill4	0.034	1.797	0.443	0.150	7.23E-03
		0.033	1.720	0.443	0.150	6.12E-03
30	NoTill1	0.099	1.884	0.439	0.143	2.76E-03
30	NoTill2	0.112	1.487	0.439	0.143	6.10E-03
30	NoTill3	0.065	1.552	0.439	0.143	3.68E-03
30	NoTill4	0.128	1.740	0.439	0.143	5.58E-03
		0.101	1.666	0.439	0.143	4.53E-03
60	NoTill1	0.022	1.699	0.418	0.134	4.20E-03
60	NoTill2	0.023	1.729	0.418	0.134	3.95E-03
60	NoTill3	0.030	1.658	0.418	0.134	7.05E-03
60	NoTill4	0.034	1.635	0.418	0.134	6.94E-03
		0.027	1.680	0.418	0.134	5.53E-03
90	NoTill1	0.037	1.331	0.437	0.120	4.20E-03
90	NoTill2	0.001	1.874	0.437	0.120	3.95E-03
90	NoTill3	0.030	1.651	0.437	0.120	7.05E-03
90	NoTill4	0.038	1.848	0.437	0.120	6.94E-03
		0.027	1.676	0.437	0.120	5.53E-03
120	NoTill1	0.004	1.608	0.425	0.070	5.49E-03
120	NoTill2	0.012	1.346	0.425	0.070	6.64E-03
120	NoTill3	0.039	1.682	0.425	0.070	6.55E-03
120	NoTill4	0.036	1.923	0.425	0.070	7.28E-03
		0.023	1.640	0.425	0.070	6.49E-03
150	NoTill1	0.066	1.565	0.453	0.100	7.26E-03
150	NoTill2	0.025	1.755	0.453	0.100	9.00E-03
150	NoTill3	0.048	1.446	0.453	0.100	4.77E-03
150	NoTill4	0.057	1.762	0.453	0.100	5.67E-03
		0.049	1.632	0.453	0.100	6.68E-03
180	NoTill1	0.084	1.630	0.385	0.130	7.26E-03
180	NoTill2	0.039	1.789	0.385	0.130	9.00E-03
180	NoTill3	0.044	1.548	0.385	0.130	4.77E-03
180	NoTill4	0.030	1.554	0.385	0.130	5.67E-03
		0.049	1.630	0.385	0.130	6.68E-03

Appendix A. Table of measured data.

Till Treatment, 8 Inch Diameter TI						
Depth (cm)	Plot	α (cm^{-1})	n	θ_s (%)	θ_r (%)	K (cm/s)
0	Till1	0.144	1.499	0.489	0.160	3.46E-03
0	Till2	0.165	1.785	0.489	0.160	6.49E-03
0	Till3	0.124	1.856	0.489	0.160	5.51E-03
0	Till4	0.172	1.771	0.489	0.160	6.05E-03
		0.151	1.728	0.489	0.160	5.38E-03
10	Till1	0.074	1.499	0.470	0.194	4.78E-03
10	Till2	0.065	1.795	0.470	0.194	6.32E-03
10	Till3	0.072	1.845	0.470	0.194	6.16E-03
10	Till4	0.089	1.822	0.470	0.194	6.05E-03
		0.075	1.740	0.470	0.194	5.83E-03
20	Till1	0.058	1.874	0.409	0.178	3.59E-03
20	Till2	0.043	1.698	0.409	0.178	6.06E-03
20	Till3	0.054	1.792	0.409	0.178	5.34E-03
20	Till4	0.046	1.728	0.409	0.178	6.06E-03
		0.050	1.773	0.409	0.178	5.26E-03
30	Till1	0.040	1.823	0.426	0.172	1.37E-03
30	Till2	0.043	1.687	0.426	0.172	6.37E-03
30	Till3	0.022	1.587	0.426	0.172	6.64E-03
30	Till4	0.032	1.569	0.426	0.172	7.94E-03
		0.034	1.667	0.426	0.172	5.58E-03
60	Till1	0.052	1.622	0.386	0.141	3.79E-03
60	Till2	0.023	1.665	0.386	0.141	7.04E-03
60	Till3	0.033	1.547	0.386	0.141	7.10E-03
60	Till4	0.042	1.572	0.386	0.141	7.74E-03
		0.037	1.601	0.386	0.141	6.42E-03
90	Till1	0.049	1.425	0.367	0.144	3.79E-03
90	Till2	0.028	1.784	0.367	0.144	7.04E-03
90	Till3	0.032	1.526	0.367	0.144	7.10E-03
90	Till4	0.037	1.678	0.367	0.144	7.74E-03
		0.037	1.603	0.367	0.144	6.42E-03
120	Till1	0.032	1.419	0.398	0.144	3.70E-03
120	Till2	0.056	1.795	0.398	0.144	6.63E-03
120	Till3	0.055	1.658	0.398	0.144	6.38E-03
120	Till4	0.080	1.580	0.398	0.144	8.28E-03
		0.056	1.613	0.398	0.144	6.25E-03
150	Till1	0.091	1.928	0.418	0.141	4.11E-03
150	Till2	0.055	1.641	0.418	0.141	3.90E-03
150	Till3	0.069	1.593	0.418	0.141	5.92E-03
150	Till4	0.043	1.669	0.418	0.141	7.25E-03
		0.064	1.708	0.418	0.141	5.30E-03
180	Till1	0.100	1.853	0.399	0.140	4.11E-03
180	Till2	0.069	1.752	0.399	0.140	3.90E-03
180	Till3	0.043	1.687	0.399	0.140	5.92E-03
180	Till4	0.046	1.558	0.399	0.140	7.25E-03
		0.064	1.712	0.399	0.140	5.30E-03

Appendix A. Table of measured data.

No-Till Treatment, 8 Inch Diameter TI						
Depth (cm)	Plot	α (cm^{-1})	n	θ_s (%)	θ_r (%)	K (cm/s)
0	NoTill1	0.019	1.773	0.460	0.150	5.38E-03
0	NoTill2	0.023	1.634	0.460	0.150	4.66E-03
0	NoTill3	0.096	1.731	0.460	0.150	7.47E-03
0	NoTill4	0.091	1.926	0.460	0.150	7.18E-03
		0.058	1.766	0.460	0.150	6.17E-03
10	NoTill1	0.053	1.821	0.482	0.178	4.69E-03
10	NoTill2	0.020	1.798	0.482	0.178	6.98E-03
10	NoTill3	0.046	1.548	0.482	0.178	4.12E-03
10	NoTill4	0.061	1.695	0.482	0.178	7.53E-03
		0.045	1.716	0.482	0.178	5.83E-03
20	NoTill1	0.055	1.849	0.443	0.150	4.07E-03
20	NoTill2	0.024	1.822	0.443	0.150	6.18E-03
20	NoTill3	0.016	1.798	0.443	0.150	7.22E-03
20	NoTill4	0.002	1.500	0.443	0.150	7.87E-03
		0.024	1.742	0.443	0.150	6.33E-03
30	NoTill1	0.042	1.855	0.439	0.143	3.68E-03
30	NoTill2	0.039	1.753	0.439	0.143	5.01E-03
30	NoTill3	0.018	1.982	0.439	0.143	6.13E-03
30	NoTill4	0.048	1.893	0.439	0.143	5.68E-03
		0.037	1.871	0.439	0.143	5.12E-03
60	NoTill1	0.039	1.859	0.418	0.134	3.85E-03
60	NoTill2	0.042	1.675	0.418	0.134	6.55E-03
60	NoTill3	0.023	1.457	0.418	0.134	7.34E-03
60	NoTill4	0.023	1.590	0.418	0.134	8.84E-03
		0.032	1.645	0.418	0.134	6.65E-03
90	NoTill1	0.051	1.482	0.437	0.120	3.85E-03
90	NoTill2	0.035	1.509	0.437	0.120	6.55E-03
90	NoTill3	0.015	1.873	0.437	0.120	7.34E-03
90	NoTill4	0.020	1.684	0.437	0.120	8.84E-03
		0.030	1.637	0.437	0.120	6.65E-03
120	NoTill1	0.022	1.842	0.425	0.070	7.90E-03
120	NoTill2	0.012	1.554	0.425	0.070	7.08E-03
120	NoTill3	0.050	1.625	0.425	0.070	6.69E-03
120	NoTill4	0.062	1.596	0.425	0.070	6.79E-03
		0.037	1.654	0.425	0.070	7.12E-03
150	NoTill1	0.012	1.612	0.453	0.100	7.88E-03
150	NoTill2	0.024	1.844	0.453	0.100	7.63E-03
150	NoTill3	0.089	1.895	0.453	0.100	5.05E-03
150	NoTill4	0.031	1.828	0.453	0.100	4.69E-03
		0.039	1.794	0.453	0.100	6.31E-03
180	NoTill1	0.019	1.811	0.385	0.130	7.88E-03
180	NoTill2	0.048	1.724	0.385	0.130	7.63E-03
180	NoTill3	0.036	1.929	0.385	0.130	5.05E-03
180	NoTill4	0.047	1.635	0.385	0.130	4.69E-03
		0.037	1.775	0.385	0.130	6.31E-03

Appendix A. Table of measured data.

Till Treatment, IPM						
Depth (cm)	Plot	α (cm^{-1})	n	θ_s (%)	θ_r (%)	K (cm/s)
0	Till1	-	-	-	-	3.02E-03
0	Till2	-	-	-	-	3.00E-03
0	Till3	-	-	-	-	3.01E-03
0	Till4	-	-	-	-	3.03E-03
						3.02E-03
10	Till1	0.065	1.450	0.435	0.150	3.00E-03
10	Till2	0.045	1.500	0.420	0.160	3.30E-03
10	Till3	0.035	1.400	0.422	0.150	2.60E-03
10	Till4	0.035	1.500	0.421	0.170	3.60E-03
		0.045	1.463	0.424	0.158	3.13E-03
20	Till1	0.078	1.490	0.446	0.150	2.80E-03
20	Till2	0.055	1.650	0.410	0.150	3.10E-03
20	Till3	0.030	1.450	0.412	0.150	2.60E-03
20	Till4	0.035	1.500	0.411	0.160	3.30E-03
		0.050	1.523	0.420	0.153	2.95E-03
30	Till1	0.065	1.450	0.439	0.150	2.30E-03
30	Till2	0.035	1.450	0.457	0.150	2.90E-03
30	Till3	0.022	1.650	0.430	0.150	2.70E-03
30	Till4	0.031	1.550	0.436	0.150	3.00E-03
		0.038	1.525	0.440	0.150	2.73E-03
60	Till1	0.020	1.750	0.427	0.150	1.60E-03
60	Till2	0.025	1.650	0.449	0.150	2.60E-03
60	Till3	0.031	1.650	0.406	0.100	2.80E-03
60	Till4	0.025	1.750	0.385	0.110	2.70E-03
		0.025	1.700	0.417	0.128	2.43E-03
90	Till1	0.015	1.650	0.440	0.120	1.30E-03
90	Till2	0.025	1.650	0.450	0.150	2.50E-03
90	Till3	0.018	1.800	0.428	0.050	2.80E-03
90	Till4	0.022	1.730	0.424	0.110	2.50E-03
		0.020	1.708	0.436	0.108	2.28E-03
120	Till1	0.012	1.750	0.429	0.120	1.10E-03
120	Till2	0.020	1.650	0.433	0.100	2.40E-03
120	Till3	0.010	1.760	0.435	0.050	2.80E-03
120	Till4	0.015	1.700	0.429	0.110	2.40E-03
		0.014	1.715	0.431	0.095	2.18E-03
150	Till1	0.011	1.650	0.418	0.120	1.00E-03
150	Till2	0.015	1.750	0.435	0.050	2.30E-03
150	Till3	0.014	1.740	0.423	0.050	2.80E-03
150	Till4	0.010	1.700	0.435	0.110	2.30E-03
		0.013	1.710	0.428	0.083	2.10E-03
180	Till1	0.015	1.550	0.409	0.120	9.00E-04
180	Till2	0.015	1.550	0.433	0.100	2.30E-03
180	Till3	0.018	1.550	0.413	0.100	2.90E-03
180	Till4	0.012	1.610	0.424	0.110	2.30E-03
		0.015	1.565	0.420	0.108	2.10E-03

Appendix A. Table of measured data.

No-Till Treatment, IPM						
Depth (cm)	Plot	α (cm^{-1})	n	θ_s (%)	θ_r (%)	K (cm/s)
0	NoTill1	-	-	-	-	1.60E-03
0	NoTill2	-	-	-	-	1.70E-03
0	NoTill3	-	-	-	-	1.40E-03
0	NoTill4	-	-	-	-	1.60E-03
						1.58E-03
10	NoTill1	0.025	1.700	0.422	0.160	1.50E-03
10	NoTill2	0.025	1.480	0.416	0.150	2.30E-03
10	NoTill3	0.026	1.550	0.394	0.170	1.50E-03
10	NoTill4	0.029	1.510	0.419	0.175	1.50E-03
		0.026	1.560	0.412	0.164	1.70E-03
20	NoTill1	0.025	1.600	0.428	0.160	1.40E-03
20	NoTill2	0.029	1.450	0.436	0.150	2.00E-03
20	NoTill3	0.025	1.520	0.413	0.170	1.50E-03
20	NoTill4	0.031	1.460	0.408	0.170	1.40E-03
		0.028	1.508	0.421	0.163	1.58E-03
30	NoTill1	0.035	1.580	0.437	0.160	1.30E-03
30	NoTill2	0.025	1.460	0.427	0.150	1.80E-03
30	NoTill3	0.022	1.600	0.405	0.150	1.40E-03
30	NoTill4	0.028	1.480	0.422	0.160	1.40E-03
		0.028	1.530	0.423	0.155	1.48E-03
60	NoTill1	0.012	1.550	0.429	0.120	1.20E-03
60	NoTill2	0.017	1.800	0.401	0.120	1.60E-03
60	NoTill3	0.012	1.850	0.372	0.130	1.40E-03
60	NoTill4	0.015	1.860	0.403	0.110	1.30E-03
		0.014	1.765	0.401	0.120	1.38E-03
90	NoTill1	0.012	1.430	0.400	0.140	1.20E-03
90	NoTill2	0.017	1.800	0.449	0.100	1.40E-03
90	NoTill3	0.012	1.810	0.425	0.110	1.30E-03
90	NoTill4	0.015	1.850	0.404	0.110	1.20E-03
		0.014	1.723	0.419	0.115	1.28E-03
120	NoTill1	0.019	1.480	0.440	0.120	1.10E-03
120	NoTill2	0.013	1.590	0.416	0.120	1.40E-03
120	NoTill3	0.012	1.810	0.370	0.110	1.30E-03
120	NoTill4	0.012	1.730	0.393	0.080	1.20E-03
		0.014	1.653	0.405	0.108	1.25E-03
150	NoTill1	0.015	1.480	0.421	0.080	1.10E-03
150	NoTill2	0.021	1.420	0.427	0.140	1.30E-03
150	NoTill3	0.018	1.670	0.428	0.080	1.30E-03
150	NoTill4	0.012	1.540	0.407	0.120	1.20E-03
		0.017	1.528	0.421	0.105	1.23E-03
180	NoTill1	0.011	1.590	0.406	0.080	1.10E-03
180	NoTill2	0.018	1.560	0.436	0.110	1.30E-03
180	NoTill3	0.021	1.530	0.407	0.100	1.30E-03
180	NoTill4	0.012	1.550	0.388	0.120	1.20E-03
		0.016	1.558	0.409	0.103	1.23E-03

Appendix A. Table of measured data.

Till Treatment, IND						
Depth (cm)	Plot	α (cm^{-1})	n	θ_s (%)	θ_r (%)	K (cm/s)
0	Till1	0.036	1.250	0.330	0.068	1.19E-04
0	Till2	0.059	1.480	0.390	0.100	3.64E-04
0	Till3	0.020	1.410	0.450	0.067	1.25E-04
0	Till4	-	-	-	-	-
		0.038	1.380	0.390	0.078	2.03E-04
10	Till1	0.036	1.250	0.330	0.068	1.19E-04
10	Till2	0.059	1.480	0.390	0.100	3.64E-04
10	Till3	0.020	1.410	0.450	0.067	1.25E-04
10	Till4	-	-	-	-	-
		0.038	1.380	0.390	0.078	2.03E-04
20	Till1	0.036	1.250	0.330	0.068	1.19E-04
20	Till2	0.059	1.480	0.390	0.100	3.64E-04
20	Till3	0.020	1.410	0.450	0.067	1.25E-04
20	Till4	-	-	-	-	-
		0.038	1.380	0.390	0.078	2.03E-04
30	Till1	0.036	1.250	0.330	0.068	1.19E-04
30	Till2	0.059	1.480	0.390	0.100	3.64E-04
30	Till3	0.020	1.410	0.450	0.067	1.25E-04
30	Till4	-	-	-	-	-
		0.038	1.380	0.390	0.078	2.03E-04
60	Till1	0.036	1.250	0.330	0.068	1.19E-04
60	Till2	0.059	1.480	0.390	0.100	3.64E-04
60	Till3	0.020	1.410	0.450	0.067	1.25E-04
60	Till4	-	-	-	-	-
		0.038	1.380	0.390	0.078	2.03E-04
90	Till1	0.036	1.250	0.330	0.068	1.19E-04
90	Till2	0.059	1.480	0.390	0.100	3.64E-04
90	Till3	0.020	1.410	0.450	0.067	1.25E-04
90	Till4	-	-	-	-	-
		0.038	1.380	0.390	0.078	2.03E-04
120	Till1	0.036	1.250	0.330	0.068	1.19E-04
120	Till2	0.059	1.480	0.390	0.100	3.64E-04
120	Till3	0.020	1.410	0.450	0.067	1.25E-04
120	Till4	-	-	-	-	-
		0.038	1.380	0.390	0.078	2.03E-04
150	Till1	0.036	1.250	0.330	0.068	1.19E-04
150	Till2	0.059	1.480	0.390	0.100	3.64E-04
150	Till3	0.020	1.410	0.450	0.067	1.25E-04
150	Till4	-	-	-	-	-
		0.038	1.380	0.390	0.078	2.03E-04
180	Till1	0.039	1.194	0.390	0.075	6.39E-05
180	Till2	0.019	1.310	0.410	0.000	7.22E-05
180	Till3	0.059	1.480	0.390	0.100	3.35E-04
180	Till4	-	-	-	-	-
		0.039	1.328	0.397	0.058	1.57E-04

Appendix A. Table of measured data.

No-Till Treatment, IND						
Depth (cm)	Plot	α (cm^{-1})	n	θ_s (%)	θ_r (%)	K (cm/s)
0	NoTill1	0.036	1.250	0.330	0.068	1.19E-04
0	NoTill2	0.059	1.480	0.390	0.100	3.64E-04
0	NoTill3	0.020	1.410	0.450	0.067	1.25E-04
0	NoTill4	-	-	-	-	-
		0.038	1.380	0.390	0.078	2.03E-04
10	NoTill1	0.036	1.250	0.330	0.068	1.19E-04
10	NoTill2	0.059	1.480	0.390	0.100	3.64E-04
10	NoTill3	0.020	1.410	0.450	0.067	1.25E-04
10	NoTill4	-	-	-	-	-
		0.038	1.380	0.390	0.078	2.03E-04
20	NoTill1	0.036	1.250	0.330	0.068	1.19E-04
20	NoTill2	0.059	1.480	0.390	0.100	3.64E-04
20	NoTill3	0.020	1.410	0.450	0.067	1.25E-04
20	NoTill4	-	-	-	-	-
		0.038	1.380	0.390	0.078	2.03E-04
30	NoTill1	0.036	1.250	0.330	0.068	1.19E-04
30	NoTill2	0.059	1.480	0.390	0.100	3.64E-04
30	NoTill3	0.020	1.410	0.450	0.067	1.25E-04
30	NoTill4	-	-	-	-	-
		0.038	1.380	0.390	0.078	2.03E-04
60	NoTill1	0.036	1.250	0.330	0.068	1.19E-04
60	NoTill2	0.059	1.480	0.390	0.100	3.64E-04
60	NoTill3	0.020	1.410	0.450	0.067	1.25E-04
60	NoTill4	-	-	-	-	-
		0.038	1.380	0.390	0.078	2.03E-04
90	NoTill1	0.036	1.250	0.330	0.068	1.19E-04
90	NoTill2	0.059	1.480	0.390	0.100	3.64E-04
90	NoTill3	0.020	1.410	0.450	0.067	1.25E-04
90	NoTill4	-	-	-	-	-
		0.038	1.380	0.390	0.078	2.03E-04
120	NoTill1	0.036	1.250	0.330	0.068	1.19E-04
120	NoTill2	0.059	1.480	0.390	0.100	3.64E-04
120	NoTill3	0.020	1.410	0.450	0.067	1.25E-04
120	NoTill4	-	-	-	-	-
		0.038	1.380	0.390	0.078	2.03E-04
150	NoTill1	0.036	1.250	0.330	0.068	1.19E-04
150	NoTill2	0.059	1.480	0.390	0.100	3.64E-04
150	NoTill3	0.020	1.410	0.450	0.067	1.25E-04
150	NoTill4	-	-	-	-	-
		0.038	1.380	0.390	0.078	2.03E-04
180	NoTill1	0.039	1.194	0.390	0.075	6.39E-05
180	NoTill2	0.019	1.310	0.410	0.000	7.22E-05
180	NoTill3	0.059	1.480	0.390	0.100	3.35E-04
180	NoTill4	-	-	-	-	-
		0.039	1.328	0.397	0.058	1.57E-04

Appendix A. Table of measured data.

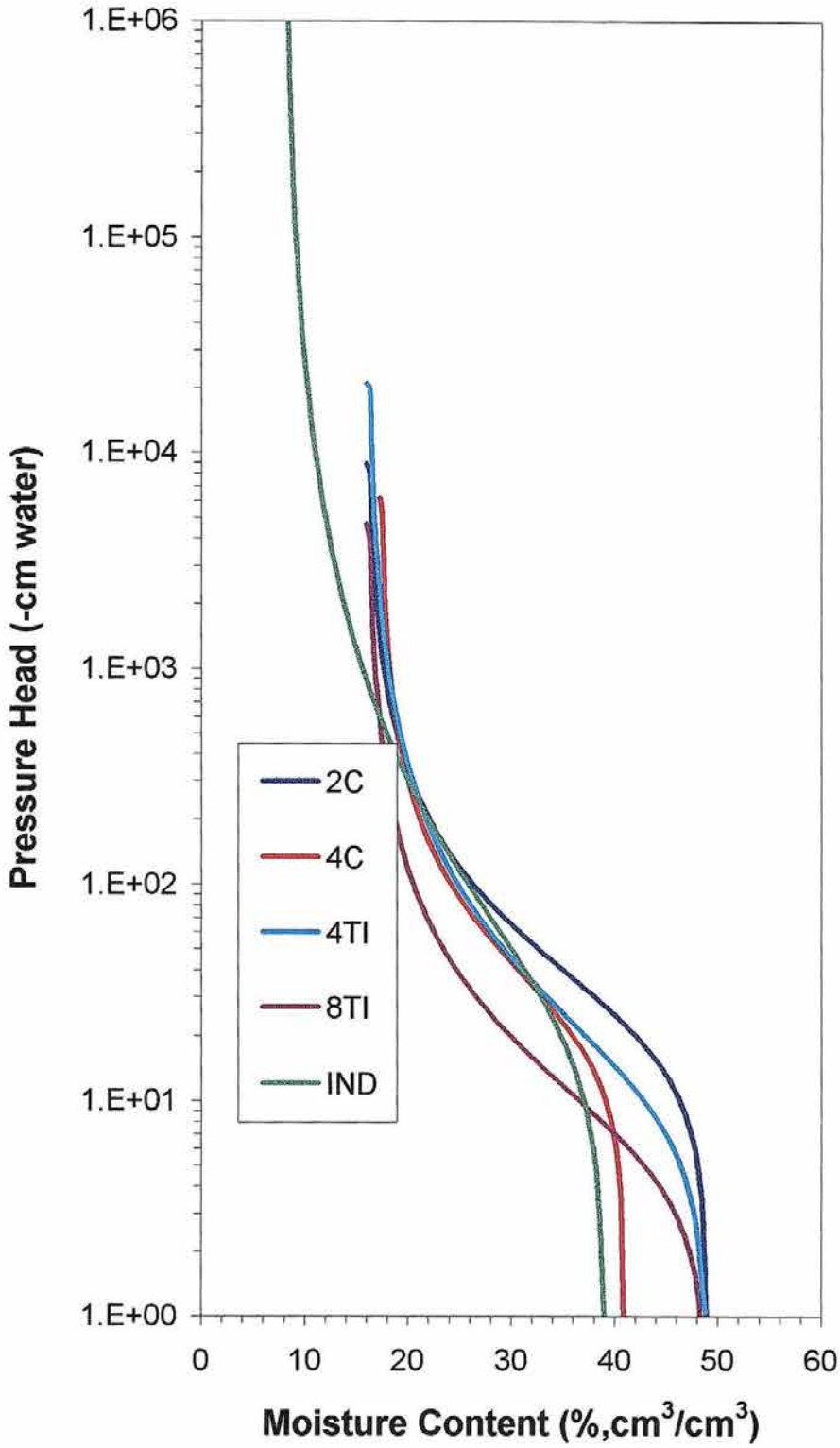

Appendix A. Moisture retention plots plots constructed using data obtained from the T treatment at the 0 cm depth.

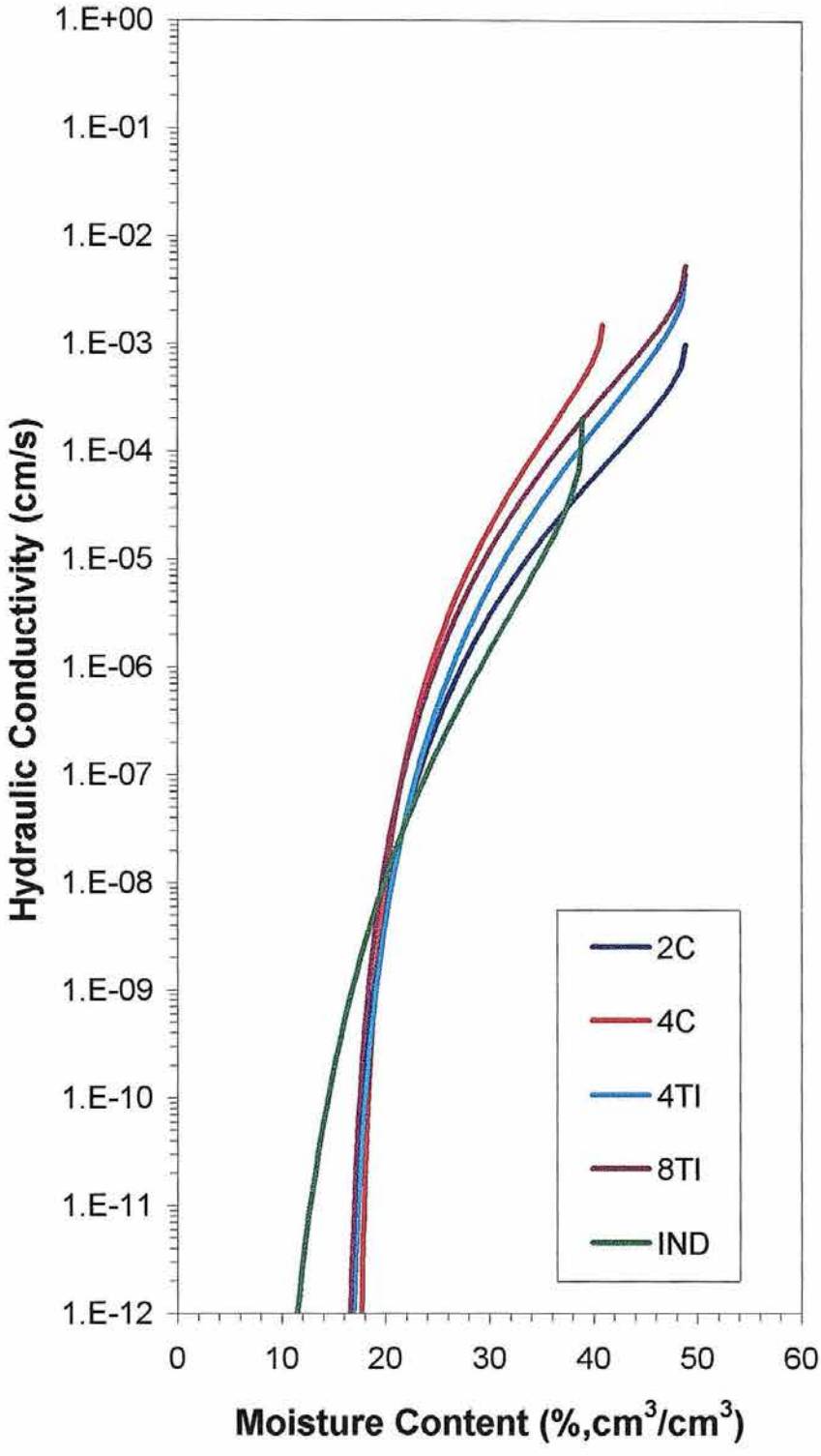

Appendix A. Unsaturated hydraulic conductivity plots constructed using data obtained from T treatment at the 0 cm depth.

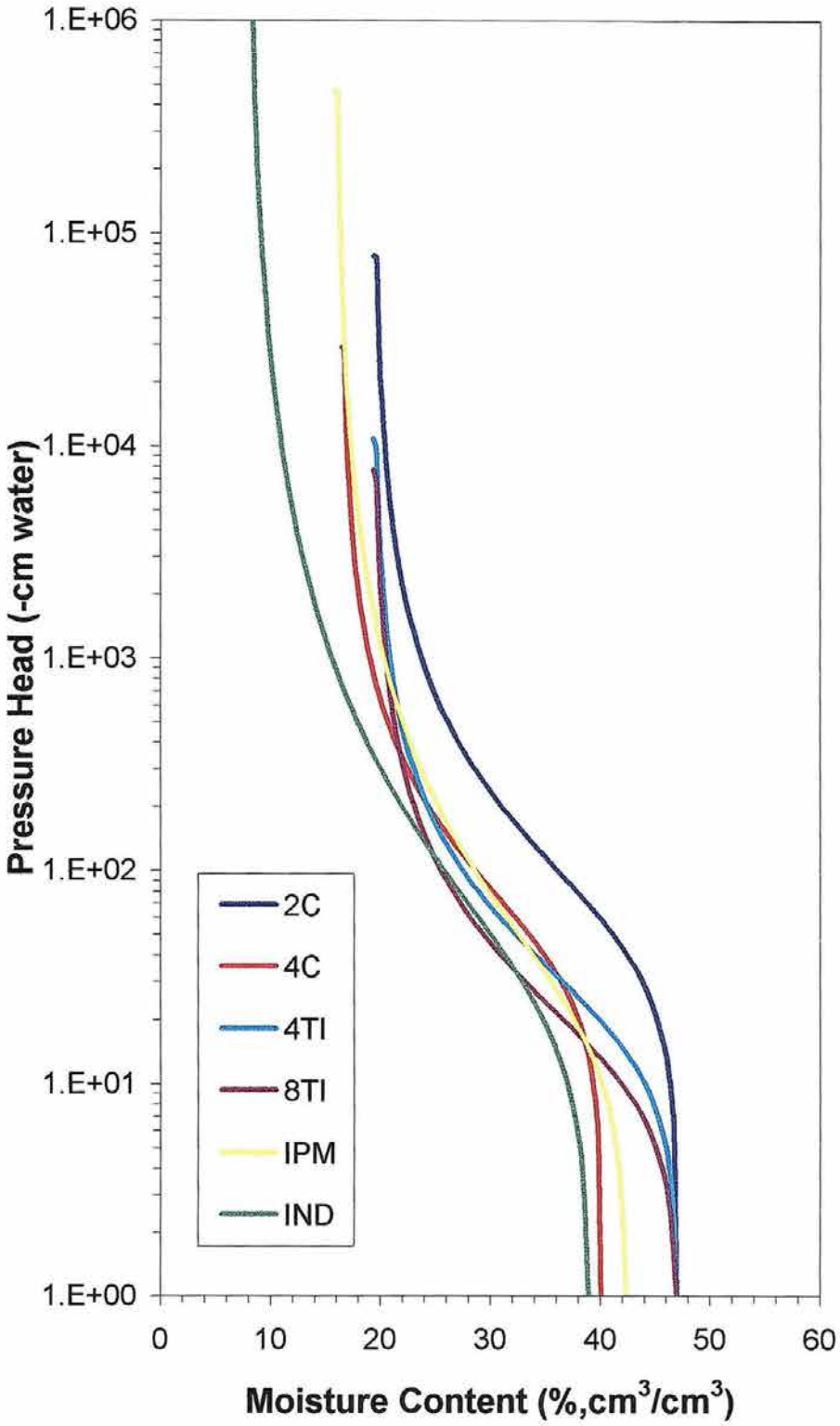

Appendix A. Moisture retention plots plots constructed using data obtained from the T treatment at the 10 cm depth.

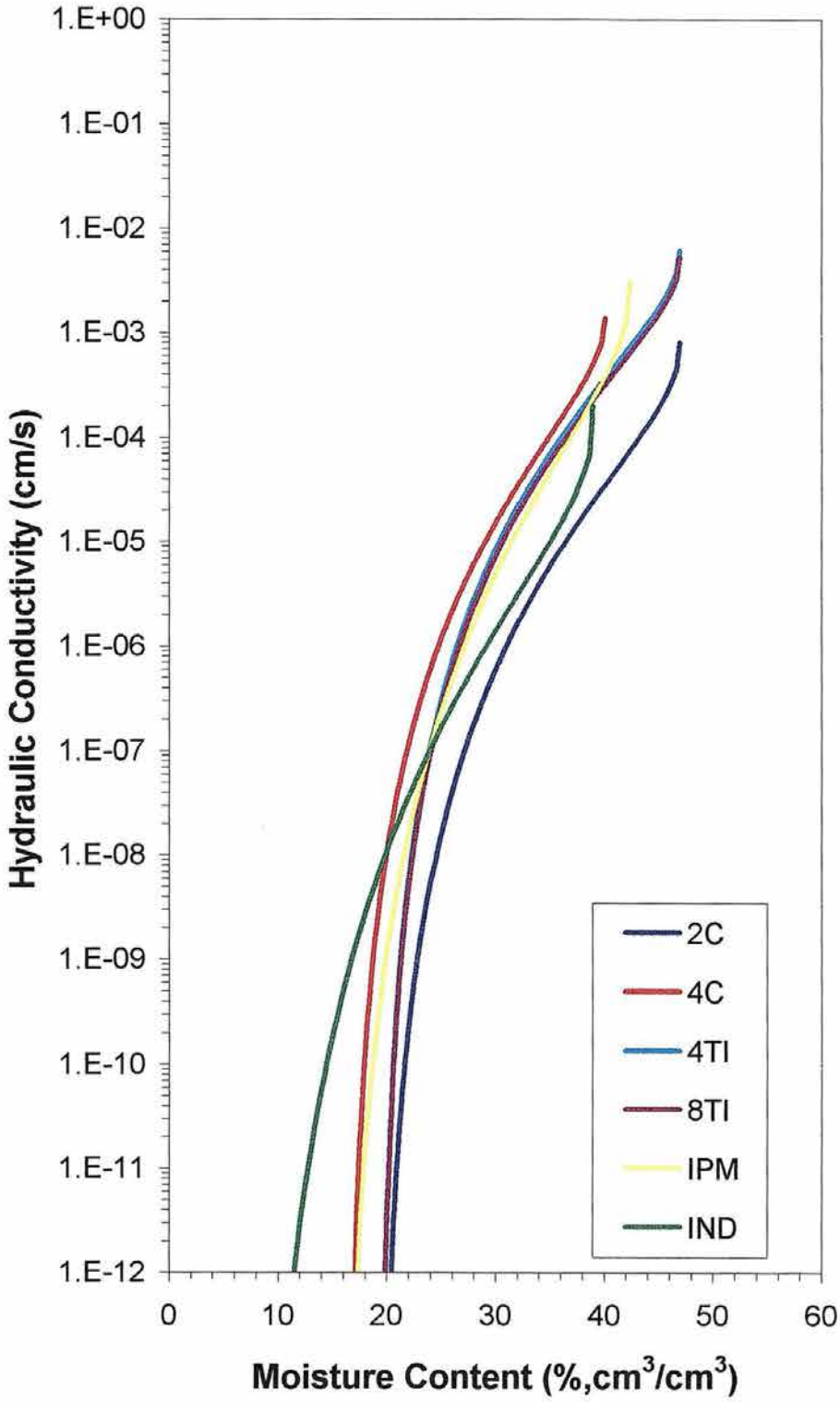

Appendix A. Unsaturated hydraulic conductivity plots constructed using data obtained from T treatment at the 10 cm depth.

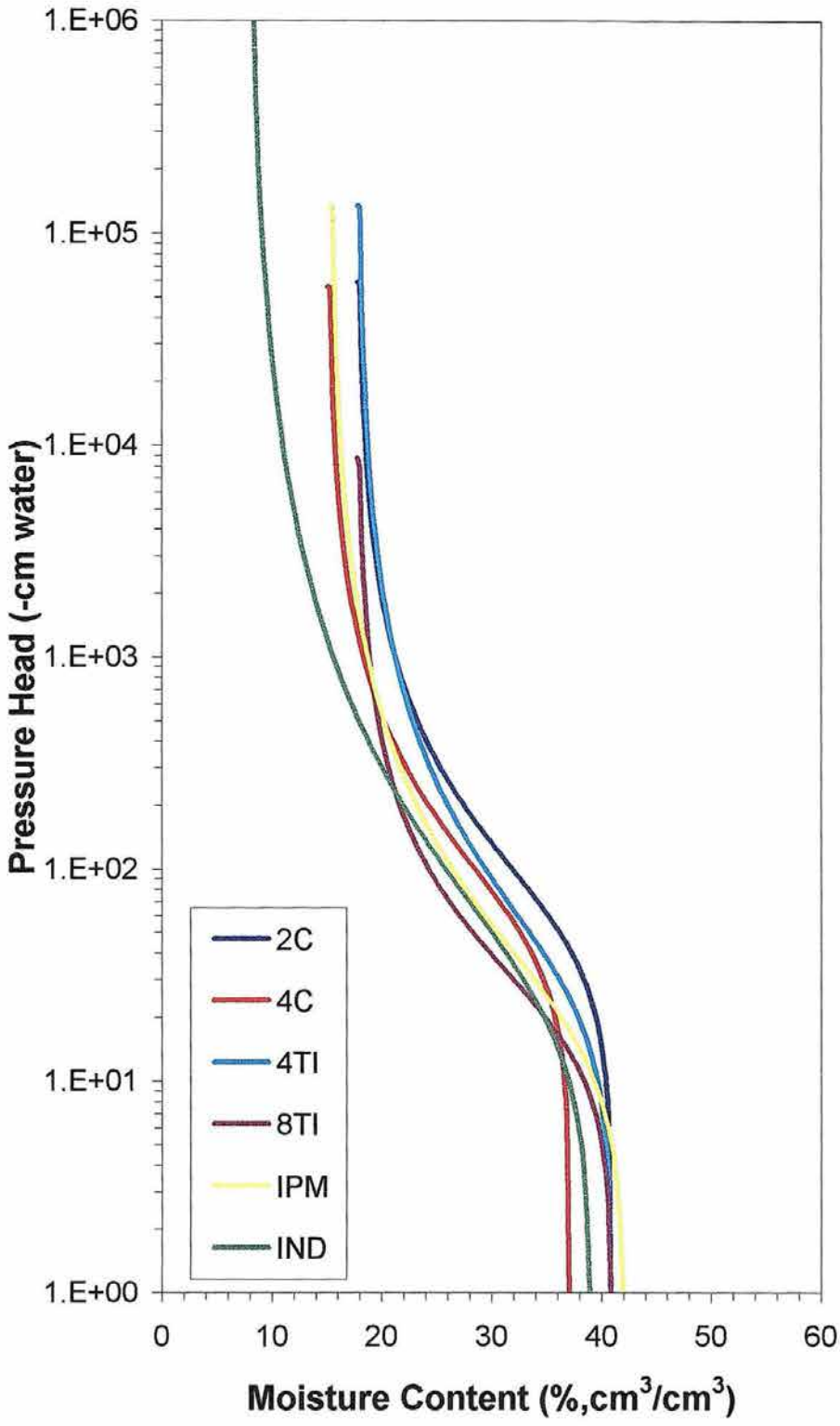

Appendix A. Moisture retention plots plots constructed using data obtained from the T treatment at the 20 cm depth.

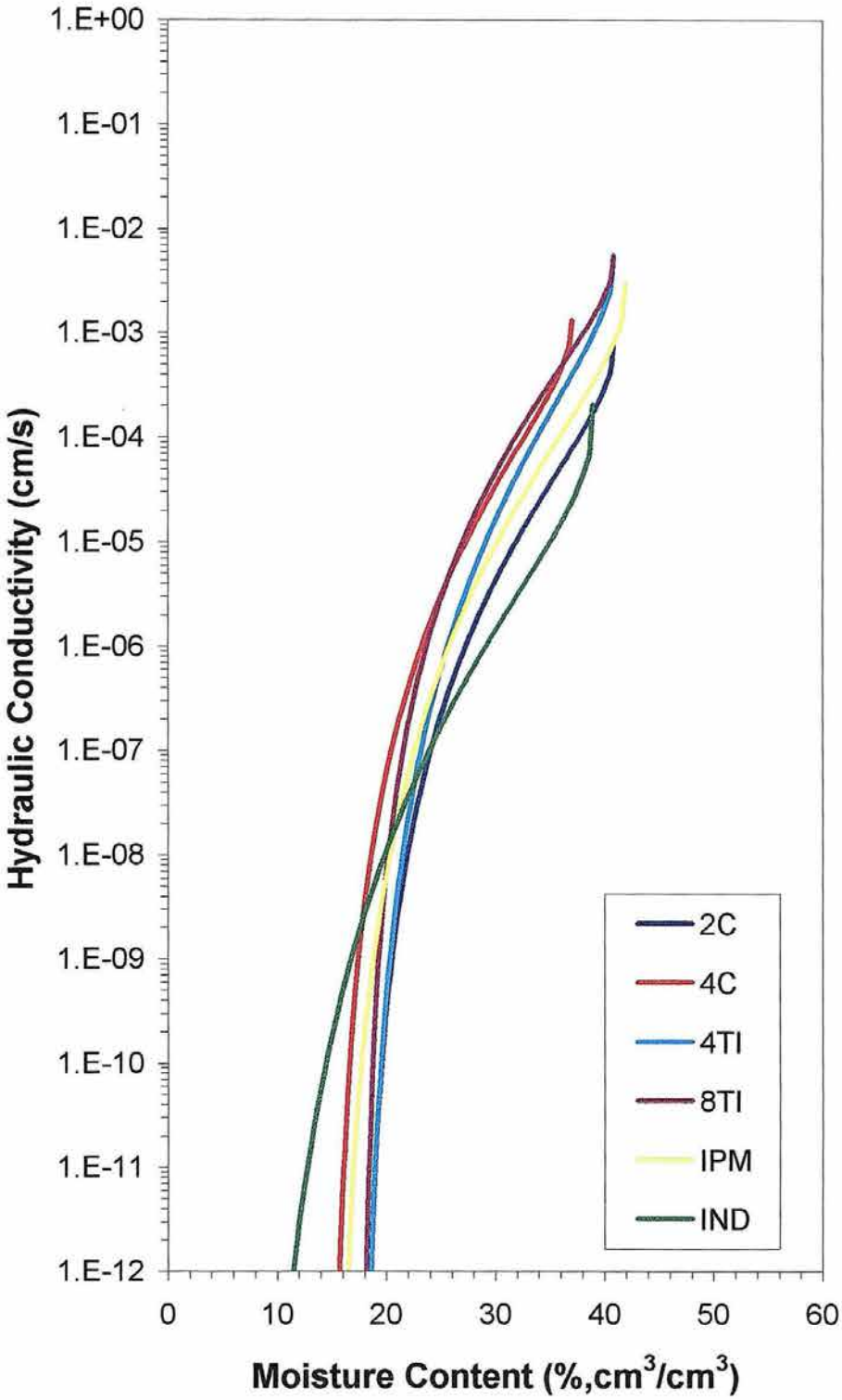

Appendix A. Unsaturated hydraulic conductivity plots constructed using data obtained from T treatment at the 20 cm depth.

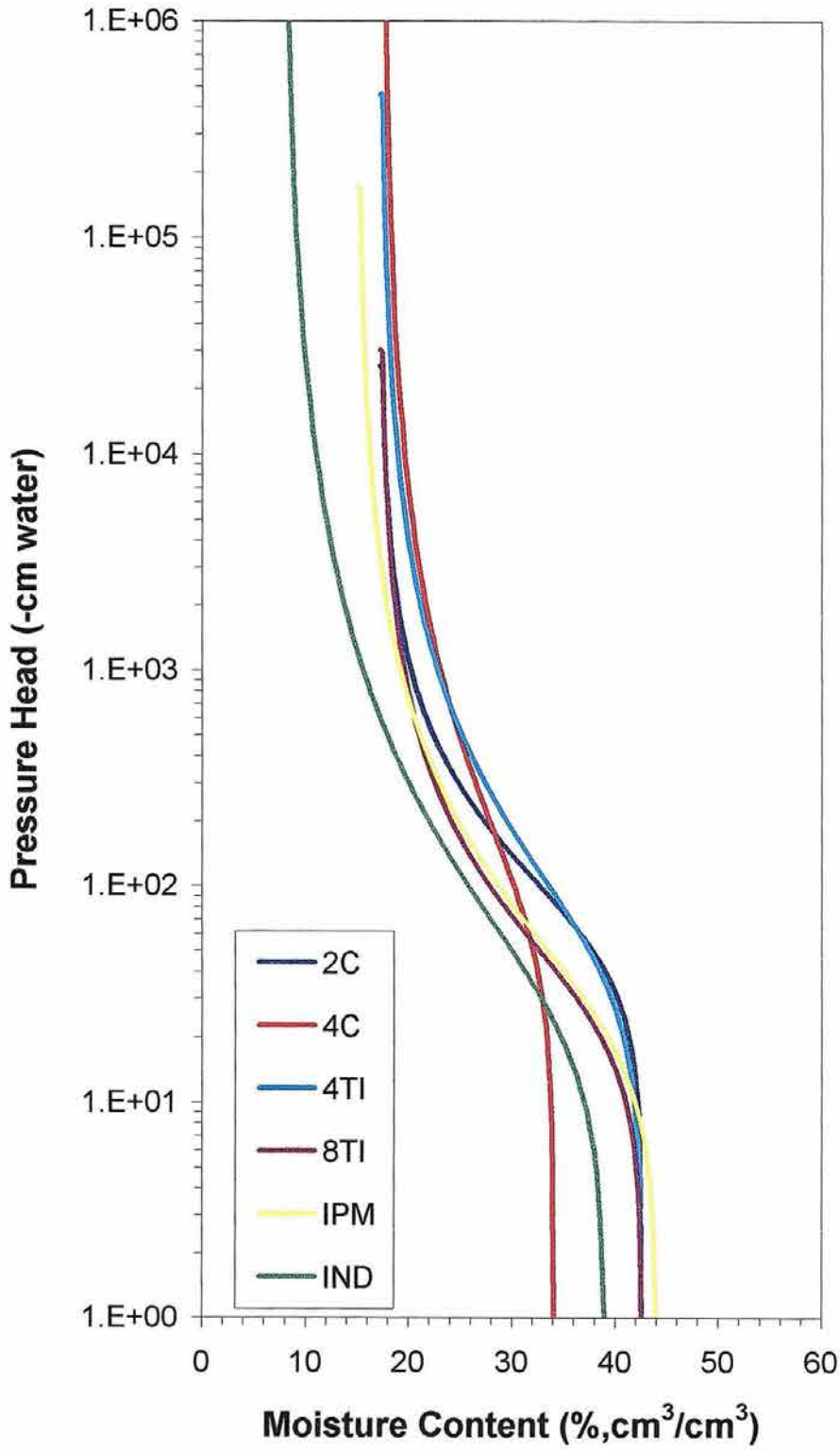

Appendix A. Moisture retention plots plots constructed using data obtained from the T treatment at the 30 cm depth.

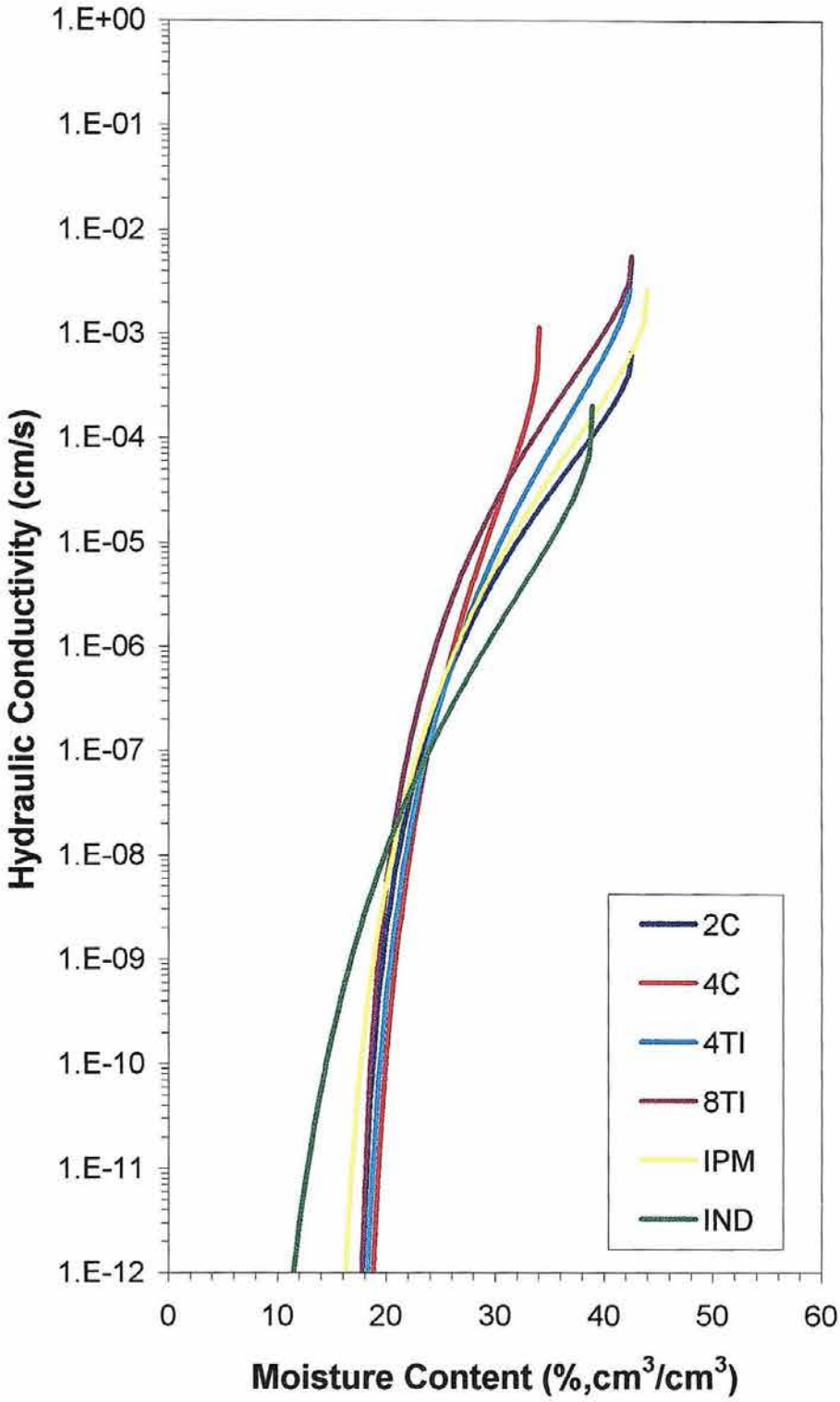

Appendix A. Unsaturated hydraulic conductivity plots constructed using data obtained from T treatment at the 30 cm depth.

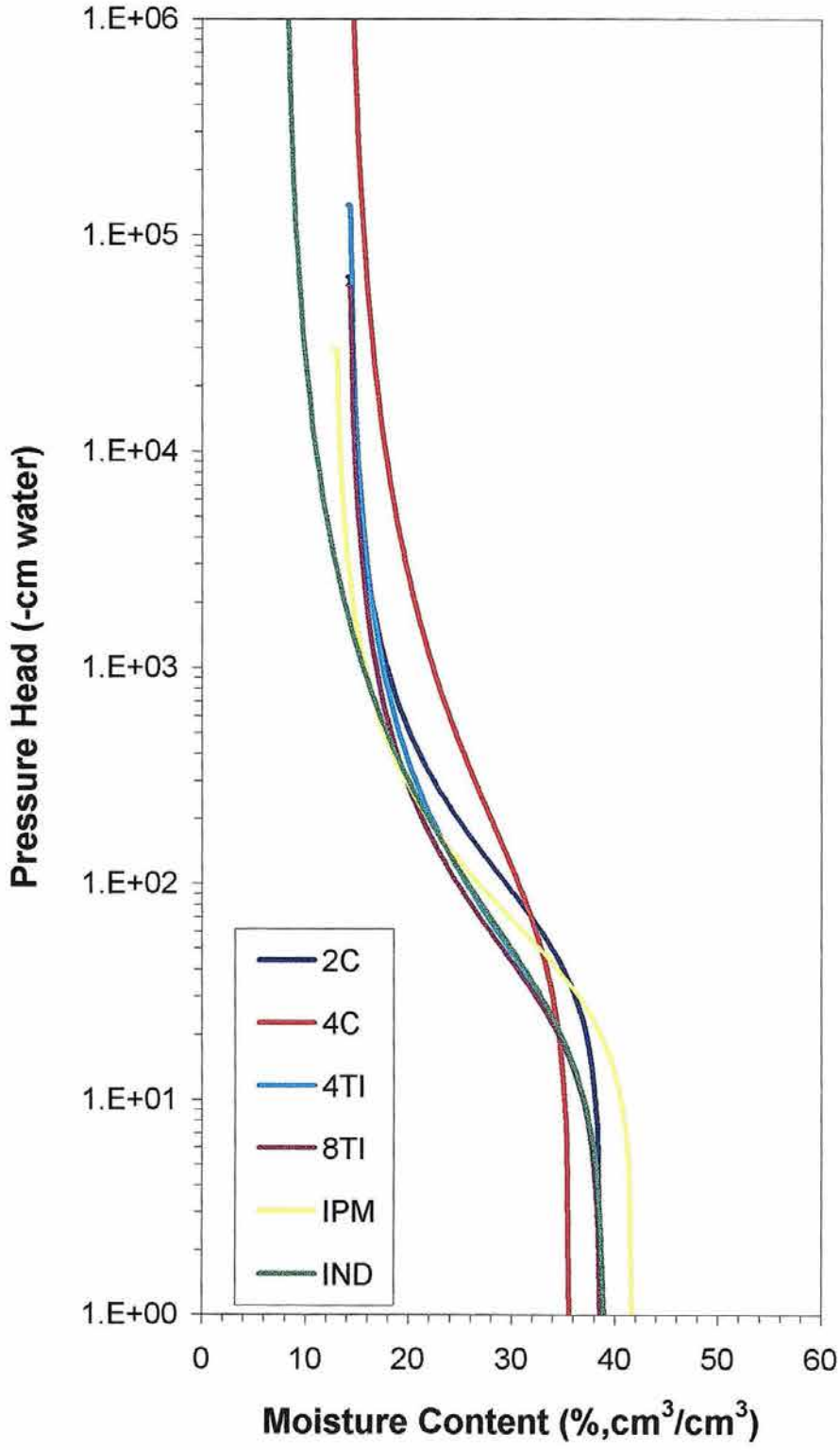

Appendix A. Moisture retention plots plots constructed using data obtained from the T treatment at the 60 cm depth.

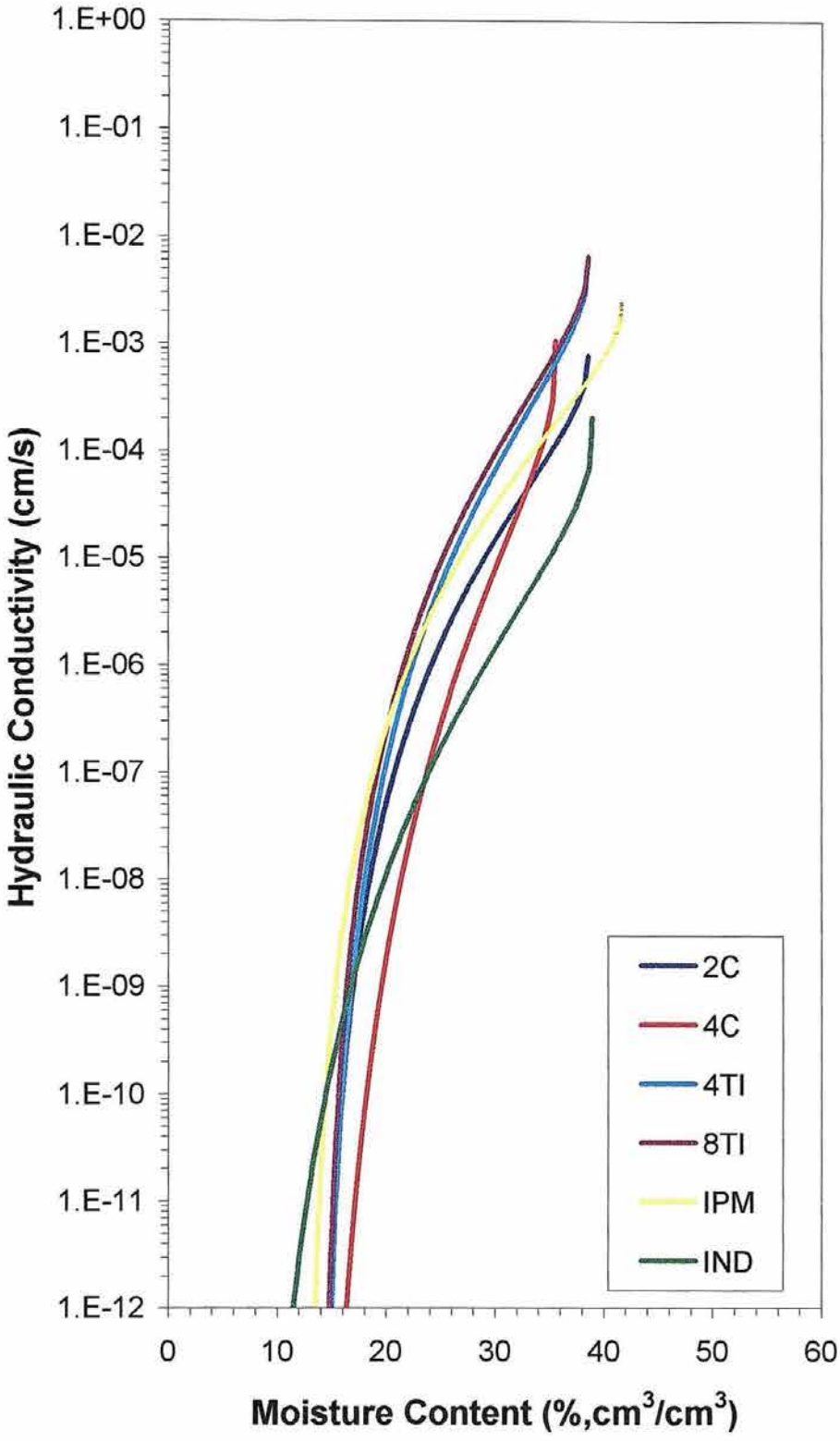

Appendix A. Unsaturated hydraulic conductivity plots constructed using data obtained from T treatment at the 60 cm depth.

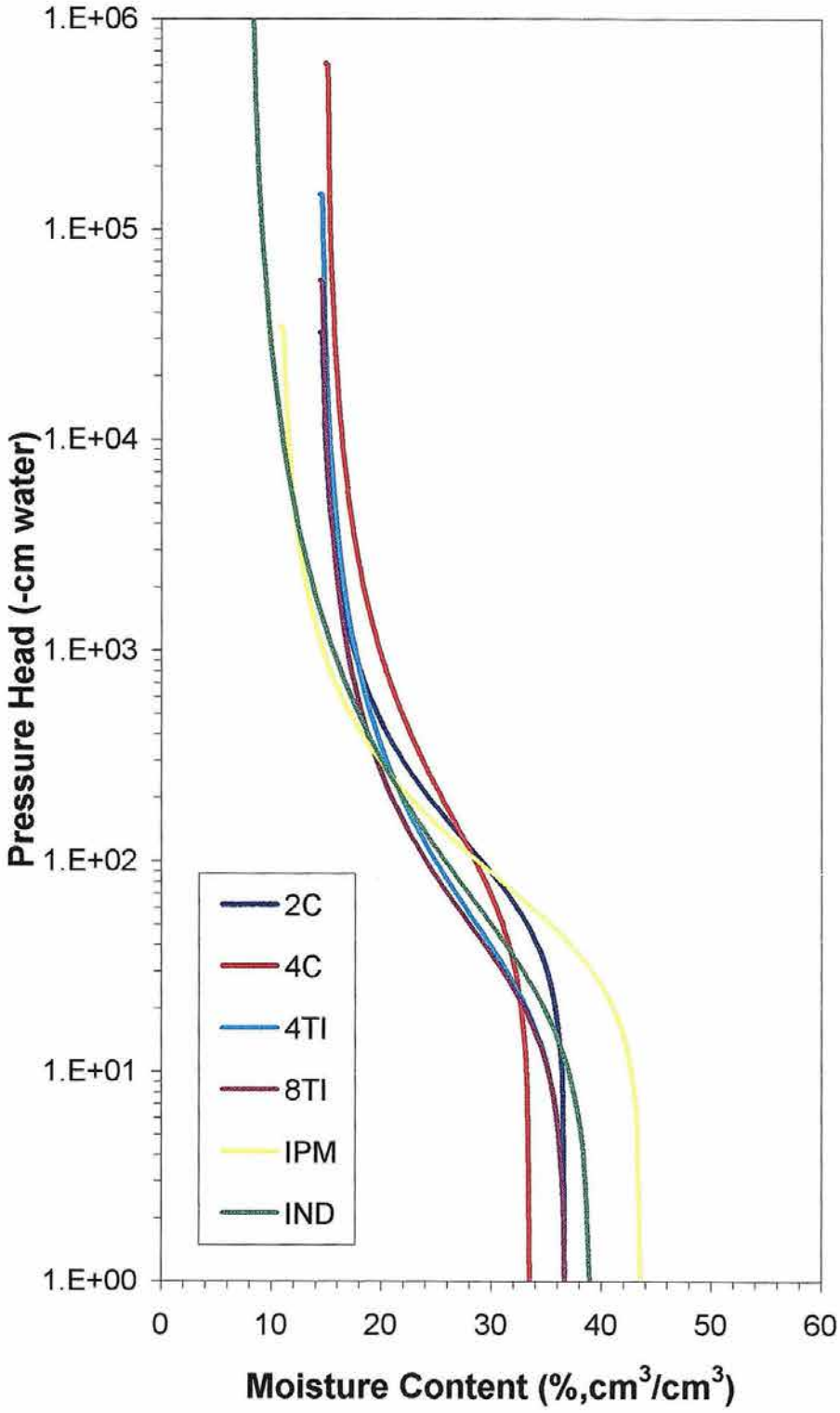

Appendix A. Moisture retention plots plots constructed using data obtained from the T treatment at the 90 cm depth.

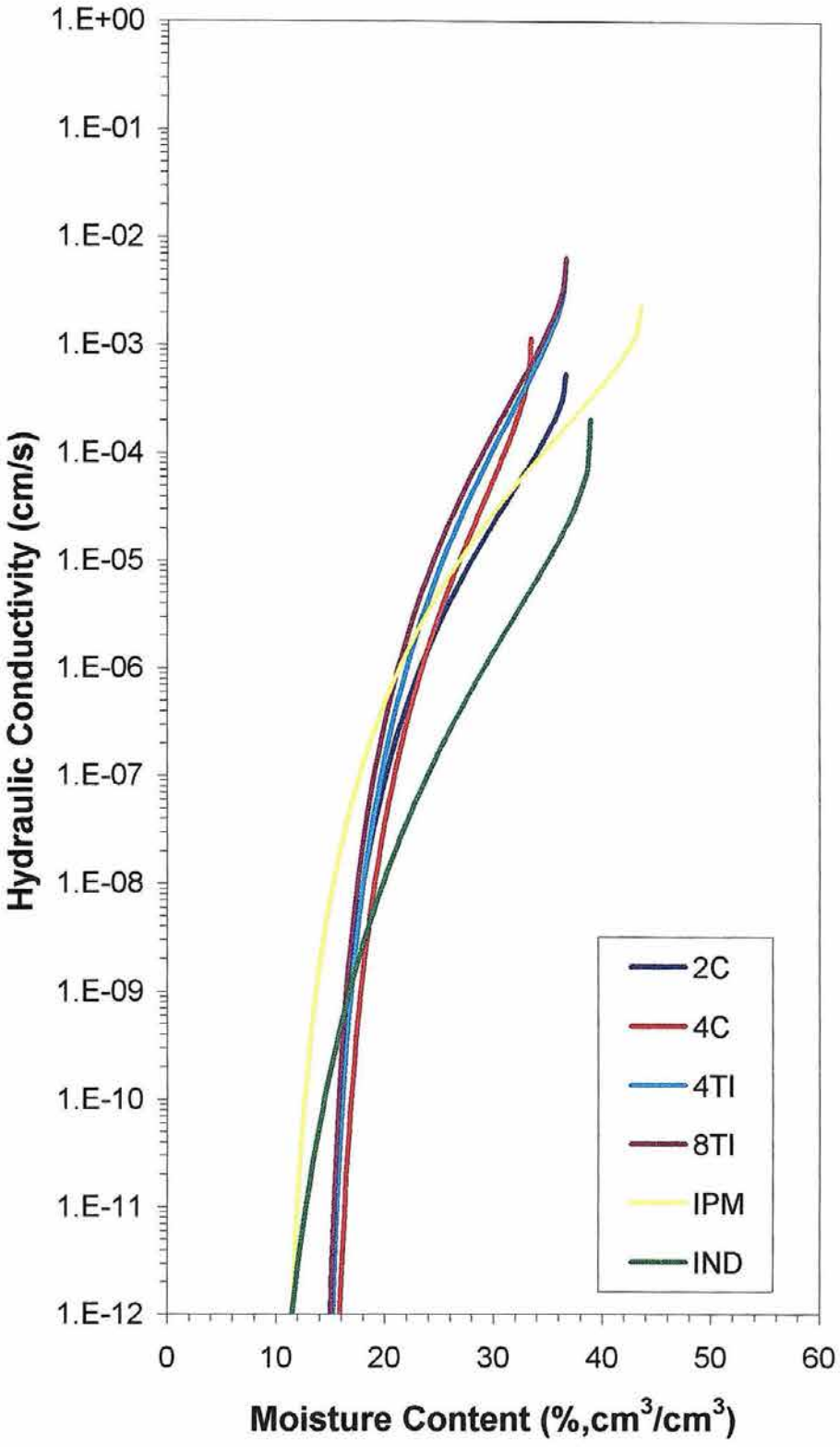

Appendix A. Unsaturated hydraulic conductivity plots constructed using data obtained from T treatment at the 90 cm depth.

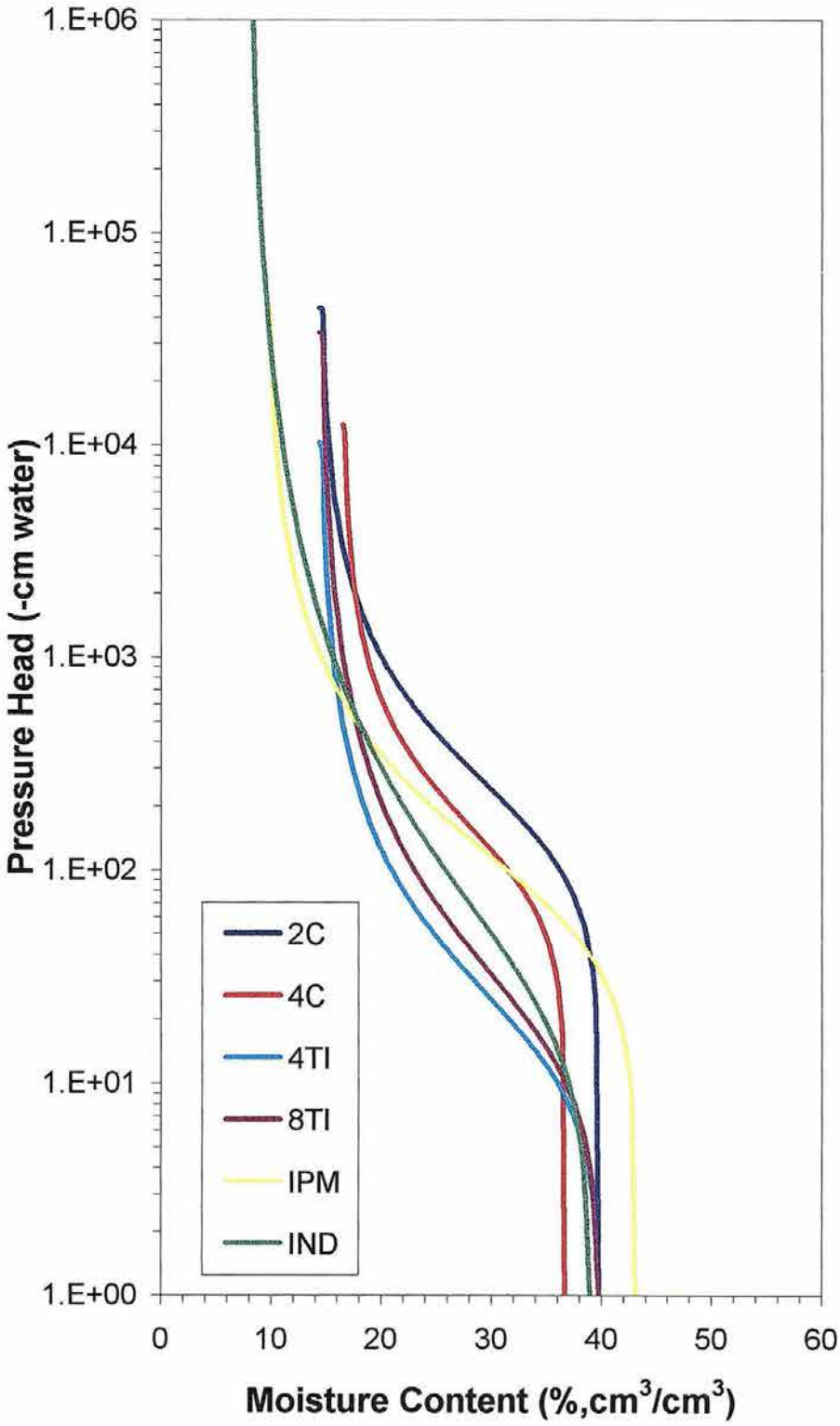

Appendix A. Moisture retention plots plots constructed using data obtained from the T treatment at the 120 cm depth.

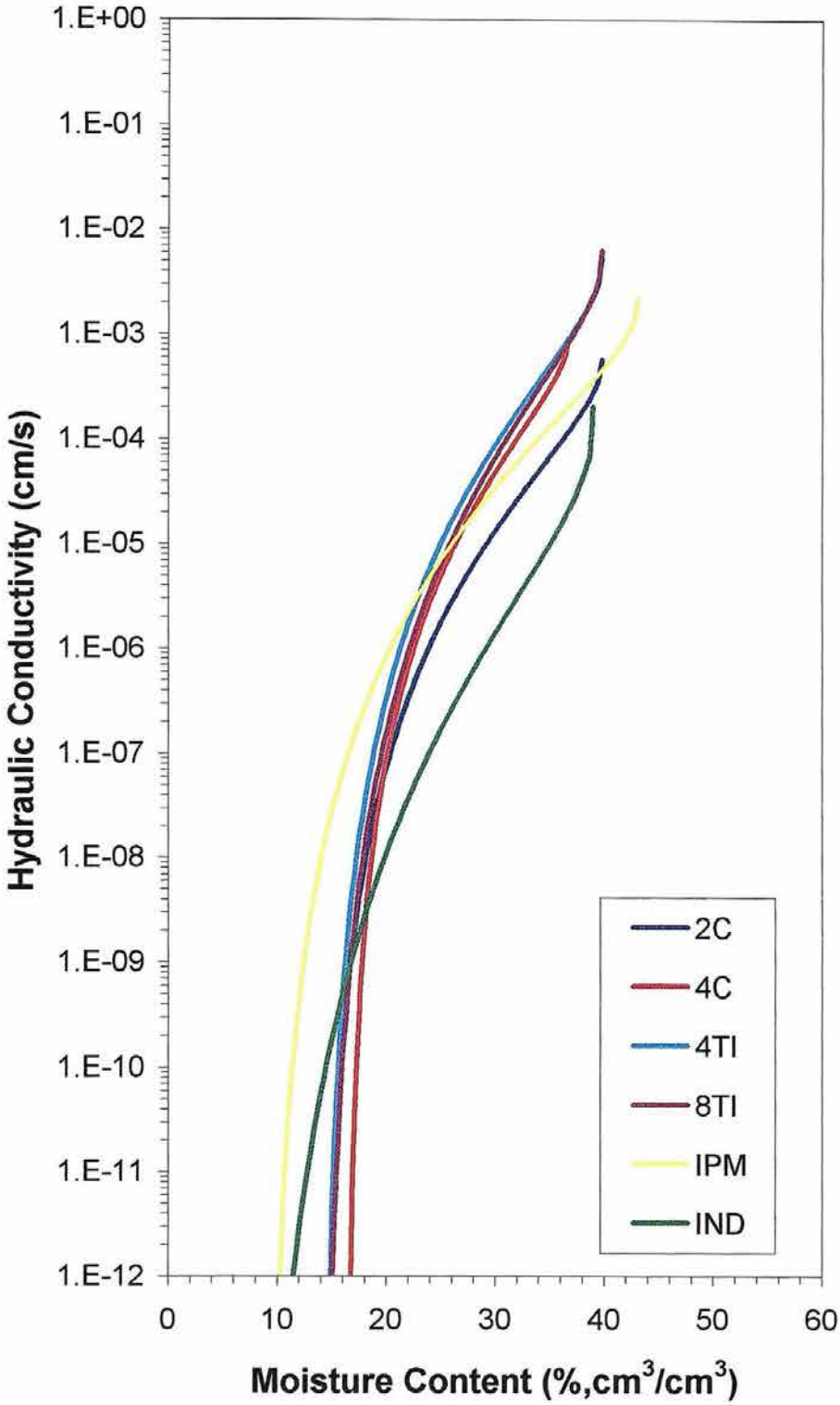

Appendix A. Unsaturated hydraulic conductivity plots constructed using data obtained from T treatment at the 120 cm depth.

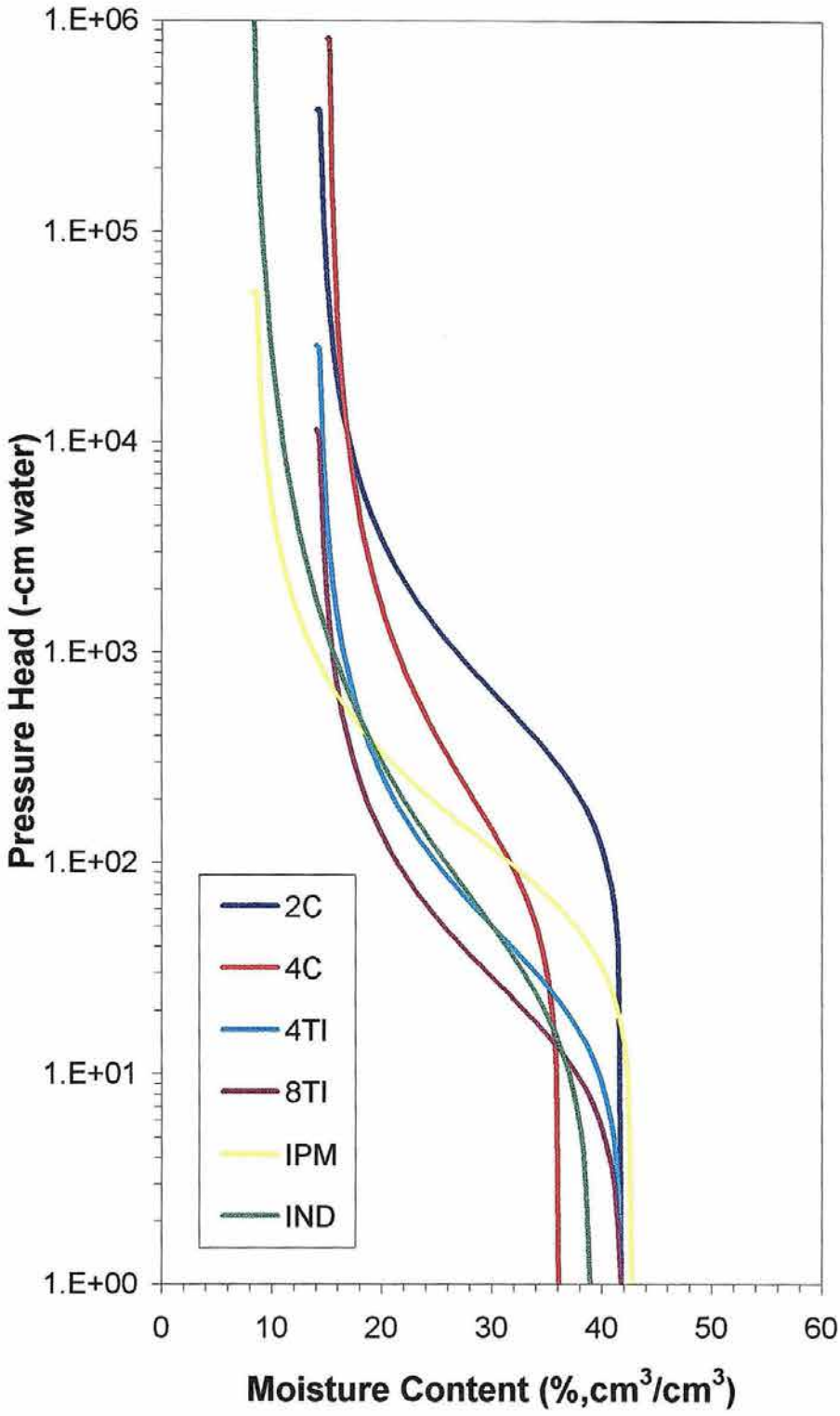

Appendix A. Moisture retention plots plots constructed using data obtained from the T treatment at the 150 cm depth.

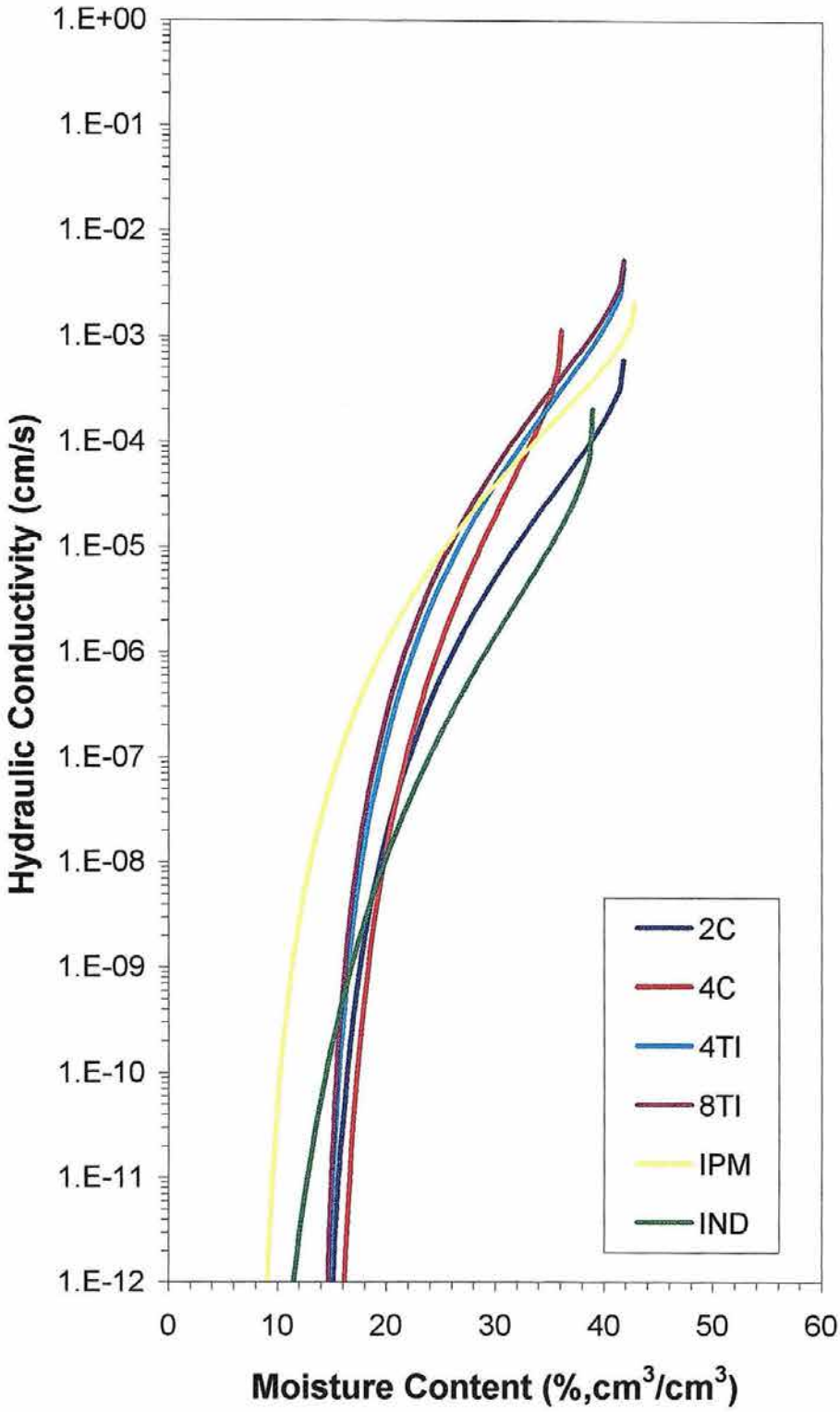

Appendix A. Unsaturated hydraulic conductivity plots constructed using data obtained from T treatment at the 150 cm depth.

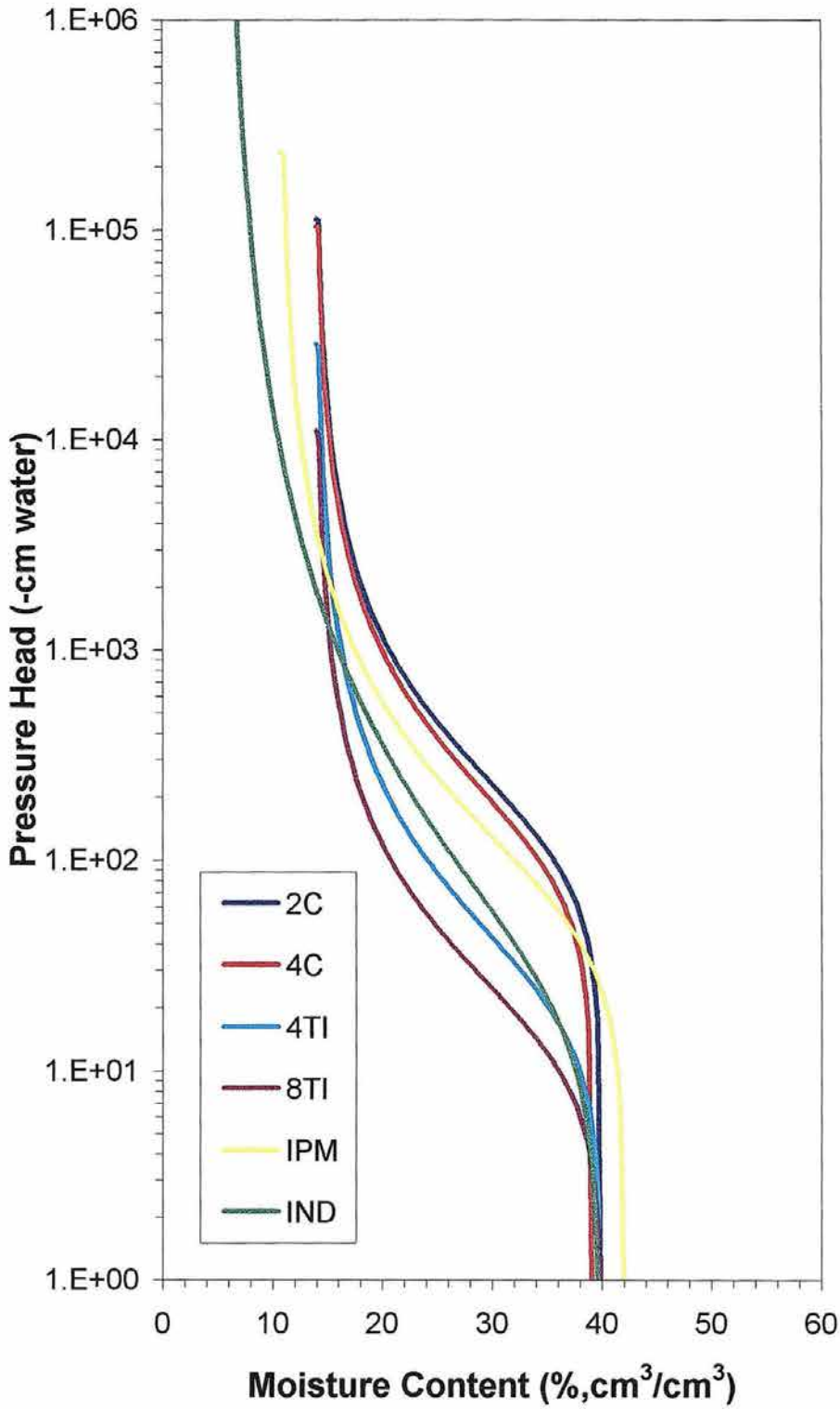

Appendix A. Moisture retention plots plots constructed using data obtained from the T treatment at the 180 cm depth.

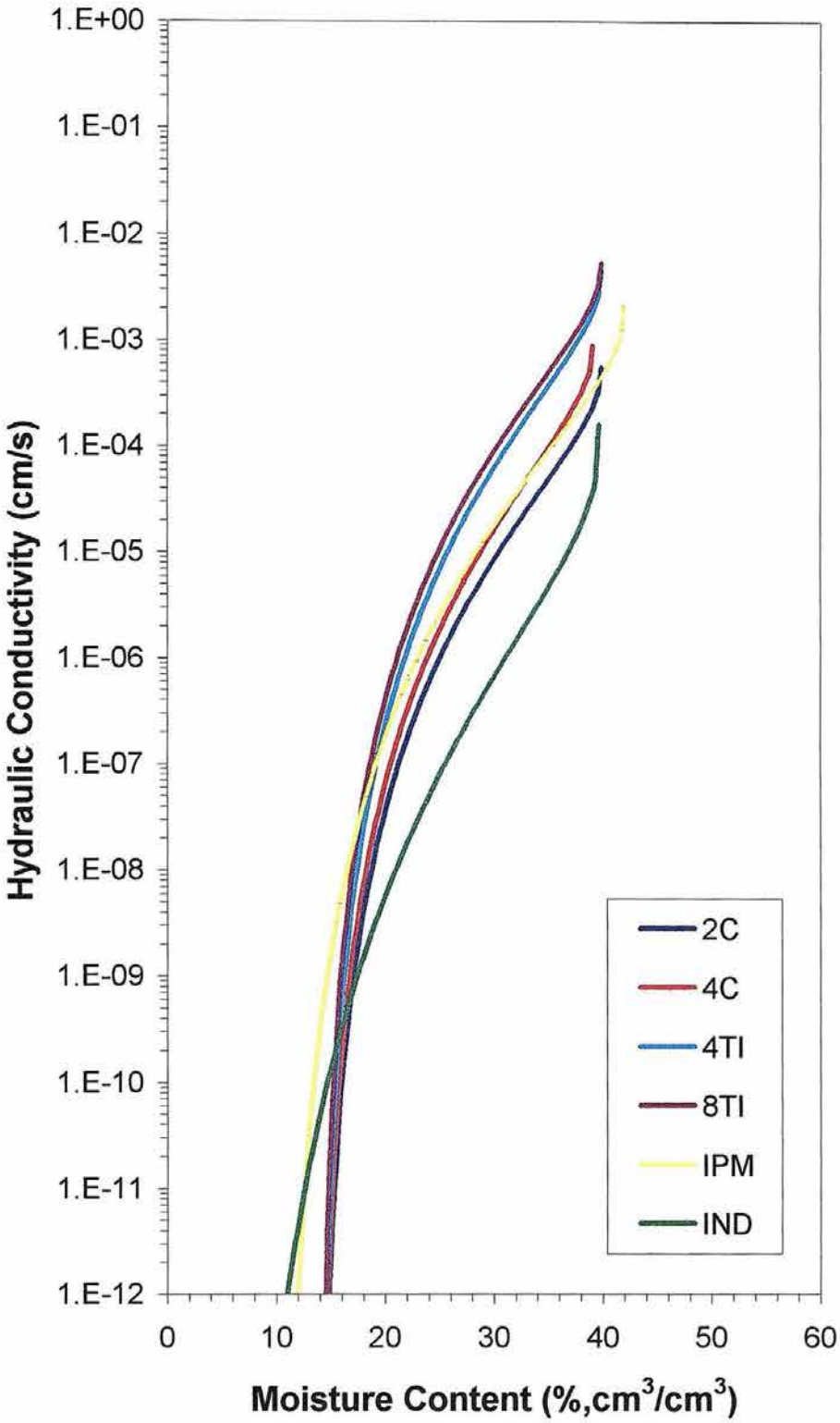

Appendix A. Unsaturated hydraulic conductivity plots constructed using data obtained from T treatment at the 180 cm depth.

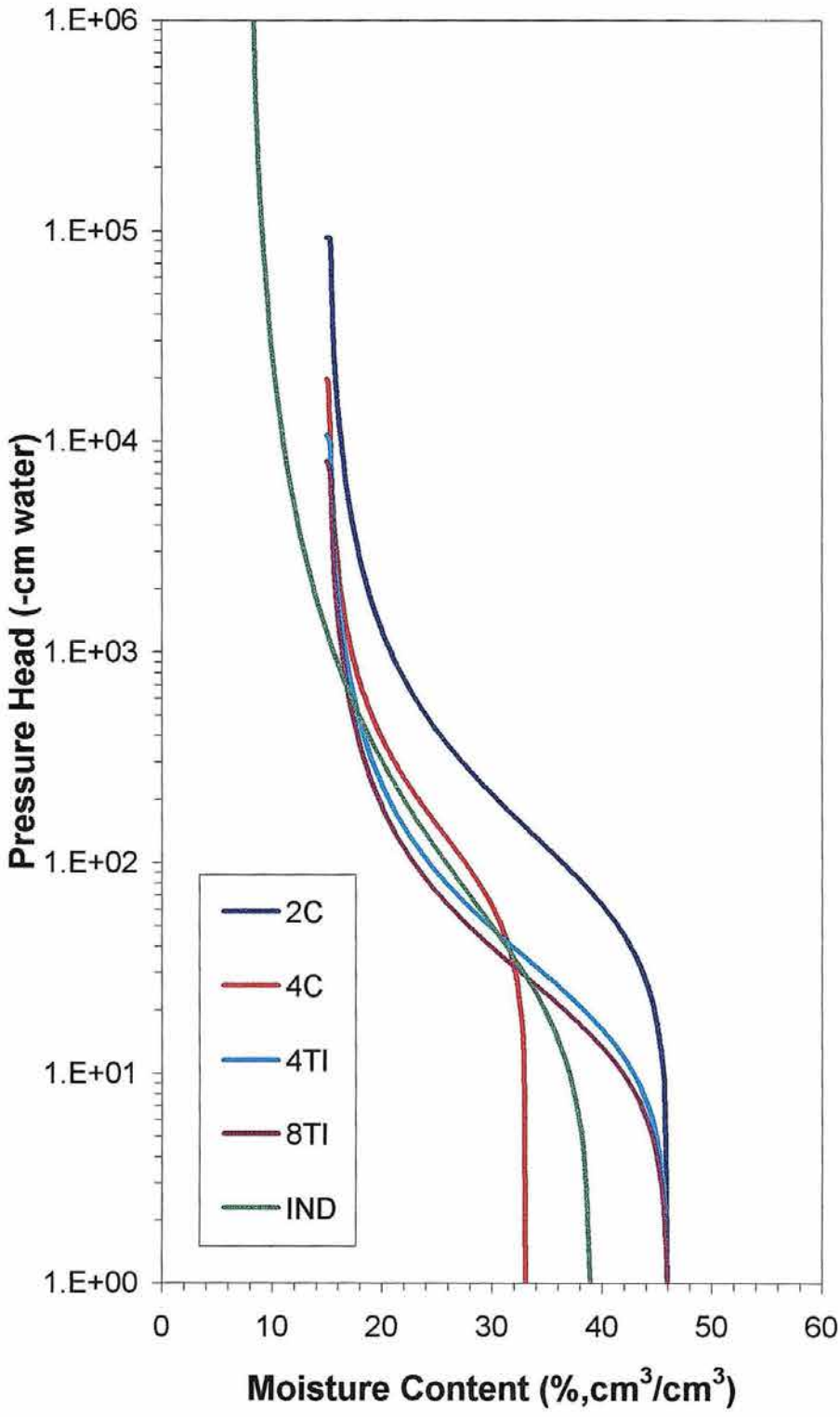

Appendix A. Moisture retention plots plots constructed using data obtained from the NT treatment at the 0 cm depth.

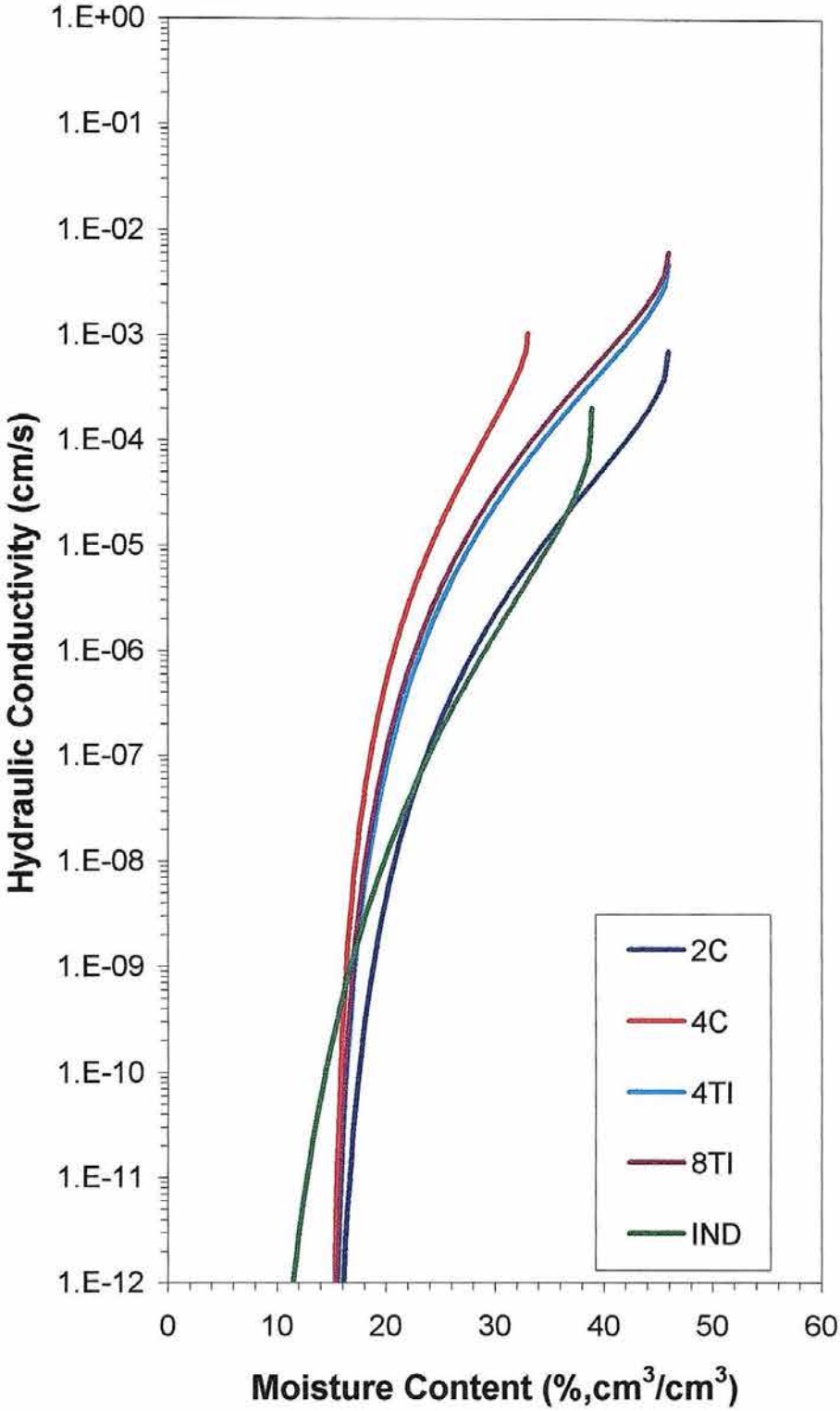

Appendix A. Unsaturated hydraulic conductivity plots constructed using data obtained from NT treatment at the 0 cm depth.

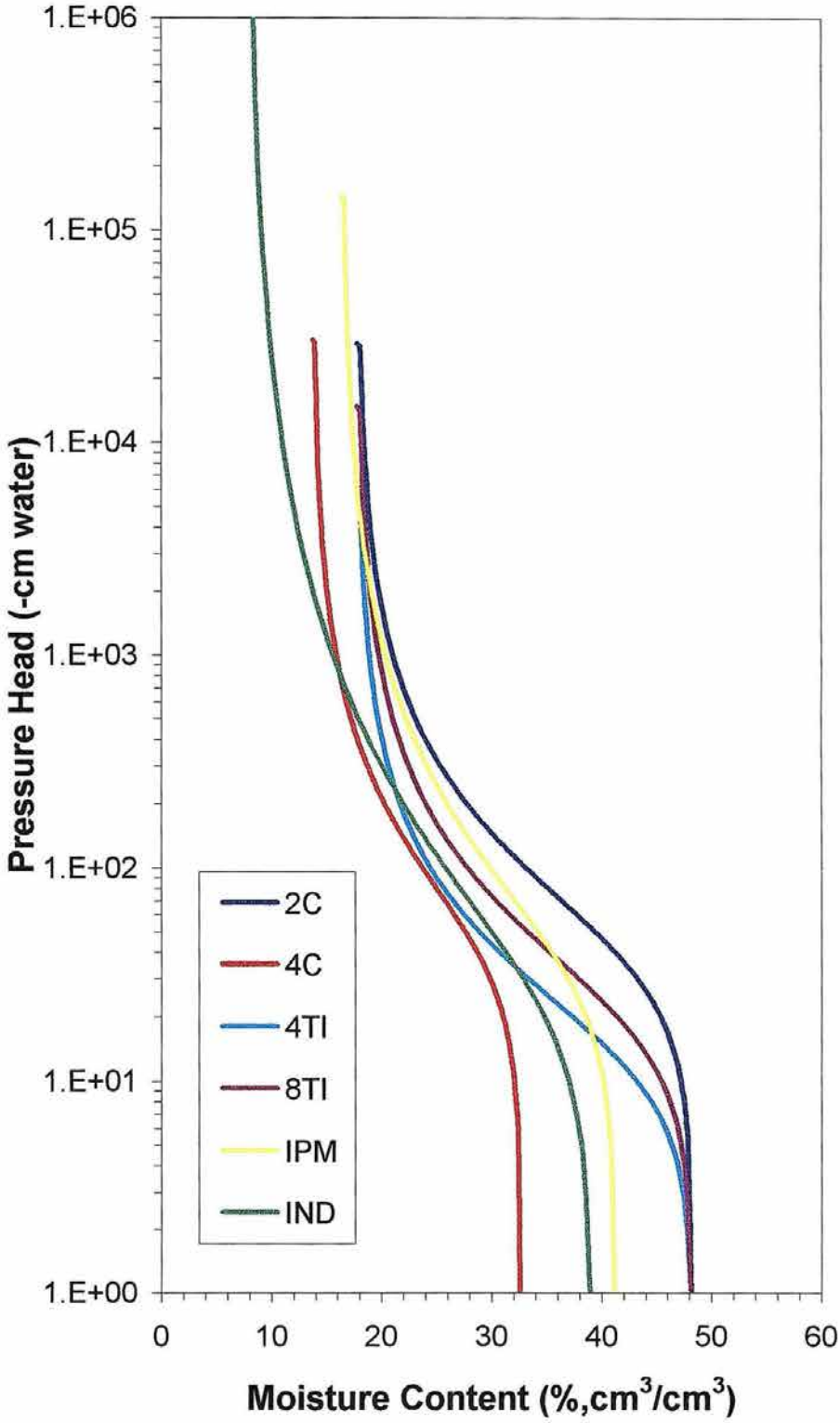

Appendix A. Moisture retention plots plots constructed using data obtained from the NT treatment at the 10 cm depth.

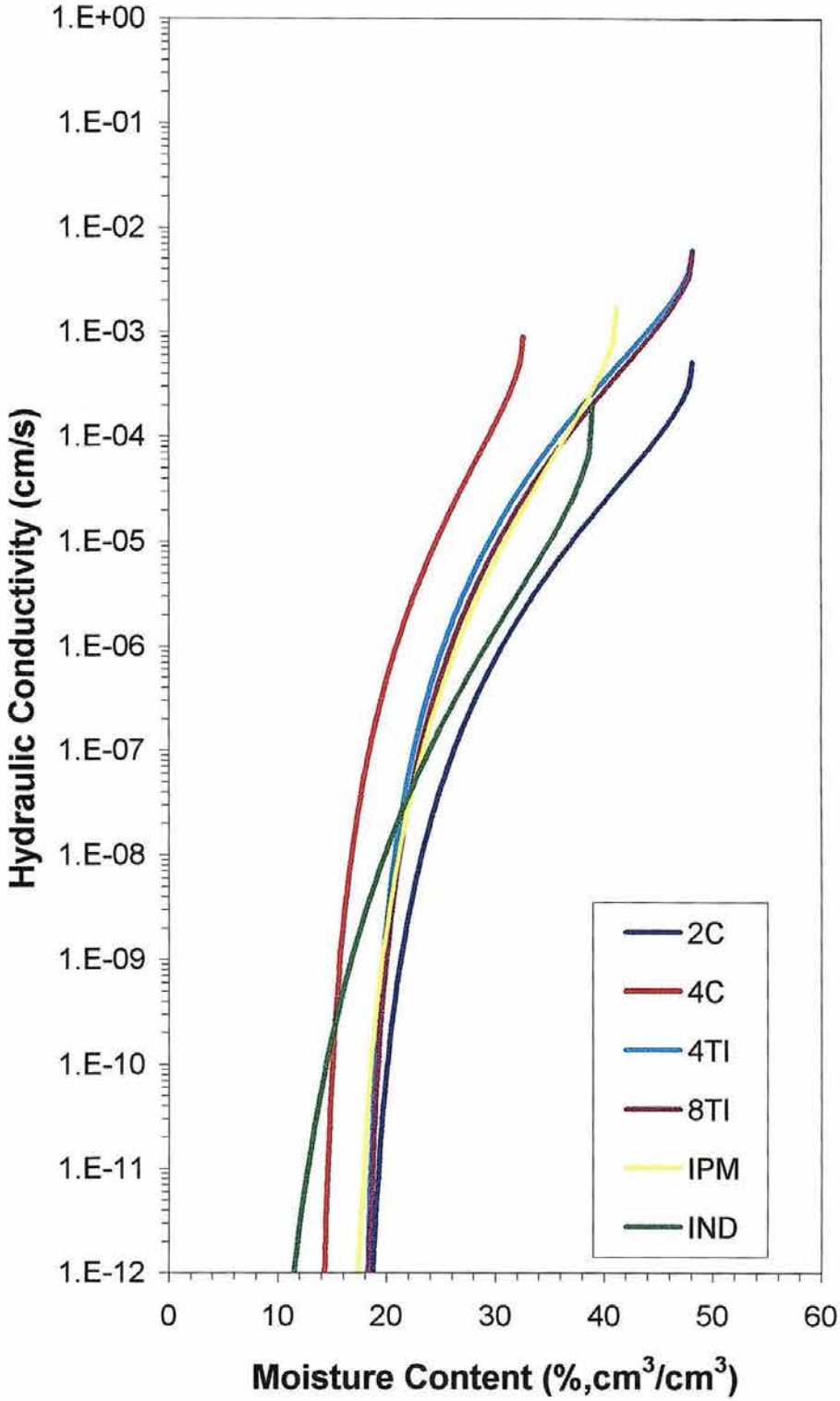

Appendix A. Unsaturated hydraulic conductivity plots constructed using data obtained from NT treatment at the 10 cm depth.

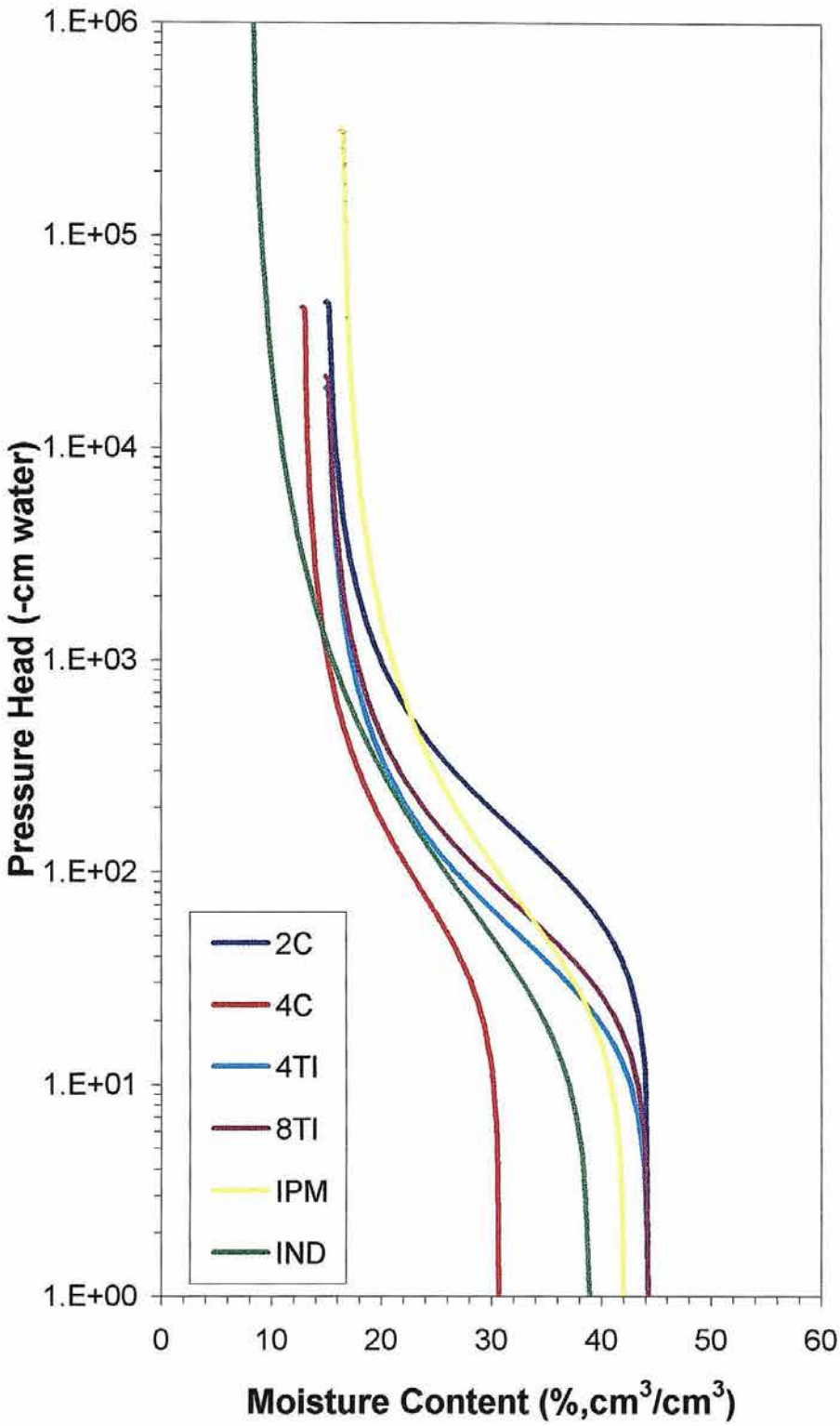

Appendix A. Moisture retention plots plots constructed using data obtained from the NT treatment at the 20 cm depth.

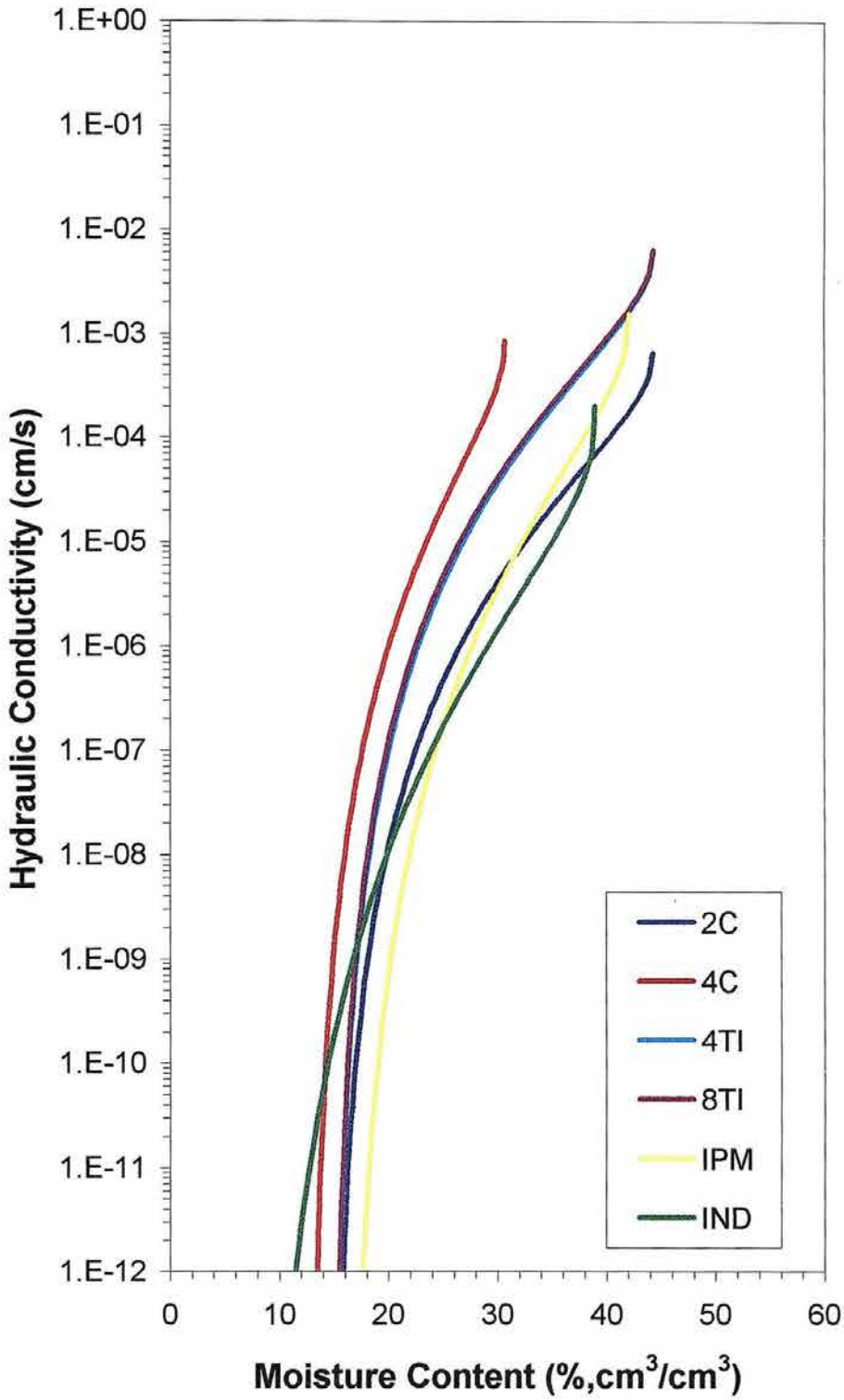

Appendix A. Unsaturated hydraulic conductivity plots constructed using data obtained from NT treatment at the 20 cm depth.

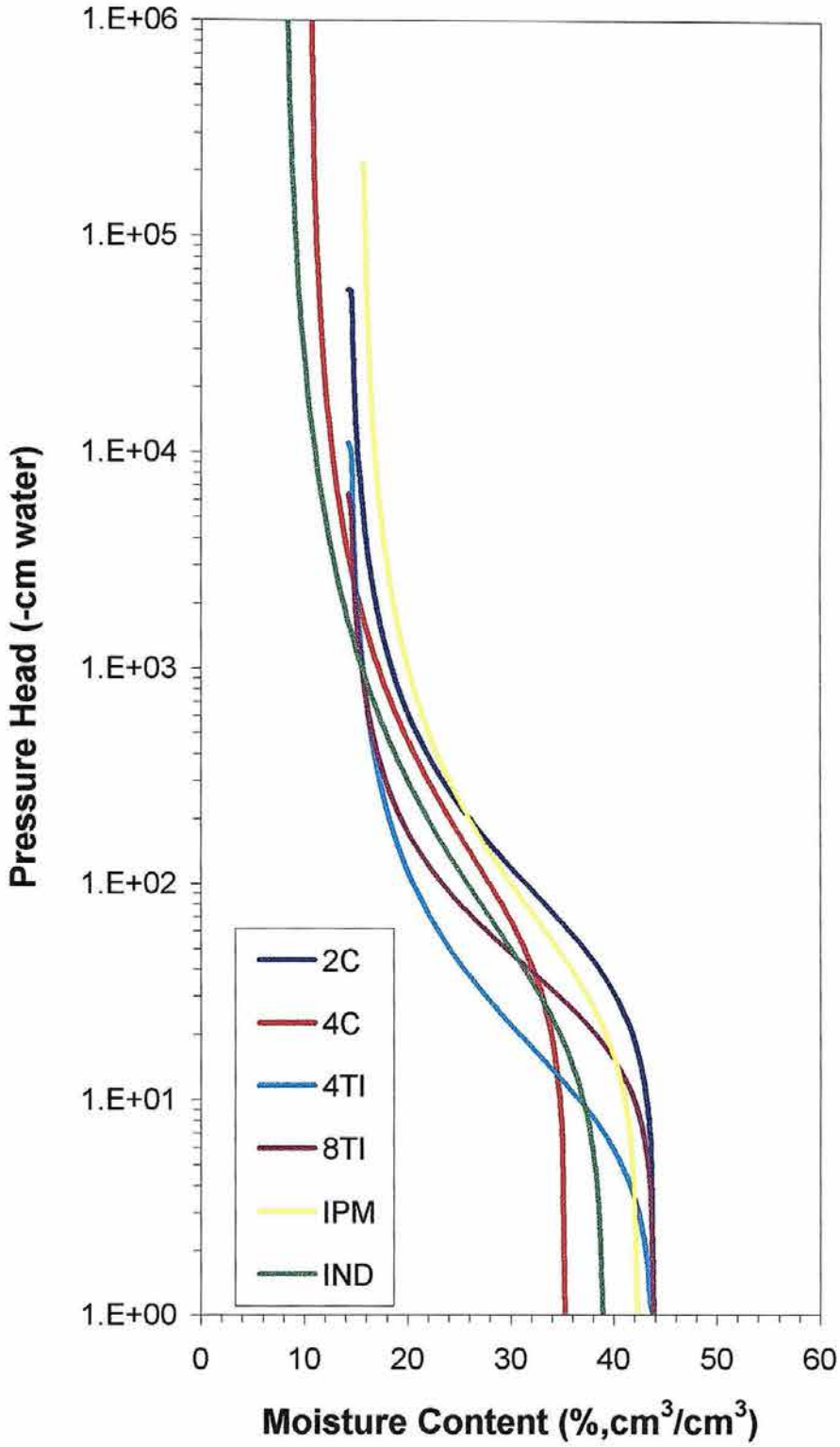

Appendix A. Moisture retention plots plots constructed using data obtained from the NT treatment at the 30 cm depth.

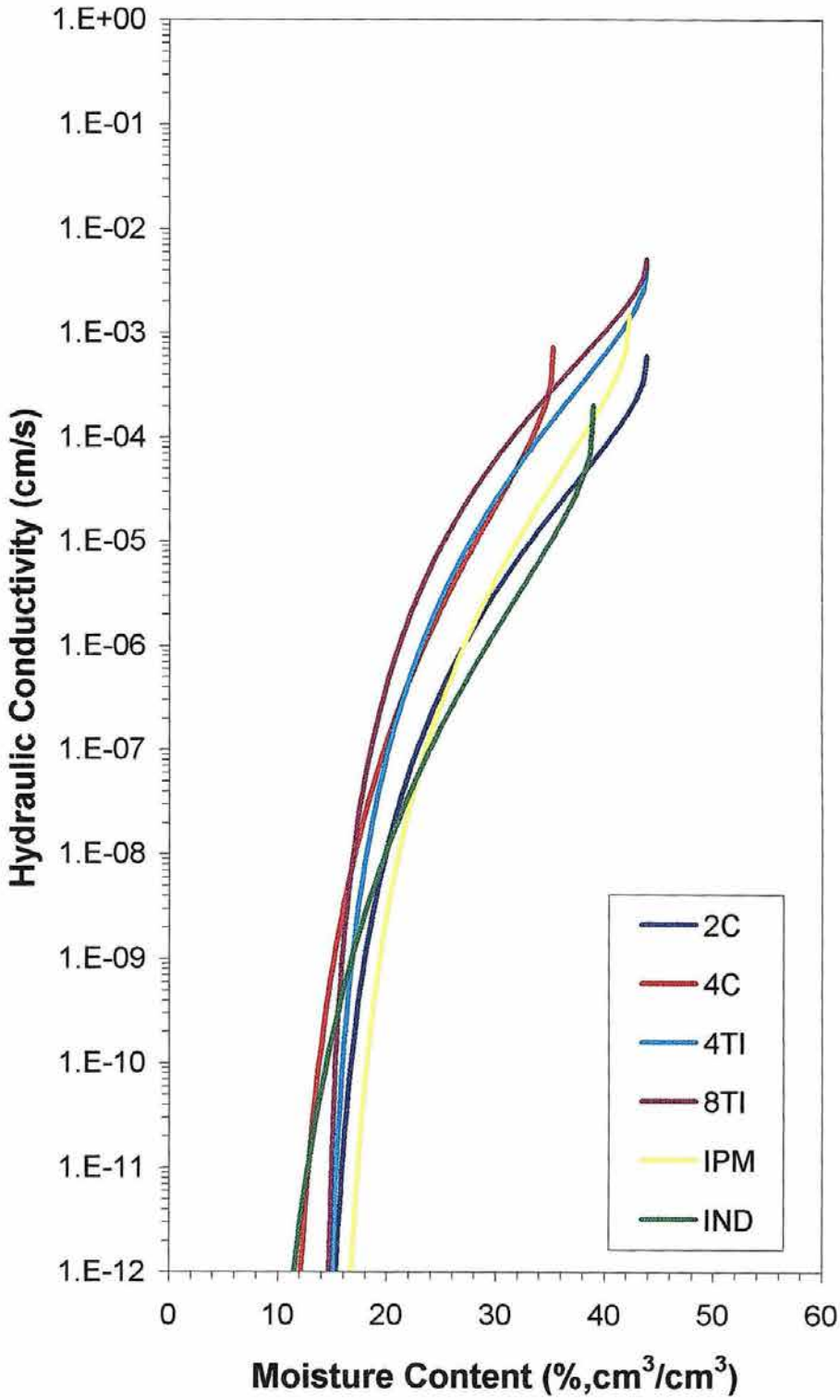

Appendix A. Unsaturated hydraulic conductivity plots constructed using data obtained from NT treatment at the 30 cm depth.

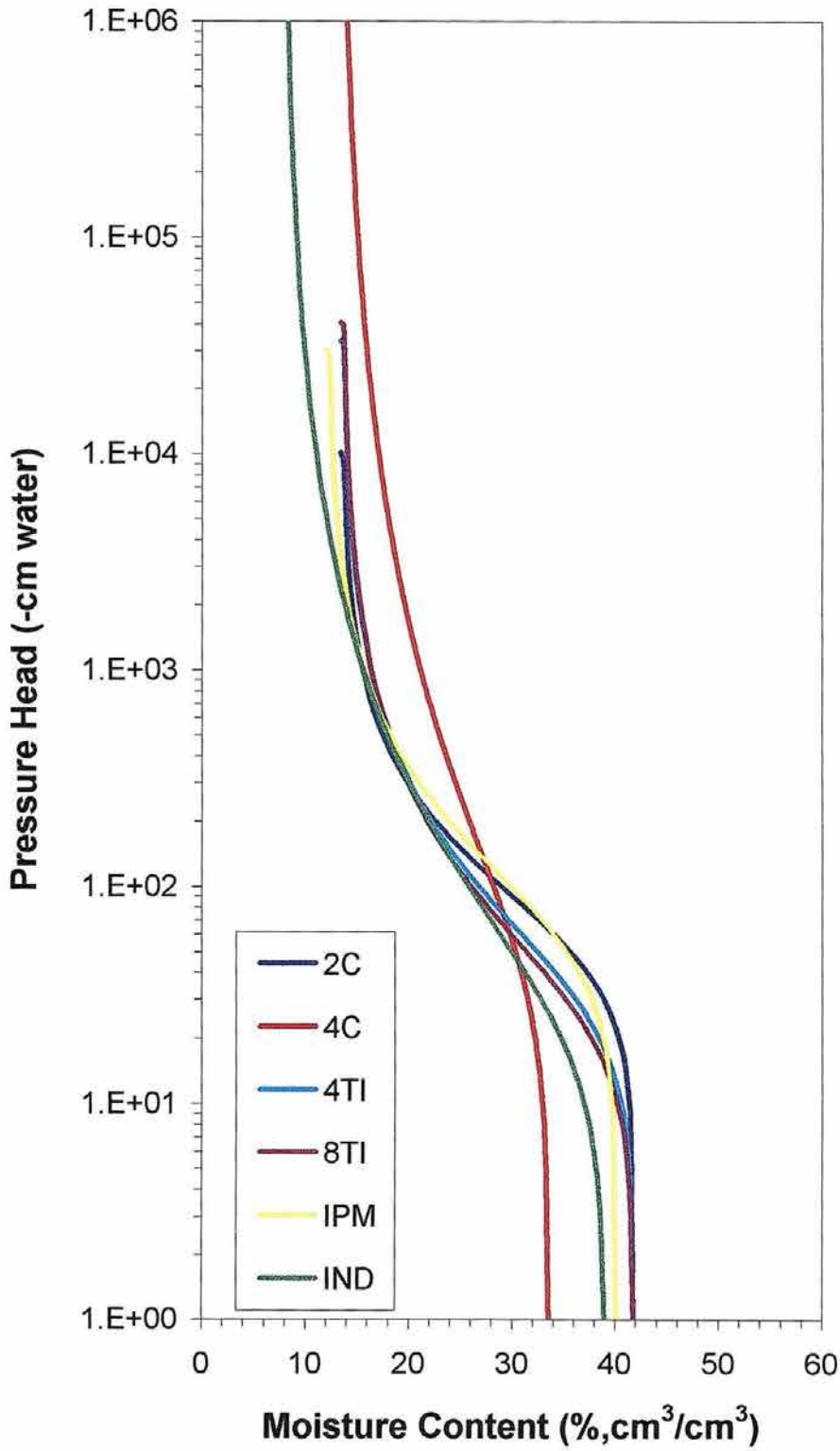

Appendix A. Moisture retention plots plots constructed using data obtained from the NT treatment at the 60 cm depth.

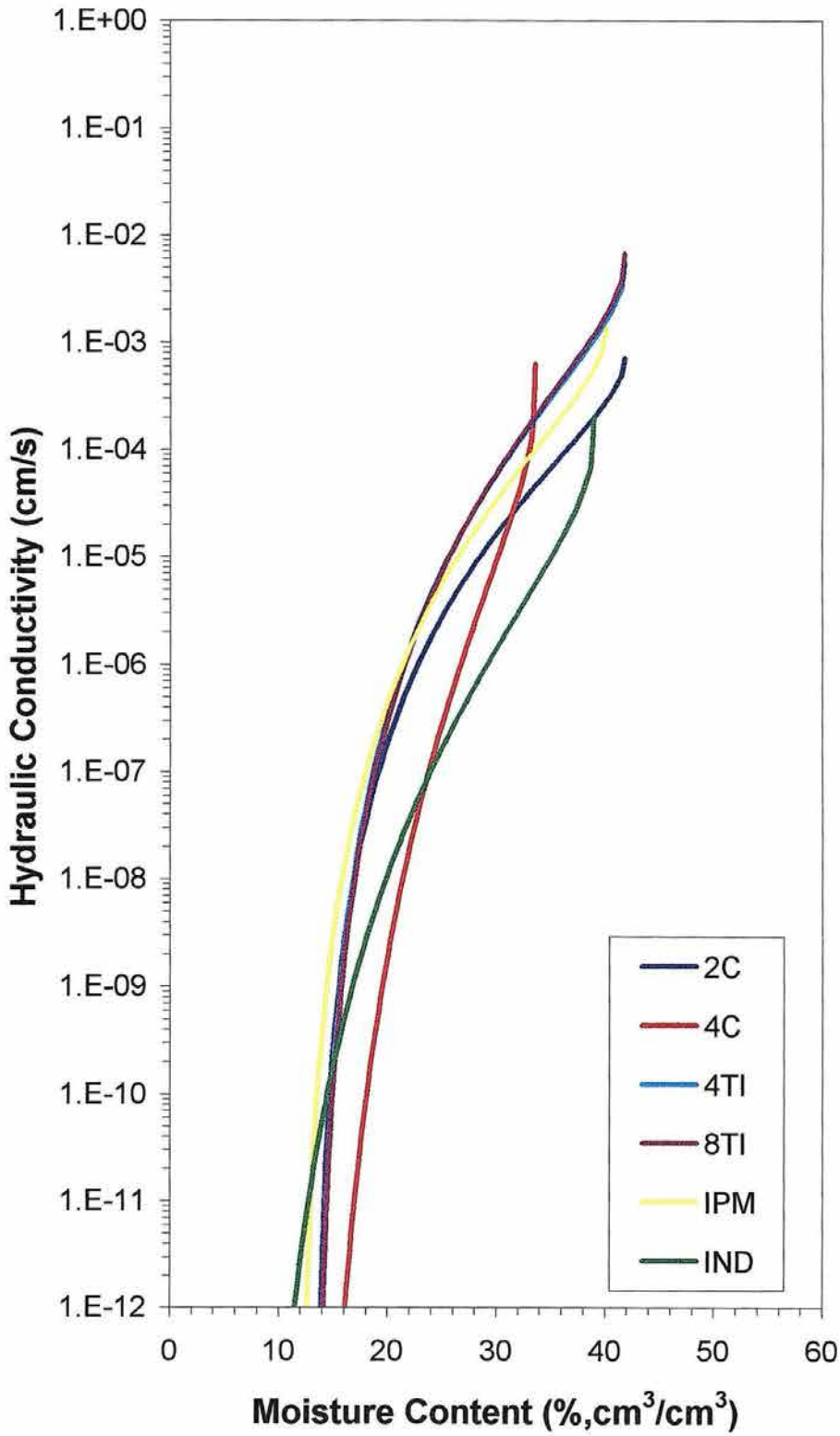

Appendix A. Unsaturated hydraulic conductivity plots constructed using data obtained from NT treatment at the 60 cm depth.

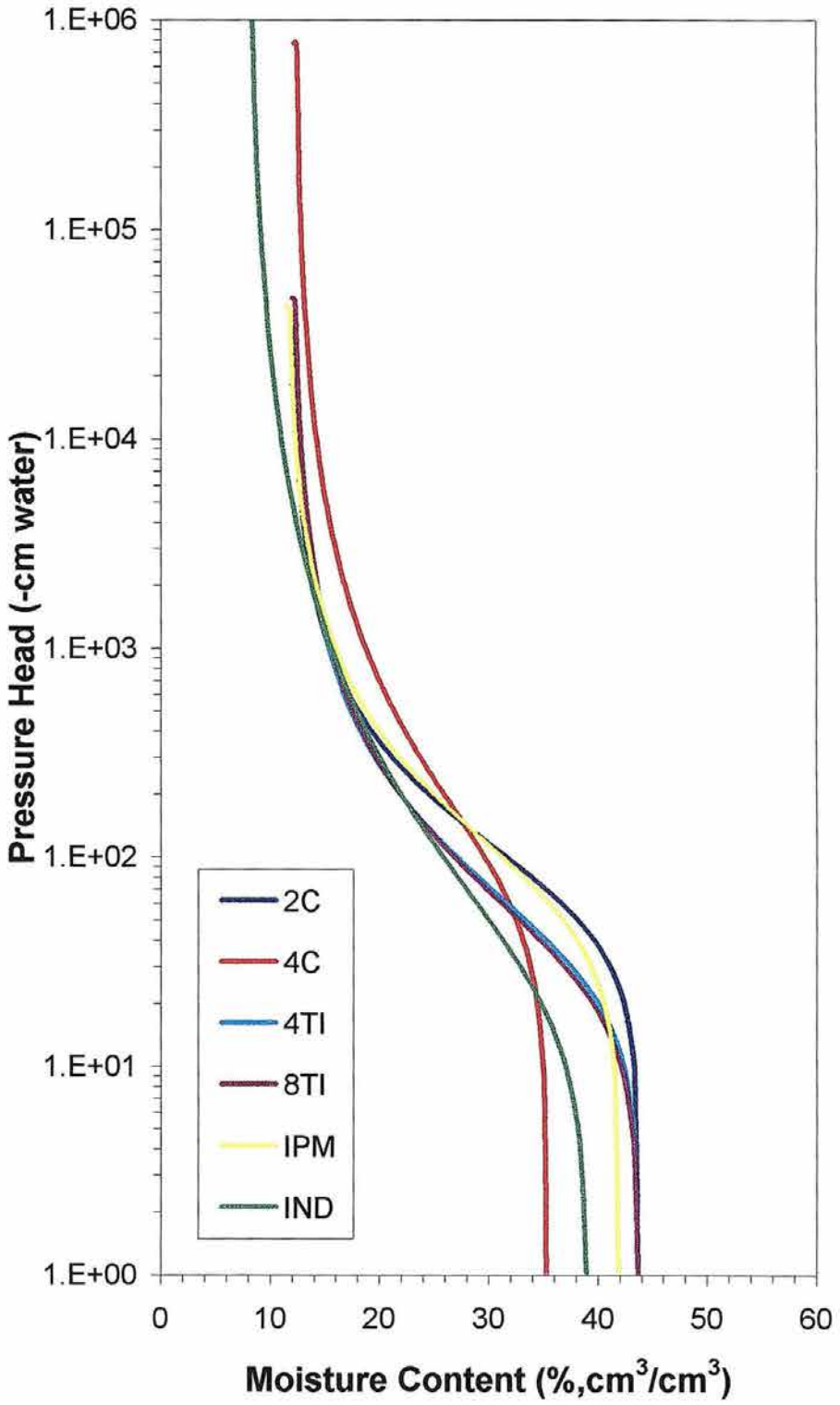

Appendix A. Moisture retention plots plots constructed using data obtained from the NT treatment at the 90 cm depth.

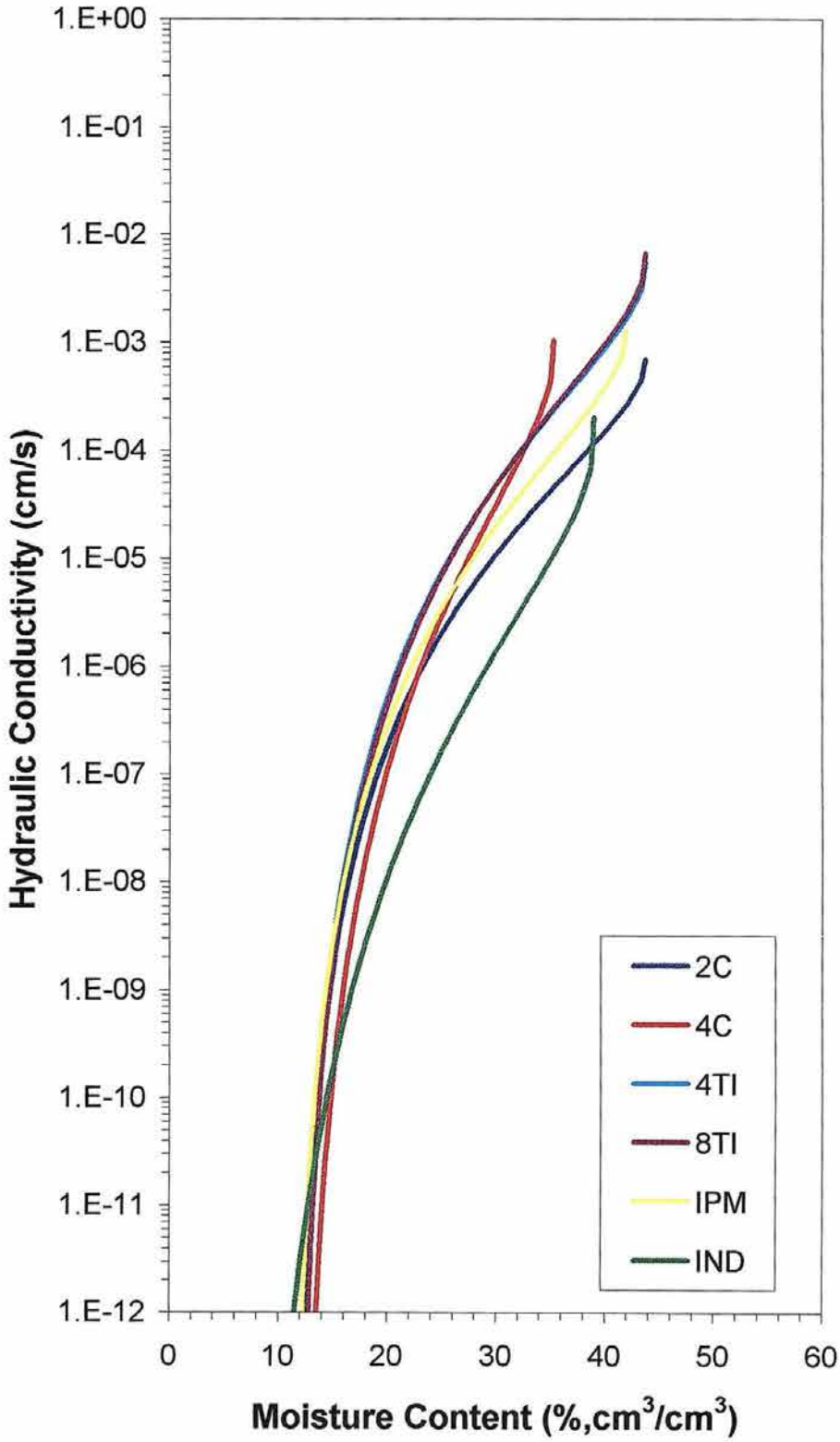

Appendix A. Unsaturated hydraulic conductivity plots constructed using data obtained from NT treatment at the 90 cm depth.

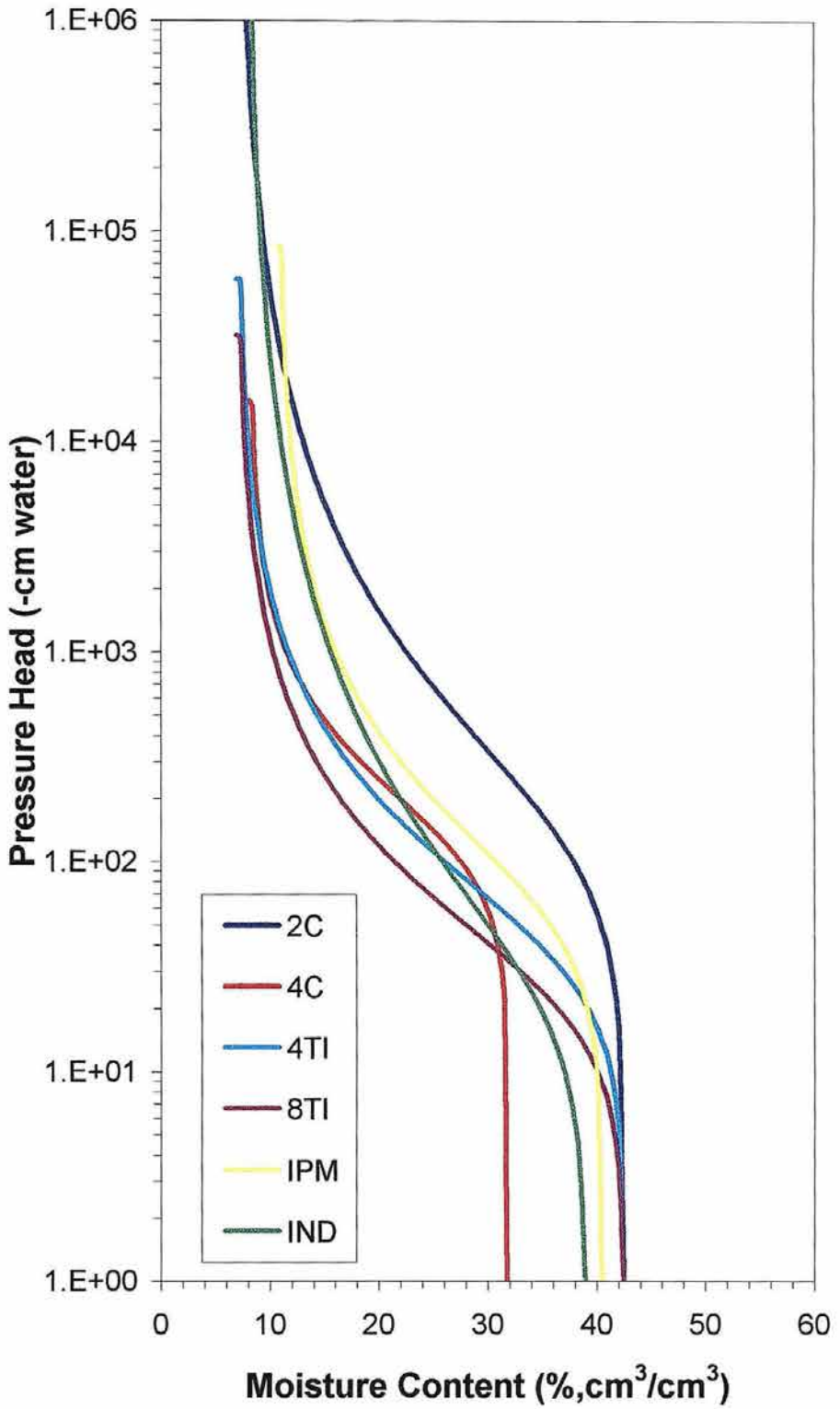

Appendix A. Moisture retention plots plots constructed using data obtained from the NT treatment at the 120 cm depth.

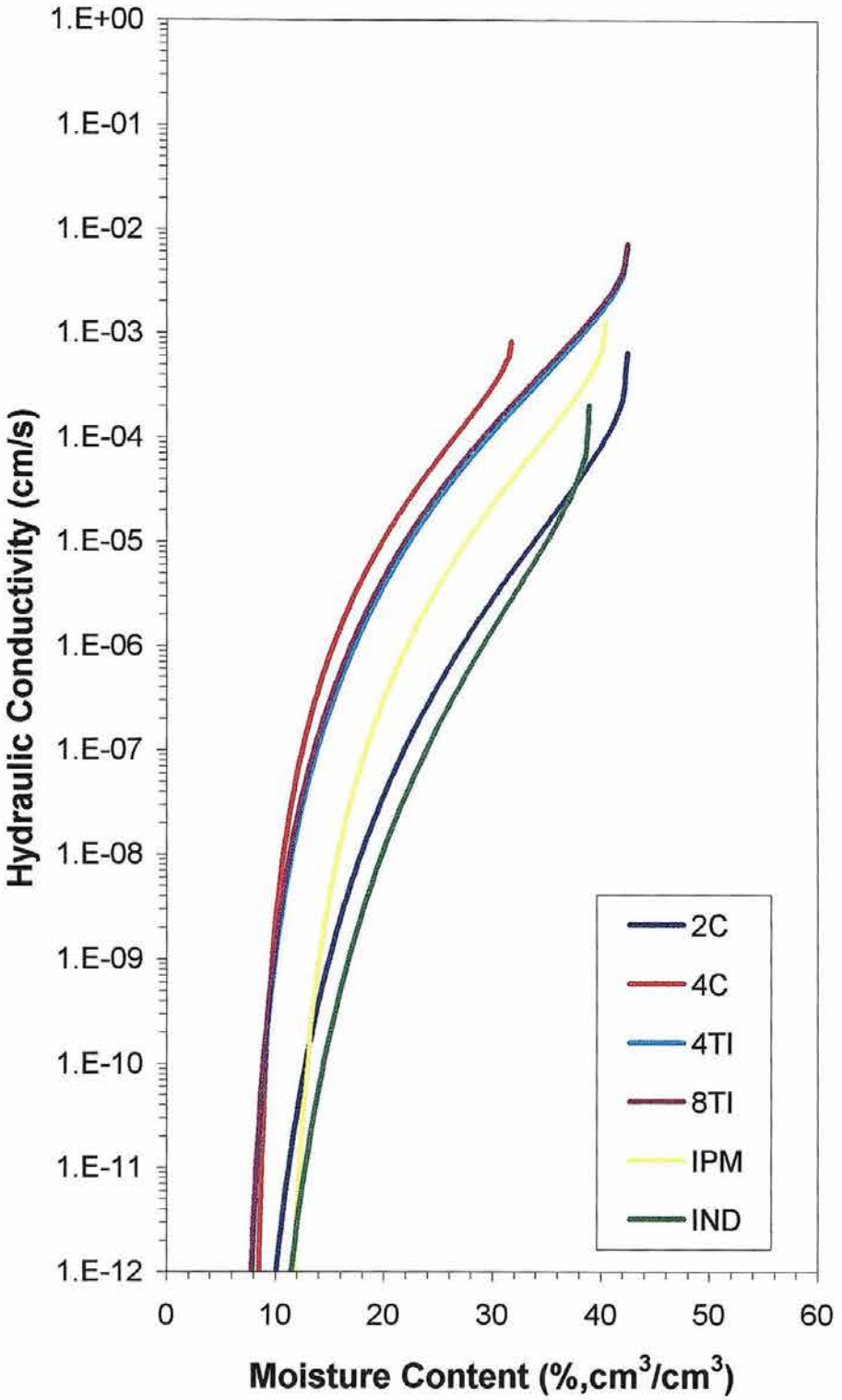

Appendix A. Unsaturated hydraulic conductivity plots constructed using data obtained from NT treatment at the 120 cm depth.

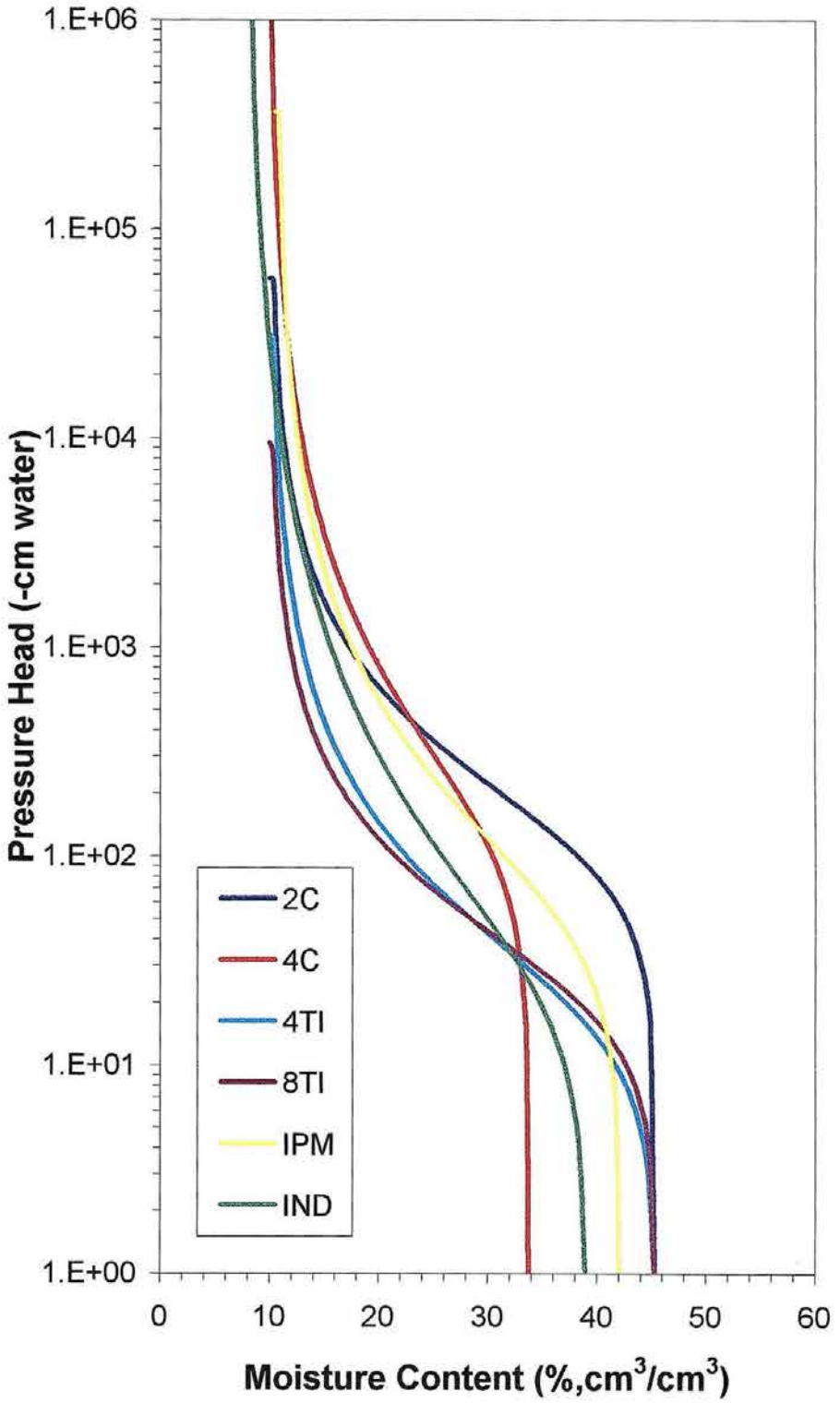

Appendix A. Moisture retention plots plots constructed using data obtained from the NT treatment at the 150 cm depth.

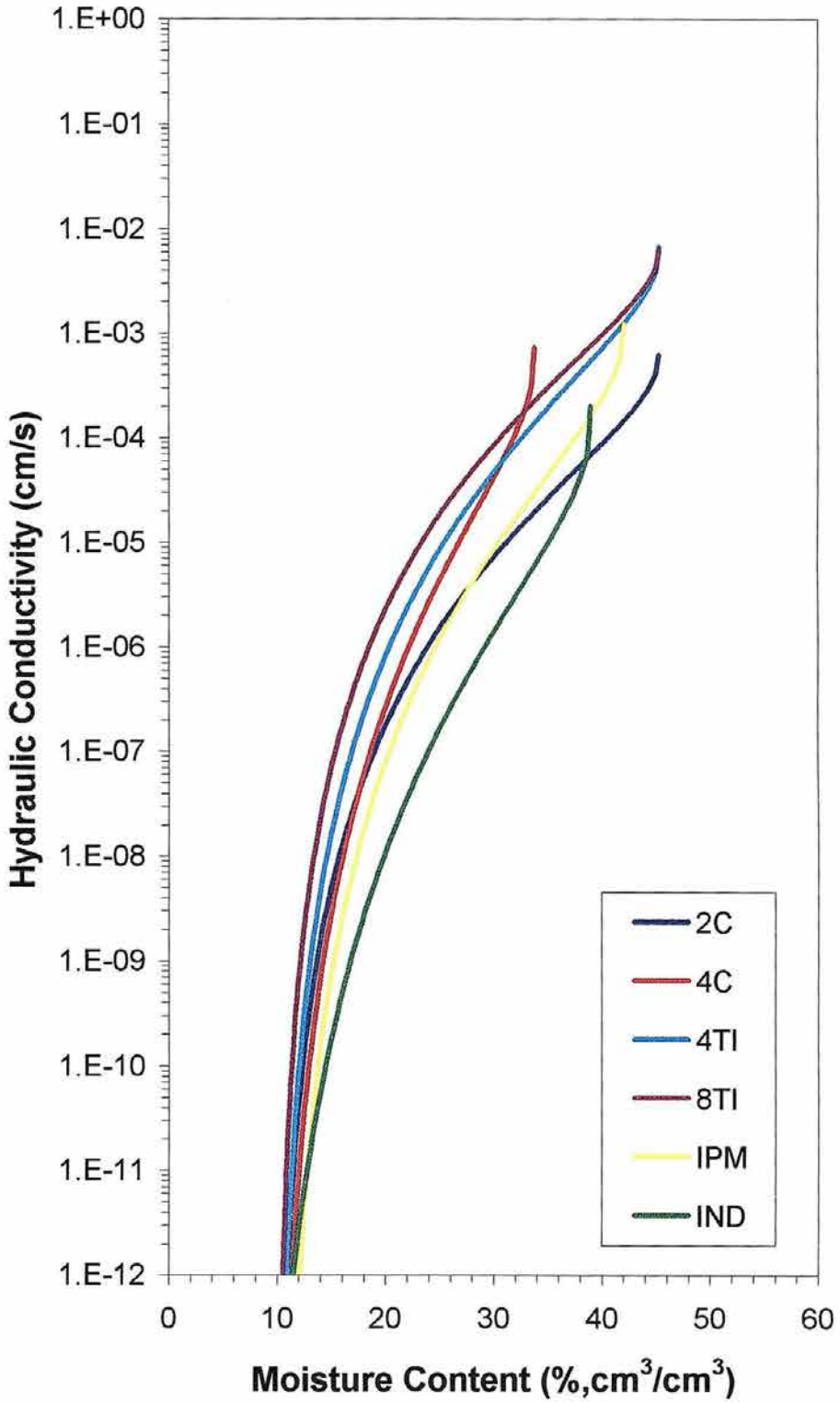

Appendix A. Unsaturated hydraulic conductivity plots constructed using data obtained from NT treatment at the 150 cm depth.

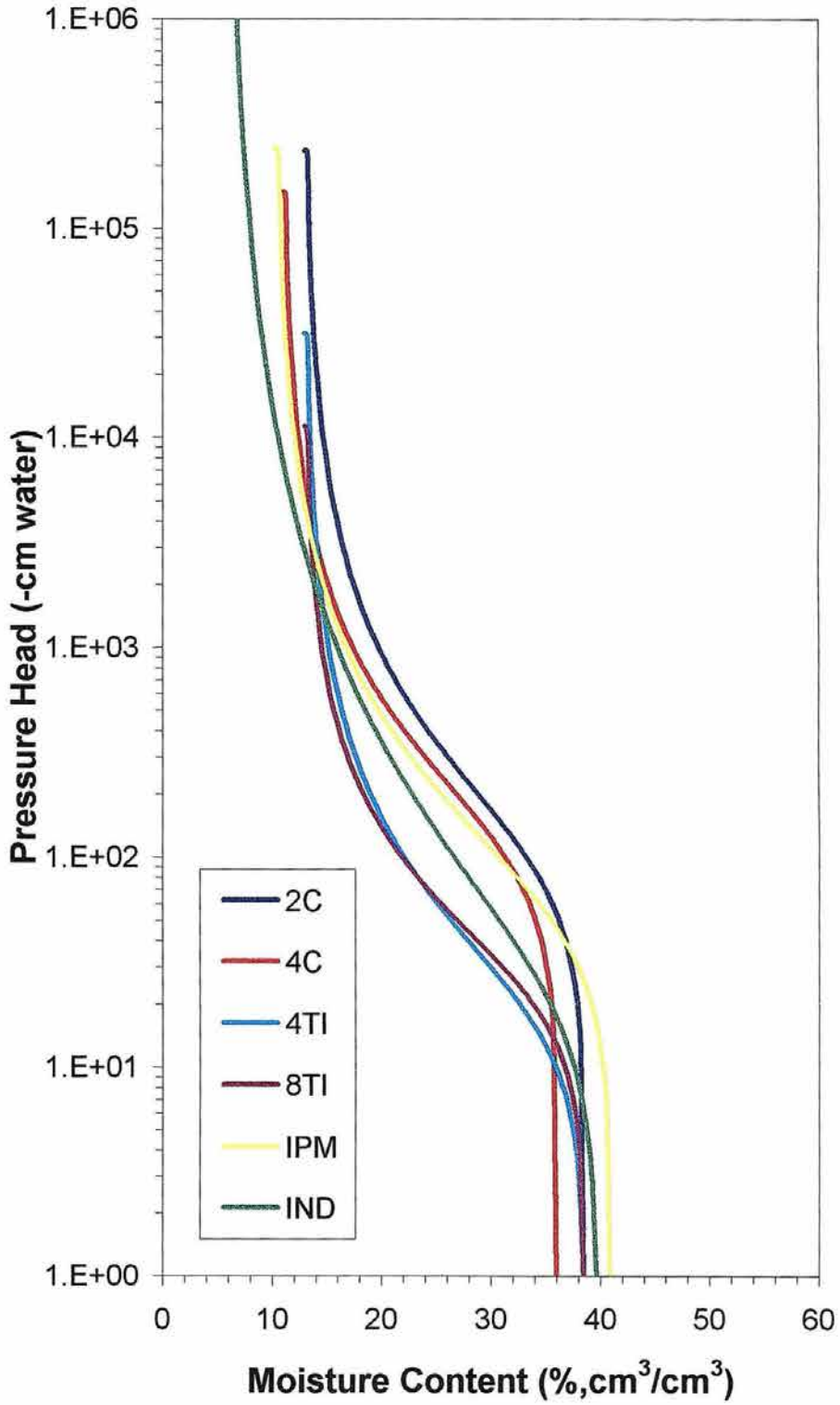

Appendix A. Moisture retention plots plots constructed using data obtained from the NT treatment at the 180 cm depth.

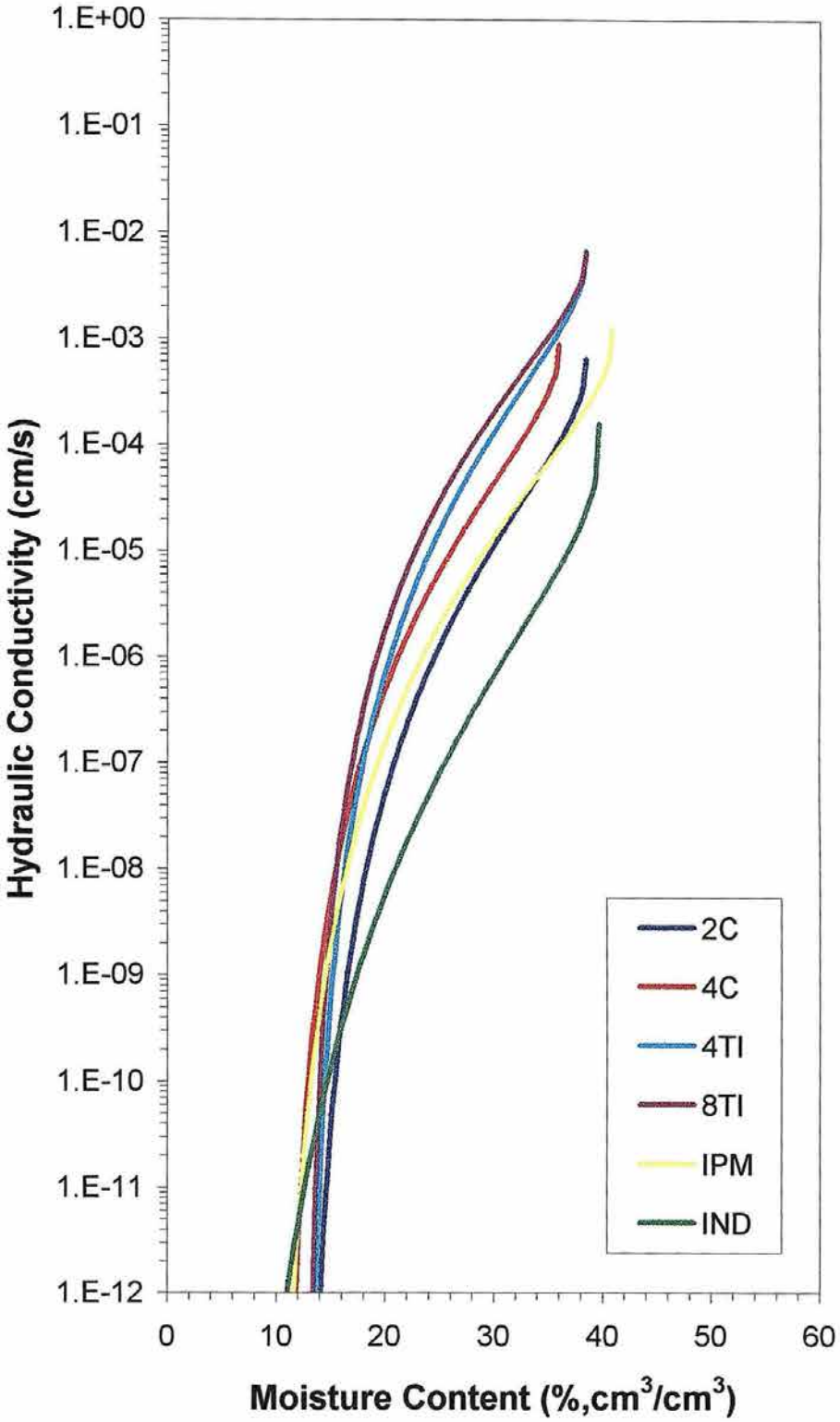

Appendix A. Unsaturated hydraulic conductivity plots constructed using data obtained from NT treatment at the 180 cm depth.

APPENDIX B

		α – Curve Fitting Parameter (cm^{-1}) by Method of Measurement													
Depth	Treatment	2C		4C		4TI		8TI		IND		IPM		Row Averages	
(cm)		Mean	CV	MEAN	CV	MEAN	CV	MEAN	CV	MEAN	CV	MEAN	CV	MEAN	CV
0	NT	0.0130	0.3016	0.0110	0.1513	0.0480	0.0589	0.0575	0.7292	0.0383	0.5114	-	-	0.0336	0.6210
0	T	0.0409	0.0381	0.0400	0.0541	0.0800	0.5401	0.1513	0.1434	0.0383	0.5114	-	-	0.0701	0.6936
10	NT	0.0226	0.3016	0.0212	0.1772	0.0384	0.1925	0.0451	0.3937	0.0383	0.5114	0.0263	0.0721	0.0320	0.3099
10	T	0.0180	0.6700	0.0218	0.0324	0.0500	0.5798	0.0750	0.1314	0.0383	0.5114	0.0450	0.3143	0.0414	0.5023
20	NT	0.0107	0.1899	0.0214	0.3213	0.0325	0.4879	0.0243	0.9191	0.0383	0.5114	0.0275	0.1091	0.0258	0.3705
20	T	0.0171	0.5099	0.0168	0.1055	0.0314	0.2768	0.0501	0.1432	0.0383	0.5114	0.0495	0.4415	0.0339	0.4399
30	NT	0.0192	0.4726	0.0155	0.2463	0.1008	0.2669	0.0365	0.3546	0.0383	0.5114	0.0275	0.2025	0.0396	0.7893
30	T	0.0152	0.9196	0.0128	0.0055	0.0195	0.7182	0.0341	0.2713	0.0383	0.5114	0.0383	0.4874	0.0263	0.4502
60	NT	0.0158	0.2878	0.0209	0.5752	0.0270	0.2221	0.0315	0.3186	0.0383	0.5114	0.0140	0.1750	0.0246	0.3837
60	T	0.0158	0.4567	0.0149	0.1095	0.0370	0.1043	0.0372	0.3378	0.0383	0.5114	0.0253	0.1782	0.0281	0.3906
90	NT	0.0142	0.0647	0.0117	0.2197	0.0265	0.6568	0.0303	0.5361	0.0383	0.5114	0.0140	0.1750	0.0225	0.4813
90	T	0.0128	0.6357	0.0129	0.1926	0.0366	0.4146	0.0366	0.2485	0.0383	0.5114	0.0200	0.2198	0.0262	0.4702
120	NT	0.0069	0.8255	0.0070	0.0000	0.0228	0.7565	0.0365	0.6433	0.0383	0.5114	0.0140	0.2374	0.0209	0.6726
120	T	0.0064	0.1654	0.0087	1.0055	0.0643	0.3498	0.0559	0.3525	0.0383	0.5114	0.0143	0.3052	0.0313	0.8040
150	NT	0.0084	0.2615	0.0070	0.2020	0.0491	0.3626	0.0390	0.8861	0.0383	0.5114	0.0165	0.2347	0.0264	0.6808
150	T	0.0025	0.6928	0.0104	1.0063	0.0392	0.0699	0.0644	0.3246	0.0383	0.5114	0.0125	0.1904	0.0279	0.8418
180	NT	0.0089	0.1761	0.0080	0.1768	0.0490	0.4858	0.0375	0.3647	0.0390	0.5128	0.0155	0.3094	0.0263	0.6703
180	T	0.0070	0.4279	0.0082	0.9831	0.0393	0.3325	0.0642	0.4136	0.0390	0.5128	0.0150	0.1633	0.0288	0.7857
Column Averages		0.0142	0.4110	0.0150	0.3091	0.0440	0.3820	0.0504	0.4173	0.0384	0.5116	0.0234	0.2385		

Appendix B. Coefficient of variation (CV) for hydraulic parameters.

		n - Curve Fitting Parameter (dimensionless) by Method of Measurement													
Depth	Treatment	2C		4C		4TI		8TI		IND		IPM		Row Averages	
(cm)		Mean	CV	MEAN	CV	MEAN	CV	MEAN	CV	MEAN	CV	MEAN	CV	MEAN	CV
0	NT	1.6500	0.1864	1.8640	0.0683	1.7500	0.0746	1.7661	0.0688	1.3800	0.0854	-	-	1.6820	0.1100
0	T	1.7968	0.2857	1.8637	0.2223	1.6250	0.1399	1.7277	0.0908	1.3800	0.0854	-	-	1.6786	0.1125
10	NT	1.7110	0.0792	1.7170	0.1128	1.7829	0.0589	1.7156	0.0726	1.3800	0.0854	1.5600	0.0626	1.6444	0.0906
10	T	1.6364	0.1381	1.7167	0.2500	1.7440	0.0934	1.7403	0.0931	1.3800	0.0854	1.4625	0.0327	1.6133	0.0967
20	NT	1.7360	0.2822	1.6730	0.1572	1.7200	0.0833	1.7424	0.0936	1.3800	0.0854	1.5075	0.0458	1.6265	0.0917
20	T	1.6678	0.1320	1.6731	0.1791	1.5532	0.0523	1.7730	0.0440	1.3800	0.0854	1.5225	0.0576	1.5949	0.0870
30	NT	1.6620	0.1421	1.4660	0.1862	1.6658	0.1085	1.8708	0.0507	1.3800	0.0854	1.5300	0.0459	1.5958	0.1095
30	T	1.7804	0.0950	1.4190	0.1644	1.5085	0.0790	1.6667	0.0700	1.3800	0.0854	1.5250	0.0628	1.5466	0.0981
60	NT	1.9240	0.2263	1.3050	0.0228	1.6800	0.0248	1.6451	0.1025	1.3800	0.0854	1.7650	0.0826	1.6165	0.1449
60	T	1.6663	0.1277	1.3425	0.1343	1.5400	0.0737	1.6015	0.0329	1.3800	0.0854	1.7000	0.0340	1.5384	0.0964
90	NT	1.8390	0.1512	1.5040	0.2360	1.6759	0.1496	1.6370	0.1103	1.3800	0.0854	1.7225	0.1139	1.6264	0.1002
90	T	1.7657	0.1824	1.5125	0.0323	1.5361	0.1506	1.6033	0.0992	1.3800	0.0854	1.7075	0.0423	1.5842	0.0882
120	NT	1.4140	0.4302	1.9950	0.0021	1.6399	0.1448	1.6542	0.0778	1.3800	0.0854	1.6525	0.0887	1.6226	0.1359
120	T	1.8291	0.2252	1.9935	0.0046	1.7210	0.0793	1.6129	0.0974	1.3800	0.0854	1.7150	0.0295	1.7086	0.1208
150	NT	1.7530	0.1512	1.4780	0.0861	1.6320	0.0944	1.7944	0.0697	1.3800	0.0854	1.5275	0.0700	1.5941	0.1014
150	T	1.6545	0.0704	1.5110	0.0777	1.6586	0.1053	1.7077	0.0879	1.3800	0.0854	1.7100	0.0266	1.6036	0.0819
180	NT	1.6020	0.1577	1.6510	0.0026	1.6300	0.0690	1.7748	0.0706	1.3280	0.1083	1.5575	0.0161	1.5906	0.0930
180	T	1.6923	0.1818	1.6855	0.0524	1.6600	0.1334	1.7125	0.0723	1.3280	0.1083	1.5650	0.0192	1.6072	0.0910
Column Averages		1.7100	0.1803	1.6317	0.1106	1.6513	0.0953	1.7081	0.0780	1.3742	0.0880	1.6081	0.0519		

Appendix B. Coefficient of variation (CV) for hydraulic parameters.

		Saturated Water Content (%, cm^3/cm^3) by Method of Measurement													
Depth	Treatment	2C		4C		4TI		8TI		IND		IPM		Row Averages	
(cm)		Mean	CV	MEAN	CV	MEAN	CV	MEAN	CV	MEAN	CV	MEAN	CV	MEAN	CV
0	NT	0.4600	0.0273	0.3314	0.0205	0.4600	0.0000	0.4600	0.0000	0.3900	0.1538	-	-	0.4203	0.1385
0	T	0.4888	0.1791	0.4085	0.2849	0.4888	0.0000	0.4888	0.0000	0.3900	0.1538	-	-	0.4530	0.1092
10	NT	0.4823	0.0191	0.3258	0.0840	0.4820	0.0000	0.4820	0.0000	0.3900	0.1538	0.4124	0.0309	0.4291	0.1507
10	T	0.4699	0.1446	0.4007	0.1620	0.4699	0.0000	0.4699	0.0000	0.3900	0.1538	0.4244	0.0168	0.4375	0.0851
20	NT	0.4433	0.0826	0.3068	0.0242	0.4430	0.0000	0.4430	0.0000	0.3900	0.1538	0.4211	0.0305	0.4079	0.1318
20	T	0.4088	0.0781	0.3708	0.2811	0.4088	0.0000	0.4088	0.0000	0.3900	0.1538	0.4196	0.0419	0.4011	0.0440
30	NT	0.4390	0.0858	0.3527	0.0265	0.4390	0.0000	0.4390	0.0000	0.3900	0.1538	0.4227	0.0322	0.4137	0.0857
30	T	0.4260	0.1732	0.3414	0.0969	0.4260	0.0000	0.4260	0.0000	0.3900	0.1538	0.4404	0.0259	0.4083	0.0902
60	NT	0.4178	0.0481	0.3365	0.0868	0.4180	0.0000	0.4180	0.0000	0.3900	0.1538	0.4012	0.0586	0.3969	0.0801
60	T	0.3859	0.1636	0.3562	0.0318	0.3859	0.0000	0.3859	0.0000	0.3900	0.1538	0.4168	0.0656	0.3868	0.0497
90	NT	0.4371	0.0170	0.3533	0.0094	0.4370	0.0000	0.4370	0.0000	0.3900	0.1538	0.4193	0.0543	0.4123	0.0831
90	T	0.3669	0.1868	0.3348	0.0471	0.3669	0.0000	0.3669	0.0000	0.3900	0.1538	0.4357	0.0271	0.3769	0.0896
120	NT	0.4251	0.1389	0.3181	0.0071	0.4250	0.0000	0.4250	0.0000	0.3900	0.1538	0.4050	0.0743	0.3980	0.1047
120	T	0.3985	0.1448	0.3673	0.2108	0.3985	0.0000	0.3985	0.0000	0.3900	0.1538	0.4314	0.0068	0.3973	0.0518
150	NT	0.4534	0.0857	0.3376	0.0343	0.4530	0.0000	0.4530	0.0000	0.3900	0.1538	0.4207	0.0228	0.4180	0.1120
150	T	0.4180	0.2612	0.3608	0.1783	0.4180	0.0000	0.4180	0.0000	0.3900	0.1538	0.4276	0.0203	0.4054	0.0623
180	NT	0.3849	0.0733	0.3596	0.0570	0.3850	0.0000	0.3850	0.0000	0.3967	0.0291	0.4089	0.0486	0.3867	0.0423
180	T	0.3987	0.1806	0.3907	0.0235	0.3987	0.0000	0.3987	0.0000	0.3967	0.0291	0.4198	0.0255	0.4006	0.0248
Column Averages		0.4280	0.1161	0.3529	0.0926	0.4280	0.0000	0.4280	0.0000	0.3907	0.1400	0.4204	0.0364		

Appendix B. Coefficient of variation (CV) for hydraulic parameters.

		Saturated Hydraulic Conductivity (cm/s) by Method of Measurement													
Depth	Treatment	2C		4C		4TI		8TI		IND		IPM		Row Averages	
(cm)		Mean	CV	MEAN	CV	MEAN	CV	MEAN	CV	MEAN	CV	MEAN	CV	MEAN	CV
0	NT	0.0007	0.1769	0.0010	0.0853	0.0048	0.1839	0.0062	0.2219	0.0002	0.6883	0.0016	0.0916	0.0024	1.1198
0	T	0.0010	0.1605	0.0015	0.8888	0.0045	0.2260	0.0054	0.2493	0.0002	0.6883	0.0030	0.1685	0.0026	0.8781
10	NT	0.0005	0.2045	0.0009	0.0058	0.0061	0.2934	0.0058	0.2875	0.0002	0.6883	0.0017	0.2697	0.0026	1.0597
10	T	0.0008	0.3139	0.0014	0.6851	0.0061	0.1261	0.0058	0.1211	0.0002	0.6883	0.0031	0.1567	0.0029	0.8815
20	NT	0.0007	0.1925	0.0009	0.1161	0.0061	0.1984	0.0063	0.2621	0.0002	0.6883	0.0016	0.2090	0.0026	1.0782
20	T	0.0008	0.2827	0.0168	0.7531	0.0055	0.1864	0.0053	0.2214	0.0002	0.6883	0.0030	0.1208	0.0052	1.1539
30	NT	0.0006	0.2295	0.0007	0.1512	0.0045	0.3469	0.0051	0.2087	0.0002	0.6883	0.0015	0.1723	0.0021	1.0196
30	T	0.0007	0.8532	0.0011	0.9271	0.0051	0.4719	0.0056	0.5180	0.0002	0.6883	0.0027	0.1302	0.0026	0.8996
60	NT	0.0007	0.2528	0.0006	0.1012	0.0055	0.3050	0.0066	0.3144	0.0002	0.6883	0.0014	0.1424	0.0025	1.1185
60	T	0.0008	0.1201	0.0010	0.2334	0.0062	0.1206	0.0064	0.2770	0.0002	0.6883	0.0024	0.2628	0.0028	0.9786
90	NT	0.0007	0.1699	0.0011	0.0829	0.0055	0.3050	0.0066	0.3144	0.0002	0.6883	0.0013	0.0861	0.0026	1.0799
90	T	0.0005	0.6604	0.0012	0.2703	0.0062	0.1206	0.0064	0.2770	0.0002	0.6883	0.0023	0.3352	0.0028	1.0043
120	NT	0.0006	0.0729	0.0008	0.0694	0.0065	0.1139	0.0071	0.0769	0.0002	0.6883	0.0013	0.1184	0.0028	1.1480
120	T	0.0006	0.3092	0.0009	0.0615	0.0053	0.1801	0.0062	0.3034	0.0002	0.6883	0.0022	0.3905	0.0026	1.0094
150	NT	0.0006	0.1466	0.0007	0.3773	0.0067	0.2786	0.0063	0.2658	0.0002	0.6883	0.0012	0.0896	0.0026	1.1474
150	T	0.0006	0.4509	0.0011	0.3482	0.0045	0.3310	0.0053	0.3001	0.0002	0.6883	0.0021	0.4204	0.0023	0.9206
180	NT	0.0006	0.5299	0.0009	0.0065	0.0067	0.2786	0.0063	0.2658	0.0002	0.9817	0.0012	0.0896	0.0026	1.1327
180	T	0.0005	0.1688	0.0009	0.1014	0.0045	0.3310	0.0053	0.3001	0.0002	0.9817	0.0021	0.4632	0.0022	0.9661
Column Averages		0.0007	0.2942	0.0019	0.2925	0.0056	0.2443	0.0060	0.2658	0.0002	0.7209	0.0020	0.2065		

Appendix B. Coefficient of variation (CV) for hydraulic parameters.

APPENDIX C

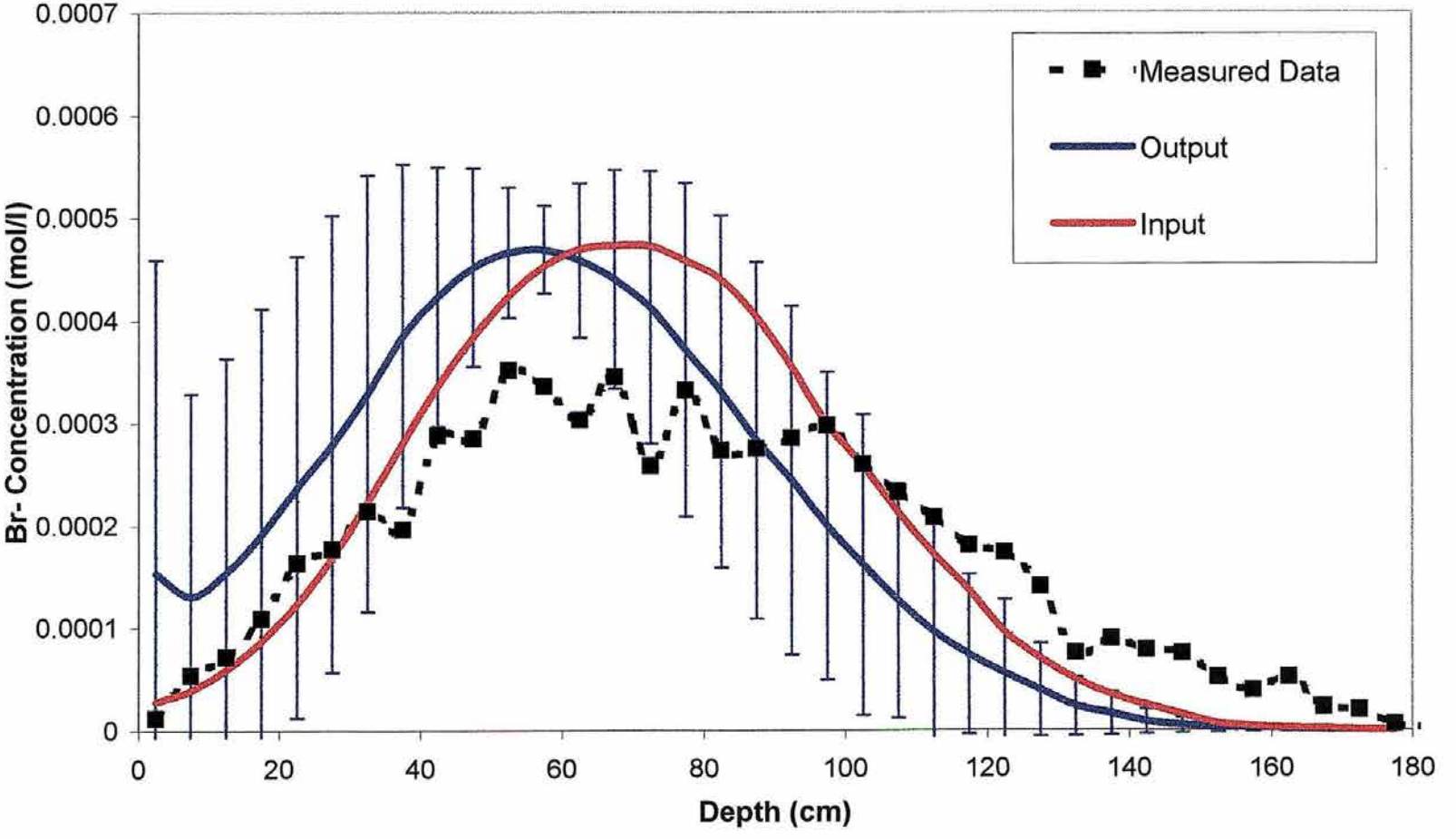

Appendix C. Bromide concentration profiles produced using average input data and averaged ouput concentration profiles for the 2C method.

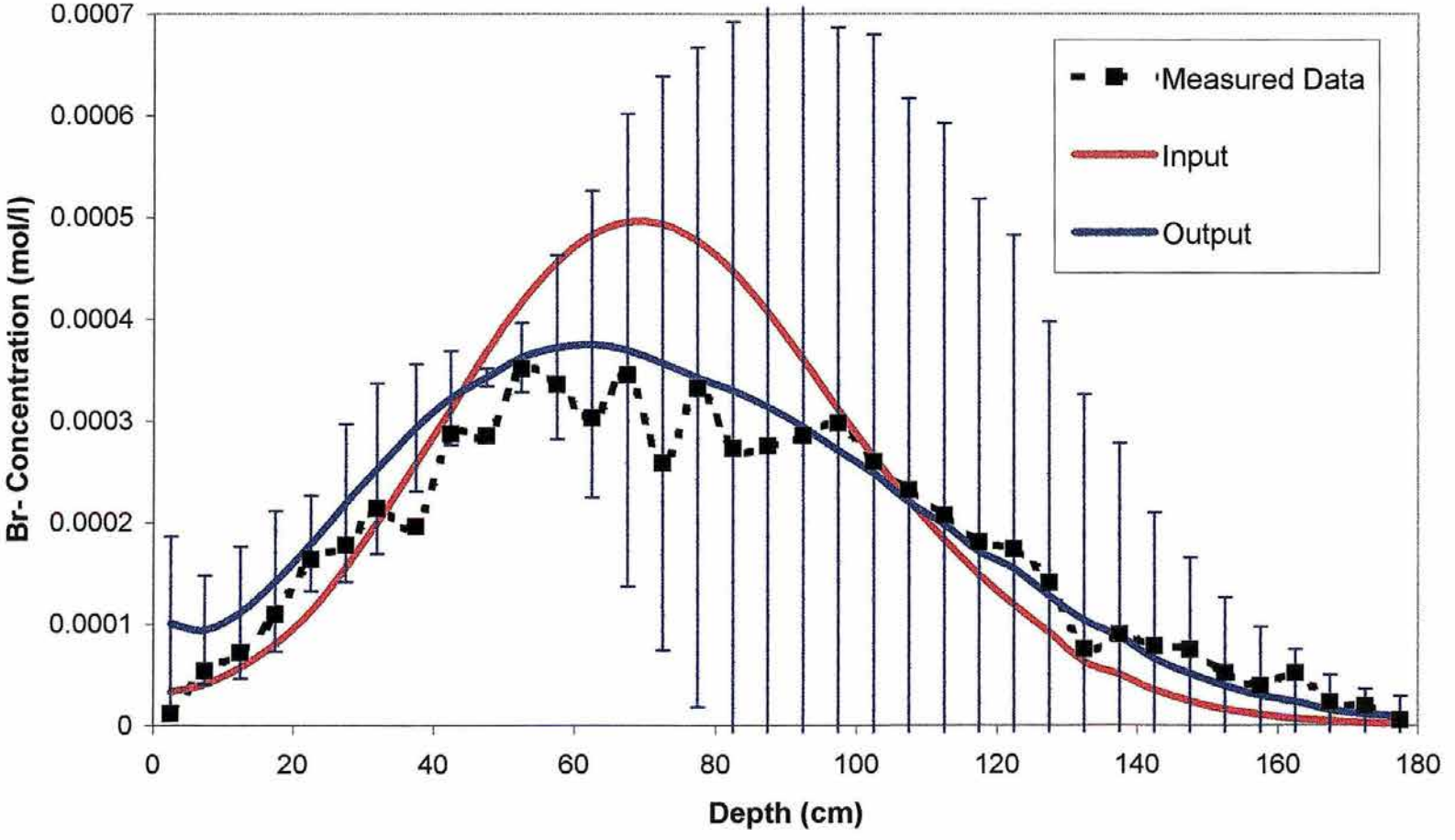

Appendix C. Bromide concentration profiles produced using average input data and averaged ouput concentration profiles for the 4C method.

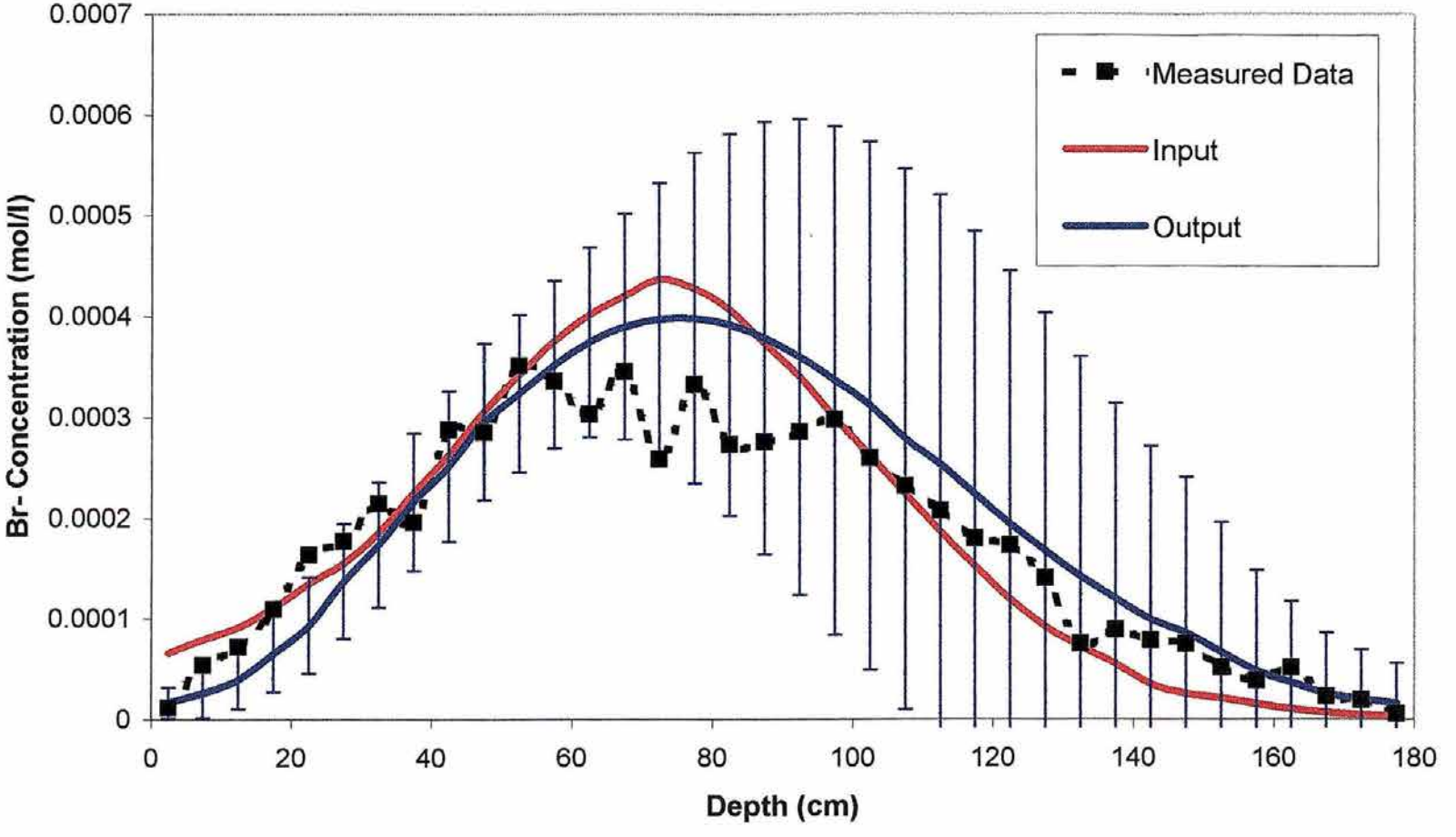

Appendix C. Bromide concentration profiles produced using average input data and averaged ouput concentration profiles for the 4TI method.

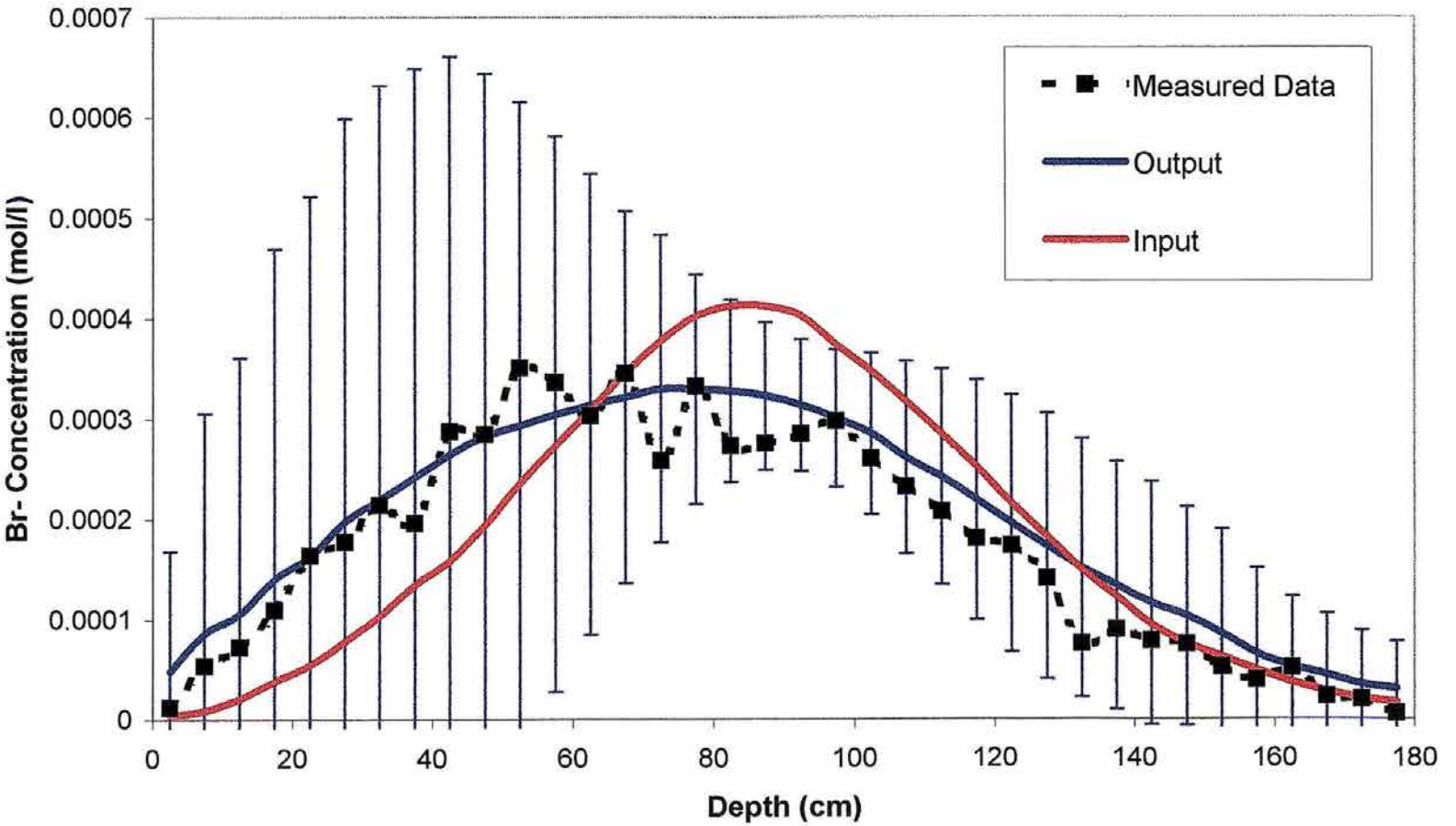

Appendix C. Bromide concentration profiles produced using average input data and averaged ouput concentration profiles for the 8TI method.

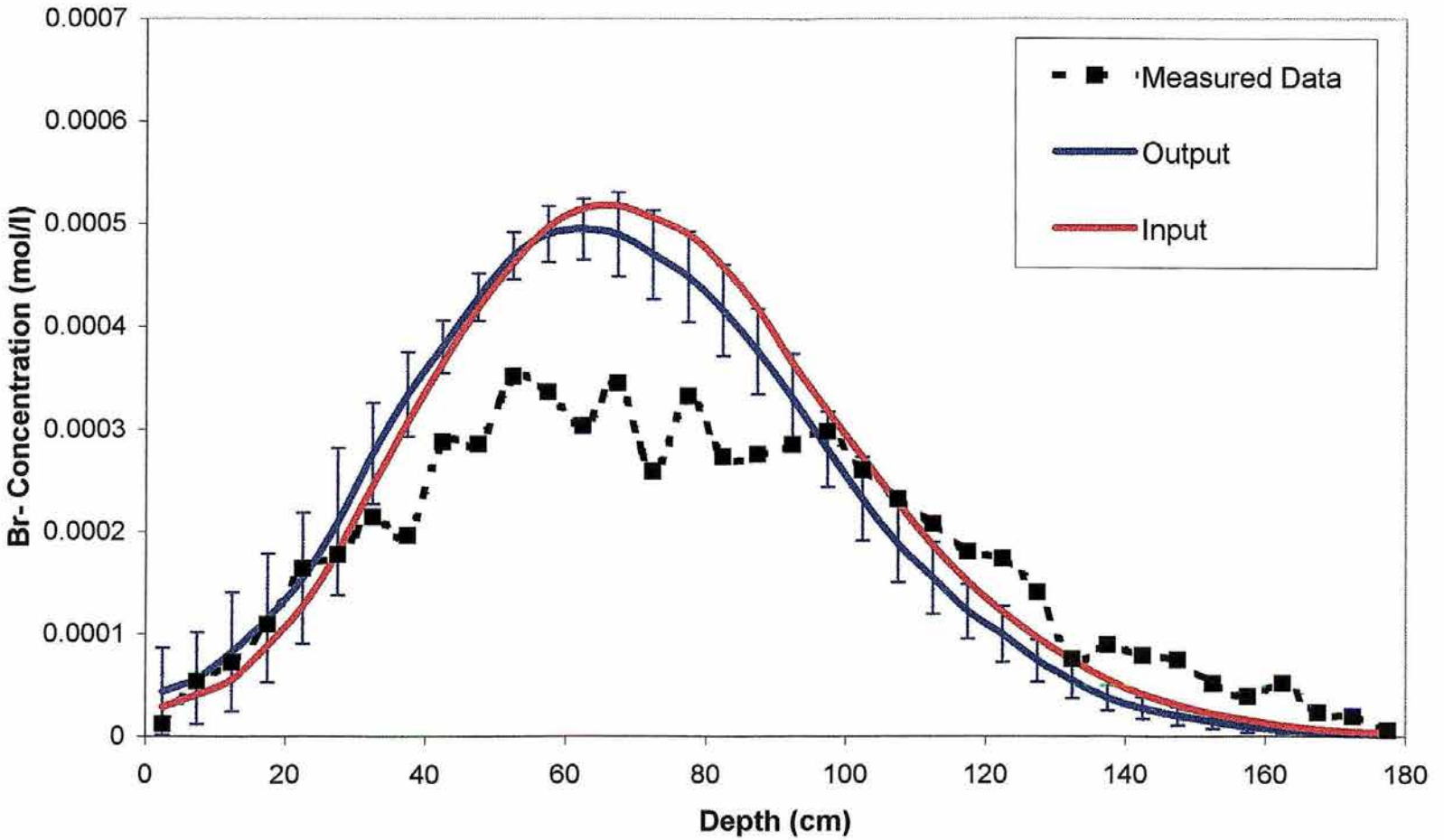

Appendix C. Bromide concentration profiles produced using average input data and averaged ouput concentration profiles for the IPM method.

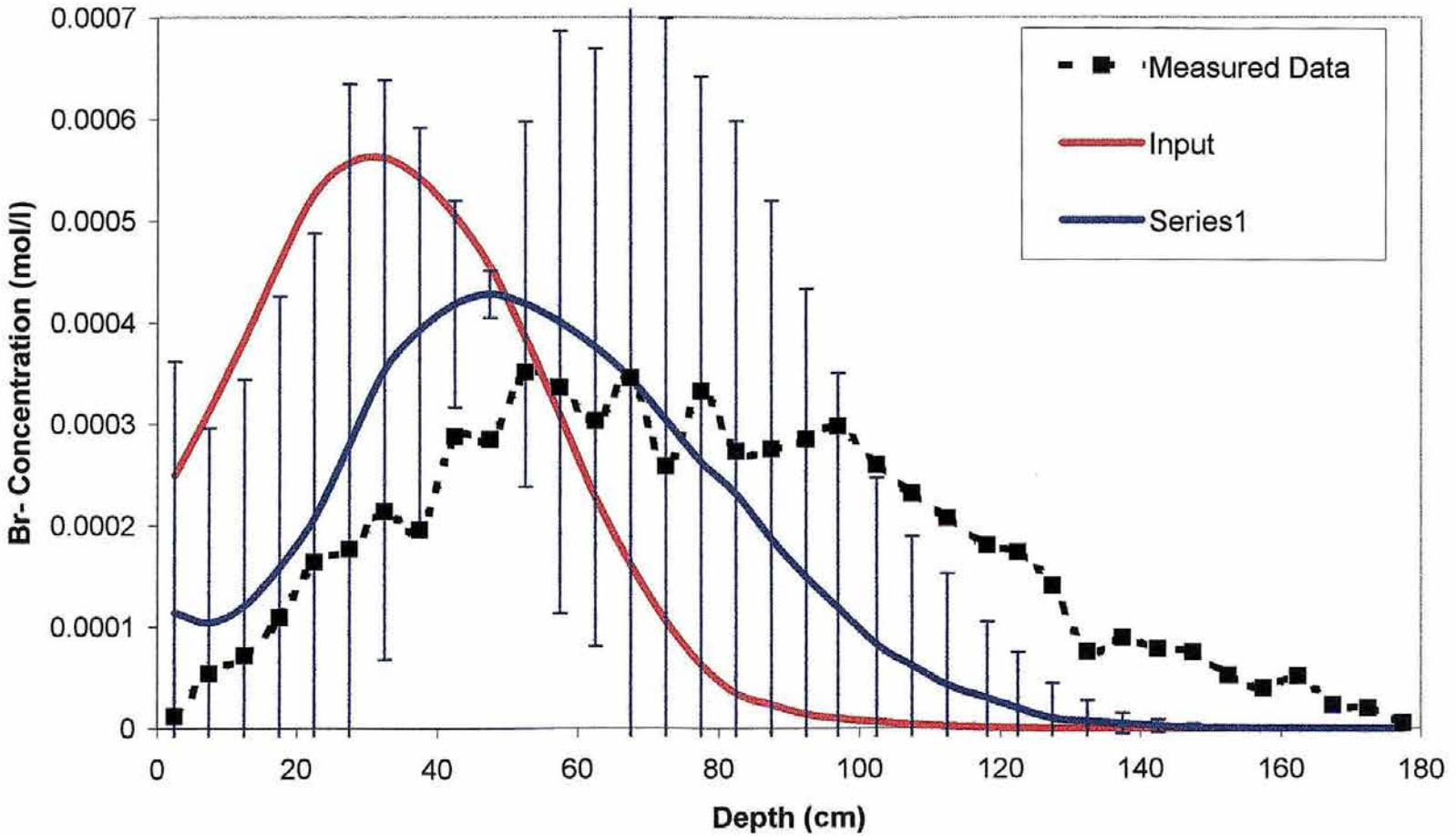

Appendix C. Bromide concentration profiles produced using average input data and averaged ouput concentration profiles for the IND method.

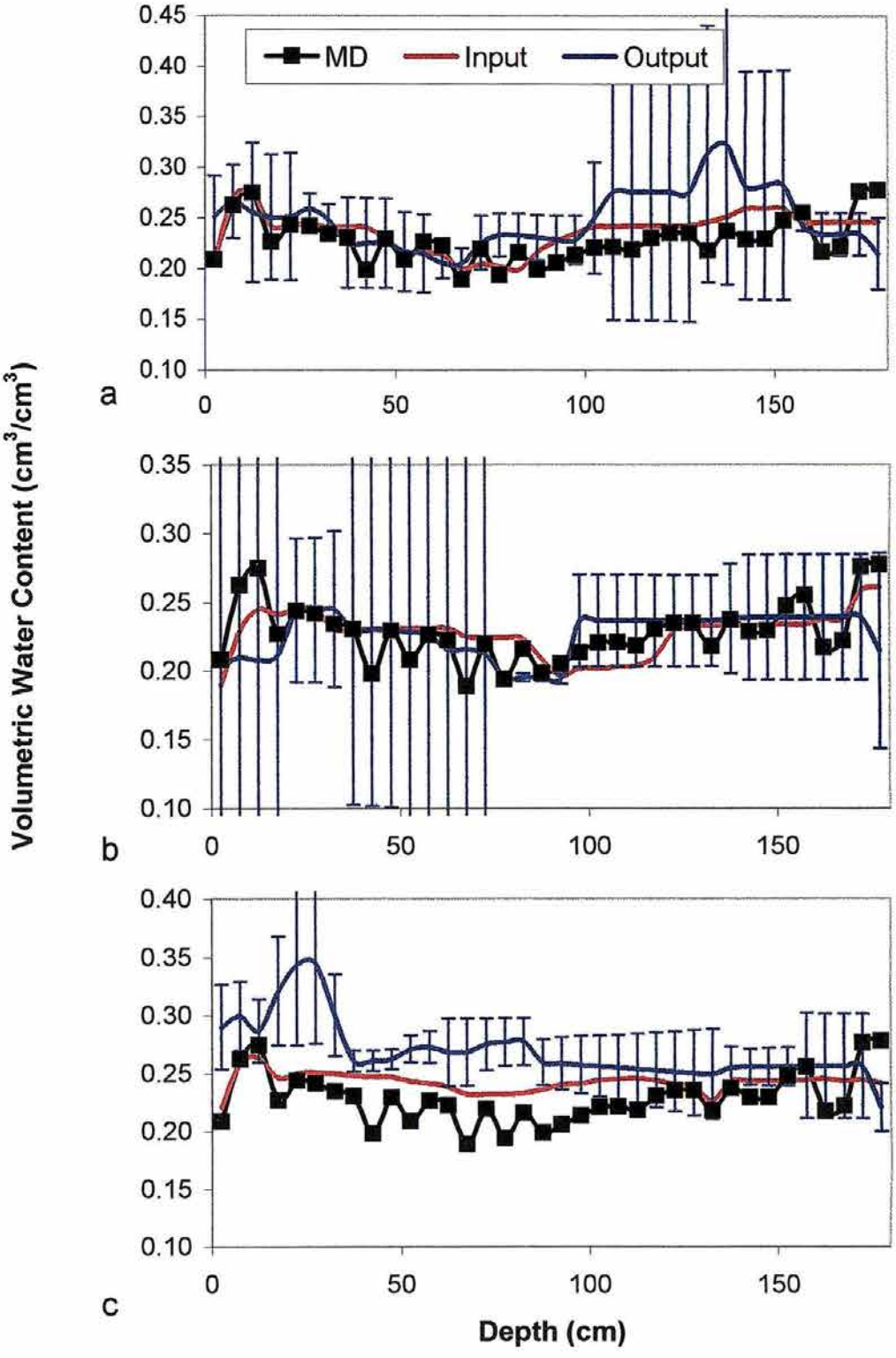

Appendix C. Water content profiles produced using averaged input parameters and averaged output water content profiles for T soil at day 117. (a=2C, b=4C, c=4TI)

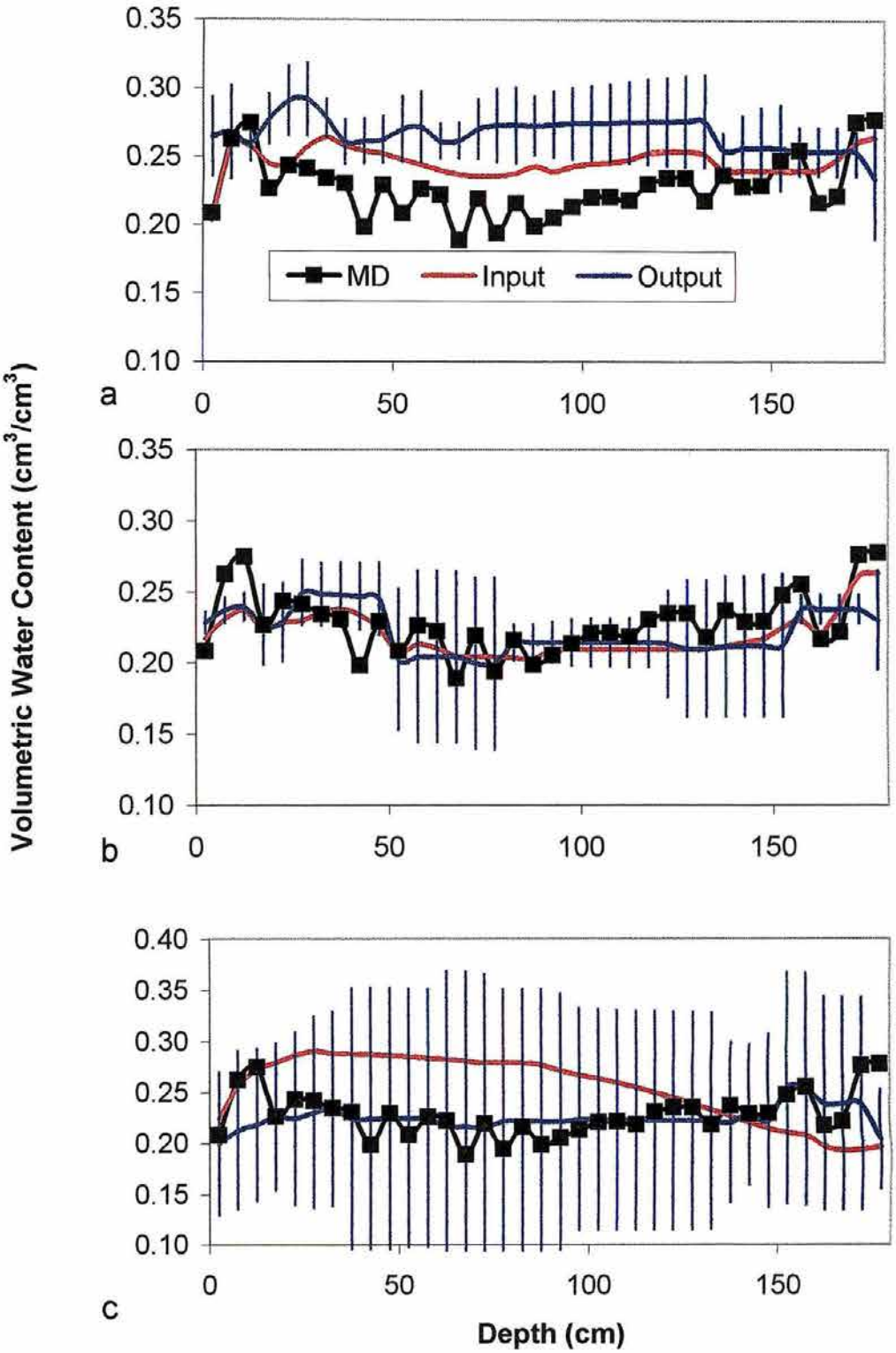

Appendix C. Water content profiles produced using averaged input parameters and averaged output water content profiles for T soil at day 117. (a=8TI, b=IPM, c=IND)